DOE/BC/14987-10
(DE97008689)

IMPROVED OIL RECOVERY IN MISSISSIPPIAN CARBONATE RESERVOIRS OF KANSAS
NEAR TERM -CLASS 2

Annual Report
September 18, 1994 to March 15, 1997

Timothy R. Carr
Don W. Green
G. Paul Willhite

April 1998

Performed Under Contract No. DE-FC22-93BC14987

The University of Kansas Center for Research Inc.
Lawrence, Kansas

National Petroleum Technology Office
U. S. DEPARTMENT OF ENERGY
Tulsa, Oklahoma

DOE/BC/14987-10
Distribution Category UC-122

Improved Oil Recovery In Mississippian Carbonate Reservoirs Of Kansas

Near Term
Class 2

Annual Report
September 18, 1994 to March 15, 1997

By
Timothy R. Carr
Don W. Green
G. Paul Willhite

April 1998

Work Performed Under Contract No. DE-FC22-93BC14987

Prepared for
U.S. Department of Energy
Assistant Secretary for Fossil Energy

Chandra Nautiyal, Project Manager
National Petroleum Technology Office
P.O. Box 3628
Tulsa, OK 74101

Prepared by:
The University of Kansas Center for Research, Inc.
Energy Research Center
Lawrence, KS 66045-2223

TABLE OF CONTENTS

FIGURES

PLATES

TABLES

FOREWORD

Contributors to this report include: Dana Adkins-Heljeson, Scott Beaty, Saibal Bhattacharya, Tim Carr, Evan Franseen, Paul Gerlach, Willard Guy, John Hopkins and W. Lynn Watney. Section 2.3.4. Rodney Reynolds, Shapour Vossoughi, and G. Paul Willhite prepared appendices D-F.

ABSTRACT

This annual report describes progress during the second year of the project entitled "Improved Oil Recovery in Mississippian Carbonate Reservoirs in Kansas". This project funded under the Department of Energy's Class 2 program targets improving the reservoir performance of mature oil fields located in shallow shelf carbonate reservoirs. The focus of this project is development and demonstration of cost-effective reservoir description and management technologies to extend the economic life of mature reservoirs in Kansas and the mid-continent. As part of the project, several tools and techniques for reservoir description and management were developed, modified and demonstrated. These include: 1) a new approach to subsurface visualization using electric logs ("Pseudoseismic"); 2) a low-cost easy-to-use spreadsheet log analysis software (PfEFFER); and 3) an extension of the BOAST-3 computer program for full field reservoir simulation. The world-wide-web was used to provide rapid and flexible dissemination of the project results through the Internet.

Included in this report is a summary of significant project results at the demonstration site (Schaben Field, Ness County, Kansas). These results include an outline of the reservoir description based on available and newly acquired data and reservoir simulation results. Detailed information is available on-line through the Internet. Based on the reservoir simulation, three infill wells will be drilled to validate the reservoir description and demonstrate the effectiveness of the proposed reservoir management strategies. The demonstration phase of the project has just begun and will be presented in the next annual report.

EXECUTIVE SUMMARY

The Kansas Class 2 project was a demonstration project in an Osagian and Meramecian (Mississippian) shallow shelf carbonate reservoir in west central Kansas. Cumulative production from Mississippian carbonate reservoirs located beneath a regional sub-Pennsylvanian unconformity is over 1 billion barrels distributed over a large number of small to medium size reservoirs. Small independent producers operate many of these reservoirs. Extremely high water cuts and low recovery factors place continued operations at or near their economic limits.

Application of cost-effective reservoir description and management strategies can significantly extend the economic life of these mature peritidal carbonate fields and recover incremental reserves. Equally important is innovative dissemination of the data, methodologies, and results to foster wider application of demonstrated technologies by the numerous operators of similar fields throughout the northern Mid-continent and US. Producibility problems in Kansas Meramecian and Osagian dolomite reservoirs include inadequate reservoir characterization, drilling and completion design problems, and non-optimal primary recovery.

The project entailed integration of existing data, drilling and coring of three new wells through the reservoir interval. Descriptive core analysis, petrophysical and petrographic analysis (e.g. capillary pressure and NMR), calibration of logs and core data, and integration of existing well data into a computerized three dimensional visualization/simulation that was used to develop a digital reservoir model and management plan for the Osagian and Meramecian rocks at the Schaben site. Analysis indicates significant potential incremental reserves through targeted infill and horizontal drilling in this major producing trend.

At the Schaben demonstration site, integrated reservoir characterization provided the basis for development of a descriptive reservoir model and the framework for simulation. A publicly accessible and comprehensive digital reservoir database using existing and newly acquired data was distributed through the Internet. New data from the three new wells provided insight into fundamental reservoir parameters (e.g., core plug NMR analysis to determine effective porosity and relationship to facies). As part of the Kansas Class 2 project a number of cost-effective tools and techniques for reservoir description were developed, modified and demonstrated. These include: 1) a new approach to subsurface visualization using electric logs ("Pseudoseismic"); 2) a low-cost easy-to-use spreadsheet log analysis software (PfEFFER); and 3) an extension of the BOAST-3 computer program for full field reservoir simulation. The Kansas Digital Petroleum Atlas model was used to provide rapid and flexible dissemination of the project results through the Internet.

The most significant Kansas Class 2 project results are 1) development of an on-line comprehensive digital reservoir database; 2) acquisition of additional core, electric log and test data; 3) construction of an integrated geologic reservoir characterization using cost-effective approaches to data analysis; 3) full-field reservoir characterization and simulation using publicly available or low-cost software; 4) identification of potential incremental reserves that can be accessed through targeted infill and possible horizontal drilling; 5) development of a regional database for evaluation of potential for horizontal and targeted infill drilling in similar Mississippian reservoirs of Kansas; and 6) new models for innovative technology transfer. An improved understanding of Mississippian subunconformity reservoirs in Kansas has been developed and new cost-effective techniques have been demonstrated for the identification of incremental reserves at the Schaben Field demonstration area and at similar reservoirs throughout Kansas and the Mid-continent

1.0 INTRODUCTION

The Kansas Class 2 project is an effort to introduce Kansas producers to potentially useful technologies and to demonstrate these technologies in actual oil field operations. In addition, advanced technology was tailored specifically to the scale appropriate to the operations of Kansas producers. The majority of Kansas production is operated by small independent producers that do not have resources to develop and test advanced technologies (90% of the 3,000 Kansas producers have less than 20 employees). For Kansas producer's, access to new technology is important for sustaining production and increasing viability. A major emphasis of the project is collaboration of university scientists and engineers with the independent producers and service companies operating in Kansas to accelerate adaptation and evaluation of new technologies. An extensive technology transfer effort is being undertaken to inform other operators of the project results. In addition to traditional technology transfer methods (for example, reports; trade, professional, and technical publications; workshops; and seminars), a public domain relational database and computerized display package are available through the Internet. The goal is figuratively to provide access to data and technology to independent producers in their office.

Project design, methodologies, data, and results are being disseminated through focused technology transfer activities. These activities include development of cost-effective technologies and software (e.g. PfEFFER, "Pseudoseismic"), open-file reports; publication in trade, professional, and technical publications; workshops and seminars; and the establishment of public access through the Internet to the data, technologies and project results domain relational database and computerized display package. The target audience includes other operators in the demonstration area, operators of other Mississippian sub-unconformity dolomite reservoirs in Kansas, operators of analogous shallow shelf carbonate reservoirs in the Mid-continent, and technical personnel involved in reservoir development and management.

1.1 OBJECTIVES AND SIGNIFICANCE

The majority of Mississippian production in Kansas occurs at or near the top of the Mississippian section just below the regional sub-Pennsylvanian unconformity. These reservoirs are a major source of Kansas oil production and account for approximately 43% (21 million barrels in 1994) of total annual production (Carr et al., 1995a, Figure 1.1). Cumulative production from Mississippian reservoirs in Kansas exceeds 1 billion barrels. Many of these reservoirs and production units are operated by small independent producers. Extremely high water cuts and low recovery factors place continued operations at or near their economic limits.

This project addresses producibility problems in the numerous Kansas fields such as the Schaben field in Ness County that produce from Meramecian and Osagian dolomites beneath the sub-Pennsylvanian unconformity. Producibility problems in these reservoirs include inadequate reservoir characterization, drilling and completion design problems, and non-optimal primary recovery. Tools and techniques will facilitate integrated, multi-disciplinary reservoir characterization. Application of cost-effective reservoir description and management strategies can significantly extend the economic life of these mature peritidal carbonate fields and recover significant incremental reserves. Equally important is innovative dissemination of the data,

methodologies, and results to foster wider application of demonstrated technologies by the numerous operators of similar fields throughout the northern Mid-continent and US.

1.2 SITE DESCRIPTION

The Schaben demonstration site consists of 1,720 contiguous acres within Schaben field, located in Township 19 South--Range 21 West, Township 20 South--Range 21 West, and Township 19 South--Range 22 West, Ness County, Kansas (Figure 1.2). The leases comprising the demonstration sites are highlighted in Figure 1.2. This site is located in the upper shelf of the Hugoton Embayment of the Anadarko Basin and produces oil from dolostones and limestones of the lower Meramecian Warsaw Limestone and Osagian Keokuk Limestone (Mississippian) at depths of 4,350-4,410 feet.

Schaben field, discovered in 1963, consists of 78 completed oil wells spaced primarily on 40-acre locations (Figure 1.3). Cumulative field production as of September, 1996 was 9.1 million barrels of oil (BO), and daily field production was 326 BOPD from 51 wells (Figure 1.2). Wells in the Schaben demonstration site have cumulatively produced 3,593,609 BO, with current (June 1993) daily production totaling 141 BOPD from 29 wells. In addition to production from the Mississippian, one well produces oil from the Cherokee Group and the Fort Scott Limestone, however, the relative volume of oil produced from these secondary zones is small. The Schaben demonstration site contains 6 plugged and abandoned oil wells, 27 actively producing oil wells, and 2 water disposal wells.

The Schaben Field demonstration site is located on the western flank of the Central Kansas uplift at the western edge of the Mississippian Osagian subcrop beneath the sub-Pennsylvanian unconformity (figures 1.4 - 1.6).

1.3 PARTICIPATING ORGANIZATIONS

University of Kansas Center for Research Inc., the University of Kansas Energy Research Center, the Kansas Geological Survey, and the Tertiary Oil Recovery Project of Lawrence Kansas, and Ritchie Exploration Inc. of Wichita, Kansas are participating in the project. Total cost sharing in the project is 50 percent.

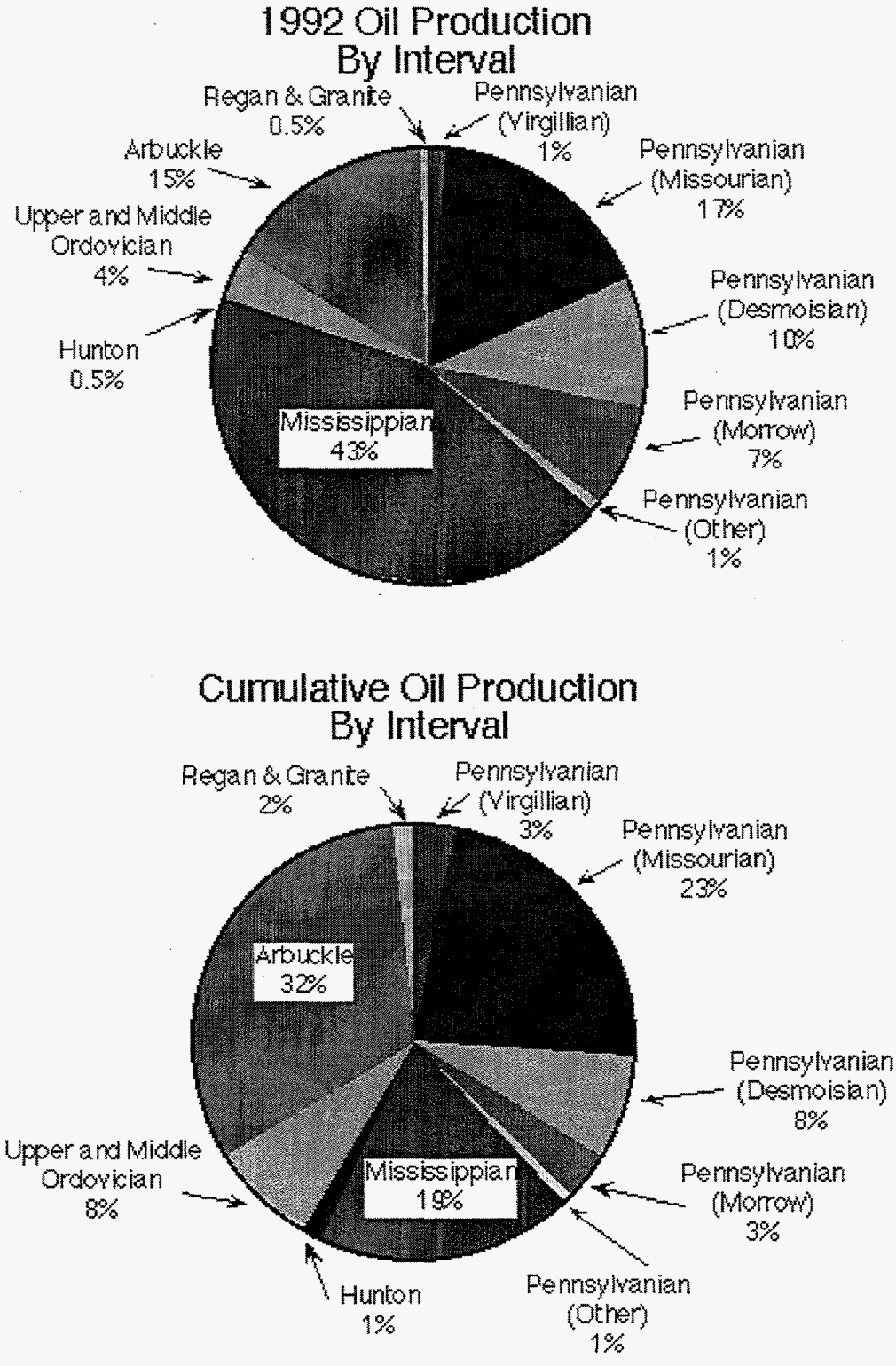

FIGURE 1.1 Kansas annual and cumulative oil production from Carr et al. 1995a. Mississippian reservoirs comprise one of the largest producing intervals in the state. Also available on-line through the Internet (http://www.kgs.ukans.edu/PRS/publication/OFR95_42/tim1.html).

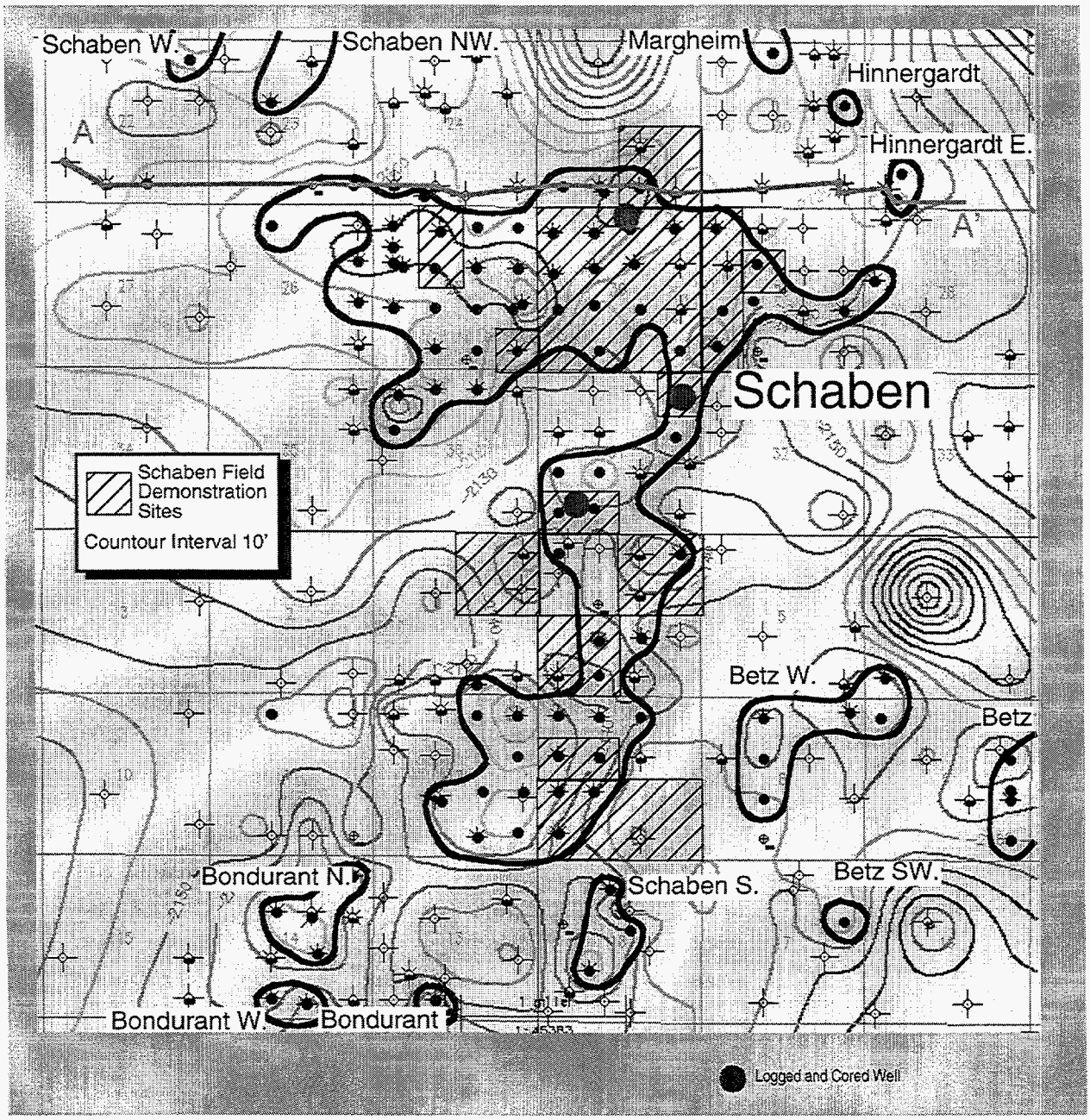

FIGURE 1.2. Schaben Field demonstration site with structure on top of the Mississippian Limestone. The Schaben Field outline and location of leases involved in demonstration are indicated. Location of the three wells, drilled, logged and cored as part of the demonstration project, are also indicated.

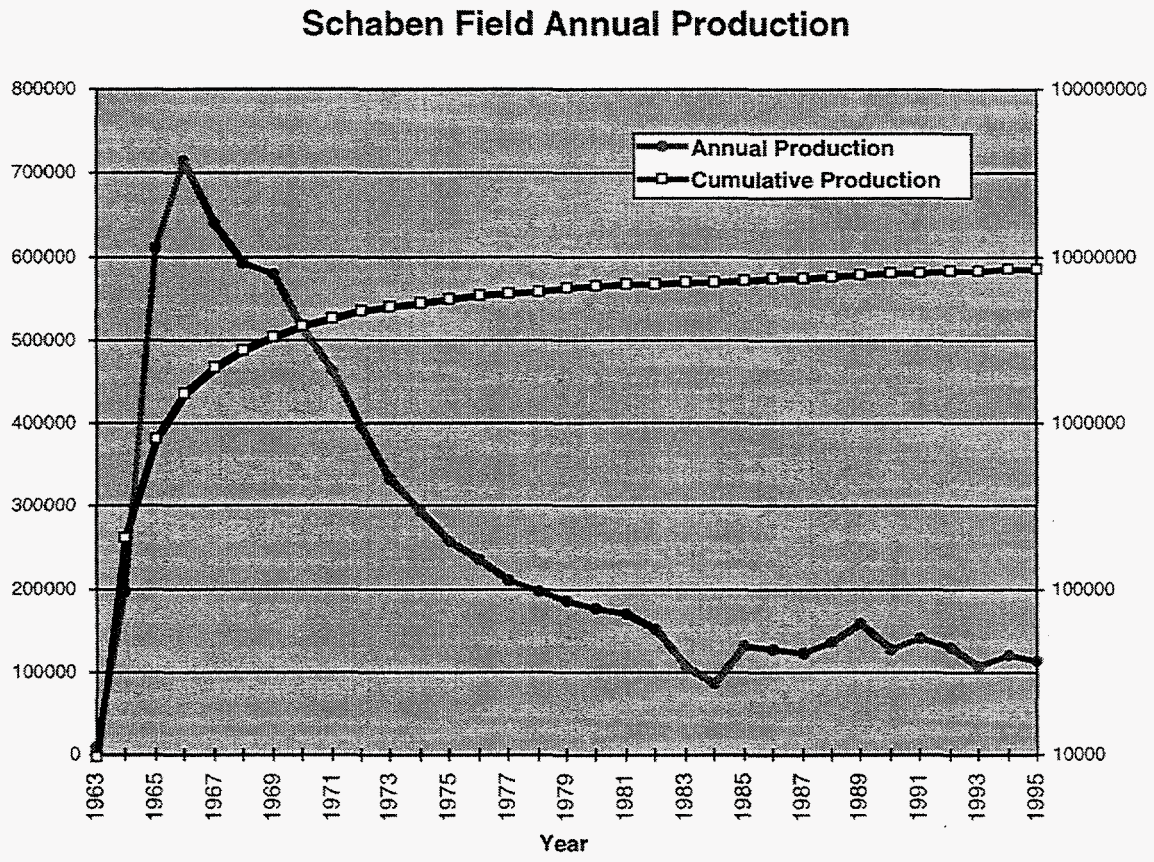

FIGURE 1.3. Annual and cumulative field production for the Schaben Field Ness County, Kansas.

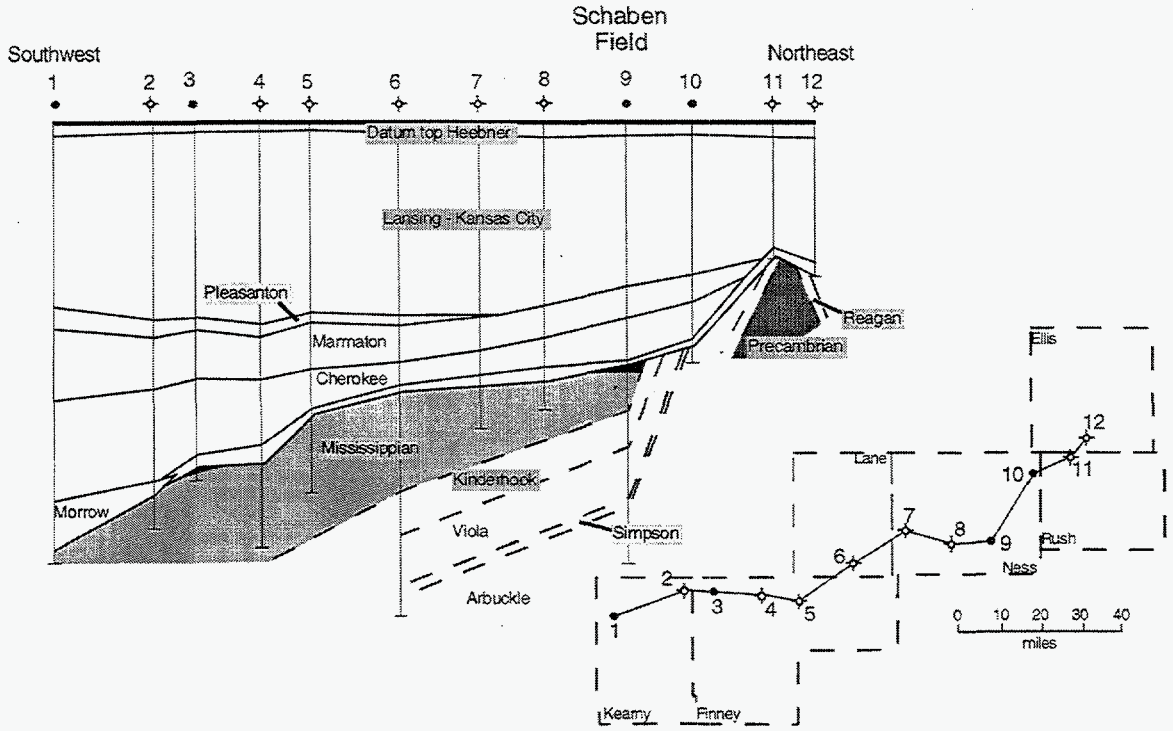

Figure 1.4. Regional southwest-northeast cross-section showing relation of Mississippian and older rocks to the pre-Pennsylvanian unconformity. Location of the Schaben Field demonstration site is indicated by the shaded area at the top of the Mississippian at well 9. Modified from Goebel and Merriam (1957).

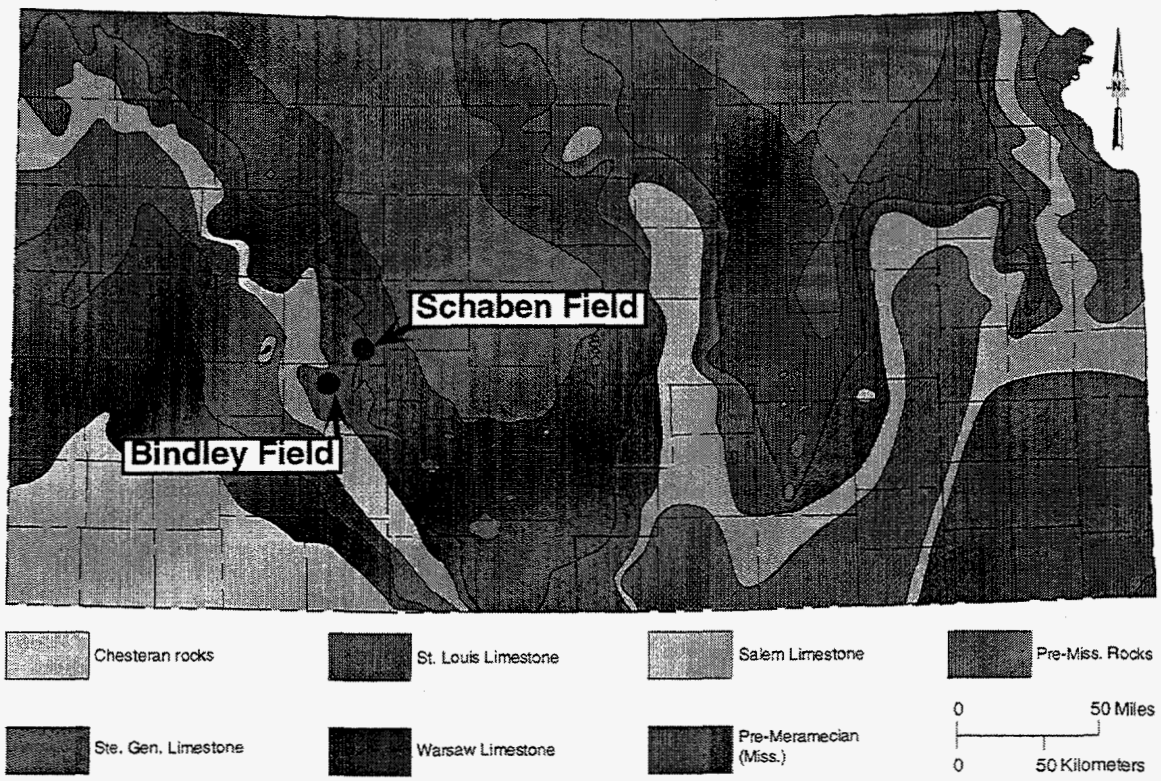

FIGURE 1.5. Mississippian subcrop map beneath the Pennsylvanian unconformity showing location of Schaben Field. Mississippian units beneath the unconformity become progressively older and are absent on the Central Kansas uplift.

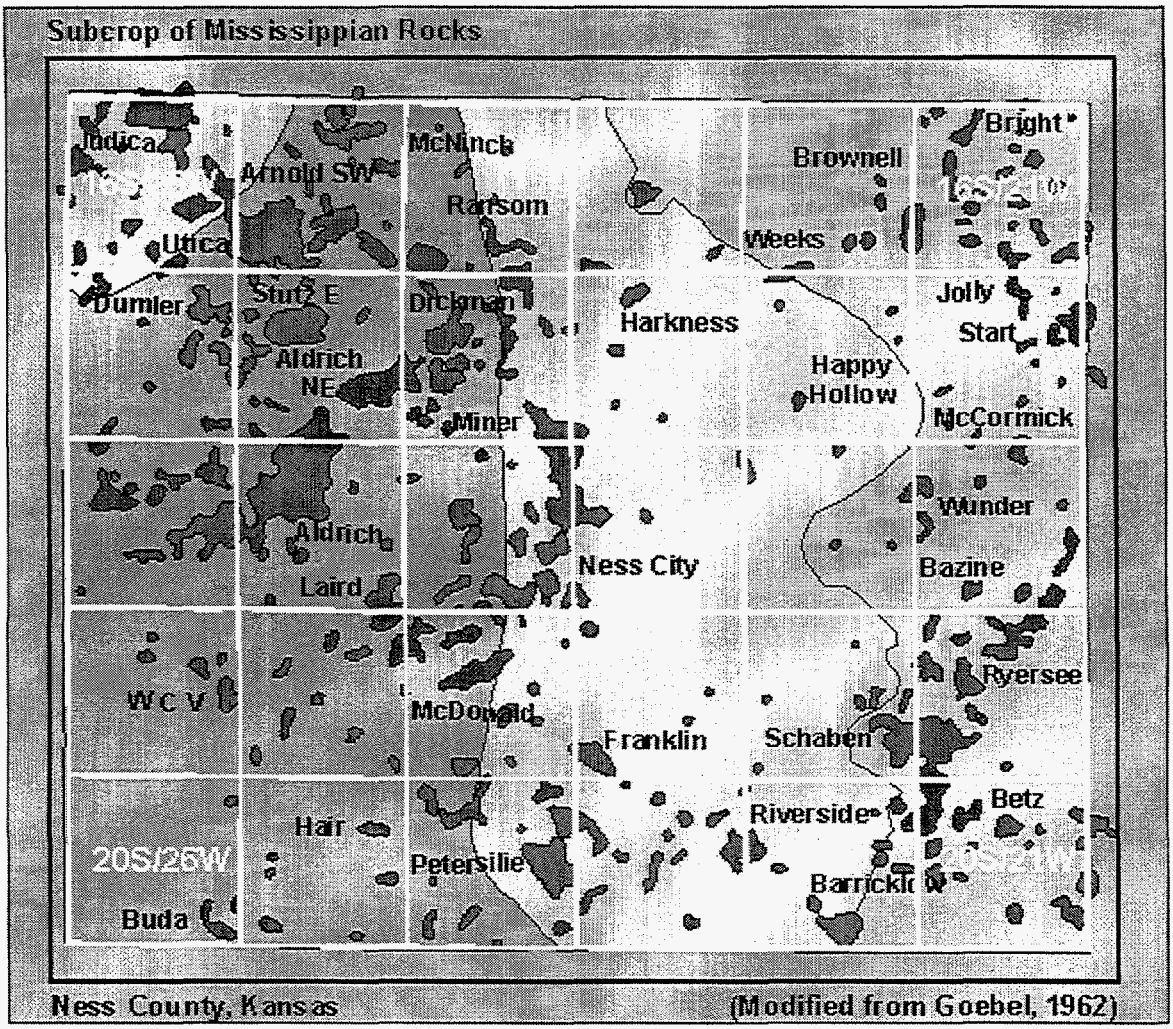

FIGURE 1.6. Mississippian subcrop map and structure on top of the Mississippian for Ness County Kansas. Field outlines for Mississippian production are shown. Schaben Field is located in the southeast corner of the county. Map available on-line through the Internet (http://www.kgs.ukans.edu/DPA/County/ness.html).

2.0 DISCUSSION

The general goal of the project is the application of existing cost-effective recovery technologies to extend the economic life of selected fields producing from shallow shelf carbonate reservoirs, and the innovative dissemination of the data, methodologies, and results for the purpose of fostering wider application of demonstrated technologies to other fields. The specific goal is to identify areas of unrecovered mobile oil in Osagian and Meramecian (Mississippian) dolostone reservoirs in western Kansas through integrated, multi-disciplinary reservoir characterization, and the demonstration of incremental primary recovery at the Schaben Field Demonstration Site.

At the Schaben site, integrated, descriptive reservoir characterization provides the basis for development of a reservoir model. Descriptive reservoir characterization entails integration and creative application of existing data, drilling and coring three new wells through the reservoir interval. Descriptive core analysis, petrophysical and petrographic analysis, calibration of logs and core data, and integration of existing well data into a computerized three dimensional visualization/simulation used to develop a descriptive reservoir model for the Osagian and Meramecian rocks at the Schaben site. This model will be compared to the existing model at the Bindley site to provide a broad foundation of modern geologic and engineering analysis for demonstration of incremental primary recovery through deepening and recompletion of existing wells and targeted infill drilling in this major producing trend.

Acquisition and consolidation of geologic, digital log, and production data are complete and all data have been entered into a database management and analysis system. Data for 267 wells distributed of 36 sections in and surrounding the Schaben project area were collected, edited and loaded into a computer database. Digital well logs for 209 of the 267 wells were obtained and loaded into the database. All digital data is available through a common computer database for use in constructing geologic maps and cross-sections and reservoir analysis (Figure 2.1).

Log analyses, core analyses and descriptions are underway to better understand the pore geometry of the carbonate reservoir in the Schaben Field. All of the complexities existing in an evaluation of an extremely heterogeneous reservoir, are present in the producing reservoir in the Schaben Field. Determination of pore size, throat size, irreducible water saturation, permeability, effective porosity, and movable oil should be possible with the techniques being used in the Schaben Field project.

2.1 FIELD ACTIVITIES

Three wells were drilled, cored, logged and tested to gather modern data for reservoir characterization. The well history for each of the wells is summarized below.

Ritchie 4 Moore "B-P" Twin
NW NE Sec. 30-T19S-R21W
Ness County, Kansas

Spudded 4/25/95. Reached TD of 4450' (log) 5/5/95. Cored Pennsylvanian conglomerate-Mississippian limestone from 4370-82' and 4390-4443. Ran Halliburton Dual Introduction Laterolog Log before running 5 1/2" casing to 4452'. Ran BPB Neutron 2, sonic, and spectral logs through casing. Final perfs 4412-17' (top Mississippian 4385'). Last one hour swab test before running tubing recovered 14.2 barrels of fluid (23% oil).). Current production is 250 barrels of fluid (6% oil) or 15 barrels of oil per day.

The core from the 4 Moore was analyzed from 4390.4-4399.4', 4410.3-4411.9, 4418.5-4442.8', and of 4443.2' for air and Klickenberg permeability, helium porosity, grain density, water saturation and oil saturation. Eight whole core samples were analyzed. The core was slabbed, photographed, and described. Thin sections were made of selected reservoir lithologies. Selected core plugs were sent out for magnetic resonance and oil-brine capillary measurements. The core was measured on a 1/4 foot spacing for permeability attributes using a mini-permeameter.

Ritchie 1 Foos "A-P" Twin
NE SW SW Sec. 31-T19S-R21W
Ness County, Kansas

Spudded 8/4/95. Reached TD of 4445' (log) 8/12/95. Cored Mississippian limestone from 4387-4441.5'. Ran BPB Induction Shallow Focused, Neutron-Photo Density, sonic, micro-resistivity, and spectral logs. Ran drillstem test from 4412-24'. Recovered 160' very slightly oil specked water. Ran 5 1/2" casing to 4444'. Final perfs 4394-95.5' (top Mississippian 4388'). Last one hour swab test before running tubing recovered 25.46 barrels of fluid (8% oil). Current production is 105 barrels of fluid (24% oil) or 25 barrels of oil per day.

The core from the 1 Foos was analyzed from 4393.3-4431.6' for air and Klickenberg permeability, helium porosity, grain density, water saturation and oil saturation. Nine whole core samples were also analyzed. The core was slabbed, photographed, and described in detail. Thin sections were made of selected reservoir lithologies. Selected core plugs were sent out for magnetic resonance and oil-brine capillary measurements. The core was measured on a 1/4 foot spacing for permeability attributes using a mini-permeameter.

Ritchie 2 Lyle Schaben "P"
400' FNL and 400" FEL, NE/4 Sec. 31-T19S-R21W
Ness County, Kansas

Spudded 2/14/96. Reached TD of 4500' (log) 2/23/96. Cored Mississippian limestone from 4409-4466'. Ran BPB Induction Shallow Focused, Neutron-Photo Density, sonic, micro-resistivity, and spectral logs. Ran drill stem test from 4318-4401'. Recovered 30' mud with an oil scum. Ran 5 1/2" casing to 4494'. Final perfs 4400-04' (top Mississippian 4389'). Last one hour swab test before running tubing recovered 12.52 barrels of fluid (22% oil). Current production is 150 barrels of fluid (35% oil) or 53 barrels of oil per day.

The core from the 2 Lyle Schaben was analyzed from 4409-4466' for air and Klickenberg permeability, helium porosity, grain density, water saturation and oil saturation. Selected whole

core samples were also analyzed. The core was slabbed, photographed, and described in detail. Thin sections were made of selected reservoir lithologies. Selected core plugs were sent out for magnetic resonance and oil-brine capillary measurements. The core was measured on a 1/4 foot spacing for permeability attributes using a mini-permeameter.

2.2 DATA ANALYSIS AND RESULTS

Acquisition and consolidation of geologic, digital log, and production data are complete and all data are entered into a database management and analysis system (Figure 2.1). Database contains data from 267 wells distributed over 36 sections in and surrounding the Schaben project area. Digital well logs for 209 of the 267 wells were obtained and loaded into the database. All digital data is available through a common computer database for use in constructing geologic maps and cross-sections, and for reservoir analysis (Figure 2.2). Data is accessible on-line through the Internet (http://www.kgs.ukans.edu/DPA/SchabenschabenMain.html).

2.2.1 Field Mapping

The Schaben digital database was used to construct a geologic model for the demonstration site and the surrounding region. On the basis of present geologic analysis, the Mississippian is an erosional karst surface. The combination of a karsted erosional surface, the influences of original depositional facies and subsequent diagenesis have had a significant control on development and preservation of reservoir quality. Mississippian (Osagian and Meramecian) reservoirs such as those present at Schaben are extremely heterogeneous. The reservoir is expected to consist of numerous vertically and laterally segregated compartments. Subsequent engineering analysis and simulation support the geologic interpretation.

Structure and isopach maps for the Schaben Field demonstration area were generated for all important stratigraphic intervals (e.g., Figure 2.2). All maps are accessible through the Internet (http://www.kgs.ukans.edu/DPA/Schaben/schabenMain.html). Using the digital well-logs and other well data, a complete network of consistently interpreted north-south and east-west cross-sections was constructed (e.g., Figures 2.3-2.6). All cross-sections display geologic tops, original oil-water contacts and other well data (e.g., logs, perforations, DST's, casing). Stratigraphic correlation was based on traditional log correlation and the results of the "pseudoseismic" analysis (see section 2.2.3). All cross-sections are accessible on-line through the Internet (http://www.kgs.ukans.edu/DPA/Schaben/CrossSect/crossSectH.html).

Production data were generated for each well in the Schaben Field demonstration area using oil sales records that are reported at the lease level. Water production was available for only a limited number of leases and wells. Annual productivity tests reported to the Kansas Corporation Commission were used to allocate oil and water production to individual wells. Oil production at the well level and water production at the lease and individual wells were estimated and subject to some error. The errors in this estimation procedure were evaluated where oil and water production were recorded for individual wells. On an annual basis the uncertainty in estimated fluid production appears small. All production data and plots are accessible on-line through the Internet using a clickable field map or custom search routines (e.g., figures 2.7- 2.9).

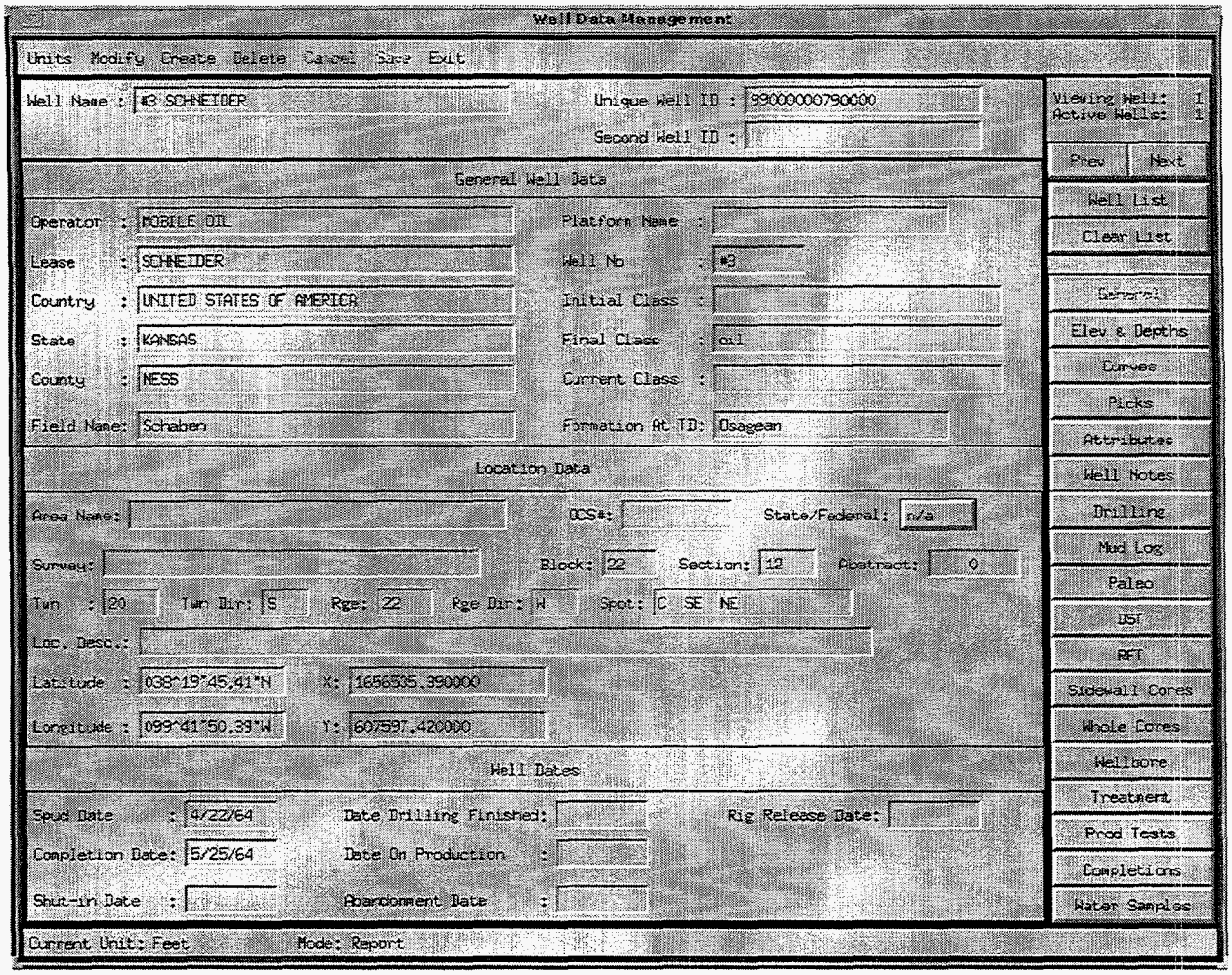

FIGURE 2.1. Sample screen from Schaben Field computer database of well data and logs. Additional data is accessed through buttons on left side of screen. Data is available through the Internet (http://www.kgs.ukans.edu/DPA/Schaben/schabenMain.html).

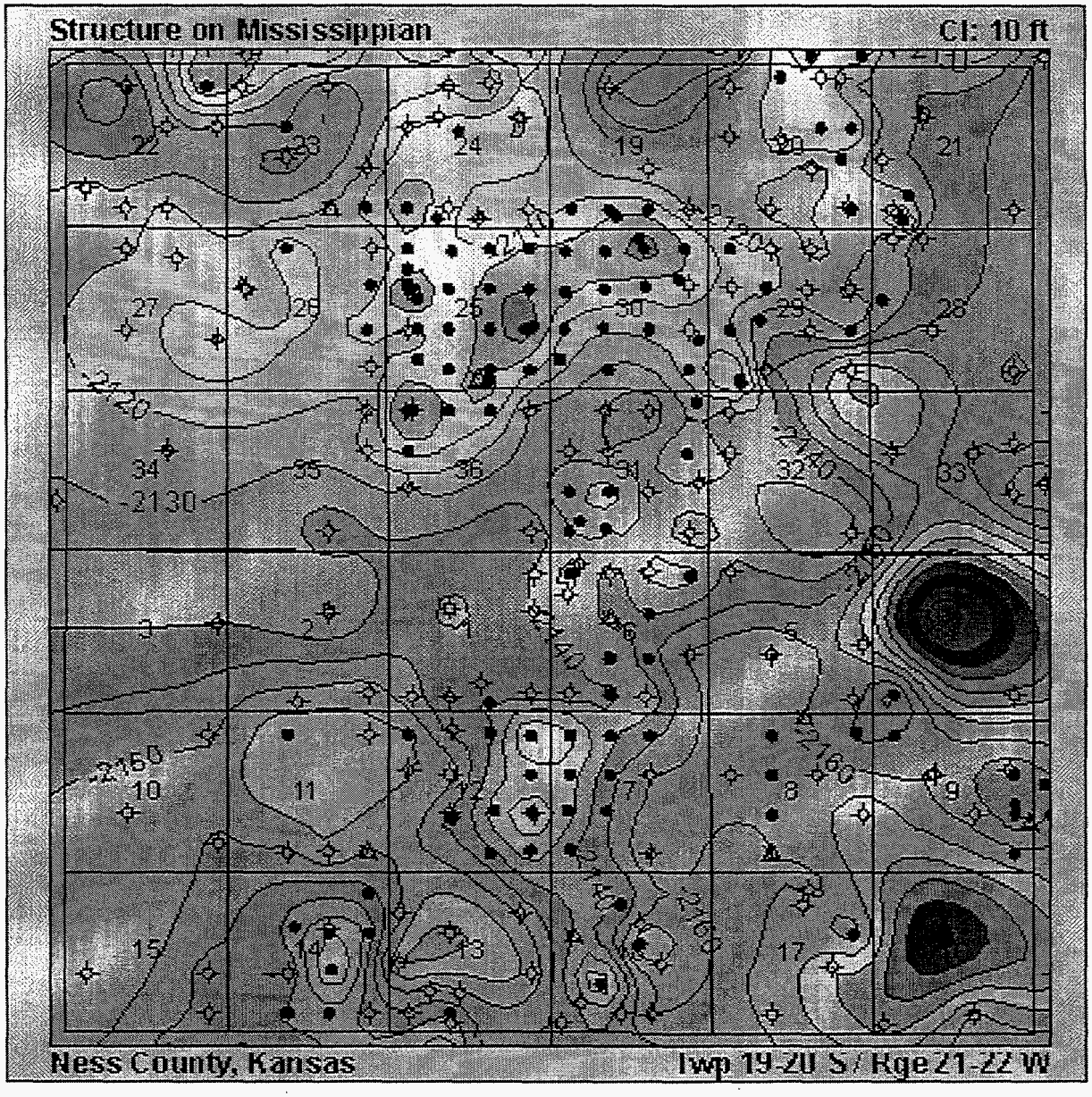

FIGURE 2.2. Structure map on the Mississippian erosional surface over Schaben Field demonstration area. Map shows irregular karst surface on top of Mississippian (Osagian). Selections of structure and isopach maps are accessible through the Internet. Figure was copied directly from the Internet (http://www.kgs.ukans.edu/DPA/Schaben/Geology/schabenGeol4.html).

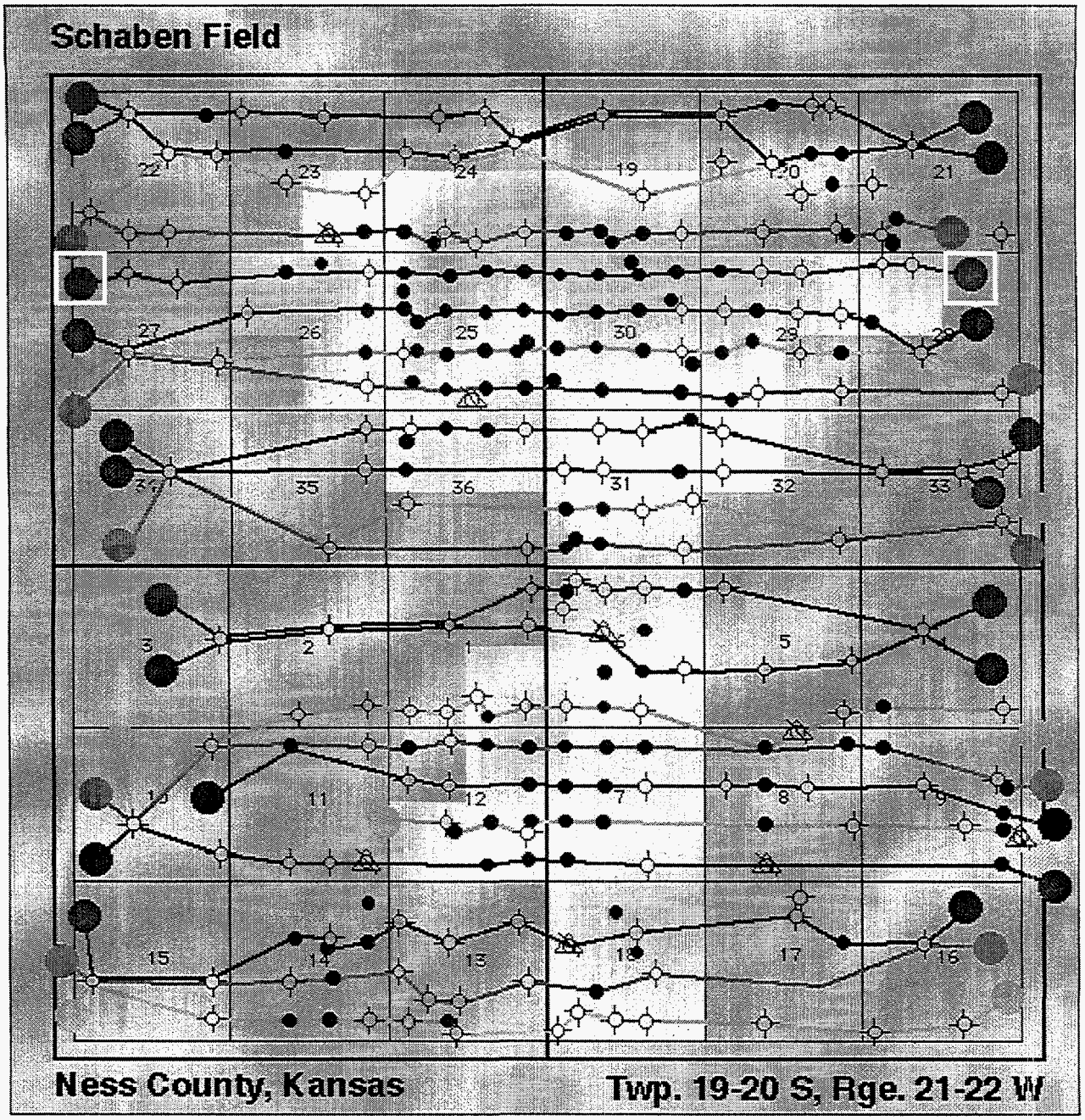

FIGURE 2.3. Map showing east-west cross-sections over Schaben Field demonstration area (http://www.kgs.ukans.edu/DPA/Schaben/CrossSect/crossSectH.html). Map is a graphical user interface and all cross-sections can be accessed on-line by clicking on the appropriate circle. Cross-section shown in Figure 2.4 is highlighted with white squares.

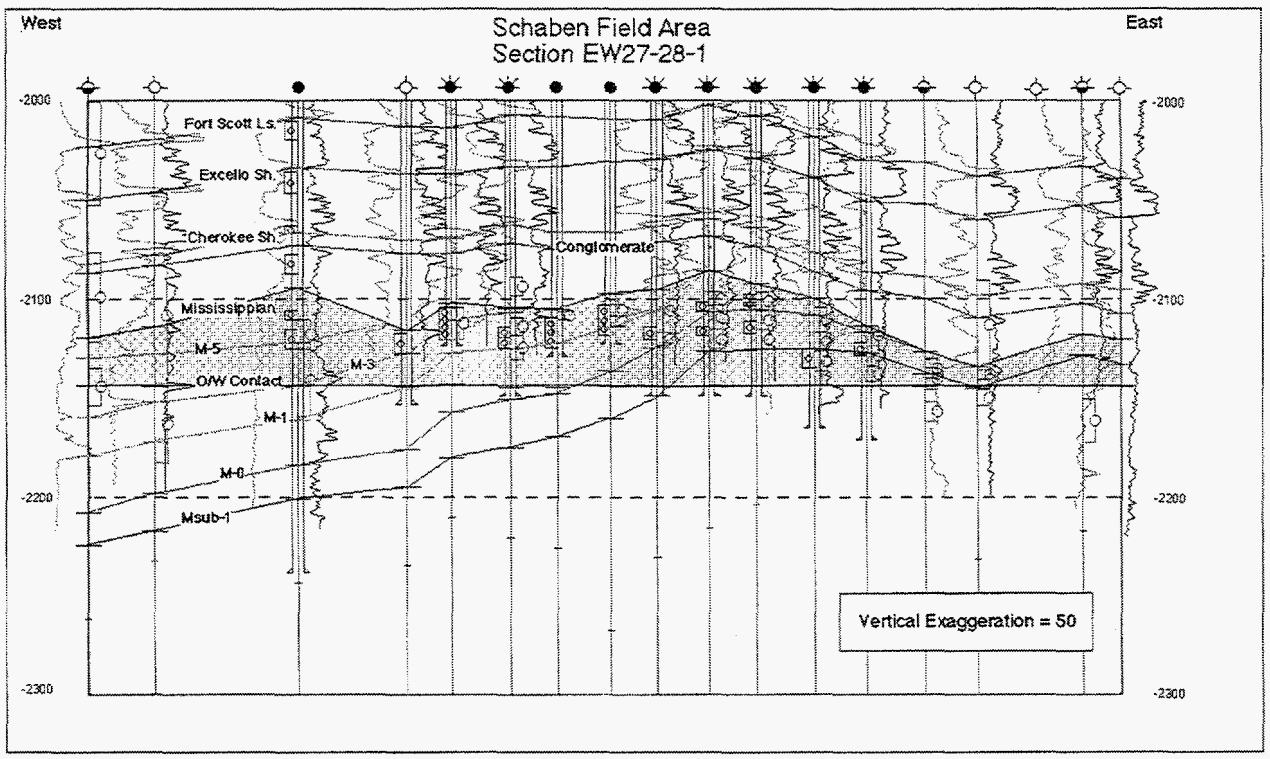

FIGURE 2.4. A selected east-west cross-section across the Schaben Field demonstration area (Cross-section EW27-26-1). Section is accessible on-line through the graphical user interface shown in Figure 2.3. Cross-section shows geologic tops, original oil-water contact and other well data (e.g., perforations, DST's, casing). Cross-section is copied directly from the Internet (http://www.kgs.ukans.edu/DPA/Schaben/CrossSect/EW27281.html).

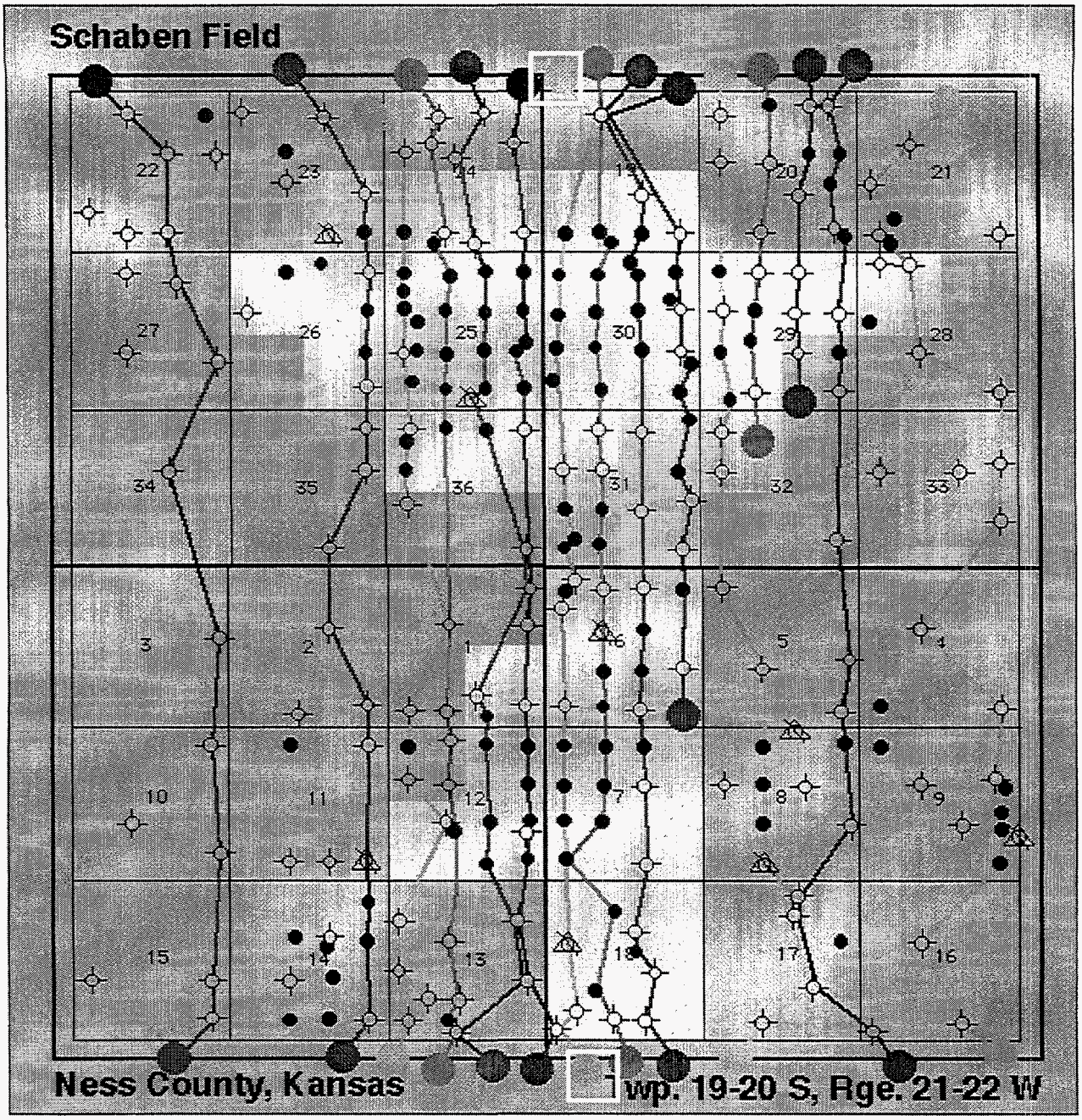

FIGURE 2.5. Map showing north-south cross-sections over Schaben Field demonstration area (http://www.kgs.ukans.edu/DPA/Schaben/CrossSect/crossSectV.html). Map is a graphical user interface and all cross-sections can be accessed on-line by clicking on the appropriate circle. Cross-section shown in Figure 2.6 is highlighted with white squares.

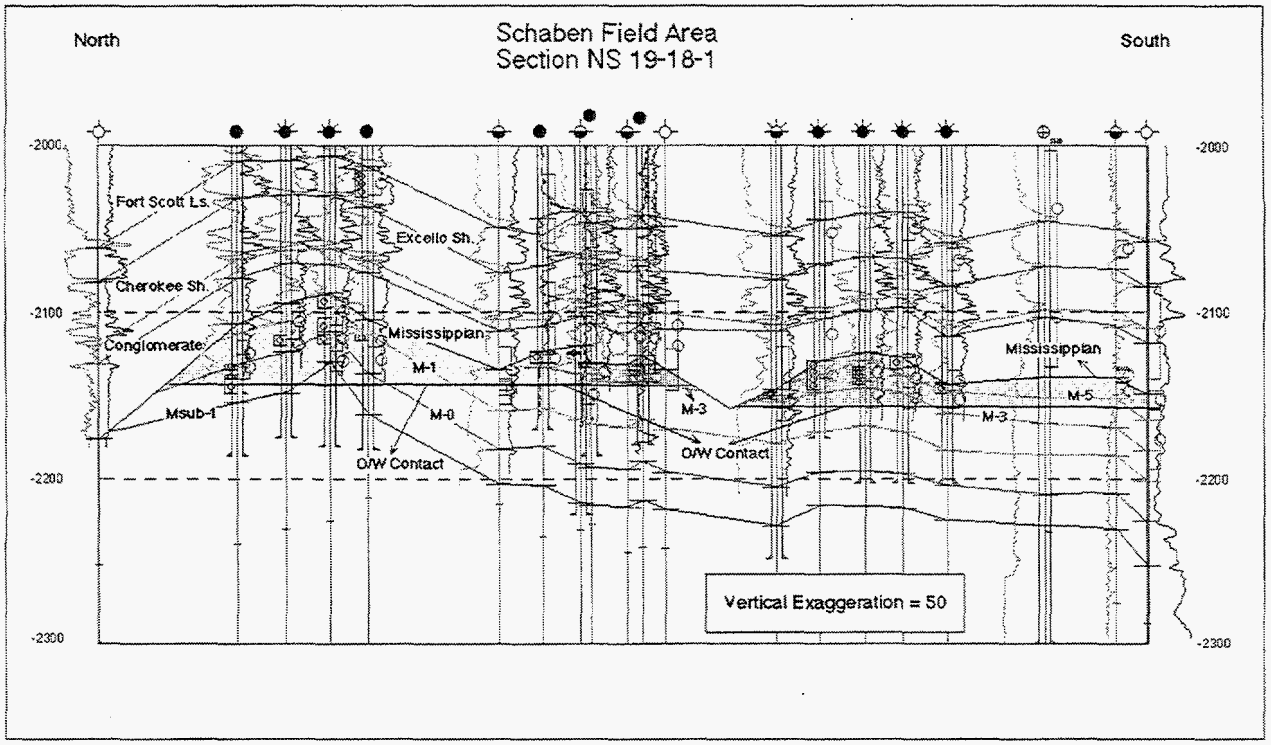

FIGURE 2.6. A selected north-south cross-section across the Schaben Field demonstration area (Cross-section 19-18-1). Section is accessible on-line through the graphical user interface shown in Figure 2.5. Cross-section shows geologic tops, original oil-water contact and other well data (e.g., perforations, DST's, casing). Cross-section is copied directly from the Internet (http://www.kgs.ukans.edu/DPA/Schaben/CrossSect/NS19-18-1.html)

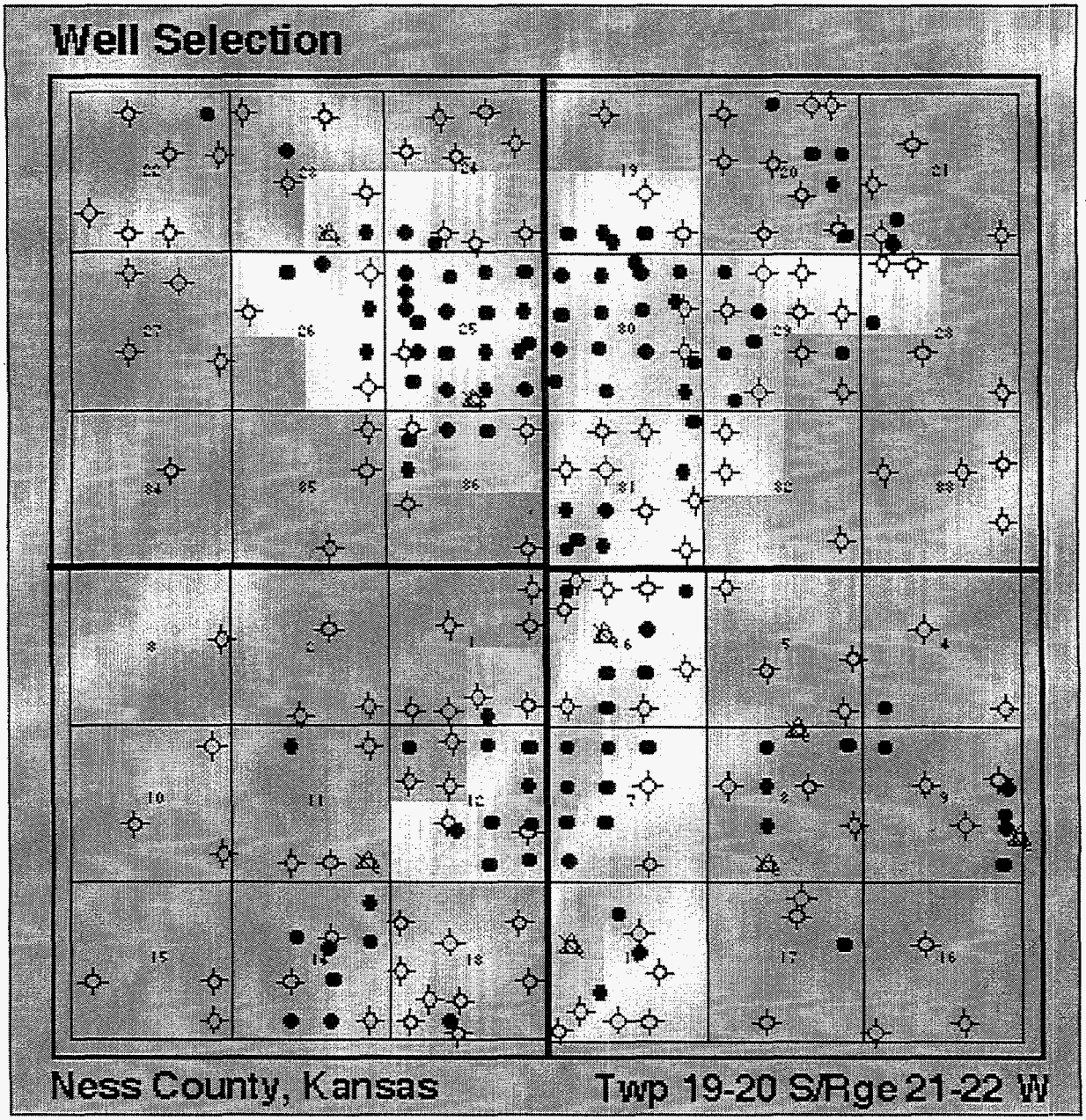

FIGURE 2.7. Map of Schaben Field demonstration area showing location of wells used in the study.. Map is a graphical user interface and all well data can be accessed on-line by clicking on the appropriate well symbol (http://www.kgs.ukans.edu/DPA/Schaben/Wells/schabenWell1.html). Searching on geographic location or API number can also access well data.

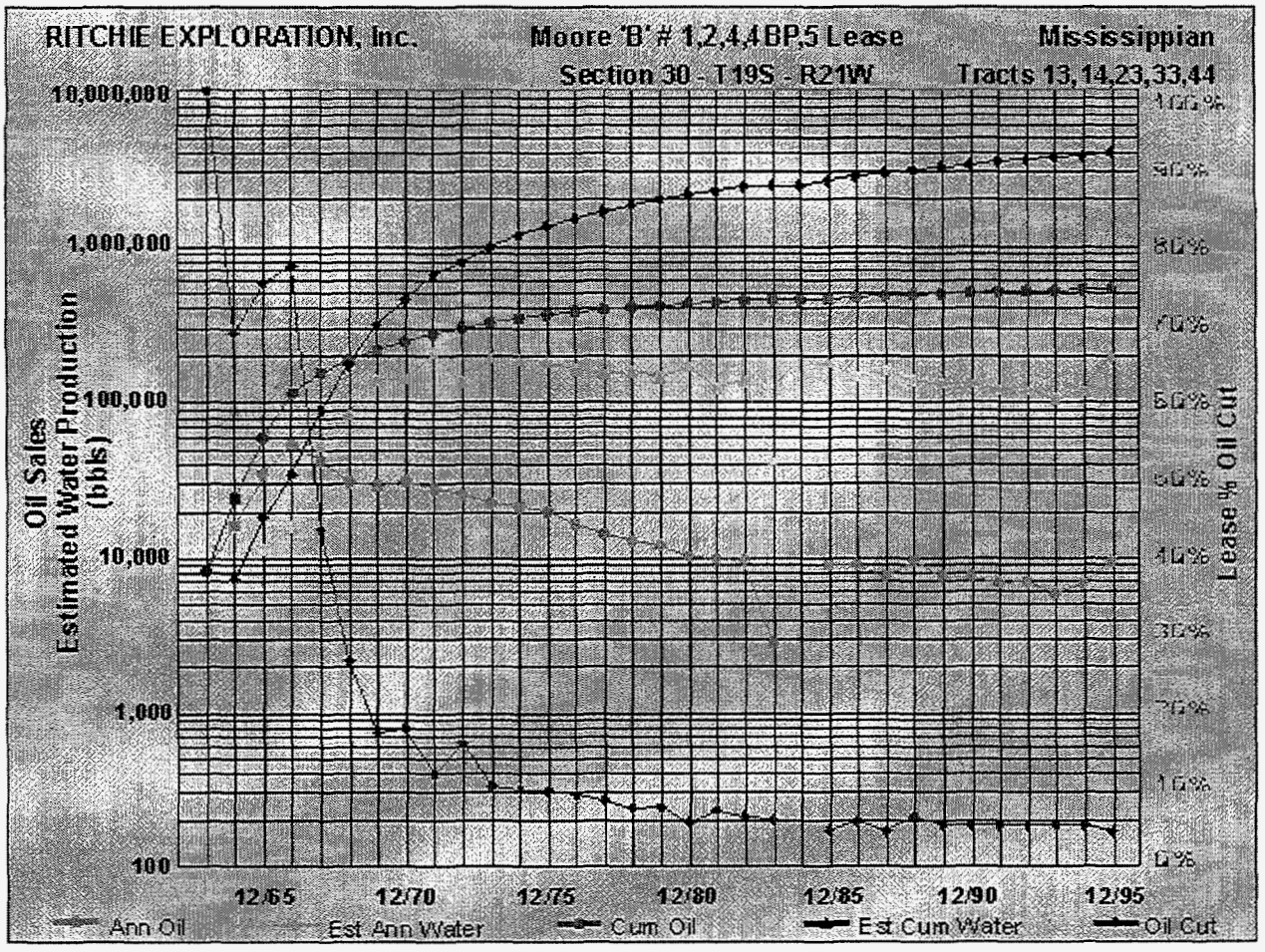

FIGURE 2.8. Fluid production plot for Moore "B" Lease. Oil production is from sales records. Water production is estimated from annual productivity tests. Plots and data are for all wells in the Schaben demonstration area are accessible through the Internet.
http://www.kgs.ukans.edu/DPA/Schaben/Wells/Pro/MooreBpro.html

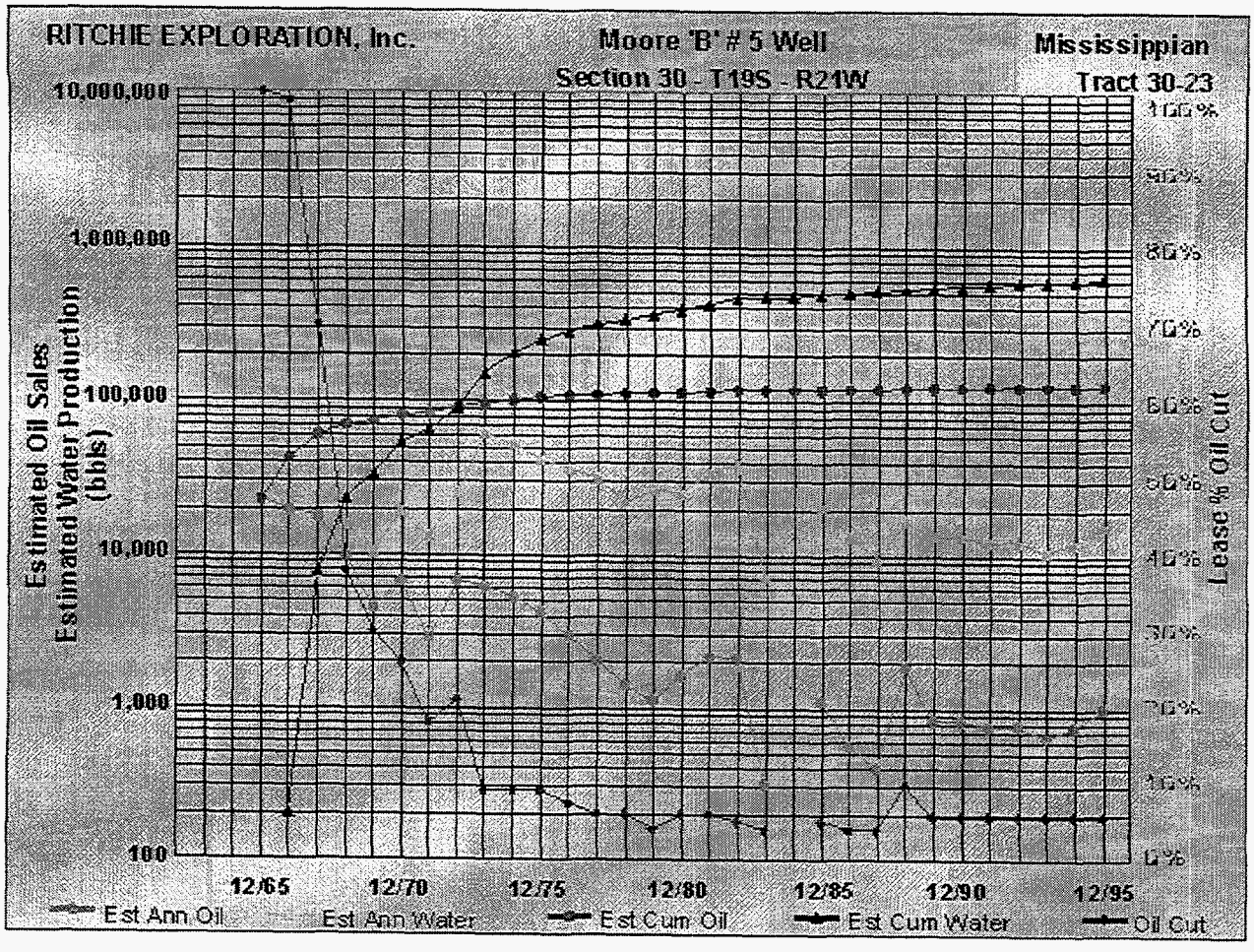

FIGURE 2.9. Fluid production for selected well on the Moore B Lease. Oil and water production estimated from lease data using annual productivity tests. Plots and data are for all wells in the Schaben demonstration area are accessible through the Internet (http://www.kgs.ukans.edu/DPA/Schaben/Wells/Pro/SCHB14pro.html).

2.2.2 Petrophysical Analysis

2.2.2.1 NMR Analysis

The magnetic resonance technique has rapidly evolved in only the last five years, but offers answers to questions that have puzzled the petroleum industry for years (Akkurt, 1990; Keller, 1990; Kleinberg and Horsfield, 1990; Kenyon, 1992: SPWLA, 1995). The magnetic resonance equipment measures the relaxation rate of hydrogen protons in porous reservoirs when excited by an applied magnetic field. The T2 relaxation time can be related to surface to volume ratio and ultimately to porosity and bulk volume irreducible.

Nuclear Magnetic Resonance (NMR) measurements were determined on 18 core plugs from the three Schaben Field wells drilled under the DOE grant. The magnetic resonance data were used to determine the fluid filled porosity, free fluid porosity, bound water porosity, pore size, grainsize, and irreducible water saturation. NMR data are interpreted as indicating pore size while the capillary pressure indicates pore throat size. After the plug is cleaned and evacuated it is saturated with a brine similar to the reservoir water. The NMR data are then obtained from the saturated core plug. The brine saturated core sample is placed into a "Core Analyzer". The relaxation times (T2) were determined at 5000 points at an inter-echo spacing of 1.2 milliseconds. The core plugs are then placed in a high speed centrifuge to determine the capillary pressure data. At selected pressures, for instance 70 and 100 psi (air-brine), the core plugs are again analyzed by the NMR lab equipment. Centrifuging is then continued until some maximum pressure (1000-psi air-brine) is reached. The final NMR data are then recorded.

Technology advances in the field of NMR logging change daily with new publications and modified techniques (e.g., Chandler et al., 1994, Murphy, 1995). Our work in the Schaben Field used only laboratory measurements. Although recent advances have occurred in wireline open hole measurements and laboratory measurements, our discussion will pertain only to the interpretation of laboratory data.

The most significant change in interpretation of reservoirs is in the determination of the T2 cutoff. The T2 cutoff is the point of division between free fluid or effective porosity, and bound water or ineffective porosity. As a result early field-testing, an initial cutoffs of 33 milliseconds for sandstone and 94-100 milliseconds for carbonates were determined. Recent experience with NMR measurements indicates that the cutoff for sandstone remains at approximately 33 milliseconds, but the cutoff for carbonates varies widely from 7 to 100 milliseconds.

The laboratory technique of making NMR measurements with the plug saturated with water similar to reservoir water and then centrifuging to revolutions equivalent to pre-determined pressures are a great aid in locating the T2 cutoff and evaluating the reservoir. The Numar technique for determining the T2 cutoff is where the saturated cumulative porosity crosses the desaturated incremental porosity. Schlumberger believes the point of divergence between the saturated cumulative and the desaturated cumulative curves best indicate the cutoff. These "rules of thumb" are not always precise and require the interpreter to make subjective judgments using all available data.

Service company literature indicates that the T2 value from NMR data can be used to determine permeability. Experience in the Schaben Field, which has a very heterogeneous carbonate lithology, indicates that the numerous permeability equations have two short-comings in that they rely on values for T2 and/or porosity. There is normally no direct relationship between porosity and permeability and the value for T2 is not always precise.

The lithology and height of oil/gas column determine the pressure value where NMR data is measured. In the Schaben field with its heterogeneous lithology and pay column of only 35-50 feet, the maximum effective pressure is only about 10-40 psi (air/brine). Therefore, the pressure recommended for NMR reservoir evaluation is 70-psi (air/brine), which is equivalent to 350 psi (air/mercury).

Comparison of the reservoir characteristics in laboratory samples using NMR data with air/brine capillary pressure data and thin section petrography is excellent. The use of mercury/air capillary pressure data would increase the resolution of the pore geometry, but would contaminate the core for future use and make it impossible to gain NMR data.

The use of NMR analysis within the Schaben Field can be illustrated by the analyses of three core plugs: the Moore 2 (4394.8'), the Moore 12 (4423.5'), and the Moore 24 (4437.8'). The M-2 is an example of a poor reservoir (Figure 2.10). The M-2 sample has a core porosity of 7.6% and a core permeability of 0.036 md. The T2 cutoff is at 5-7 milliseconds. NMR analysis indicates a total porosity of 7.34%, and a bound water porosity of 4.63%. Thus, the effective or free fluid porosity is only 2.71%. Figure 2.10 illustrates that almost all of the bound water porosity has a T2 value of less than 7 milliseconds, and places it in the zone of microporosity similar to that in shale. Even the free fluid or effective porosity never exceeds 20 milliseconds, and even the best reservoir quality in the core plug has very fine pores.

The M-12 is an example of an excellent very fine crystalline unimodal homogeneous dolomite. The M-12 sample has a porosity of 19.8%, and a permeability of 8.54 md. NMR analysis indicates a total porosity of 19.89% and a bound water porosity of 3.21%. Thus, the effective or free fluid porosity is 16.68 %. The saturated incremental porosity curve (Figure 2.11) is almost totally between a T2 value of 35 to 200 milliseconds. Using a T2 cutoff of 35 milliseconds indicates that the reservoir has a homogeneous unimodal pore geometry. The absence of pores above 200 milliseconds indicates that the reservoir has no vugular porosity, and is verified by examination of thin-sections.

The M-24 is an example of a very fine crystalline bimodal dolomite with a core porosity of 14.7% and a core permeability of 149 md. The T2 cutoff is at 50 milliseconds (Figure 2.12). The NMR analysis indicates a total porosity of 14.74%, a bound water porosity of 6.09% and a free fluid or effective porosity of 8.65%. The saturated incremental porosity curve indicates that the dolomite reservoir has a T2 value from 50 to 2000 milliseconds. Analysis would indicate that the T2 values between 50 and 200-225 milliseconds represent a dolomite with fine pores and that T2 values exceeding 200 milliseconds represent large vugular porosity, some of which is not effective. Comparisons with thin sections confirm the NMR observations.

The NMR data from these three core plugs were determined at a pressure of 1000 psi (air-brine) and are therefore too optimistic for the Schaben Field where data should have been analyzed at about 70 milliseconds. However this does not affect the interpretation to any significance.

Another good example is to compare the capillary pressure, NMR, and thin sections of Schaben 22 and 27 core plugs. Schaben 27 has little to no effective porosity (9.86%, total 17.27% from NMR while Schaben 22 has excellent effective porosity (11.38%, total 18.82% from NMR). Comparison of the thin sections indicates that the Schaben 22, although appearing very similar to the Schaben 27, has a much higher amount of effective porosity. The primary difference is that Schaben 22 is a mottled, wispy mudstone-wackestone, while Schaben 27 is a very homogeneous mudstone. The capillary pressure curves of the two core plugs verify that Schaben 22 has a greater percentage of effective porosity.

The reservoir data, determined by the NMR, capillary pressure, and thin sections, were used to determine reservoir parameters used in the reservoir evaluation and simulation.

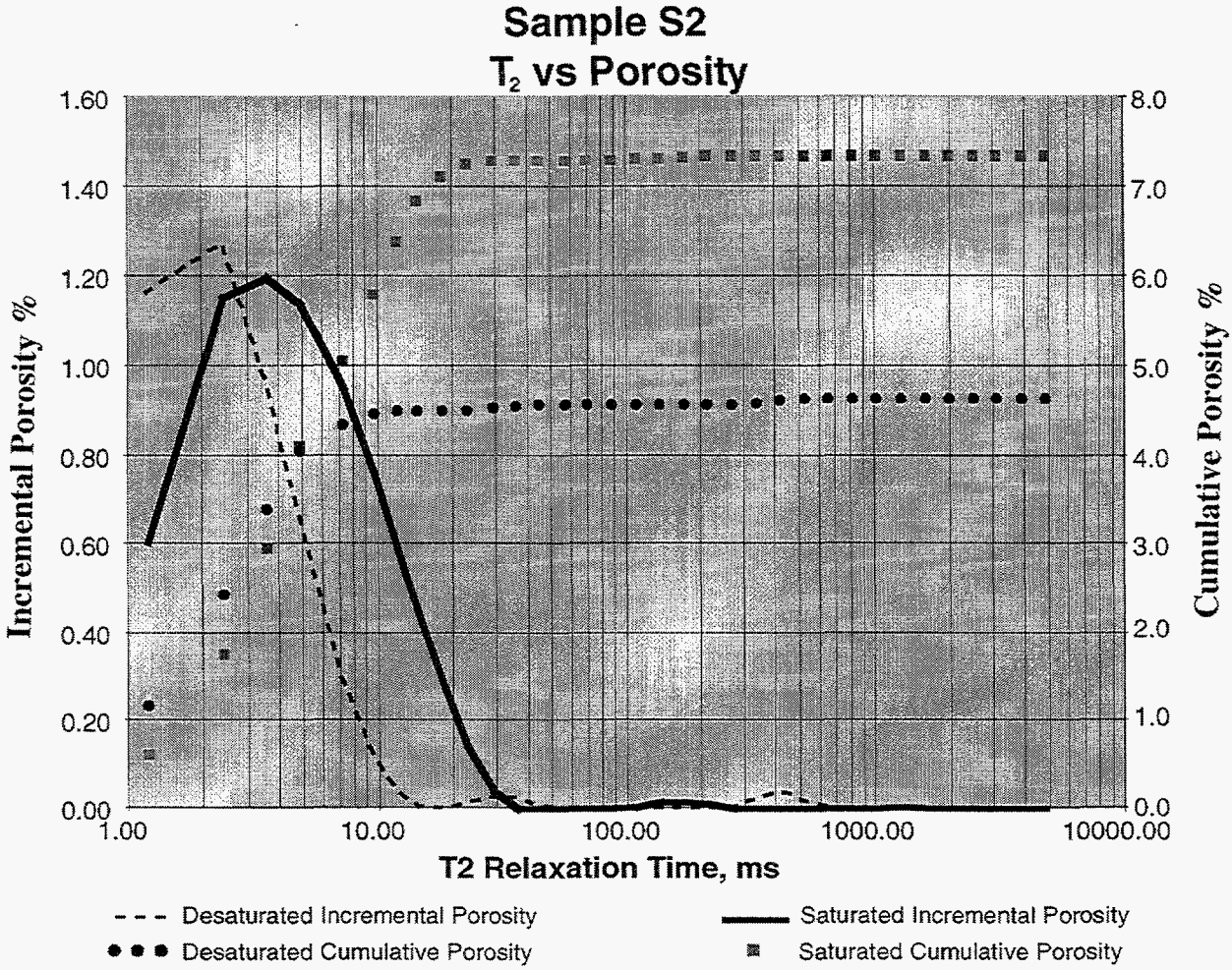

FIGURE 2.10. NMR analysis from Sample 2 (4394.8') in the Moore "B-P" Twin. The T2 cutoff is at 5-7 milliseconds. NMR analysis indicates a total porosity of 7.34%, and a bound water porosity of 4.63%. Thus, the effective or free fluid porosity is only 2.71%.

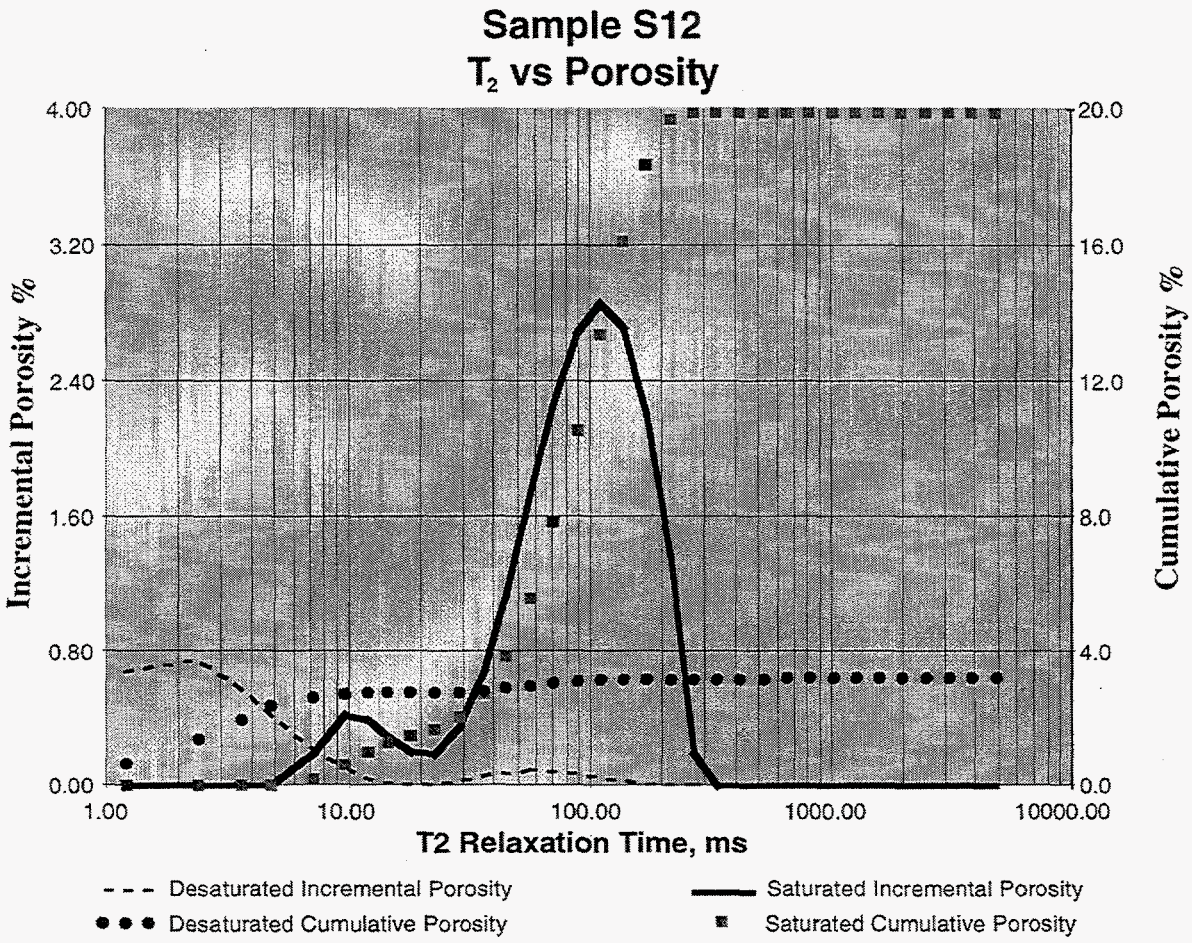

FIGURE 2.11. NMR analysis from Sample 12 (4423.5') in the Moore "B-P" Twin. The M-12 is an example of an excellent very fine crystalline unimodal homogeneous dolomite with a porosity of 19.8%, and a permeability of 8.54 md. NMR analysis indicates a total porosity of 19.89% and a bound water porosity of 3.21%. Thus, the effective or free fluid porosity is 16.68 %.

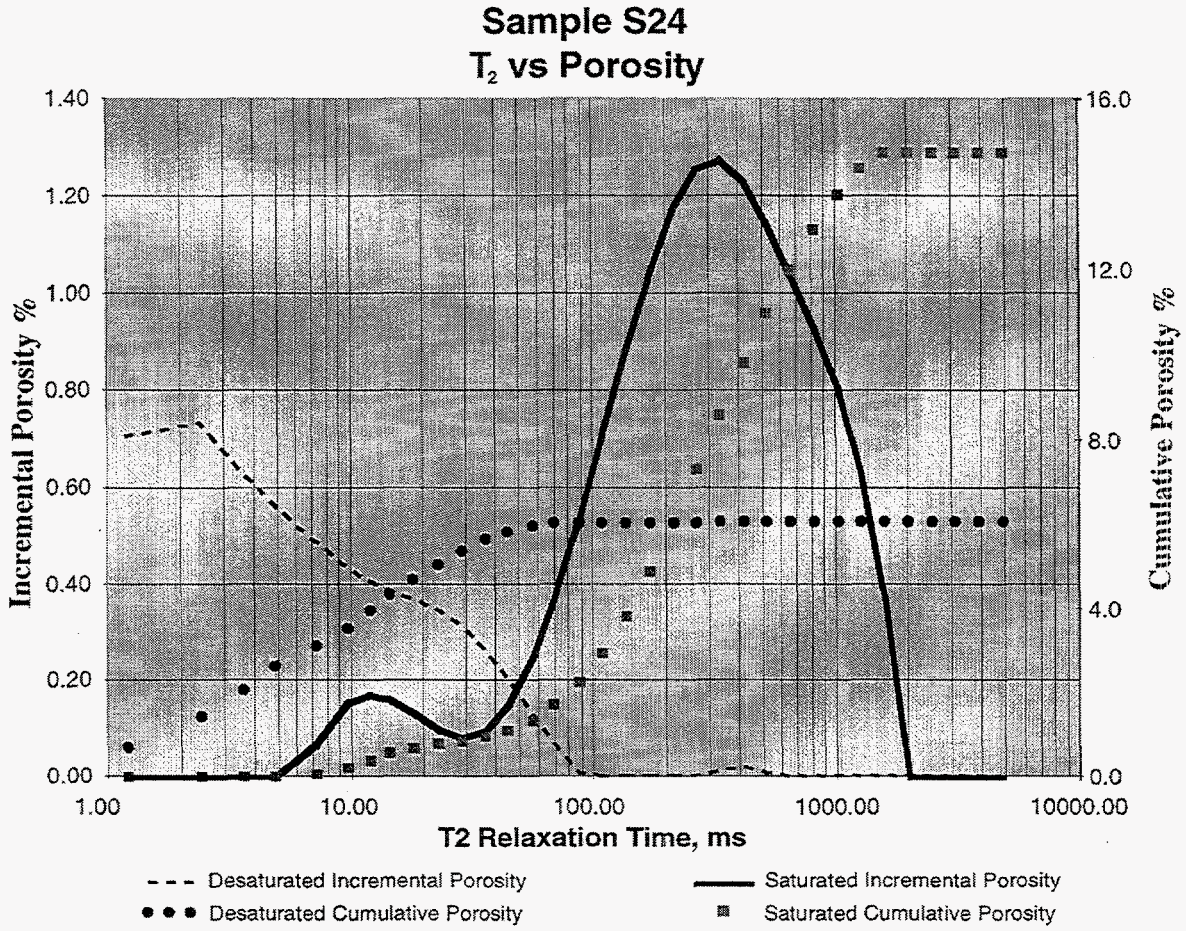

FIGURE 2.12. NMR analysis from Sample 24 (4437.8') in the Moore "B-P" Twin. The M-24 is an example of a very fine crystalline bimodal dolomite with a core porosity of 14.7% and a core permeability of 149 md. The T2 cutoff is at 50 milliseconds (Figure 2.12). The NMR analysis indicates a total porosity of 14.74%, a bound water porosity of 6.09% and a free fluid or effective porosity of 8.65%.

2.2.2.2 Capillary Pressure

Air-brine capillary pressure measurements were taken on 18 core plugs from the three Schaben Field wells drilled under the DOE grant program. These were taken using a high speed centrifuge. Capillary pressures were taken to study the pore geometry, the height of oil column, the irreducible water saturation, and the effective porosity. These measurements were taken in association with a Nuclear Magnetic Resonance (NMR) study. Air-mercury capillary pressure measurements, which are less expensive, were not done because of the mercury contamination that would not permit NMR measurements to be made.

Air-brine capillary measurements were made primarily at pressures of 7, 10, 20, 40, 70, 100, 200, 400, 700, and 1000 psi. However, if we take the normal maximum carbonate pore size cutoff of 0.5 microns, any pressure higher than 40 psi will not be of value in the reservoir evaluation. The Schaben Field has only a 35-50 foot oil column that is equivalent to about 10 psi (air-brine). Thus, in reality, no pore-size less than about 2.0 microns will be effective.

The capillary pressure data, therefore, indicates that the Schaben Field will have a water saturation of approximately 50% even though the "irreducible" water saturation of some of the reservoir can be as low as 20% at 1000 psi (air-brine). This low saturation would be in non-effective microporosity.

The air-brine capillary data indicates that the Schaben reservoir is primarily unimodal in pore size within a very fine crystalline dolomite. Pore size histograms made from the capillary data shows that most of the effective reservoir has macro porosity (2-10 microns). A few of the core plugs have a bi-modal porosity, yet NMR data indicates that many of the larger vugs are not effective unless they are connected by microfractures.

The use of capillary measurements remains as an under utilized reservoir evaluation tool. Results in the Schaben Field using capillary measurements in association with NMR data and petrography using thin sections were very useful in understanding the reservoir.

2.2.2.3 Minipermeameter

In order to analyze the degree of vertical stratification present in Schaben Field, permeability values were measured in all three cores using a portable field permeameter (minipermeameter). The values obtained using the minipermeameter were compared with permeability analyses of plugs taken from the core at the same interval. Core plug measurements were collected at an interval spacing of approximately 1.0 foot whereas the minipermeameter measurements were collected at an interval spacing of 0.25 feet (3 inches). Because a larger volume of the rock was tested, core plug permeability values were thought to be more accurate than minipermeameter results. Regression analysis allowed us to establish a correlation line between the minipermeameter and core plug permeability results and minipermeameter values were corrected to the equation of this line.

Vertical profiles of minipermeameter and core plug permeability values from the reservoir interval of the Ritchie Exploration, #1 Foos AP Twin are shown in Figure 2.13. The

minipermeameter profile demonstrates that a high degree of vertical stratification is present in the reservoir interval. Comparison of the minipermeameter profile to the core plug profile indicates that core plug permeability values were sampled at a spacing insufficient for representing the vertical stratification present in the Mississippian reservoir at Schaben Field. The same type of vertical stratification of flow units is present in the reservoir interval of the Ritchie Exploration, #4 Moore BP Twin and #2 Lyle Schaben P cores (figures 2.14, 2.15).

A plot of minipermeameter values, simplified depiction of facies, fracturing, brecciation and other features as related to these values, and locations of oil staining are shown for the Ritchie Exploration, #1 Foos AP Twin (Figure 2.16).

Further discussion of minipermeameter measurements and the relationship to facies and diagenetic features is given in section 2.2.4.

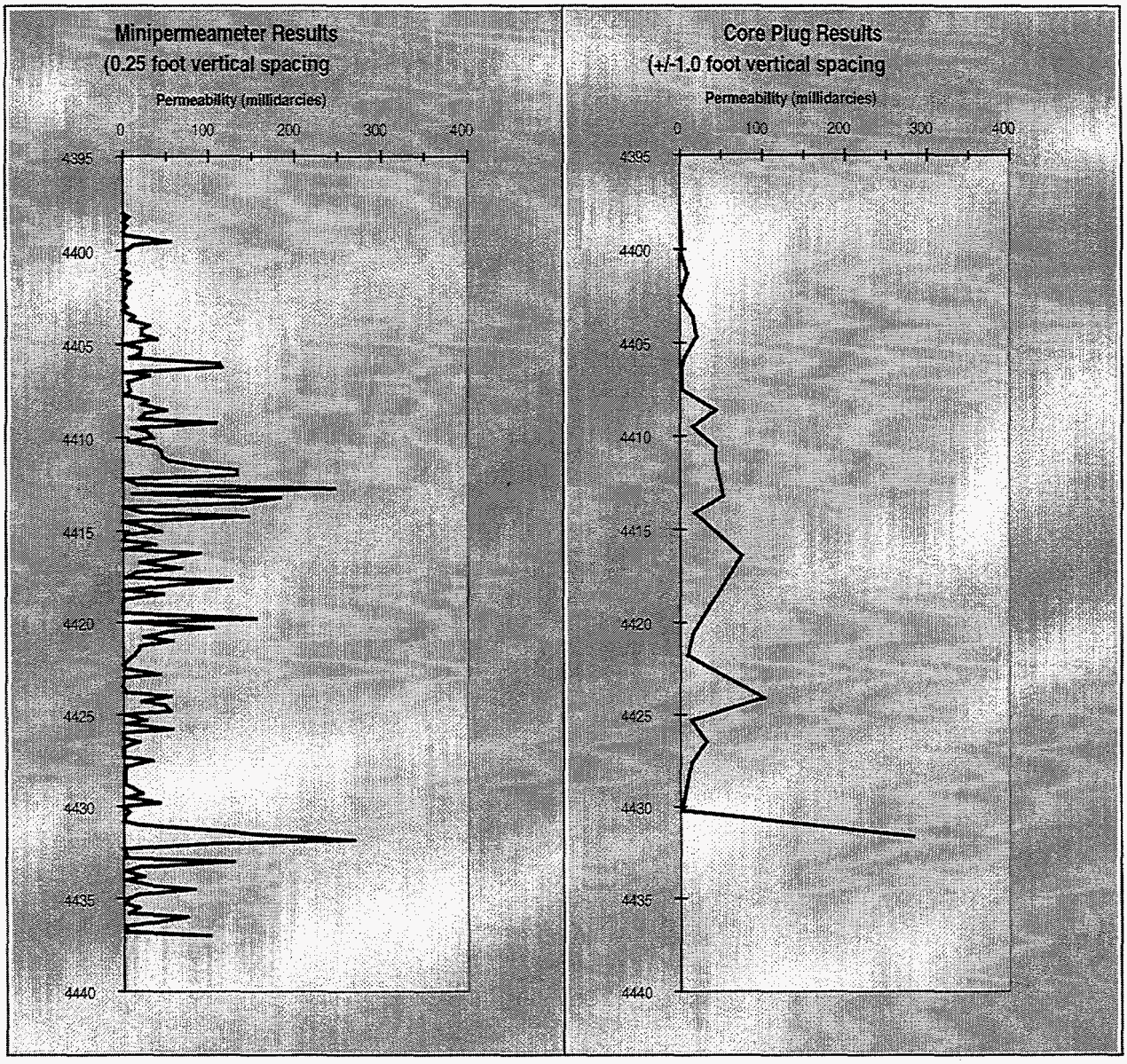

FIGURE 2.13. Vertical profiles of minipermeameter and core plug permeability values from the reservoir interval of the Ritchie Exploration, #1 Foos AP Twin. The minipermeameter profile demonstrates that a high degree of vertical stratification is present in the reservoir. Comparison of the minipermeameter profile to the core plug profile indicates that core plug permeability values were sampled at spacing insufficient for representing the vertical stratification present in the Mississippian reservoir at Schaben Field

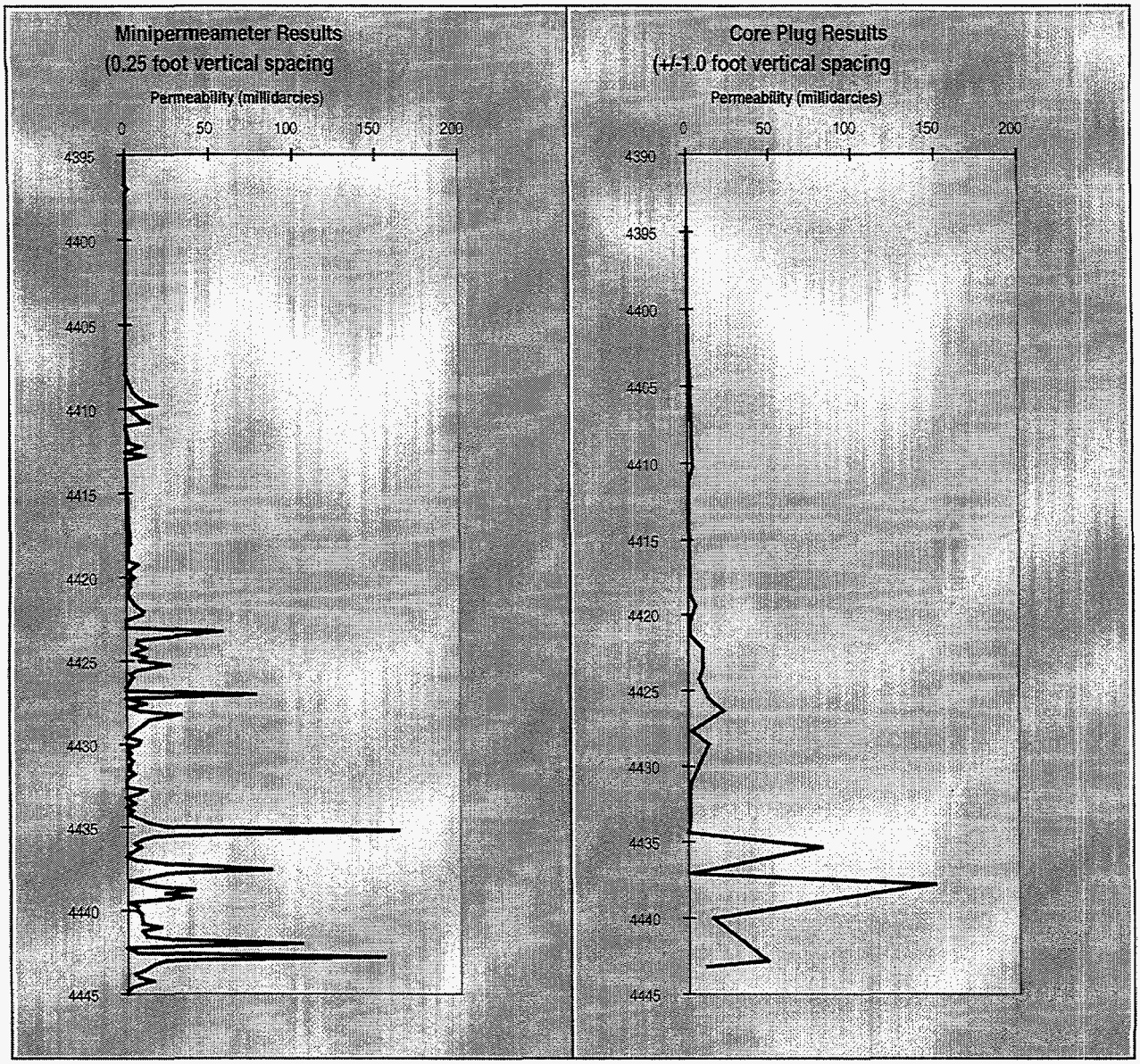

FIGURE 2.14. Vertical profile of minipermeameter values from the reservoir interval of the Ritchie Exploration, #4 Moore BP Twin. The minipermeameter profile demonstrates that a high degree of vertical stratification is present in the reservoir. Comparison of the minipermeameter profile to the core plug profile indicates that core plug permeability values were sampled at a spacing insufficient for representing the vertical stratification present in the Mississippian reservoir at Schaben Field.

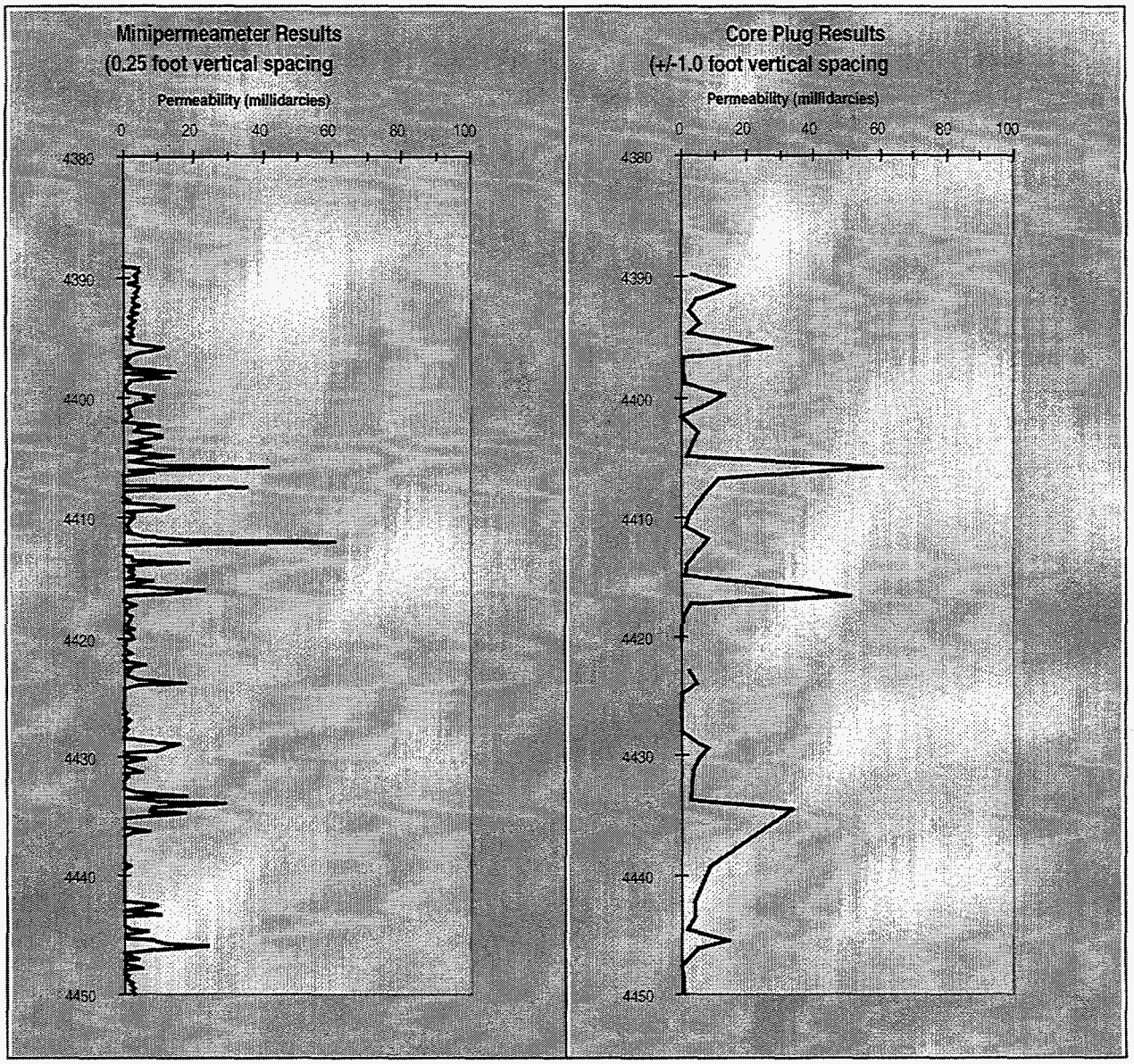

FIGURE 2.15. Vertical profile of minipermeameter values from the reservoir interval of the Ritchie Exploration, #2 Lyle Schaben. The minipermeameter profile demonstrates that a high degree of vertical stratification is present in the reservoir. Comparison of the minipermeameter profile to the core plug profile indicates that core plug permeability values were sampled at spacing insufficient for representing the vertical stratification present in the Mississippian reservoir at Schaben Field.

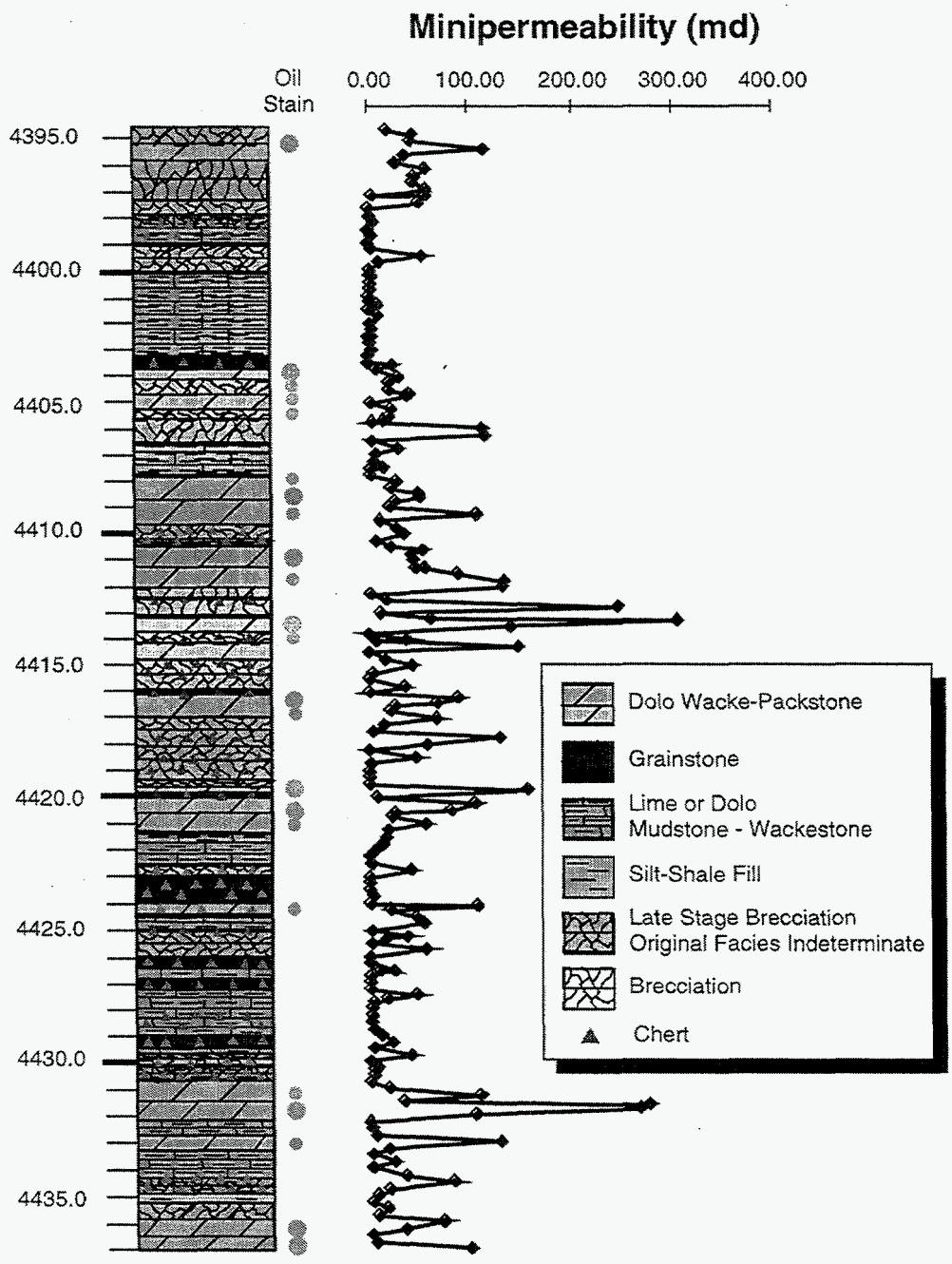

FIGURE 2.16. Graphical core description showing facies discussed in text for the Ritchie Exploration, #1 Foos AP Twin compared with the vertical profile of minipermeameter values. Depositional facies appear to influence permeability development and the reservoir is very vertically heterogeneous. Individual facies are discussed in text.

2.2.2.4 PfEFFER

Petrophysical analysis and reservoir evaluation used a new computer package (PfEFFER) that was developed in conjunction with this project. Prototype software was tested and successfully applied in Schaben Field, and grew out of the "Super-Pickett" crossplot that was developed and applied as part of other DOE funding (DOE/BC/14434-13). PfEFFER stands for "Petrofacies Evaluation of Formations For Engineering Reservoirs" (Doveton et al., 1995). PfEFFER v.1 was released January 2, 1996 as a commercial spreadsheet-based well-log analysis program developed and distributed through the Kansas Geological Survey. PfEFFER v.1 software was developed as a separate project with one year of additional funding provided by twelve major and small independent companies. Industry and BDM/Oklahoma are providing additional funding for development of an enhanced PfEFFER. PfEFFER was designed as a means to obtain timely, inexpensive, but reliable reservoir characterization using the limited available information, staff, and technical resources (a major problem for independent producers).

PfEFFER is an interactive spreadsheet-based program that is designed to run as a Visual Basic add-in to Excel version 5.0 or later. The minimum logs required are a porosity log and a resistivity log. The focal point of the analytical routines and graphical displays is the "Super Pickett" crossplot, an extension of the standard log-log porosity/resistivity plot. The special features include: tracking the pattern of data points by depth, and annotation with bulk volume water and permeability lines in addition to the standard water saturation lines. Color is used on the "Super Pickett" crossplot to display attributes such as well log data, completion information, and other derived data. Color ranges are automatically or manually selected to highlight and emphasize reservoir components, adding new perspectives. If neutron/density porosity and PEF logs are available, proportions of complex lithologies can be solved with the Rhomaa Umaa option. A variety of lithologies can be selected and easily changed through menu choices to modify the matrix coefficients. Explicit lithologic information can be displayed as attributes on the crossplot or shown as compositional profiles keyed to depth. Lithology solutions can be presented as attribute colors on the crossplot or the information can be presented along with other depth-related information as a vertical depth display by activating the "LOG" button and corresponding dialog boxes and menus. Log traces can be combined on single or multiple tracks. Additional details can be found in Doveton et al. (1995, 1996).

Well log analyses of the Schaben Field uses PfEFFER. Logging suites in the Schaben Field are as diverse as the reservoir. There are about 41 wells that have only the Microlateralog to use in determining porosity, 46 wells have only the uncalibrated neutron for determining porosity, 56 wells with sonic porosity logs, and 23 wells with a combination density neutron porosity. Using the PfEFFER program, we have been able to determine reservoir parameters that are reasonably accurate and comparable, no matter which porosity tools were run. Petrophysical results indicate that the reservoir is highly stratified vertically, of variable lithology (limestone, dolomite, and chert), and has high BVW (Bulk Volume Water). PfEFFER analysis on all wells in the Schaben Field demostration area with an adequate suite of logs provided the input parameters for reservoir simulation. Examples of PfEFFER plots and petrophysical interpretations for the three new wells drilled as part of the project are attached (Appendices A - C). The petrophysical results from the PfEFFER analyses are being tied into advanced core analysis (for example, Minipermeability, Capillary Pressure and NMR).

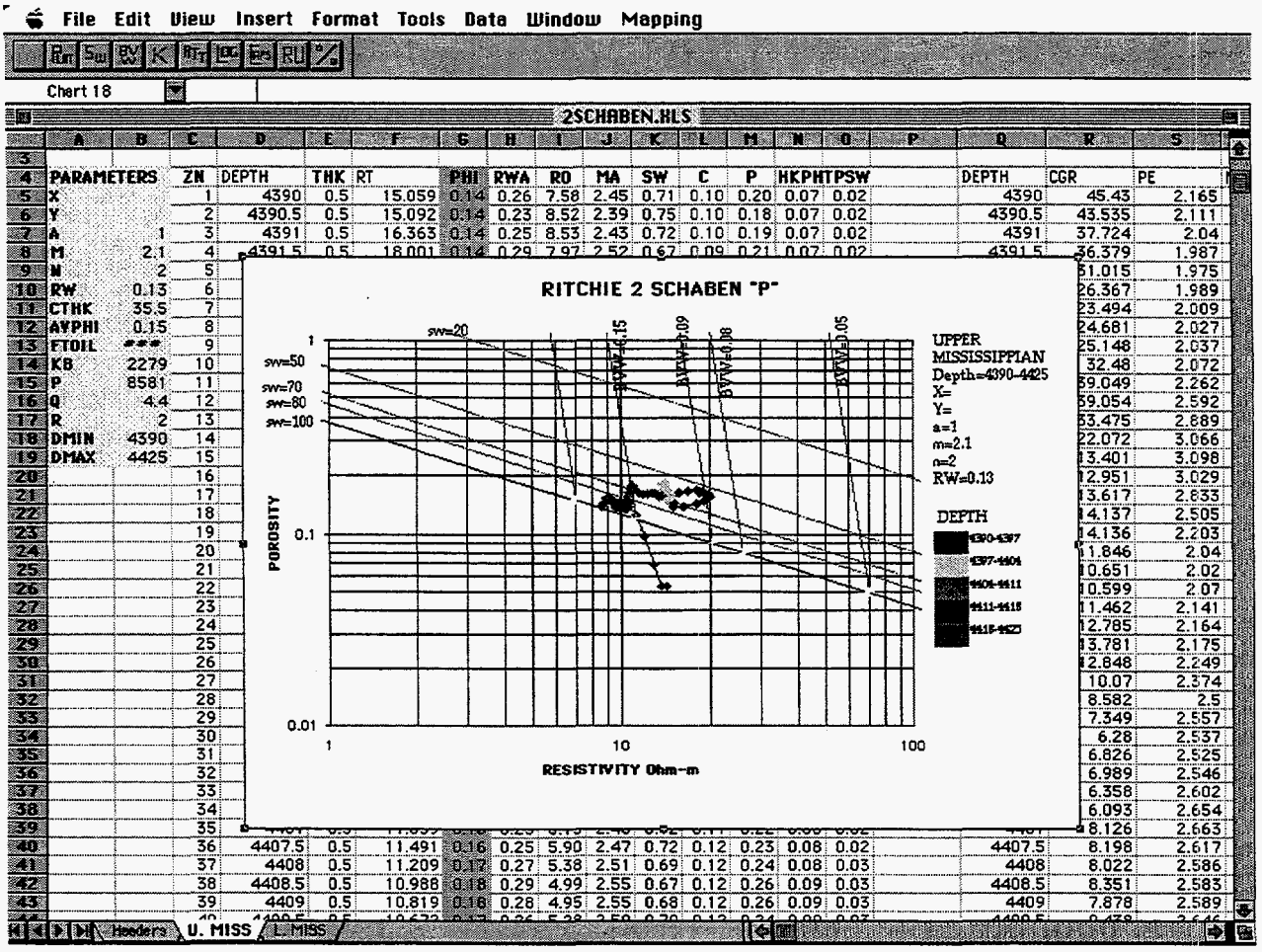

	A	B	C	D	E	F	G	H	I	J	K	L	M	N	O	P	Q	R	S
4	PARAMETERS		ZN	DEPTH	THK	RT	PHI	RWA	RO	MA	SW	C	P	HKPHTPSW			DEPTH	CGR	PE
5	X		1	4390	0.5	15.059	0.14	0.26	7.58	2.45	0.71	0.10	0.20	0.07	0.02		4390	45.43	2.165
6	Y		2	4390.5	0.5	15.092	0.14	0.23	8.52	2.39	0.75	0.10	0.18	0.07	0.02		4390.5	43.535	2.111
7	A	1	3	4391	0.5	16.363	0.14	0.25	8.53	2.43	0.72	0.10	0.19	0.07	0.02		4391	37.724	2.04
8	M	2.1	4	4391.5	0.5	18.001	0.14	0.29	7.97	2.52	0.67	0.09	0.21	0.07	0.02		4391.5	36.379	1.987
9	N	2	5															31.015	1.975
10	RW	0.13	6															26.367	1.989
11	CTHK	35.5	7															23.494	2.009
12	AVPHI	0.15	8															24.681	2.027
13	FTOIL	***	9															25.148	2.037
14	KB	2279	10															32.48	2.072
15	P	8581	11															39.049	2.262
16	Q	4.4	12															39.054	2.592
17	R	2	13															53.475	2.889
18	DMIN	4390	14															22.072	3.066
19	DMAX	4425	15															13.401	3.098
20			16															12.951	3.029
21			17															13.617	2.833
22			18															14.137	2.505
23			19															14.136	2.203
24			20															11.846	2.04
25			21															10.651	2.02
26			22															10.599	2.07
27			23															11.462	2.141
28			24															12.785	2.164
29			25															13.781	2.175
30			26															12.848	2.249
31			27															10.07	2.374
32			28															8.582	2.5
33			29															7.349	2.557
34			30															6.28	2.537
35			31															6.826	2.525
36			32															6.989	2.546
37			33															6.358	2.602
38			34															6.093	2.654
39			35															8.126	2.663
40			36	4407.5	0.5	11.491	0.16	0.25	5.90	2.47	0.72	0.12	0.23	0.08	0.02		4407.5	8.198	2.617
41			37	4408	0.5	11.209	0.17	0.27	5.38	2.51	0.69	0.12	0.24	0.08	0.03		4408	8.022	2.586
42			38	4408.5	0.5	10.988	0.18	0.29	4.99	2.55	0.67	0.12	0.26	0.09	0.03		4408.5	8.351	2.583
43			39	4409	0.5	10.819	0.18	0.28	4.95	2.55	0.68	0.12	0.26	0.09	0.03		4409	7.878	2.589

FIGURE 2.17. PfEFFER spreadsheet showing data and structure of the program. The focal point of the PfEFFER analytical routines and graphical displays is the "SuperPickett" crossplot, an extension of the standard log-log porosity/resistivity plot. Specific parameters obtained from the PfEFFER crossplots include minimum bulk volume water and associated porosity and water saturations, permeability estimates, resistivity gradients reflecting hydrocarbon transition zones and depth of possible free water levels, and reservoir zonation/permeability barriers and associated heterogeneities

2.2.3 Pseudoseismic Analysis

Additional petrophysical/seismic procedures were developed to modify, load, and display well log data from Schaben Field as a 3D "pseudoseismic" volume (figures 2.18-2.20). The pseudoseismic volume can be displayed and interpreted on any commercial geophysical workstation (PC or UNIX). At Schaben the "pseudoseismic" approach was used to recognize and map previously unknown small faults and subtle stratigraphic heterogeneities within the reservoir units. The pseudoseismic approach adapts technologies and leverages previously existing data (i.e., electric logs). The pseudoseismic approach developed at Schaben has been presented and published through technical meetings, industry newsletters and technical publications (Carr et al. 1995b; Hopkins et al., 1996; Hopkins and Carr, in press). Copies of abstracts and manuscripts are attached as appendices (D-F). Numerous producing companies have inquired concerning software and assistance in using the 3D pseudoseismic approach in their projects.

Genesis of a seismic approach to wireline logs arose from efforts to use the computer workstation to integrate geologic and geophysical approaches to subsurface analysis, and the challenge of trying to apply computer-aided exploration and development techniques to mature producing areas that are dominated by well data such as the Schaben demonstration site. Wireline well logs resemble seismic traces in many respects. Fundamentally, both wireline log data and seismic data are simple x-y series. The wireline log records amplitude in the depth domain, and the seismic trace records amplitude in the time domain. Wireline well logging tools record various rock properties and output these data as a depth series. Ultimately, the goal of seismic processing is to approach on a trace-by-trace basis the resolution of geophysical well logs. If wireline logs can be transformed to more closely resemble the seismic trace one can interpret wireline logs within existing seismic interpretation software. This change in approach is labeled *pseudoseismic* . The pseudoseismic approach significantly increases the scope, power, and resolution of the interpretation.

In a series of papers during the 1980's John Doveton and Dave Collins of the Kansas Geological Survey proposed a color image transformation that achieves a significant improvement in the stratigraphic interpretation of wireline log data (Collins and Doveton, 1986, 1989). When well designed, such a transformation of wireline log data from multiple wells can maximize both spatial and compositional information contents, and provide a readily interpretable image of the subsurface geology. They introduced the concept of a color cube subdivided into a series of discrete cells to represent the log data. The planes between cells were selected to coincide with coordinate values that discriminate between lithologies, porosity levels, or shale mineralogy. The transformation operates as an automatic classification device that provides visual meaning. The color image transformation was used to construct single well displays and a single cross-section across western Kansas. The cross-section was constructed on a well-by-well basis, and resembles in many ways a standard 2D seismic display (See: Doveton, 1994, p. 43).

The pseudoseismic approach uses a similar transform of a single curve or combination from multiple tools (e.g., gamma ray, density and neutron) to generate a color coded "crossplot log" for each well as the single trace input to the pseudo-seismic approach. The key is to take the transformed log data and treat it as either 2D or 3D "seismic" data. A conversion program to

transform wire-line or transformed wireline log data into a binary SEGY file accomplishes the actual conversion of digitized well data to pseudo-seismic data.

LAS and SEGY formats are "standard" formats for digital well log and seismic data, respectively. SEGY was designed primarily as a format for recording and processing seismic data. This format consists of a 3600 byte reel header containing general information about the seismic line or survey. The first 3200 bytes of the SEGY reel header are in ASCII and the remaining 400 bytes are binary. Following the reel header are the binary trace data. Each trace also has its own header (240 bytes binary) and is followed by the seismic trace data (Barry, Cavers, and Kneale, 1975). The data are arranged serially. A common starting point (the seismic datum) and time increment (sample interval) are assigned to all traces. The data appear as a listing of numbers, time increasing at an equal interval from left to right across rows and downwards between rows. The data one encounters within a seismic trace are normally seismic reflection amplitudes, or, loosely, waves.

LAS formatted well log data contrast strongly in appearance with SEGY seismic data. LAS was developed to insure that there was a standard digital well log format that anyone with a computer could read (Canadian Well Logging Society's LAS Committee, 1993). The entire well log data set is in ASCII and can be opened like any ASCII file. The data structure is relatively straightforward. The well header contains LAS version, general well, logging parameter, and curve information. The curve data following the header is set up much like a spreadsheet. Depth values appear in the far left column followed by one or more data points for that depth, corresponding to the various well logging tools run in that well.

The pseudoseismic transform "maps" LAS header and curve data onto corresponding SEGY data fields creating a file formatted like seismic reflection data. Coding of the pseudo-seismic transform uses a "C" program (Appendix F). The transform reads LAS files containing one curve (depth-value pairs) plus the well header. For instance, if it was desired to transform neutron-porosity readings from LAS to SEGY, files must exist which contain only the well log header and depth-porosity pairs. It is also required that all the digital well logs have the same sample interval. The transform program reads the LAS files, writes portions of the curve header to specific locations in the SEGY trace header, and writes the log data to the SEGY trace data field (Table 1). Data from the well header that are used in the trace header are location (X, Y or latitude and longitude) and kelly bushing elevation. Many of the fields in the reel and trace headers are filled with null values because they have little relevance to well log data. For instance, there are SEGY fields set aside for filter parameters and vibrator sweep characteristics. Data handling and loading are made somewhat easier by using SEGY data fields in the standard manner.

The pseudo-seismic transform combines data from many individual wells and creates a 2-D or 3-D data set. In doing so, the program also assigns a datum for the data set (the largest K. B. value), pads the tops and bottoms of well logs to ensure the "traces" are of equal length and writes this information to a binary SEGY file. Trace spacing is determined from well spacing based on the nearest neighbors to an arbitrary spacing unit (e.g., an 80-acre bin or a 330-foot spacing). Transformation of well locations to trace spacing can be computed rounding to the nearest whole spacing unit or bin. Empty bins or blank traces can represent areas without wells.

The net result is that the SEGY file contains a structural volume created from geophysical well logs.

After the transform, the ASCII well log data looks like a binary seismic data set. This allows the data set to be loaded into a seismic workstation for display, manipulation, and interpretation purposes. It also facilitates the compiling of very large digital well log databases, which eases data handling burdens. For example, a cross-section containing 300 gamma-ray traces (one well per mile) was constructed for a project at the Kansas Geological Survey. If this cross-section had been constructed using 4 inch wide paper logs, at a scale of 4 inches per mile, the section would have been a 100 feet long. A section of these monumental proportions would be unwieldy and impractical. However, as a pseudo-seismic line it contains only 300 traces, about as many traces as a 3 mile seismic reflection line shot with 55 foot C. D. P. spacing, and is readily manipulated or interpreted.

Using a seismic approach to well data can significantly ease the data handling burdens through use of computerized techniques designed for interpretation and display of seismic data. The use of interpretation and processing packages developed for seismic data offers flexibility in displaying and picking horizons, and opens new opportunities for increasing the efficiency of stratigraphic interpretation. The change in approach from the traditional well-by-well examination to treating the wireline logs in a field or basin as a data volume permits comprehensive study and cost-effective analysis of data sets that were previously considered intractable.

The examples from the Schaben demonstration site use gamma ray logs to map small faults and subtle stratigraphic geometries in the Pennsylvanian rocks overlying the Mississippian reservoirs. Data was "binned" at a 40-acre spacing resulting in a volume that covers approximately six square miles with a trace every 1320 feet (figures 2.19, 2.20). The "hot" Pennsylvanian core shales make excellent markers that can be traced using the gamma-ray log across the demonstration site (Figure 2.19). The pseudoseismic technique was used to efficiently map internal Mississippian markers across the Schaben Field demonstration area.

WELL LOG HEADER & OTHER INFORMATION	SEGY BYTE NUMBERS FOR REEL HEADER	DESCRIPTION
1	3213-3214	Number of traces per record, always 1 for curve data
1000, 2000, ...	3217-3218	Sample interval in feet *1000
XXX	3221-3222	Number of samples per curve
1	3225-3226	Data format: 4 byte floating point
1	3227-3228	Number of traces per record or C. D. P.
1 or 2 ...	3255-3256	Measurement system: 1 = metres 2 = feet
WELL HEADER & OTHER INFORMATION	SEGY BYTE NUMBERS IN TRACE HEADER	DESCRIPTION
1, 2, 3, ...	1-4	Trace sequence number, numbers increase for each curve.
K. B. elevation	41-44	Elevation of well, used to place wells in correct relative vertical position.
Max K. B. elevation	53-56	elevation used as datum
X coordinate or Longitude	81-84	Survey coordinates
Y coordinate or Latitude	85-88	Survey coordinates
1 or 2	89-90	Coordinate units: 1 = length (meters or feet) 2 = seconds of arc
XXX	115-116	Maximum number of samples
1000, 2000 ...	117-118	Sample interval in feet *1000

Table 1: Data field and header information and the corresponding SEGY reel and trace header byte numbers. Not all SEGY fields are used in the transform. The unused fields are filled with null values.

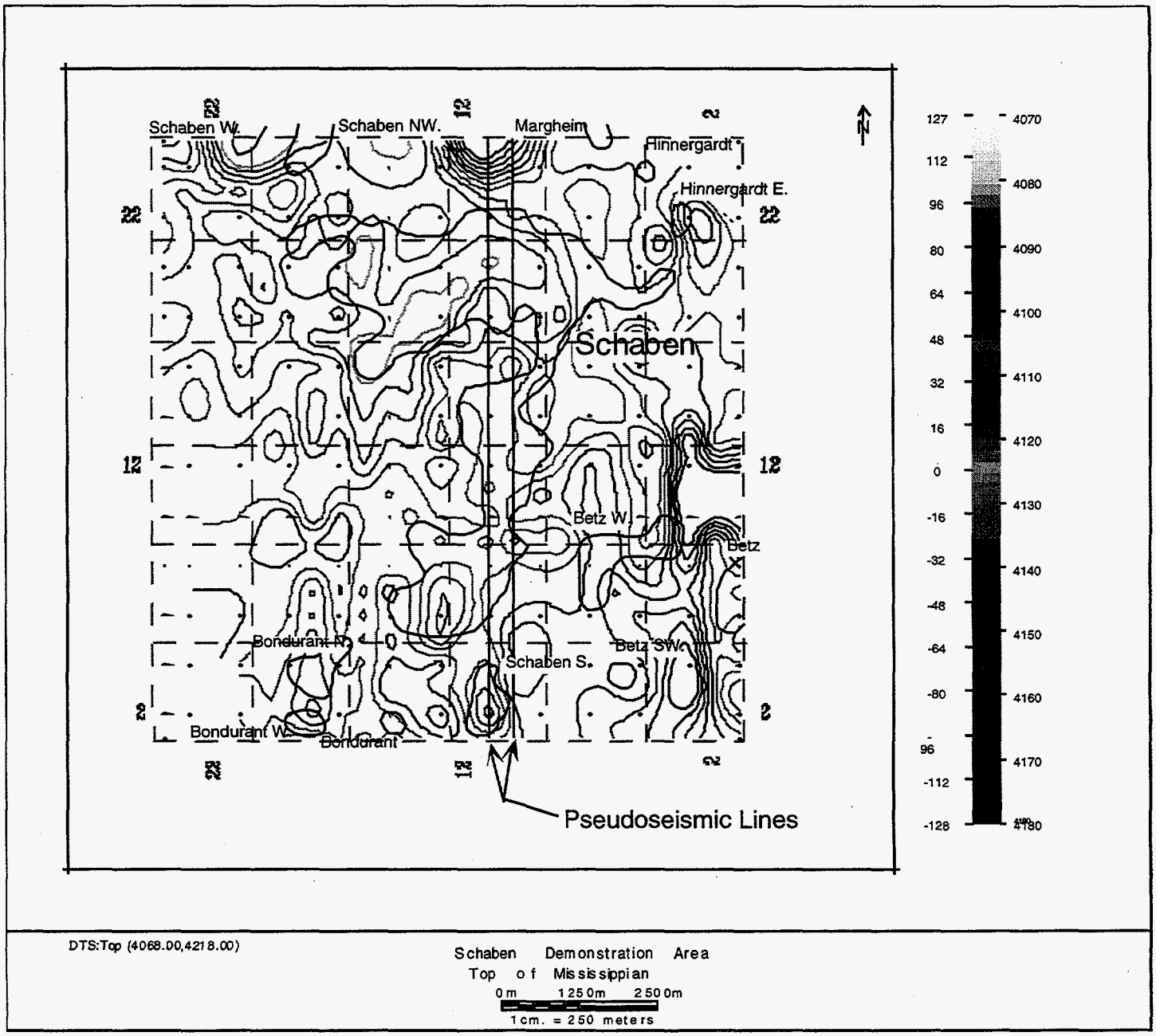

FIGURE 2.18. Map of selected pseudoseismic surface (Top of Mississippian) from the Schaben demonstration site 3D *pseudoseismic* volume. Note correspondence to contour map generated from well tops (Figure 2.2). Locations of selected pseudoseismic profiles are shown (figures 2.19 and 2.20). Hotter colors represent higher subsea depths.

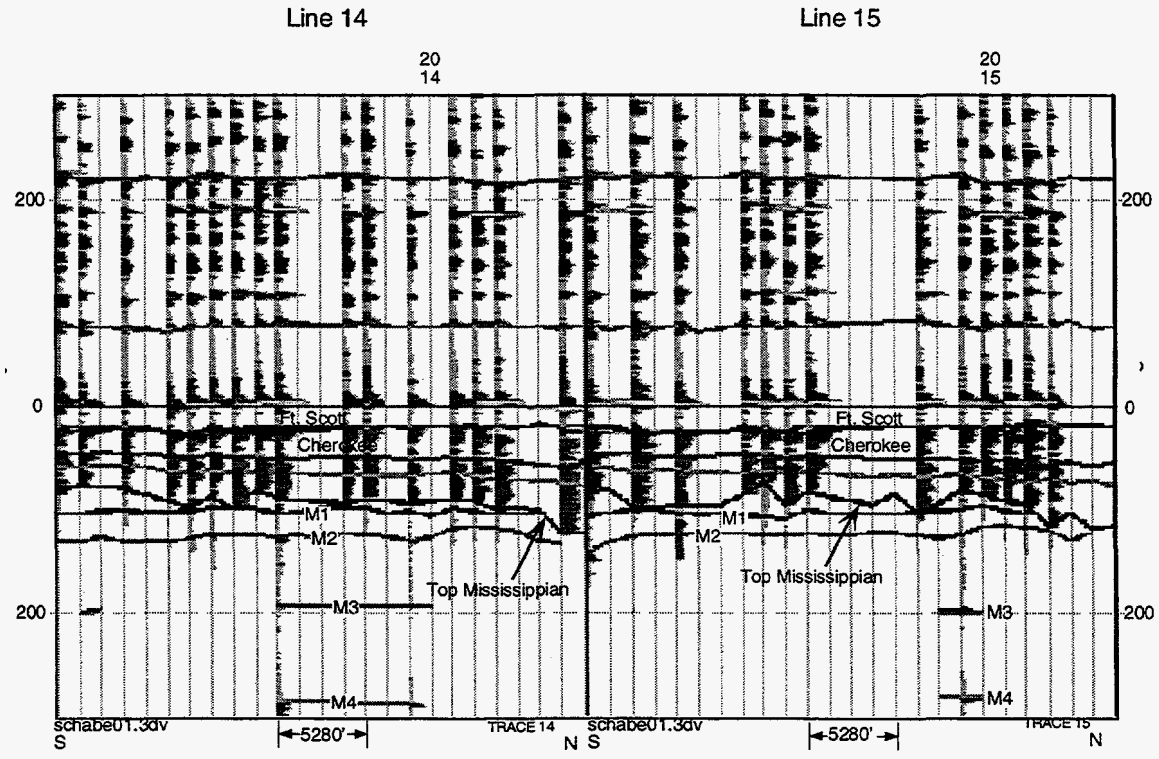

FIGURE 2.19 A group of two north south pseudoseismic profiles of gamma-ray across Schaben Field. Individual profiles extracted from the Schaben demonstration site 3D volume are datumed on the top of the Fort Scott and are 1320' apart. Volume contains data from over 200 wells and is "binned" at forty-acre spacings. Note the east to west truncation of Mississippian markers and the irregular nature of the Mississippian erosional surface. Location of profiles shown on figure 2.18.

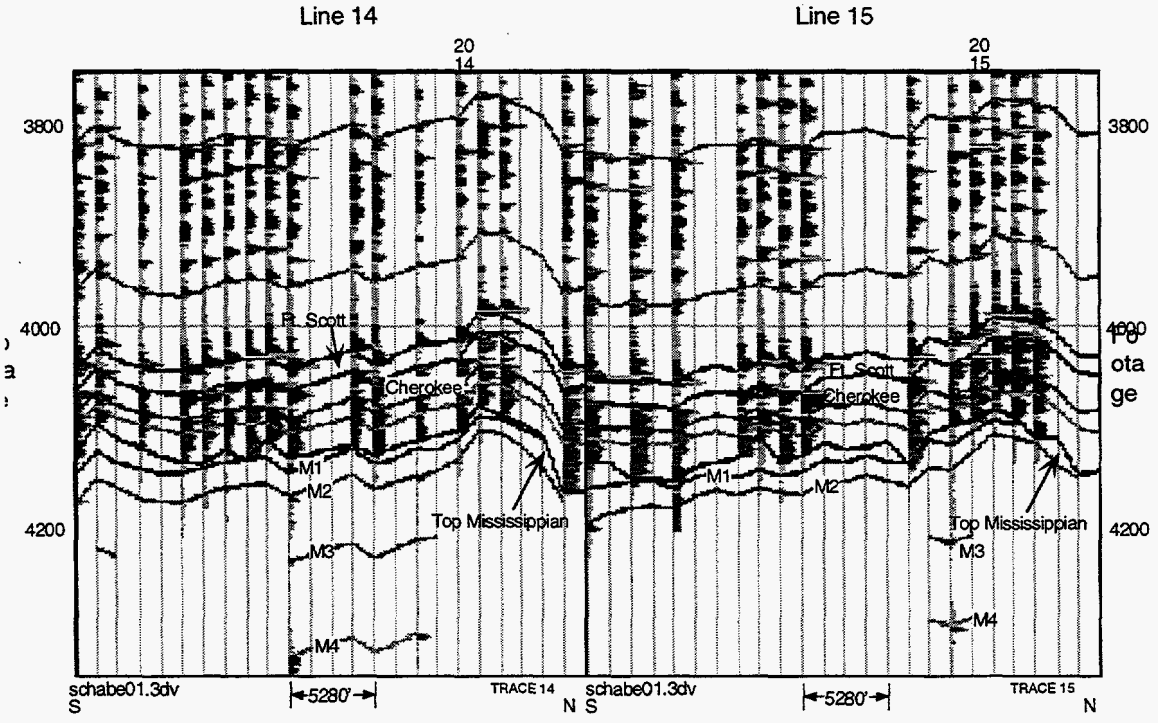

FIGURE 2.20. A group of two north south pseudoseismic profiles of gamma-ray across Schaben Field. Individual profiles extracted from the Schaben demonstration site 3D volume are structurally datumed and are 1320' apart. Volume contains data from over 200 wells and is "binned" at forty-acre spacings. Note consistent east to west offset of shale markers on both profiles across the demonstration site. Location of profiles shown on Figure 2.18.

2.2.4 Lithofacies, Depositional Environment, Paragenesis: Controls on Reservoir Facies

The following discussion is based on examination of the three cores recovered from the Schaben Field demonstration area. All core photographs are available online at http://www.kgs.ukans.edu/DPA/Schaben/CoreScans/Core.html

Depositional Facies

Dolomite or Lime Mudstone-Wackestone (MW).--This facies is typically light gray to olive green in color or dark gray to brown. Typically this facies is laminated, or wavy to wispy laminated. Locally it is massive. Laminations are imparted locally by interbedded green shale-siltstone and by horsetail stylolites (Plate 1A). Much of this facies has a mottled texture apparently imparted by burrowing organisms and locally microscopic fracturing. Other features include soft sediment deformation. Fenestral fabric, indicating early subaerial exposure, occurs locally. Identifiable skeletal grains are rare; sponge spicules (mostly monaxon) and their molds are locally identifiable and appear to be the most common grain type with echinoderm and bryozoan, brachiopod, gastropods, peloid, and glauconite locally present. The sponge spicules are locally concentrated in layers or in "pockets" presumably as a function of currents and reworking by burrowing organisms. Rare concentrations of very fine grained (~ 100 μm) detrital quartz grains also likely occur from reworking by burrowing organisms. This facies is typically tight or has moldic, intercrystalline, and vuggy porosity (up to ~25%, visual estimate) locally developed; mottling texture and lamination locally results in variable tight and porous areas at a thin section scale. Dolomite occurs as very finely crystalline to micrite size (~20 μm to <100 μm), subhedral to anhedral crystals; euhedral crystals are locally developed and more commonly identified in areas with intercrystalline porosity. This facies often contains silica that replaced evaporite crystals, nodules and coalesced nodules that form layers. Silica also locally replaces matrix and grains in this facies.

Sponge Spicule-Rich Dolomitic or Lime Wackestone-Packstone (SWP).--This facies is defined because of its abundance in all three cores, especially in the upper portions of each core and because of its importance as a reservoir facies. This facies is dark to light gray, olive green, tan, or brown in color. Mottled, wispy horizontal laminated, and wavy horizontal laminated textures are common. This facies is typically characterized by mottling from burrowing organisms (Plate 1B). Laminations are imparted locally by interbedded green-gray shale-siltstone and by horsetail stylolites. Sponge spicules (mostly monaxon) and their molds (Plate 1C) are the most common grain type and commonly the exclusive grain type. Echinoderm, bryozoan, gastropod, and peloid grains occur more rarely. The sponge spicules are locally concentrated in layers or in "pockets" as a function of depositional processes (currents) and reworking by burrowing organisms. Moldic, intercrystalline, and vuggy porosity is locally abundant (up to ~65%, visual estimate). Fenestral fabric occurs locally. Some primary porosity is solution enlarged forming vugs. The mottling texture and concentration of grains in layers locally results in variable tight and porous areas at a thin section scale. Dolomite occurs as very finely crystalline to micrite size (~20 μm to <100 μm), subhedral to anhedral crystals; euhedral crystals are locally developed and more common in areas with intercrystalline porosity. This facies commonly contains chert after replacement of evaporite crystals, nodules and coalesced nodules that form layers. Chert also replaces matrix and grains (Plate 1D, Plate 2A). A breccia fabric is common from dissolution

and collapse of evaporites and due to early differential compaction between brittle chert and soft dolomitic matrix. This facies is the most common to contain oil staining.

Echinoderm-Rich Dolomitic or Lime Wackestone-Packstone-Grainstone (EWPG).--This facies occurs in all three cores and is most abundant in the lower parts of the cores. This facies is typically dominated by echinoderm fragments but also contains abundant sponge spicules, bryozoan fragments, brachiopods, coral fragments, gastropods, ostracods, ooids, peloids, grapestone, calcispheres, oncolites, and other unidentifiable skeletal debris. Very fine to fine-grained detrital quartz grains occur locally. Where replaced by silica, the grain textures may be preserved or are molds filled with chert, silica or calcite cement (Plate 2B). Grainstones locally have an isopachous chalcedony cement that coats grains and lines primary pores (Plate 2B). Where still dolomitic, the grains are typically preserved as molds (Plate 2C). Horizontal laminations and low-angle cross laminations are locally preserved. Some intervals show sorting of grains into fine-grained layers and coarser-grained layers. Other intervals show normal grading of grains. Locally, grains in this facies show compromise boundaries, overly close packing, grain breakage and flat, horizontal alignment of skeletal fragments, but typically there is not much over compaction or other evidence for much early compaction.

Where still dolomite, this facies is characteristically tan to dark brown in color and typically has a wispy laminated or mottled texture; locally it has a massive texture. Locally, interbedded skeletal rich layers (more porous) and skeletal poor layers (tighter) result in an alternating porous and tight layering within this facies. Porosity in this facies can exceed 35% (visual estimate). Common porosity types include moldic, moldic reduced, intercrystalline, and vugs. Oil staining occurs commonly in this facies where still mostly dolomitic. Dolomite is typically very finely crystalline (~50 μm or less) but locally exceeds 150 μm. Crystals are typically subhedral to euhedral. Some of the crystals are zoned with a clear to turbid (locally calcian) center and clear dolomite rim. Some dedolomite textures were identified. Locally, calcite cement and neomorphic spar occludes porosity and replaces original textures; some areas have dolomite rhombs or silica "floating" in calcite.

This facies commonly has been partially or pervasively replaced with porcelanous (tight) or tripolitic (porous) chert/megaquartz. Abundant vuggy and microcrystalline porosity occur within tripolitic chert areas (Plate 2D) and both tripolitic and porcelanous chert typically contains micro- and mega-fracture porosity. Only locally are vugs developed within chert areas and partially or fully filled with silica cement. Fenestral pores either partially or fully filled with silica cement occur locally.

Other Lithologies and Features

Chert/Chalcedony/Megaquartz Replacement.--Silica replacement of original lithologies is abundant throughout all three cores and replaces all facies types described above. Silica replacement occurs either as pervasive or partial replacement of original facies textures or grains. The silica is typically white to light gray in hand sample and has a porcelanous or tripolitic texture. Typically, several stages of silica replacement and cementation can be identified microscopically. A typical sequence shows a first stage of brown/black chert replacing facies and grains, a second stage of isopachous brown chalcedony cement, and a third stage of

megaquartz replacement or cementation. This sequence is repeated at least two times stratigraphically.

The abundance of silica replacement is likely at least partially due to the abundance of sponge spicules. Silica locally preferentially replaces spicules imparting a wispy texture or replaces the matrix surrounding the spicules and leaves the spicules as molds. Much of the chert replacement appears to follow original burrow mottling and networks. The silica replacement is typically tight and forms impermeable layers where replacement is massive and porcelanous. Where the silica replacement is tripolitic the chert contains abundant microcrystalline porosity. Chert areas commonly exhibit a fracture and brecciated texture due to early differential compaction between brittle chert areas and surrounding matrix areas that were still soft (Plate 3A, 3B), and from later fracturing related to subaerial exposure and later burial compaction. Variable micro-and macro-fracture porosity results from these processes.

Silica also occurs as replacement of original evaporite crystals, isolated nodules, horizontal layers of isolated or laterally coalescing nodules, or as horizontal layers of vertically elongate nodules. This silica replacement is typically dark gray in color and has more associated vuggy porosity. Some of these nodules preserve a bladed or radiating bladed crystal morphology (Plate 3C), bladed and twined morphology or zebraic chalcedony texture (Plate 3D) when viewed with a petrographic microscope, indicating replacement of an original evaporite mineral (anhydrite or gypsum). Typically, the original evaporite crystals and nodules display replacement by clear to dark brown chert followed by dissolution/corrosion/erosion forming an irregular surface by precipitation of megaquartz cement in remaining pore space (Plate 4A).

Sandstone/Siltstone/shale.--This facies is typically green to gray in color. It is wavy to wispy laminated and locally displays low-angle lamination. This facies is composed predominantly of very-fine grained sand (~100 μm) to silt-sized (<50 μm) quartz grains. Intergranular porosity is locally developed (> 20% locally, visual estimate). This facies occurs as fracture fill (Plate 4B) and breccia matrix. The shale locally occurs as wispy layers in dolomitic mudstone or wackestone facies (Plate 1A).

Breccia and Fracturing.--Brecciation and fracturing are ubiquitous throughout the three cores. Fracturing and brecciation results in fracture and mosaic breccias, with textures ranging from little to no rotation on clasts (indicating in-situ brecciation) (Plate 4C), to matrix-supported and clast-supported chaotic breccias that represent mixtures of autochthonous and allochthonous materials resedimented by gravitationally driven processes (Plate 4D).

Fracturing and brecciation occur on macroscopic and microscopic (Plate 5A) scales. Fracture fill and breccia matrix includes shale, subangular to rounded, silt- to coarse-grained size detrital quartz, chert, megaquartz, chalcedony grains, carbonate micrite, carbonate grains, and skeletal grains. Clasts (ranging from rounded to angular) include chert/chalcedony/megaquartz fragments, clasts of original carbonate facies, replacive poikilotopic calcite clasts, coarse calcite cement fragments, and rubble of red and greenish limy clay. Porosity associated with fracturing and brecciation is quite variable, ranging from tight to very porous, and depends on amount of fracturing and brecciation, "openness" of fractures, types and grain size of fracture fill, and types

and grain size of breccia clasts and matrix. Interparticle, intercrystalline, vuggy and fracture porosity are common porosity types in breccia matrix.

Brecciation and fracturing were caused by a variety of processes interacting at different times. Some areas reveal several generations of fracturing, brecciation, cementation and sediment fills. The overprinting of these different events results in complex fabrics. Relatively early silica replacement resulted in layers and areas that were cemented versus surrounding original matrix that was still soft. Early compaction resulted in differential brittle and soft deformation between the chert and surrounding matrix which imparted a fracture and breccia fabric. Displacive growth of chert nodules in soft dolomitic sediment resulted in soft sediment deformation textures and some brecciation. Some breccia was locally caused by depositional processes (e.g. current rip-up). Other brecciation and fracturing were caused by early (intra-Mississippian) subaerial exposure, dissolution and collapse of evaporites, post-Mississippian subaerial exposure, and late burial compaction that resulted in brittle deformation of all lithologies.

Depositional Environment

A general upward facies change is discernible in all three cores. Echinoderm facies predominates in the bases of all the cores (up to 4435' in Moore, up to 4428' in Schaben and up to 4436' in Foos). Although other facies occur as well, importantly, evidence of evaporites is generally lacking. The upper portions of all cores (above 4435' in Moore, above 4428' in Schaben and above 4436' are dominated by the sponge spicule-rich and mudstone/wackestone facies and contain abundant evidence of evaporites. Figure 2.21 shows correlation of the cores that was made with the aid of well logs. Although dips are accentuated by structural elements, the correlation and general facies trends indicate deposition on a ramp with the Moore core at the updip area, Schaben in the middle, and the Foos core in a downdip area. The abundance of the echinoderm facies with abundant other diverse fauna, abundance of burrowing organisms and only rare occurrence of evaporites in the basal portions of the cores suggest deposition in relatively normal to somewhat restricted marine environments. In contrast, the abundance of mudstone, wackestone and spicule-rich facies, relative rarity of echinoderm-rich facies, and abundance of evaporites in upper portions of the cores suggest deposition in restricted, evaporitive ramp or lagoon environments. However, the abundance of burrow mottling indicates conditions sufficient to support organisms that reworked the sediment. The morphology and alignment of the evaporite crystals, nodules, and layers likely indicates formation in a supratidal to shallow subaqueous setting at or just below the sediment/water interface (Warren, 1989). Local fenestral fabric indicates at least intermittent subaerial exposure.

Overall, each core shows an upward shoaling trend leading up to the post-Mississippian subaerial exposure event. Correlations reveal lateral facies shifts accross the ramp through time with the evaporitic ramp to lagoon environment existing earliest in the Moore core (correlating with open to restricted marine ramp environments in the Schaben and Foos cores) and shifting down ramp through time in response to the relative sea level drop leading to the eventual post-Mississippian subaerial exposure event.

The echinoderm-rich facies are mostly characteristic of a shallow subtidal shelf setting. The lamination, cross lamination, normal grading, packing of grains, grain breakage, and scoured

contacts evidence at least intermittent high energy. In the normal to restricted portion of the ramp, this facies likely represents deposition from storm and turbidity currents or from migration of subtidal shoals or banks. Local fenestral fabrics in the echinoderm facies, especially in the evaporite ramp or lagoon portion of the section, indicate at least local subaerial exposure in a supratidal setting. The echinoderm-rich facies in this part of the ramp may represent shelfward migration of a subtidal shoal or shelfward deposition from tide or storm currents. The sponge spicule dolowackestone-packstone and dolomudstone-wackestone facies are likely indicative of a low energy and slightly more restricted setting as compared to the echinoderm-rich facies. In this environment sponges thrived and likely formed sponge "gardens" or "mounds" (Rogers et al., 1995). Wispy and wavy horizontal lamination, alternating grain-rich and grain-poor layers, some apparent normally graded beds and local interbeds of grainstone in mudstone to packstone indicate transport and reworking of sediment by currents likely generated from tides or storms.

The change between the normal to restricted marine ramp and the evaporitic ramp to lagoon in the Schaben core is marked by a sharp contact at 4424' (MO sufrace). This surface and the strata immediately below for several meters show significant alteration. A coarse calcite cement and replacive poikilotopic calcite is associated with the MO surface and occurs variably throughout strata below this surface to the bottom of the core (Plate 5B). This cement is very important for making these strata relatively tight compared to overlying strata. The cement does not occur in strata above the MO surface. There is a similar cement at the very top of the Schaben core (Plate 5C) but it only affects strata in the upper five feet of the core and is presumably related to the post-Mississippian subaerial exposure event. Strata from about 4390' to 4424' do not contain any coarse poikilotopic calcite cement. In addition, the strata below the MO surface contain local fenestral fabric (Plate 5D), autobreccia, clay-rich "crusts" (most now chertified) with abundant horizontal fenestrae interlaminated with fine-coarse grained detrital quartz layers, locally abundant glauconite, pyrite, fractures and breccia with dolomite, clay, detrital quartz matrix locally cemented with coarse calcite cement (Plate 6A), dolomite facies clasts, chalcedony, megaquartz and chert clasts, and, locally, poikilotopic calcite clasts (Plate6B). In addition, round or oblong to elongate areas altering original facies occur for several meters below the surface. These areas are characterized by a central area filled with poikilotopic calcite that is surrounded by a halo of iron staining and local fenestral fabric (Plate 6C). Some of these areas show associated microscopic horizontal and downward "branching" of microfractures. These altered areas may reflect the presence of land plant roots. The fenestral fabric, crusts, autobreccia, coarse calcite and poikilotopic cement, possibly associated with meteoric water, are consistent with subaerial exposure as well. An early, intra-Mississippian exposure event at the MO surface versus the alteration and features being related to the post-Mississippian exposure event is supported by several crosscutting relationships. Below the MO surface, original dolomitic facies and silica-replaced facies are fractured and brecciated and infilled with dolomite matrix, detrital quartz and replacive silica clasts. These facies and previously fractured and brecciated areas are crosscut by coarse calcite-filled fractures, replaced by poikilotopic calcite, and the previously fractured and brecciated areas are locally cemented by the poikilotopic calcite (Plate 6A). These fabrics, including the coarse calcite cement and poikilotopic calcite, are crosscut by fractures filled with dolomite (Plate 6D) and locally, evaporite crystals and evaporite nodules from facies overlying the MO surface. These dolomite-filled fractures contain clasts of poikilotopic cement (Plate 6B, 6D) and clasts of replacive silica (Plate 6A). Importantly, none of these features are identified above the MO which strongly suggests a subaerial exposure event at

the MO surface prior to deposition of overlying strata. The MO surface in the Schaben core appears to correlate with an area of siliciclastic-rich and shallow water carbonate rubble and missing strata in the Moore core (~4400-4410') (Figure 2.21). This may represent extreme erosion in the updip Moore core during the MO subaerial exposure event. The Foos core does not extend down to the level that correlates with the MO surface in the Schaben core.

Paragenetic Sequence

The following is a preliminary paragenetic sequence of depositional and diagenetic events for the strata from the Schaben field based on macroscopic and standard petrographic observations of crosscutting relationships. Although in general this paragenetic sequence is thought to be applicable to all three cores, further analyses utilizing cathodoluminescence, fluid inclusion data, XRD, SEM and geochemical analyses will be necessary to determine the details of timing, environment and lateral continuity of the different events. This preliminary paragenetic sequence is given here to highlight the complexity of events that have affected Schaben field strata and, in turn, affected reservoir properties.

1) Deposition of pre-MO surface sediments.
2) Local syntaxial overgrowths on echinoderm fragments. Some minor early compaction in grainstone facies.
3) Dolomitization dominated by very finely crystalline (<10-50 μm) dolomite characteristic of early dolomitization possibly associated with reflux or mixing zone.
5) Dissolution of grains, silica cementation and replacement of dolomite facies and grains. Early silica cementation and replacement is evidenced by silica replacement closely following burrow networks, brittle fracturing of silica areas and fractures in silica filled with surrounding dolomite, displacive growth of silica nodules and soft-sediment deformation of surrounding dolomite. A typical sequence of silica replacement and cementation events is as follows:

A) pervasive chertification of matrix and many grains.
B) dissolution, erosion and corrosion of grains and matrix
C) precipitation of brown, isopachous to equant pore lining or filling chalcedony cement (lines or fills molds, shelter pores, and interparticle pores). This cement does not typically line or fill echinoderm molds possibly indicating later dissolution of echinoderms (Plate 2B).
D) Clear megaquartz pore filling cement; this cement also fills echinoderm molds (Plate 2B).

6) Subaerial exposure at MO surface results in following events and features in underlying strata:

A) fracturing, brecciation, dissolution (Plate 6).
B) development of crusts, fenestral fabric (Plate 5D, 6C), autobreccia.
C) infill of fractures with various dolomite, detrital quartz, clay, and replacive silica matrix and clasts (Plate 6A).
D) fracturing and precipitation of coarse calcite cement in fractures and calcite cementation of fracture matrix (Plate 6A); replacement of dolomite facies (Plate 6B) and replacive silica with poikilotopic calcite. Some dedolomite.
E) possible early precipitation of glauconite (reducing conditions).

7) Deposition of post MO surface facies including abundant evaporites crystals and nodules.
8) Dolomitization dominated by very finely crystalline (<10-50 μm) dolomite characteristic of early dolomitization associated with reflux or mixing zone. Predominance of evaporites is supportive of reflux mechanism.
9) Dissolution of grains and evaporite minerals, silica cementation and replacement of dolomite facies and grains. In addition to previously cited evidence for early silica cementation and replacement, additional evidence includes replacement of radiating bladed evaporite crystal and nodule textures without much breakage or compaction (Plate 3C). The typical sequence of silica replacement fabrics and cements is similar to previously described. In addition, evaporite crystals and nodules were replaced with a generally clear to light brown chert followed by a corrosion/erosion event in which crystals and nodules have a dark brown (Fe-stained?) irregular surface that is overlain by clear megaquartz cement that fills or partially fills remaining porosity (Plate 4A). Evidence for several sequences of silica replacement and cementation include fractures in pre MO surface strata that crosscut all silica replacement fabrics and cements and are filled with a sequence of chert and or chalcedony cement followed by megaquartz cement.
10) Fracturing and brecciation, including collapse breccia from dissolution of evaporites (Plate 7A). Fractures extend into pre-MO surface strata where they crosscut all previous dolomite and chert facies as well as coarse calcite cement and poikilotopic replacive calcite (Plate 6B, 6D, 7C). The fractures are filled with dolomite and, locally, evaporite crystals and nodule fragments from post MO surface sediment and contain clasts of calcite cement, replacive poiklotopic calcite, replacement silica, and silica cement.
11) Post-Mississippian subaerial exposure, resulting in the following:
A) Additional fracturing and brecciation
B) Infiltration of clay and detrital siliciclastic grains
C) Precipitation of coarse calcite cement and replacive poikilotopic calcite (Plate 5C).
12) Burial resulting in the following:
A) Precipitation of coarser (up to 150 μm) baroque dolomite (Plate 7B).
B) Precipitation of pyrite and glauconite.
C) Compaction resulting in stylolites and brittle fracturing of all facies (Plate 7C).

Although reservoir characteristics in strata underlying major subaerial exposure unconformities, such as the Schaben field, are thought to be controlled by processes associated with subaerial exposure, the value of sorting out the different depositional and diagenetic events in these types of fields as listed above is demonstrated by comparing minipermeameter measurements and locations of oil stains in relationship to core data (Figure 2.22). An original depositional facies control for favorable reservoir strata is shown by the predominance of the highest minipermeameter readings and most oil shows occurring in spicule-rich facies that originally had abundant evaporites present and, less commonly, echinoderm-rich wackestones/packstone facies. Burrow mottling was very important in creating and locating fluid flow networks for later diagenetic fluids that resulted in variable porous and non-porous areas on macroscopic and microscopic scales. Early diagenetic events such as dolomitization, dissolution, silica cementation and replacement, associated fracturing and brecciation and poikilotopic calcite

replacement and cementation were important for reservoir architecture. Dissolution of grains and dolomitization created the moldic, intercrystalline and vuggy porosity important for favorable reservoir facies. Early silica cementation and replacement was important in creating the vertical heterogeneity illustrated by minipermeameter measurements and oil staining patterns (Figure 2.22) Whereas silica replacement and cementation tend to result in relatively tight and pervasive replacement in echinoderm-rich facies, the silica replacement and cementation in spicule-rich facies tends to be more variable, especially where evaporites were replaced and tend to contain more moldic and vuggy porosity. The poikilotopic cement associated with the MO subaerial exposure event was extremely important in occluding porosity in underlying strata in the Schaben field as reflected by the low minipermeameter readings and relative lack of oil staining. Both early and late fracturing and brecciation variously enhanced or destroyed reservoir characteristics as indicated by minipermeameter measurements and oil stain patterns (Figure 2.22). Certainly the late fracture and breccia matrix porosity that remained open are important for creating effective porosity when intersecting favorable reservoir facies.

In summary, historically, topographic highs just underlying the post-Mississippian unconformity are viewed as the most favorable locations for petroleum exploration and production. This study shows that the dipping Mississippian ramp strata, accentuated by structural uplift, were differentially eroded at the post-Mississippian unconformity resulting in paleotopographic highs (buried hogbacks, Figure 2.3). The sedimentologic, stratigrahic and paragenetic portion reported in this section indicate that the most favorable areas for successful production may be where spicultic-rich facies containing abundant evaporites intersect fractures associated with the post-Mississippian unconformity and form the topographic highs. In contrast, areas in which echinoderm-rich facies intersect fractures associated with the unconformity and form topographic highs may not be as favorable reservoirs, especially for pre-MO strata.

Clearly, additional studies are necessary to evaluate and confirm the details of paragenesis and determine more fully the relationship of the different events to reservoir architecture. This detailed understanding not only has important implications for Schaben field, but for other similar Mississippian reservoirs in Kansas such as Glick field (Osagian, Rogers et al., 1995), Western Sedgwick basin (Osagian; Thomas, 1982), Bindley field (Warsaw, Ebanks, 1991; Johnson and Budd, 1994) and other similar Mississippian strata outside of Kansas (e.g. Madison Group strata from the Williston Basin of Southeast Saskatchewan, pers. comm. Paul Gerlach).

PLATE 1:

A) Dolomite Mudstone-Wackestone facies. Wispy lamination imparted by clay and horsetail stylolites. This facies is typically tight. Plane polarized light.

B) Sponge Spicule-rich Dolomite Wackestone-Packstone facies. Burrow mottling has created variably tight and porous (blue) areas with abundant moldic and intercrystalline porosity. Plane polarized light.

C) Sponge Spicule-rich Dolomite Wackestone-Packstone facies with abundant sponge spicule moldic and intercrystalline porosity. Plane polarized light.

D) Sponge Spicule-rich Dolomite Wackestone-Packstone facies. In this sample the sponge spicules are siliceous and only a minor amount of intercrystalline porosity is present. Plane polarized light.

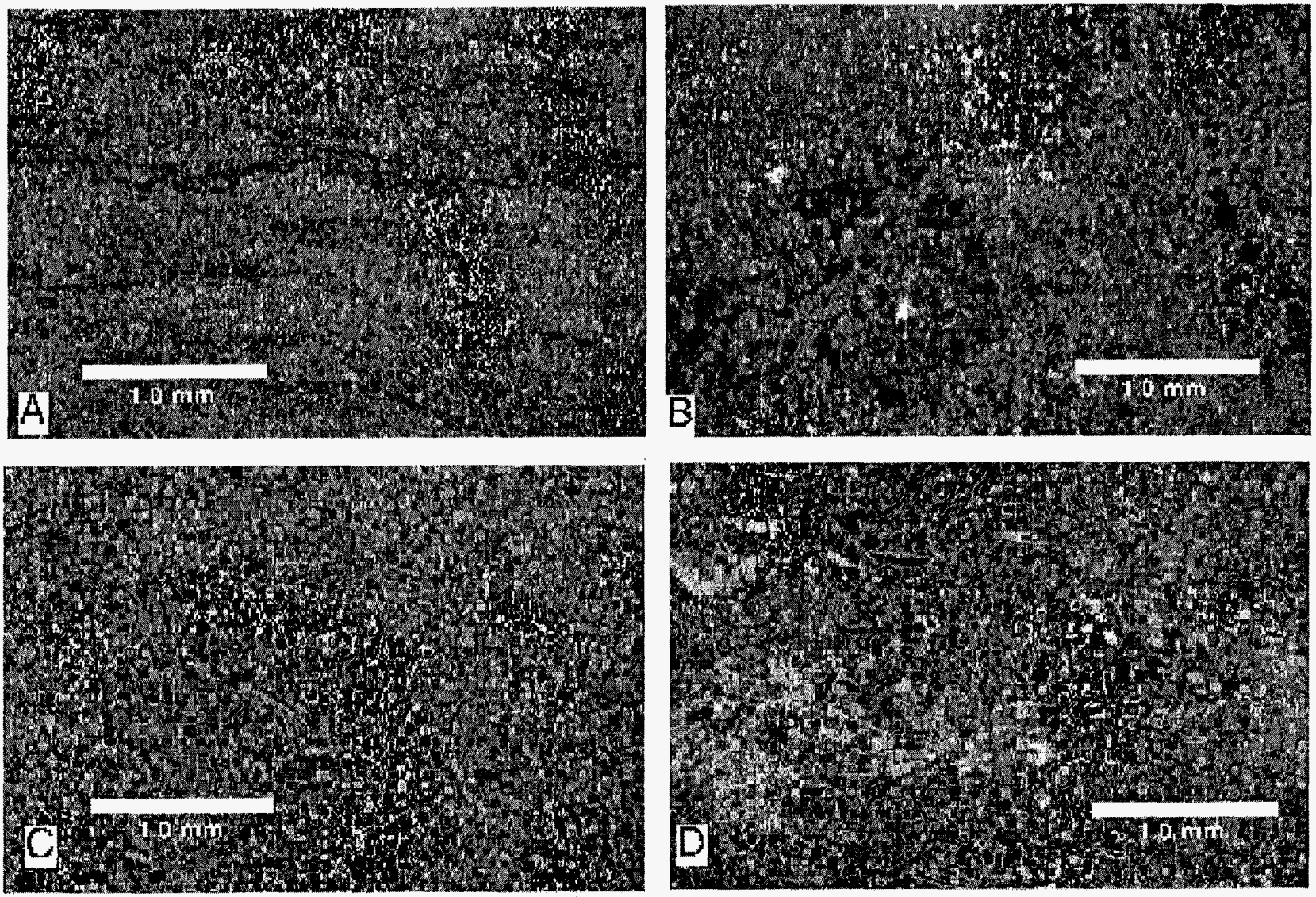

Plate 1

PLATE 2:

A) Sponge Spicule-rich Dolomite Wackestone-Packstone facies. In this sample sponge spicules have been dissolved leaving molds (blue areas) and the surrounding matrix has been replaced by chert. Note the upper left corner of this photomicrograph has not been replaced by chert and is dolomitic. Plane polarized light.

B) Echinoderm-rich Wackestone-Packstone-Grainstone facies. Echinoderm, brachiopod, and other skeletal fragments in this sample have been entirely replaced and cemented by silica. Red arrow points to initial chert replacement, white arrow points to brown isopachous chalcedony cement that lines primary pores, and the green arrow points to clear pore-filling micro-megaquartz cement. Plane polarized light.

C) Echinoderm-rich Dolomitic Wackestone-Packstone-Grainstone facies. Echinoderm fragments and other skeletal fragments, including sponge spicules (white arrow), have been dissolved leaving abundant moldic porosity (blue areas). Plane polarized light.

D) Echinoderm-rich Wackestone-Packstone-Grainstone facies. This is an example of porous (tripolitic) chert texture. The grains in this sample have been preserved by chert replacement and surrounding matrix has been dissolved leaving abundant interparticle, vuggy, and some intercrystalline porosity. Plane polarized light.

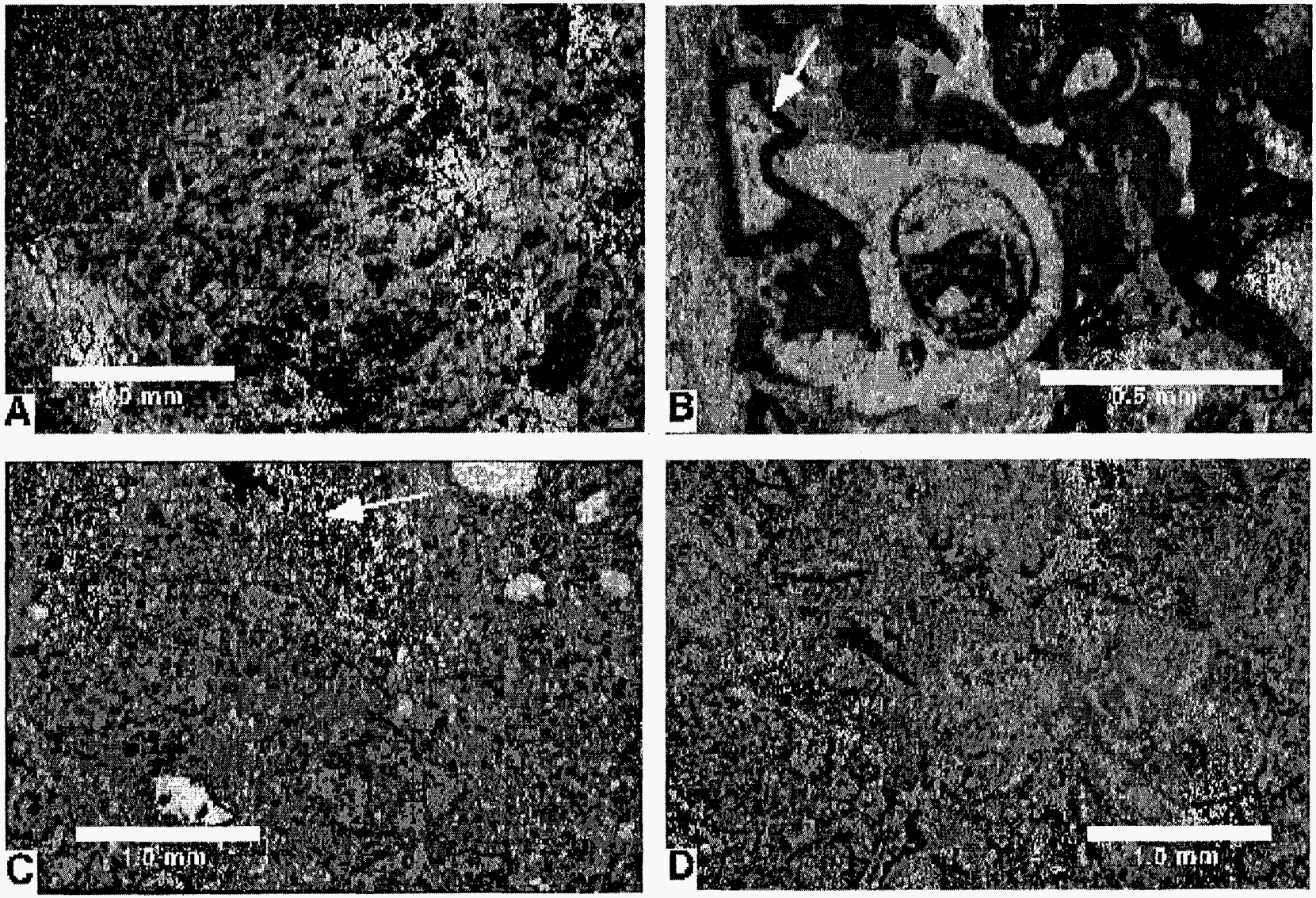

Plate 2

PLATE 3:

A) Chert and chalcedony filled fracture in dolomitic mudstone-wackestone facies. Note the fracture was subsequently fractured and the surrounding dolomitic matrix fills in around fractured areas without brittle fracture. Plane polarized light.

B) Partial chert replacement of Sponge Spicule-rich Dolomite Wackestone-Packstone facies. Some sponge-spicule molds (blue areas) can be identified in chert areas. Note brittle fracturing of chert and infill by surrounding dolomitic matrix indicating early chert replacement and differential compaction. Plane polarized light.

C) Silica-replaced bladed and radiating bladed texture of original evaporite (anhydrite/gypsum) minerals. This sample exhibits displacive growth of crystals and formation of nodules in dolomitic sediment. Preservation of the radiating crystal/nodule texture suggests early replacement by silica prior to any significant compaction. Plane polarized light.

D) Zebraic chalcedony pore-filling cement which is assorted with evaporite minerals. Crossed nicols.

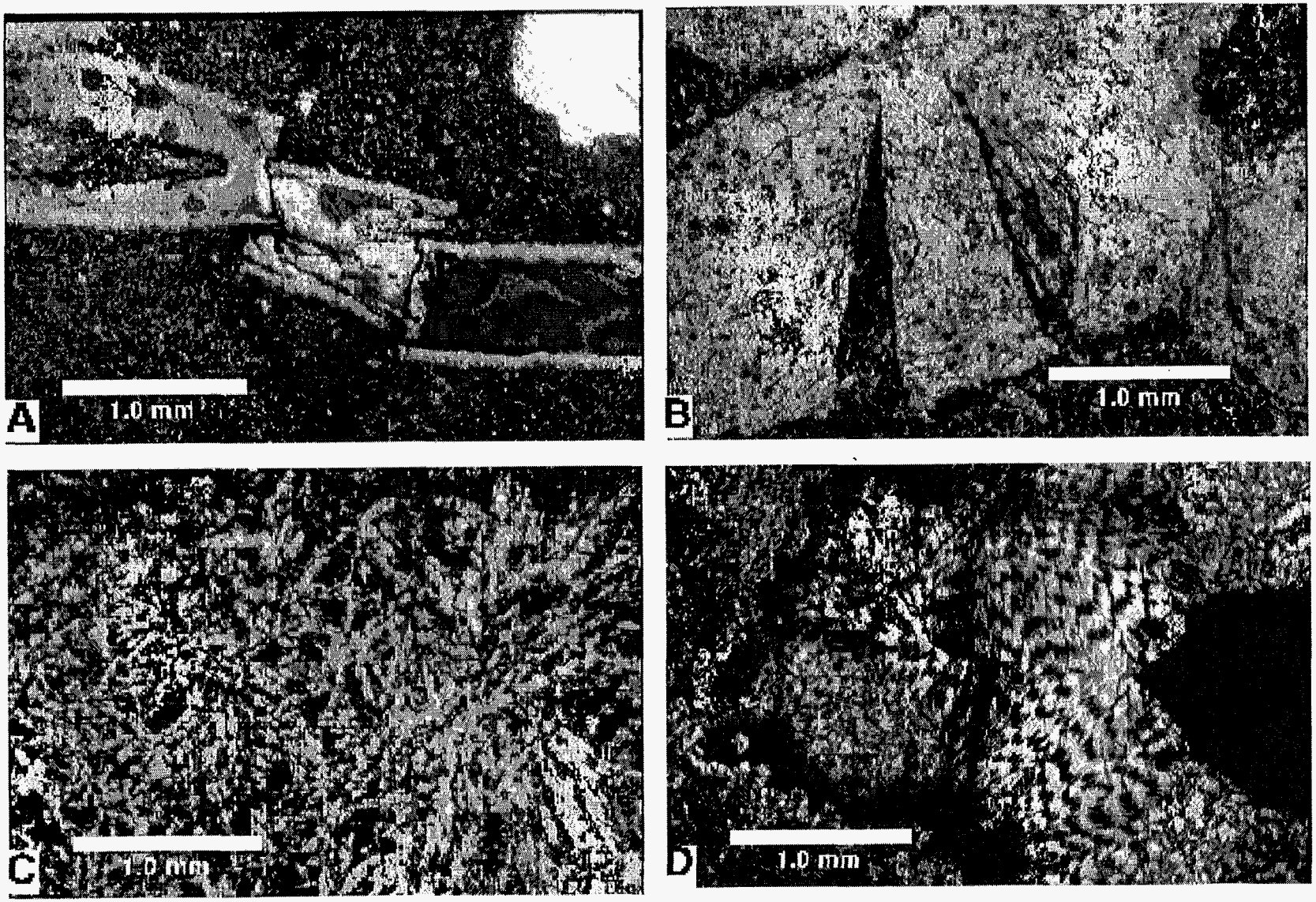

Plate 3

PLATE 4:

A) Replacement of original evaporite crystals and nodule by clear to brown chert (white arrow). This was followed by a dissolution/corrosion/erosion event (blue arrow). Remaining porosity was filled by clear megaquartz cement (black arrow). Plane polarized light.

B) Dolomitic matrix cut by a fracture filled with chert and detrital quartz. Plane polarized light.

C) Autobreccia fabric indicative of in-place brecciation. Plane polarized light.

D) Chaotic breccia fabric with subround to round detrital quartz and megaquartz cement grains and angular to subangular chert fragments in dolomitic and chert matrix. Plane polarized light.

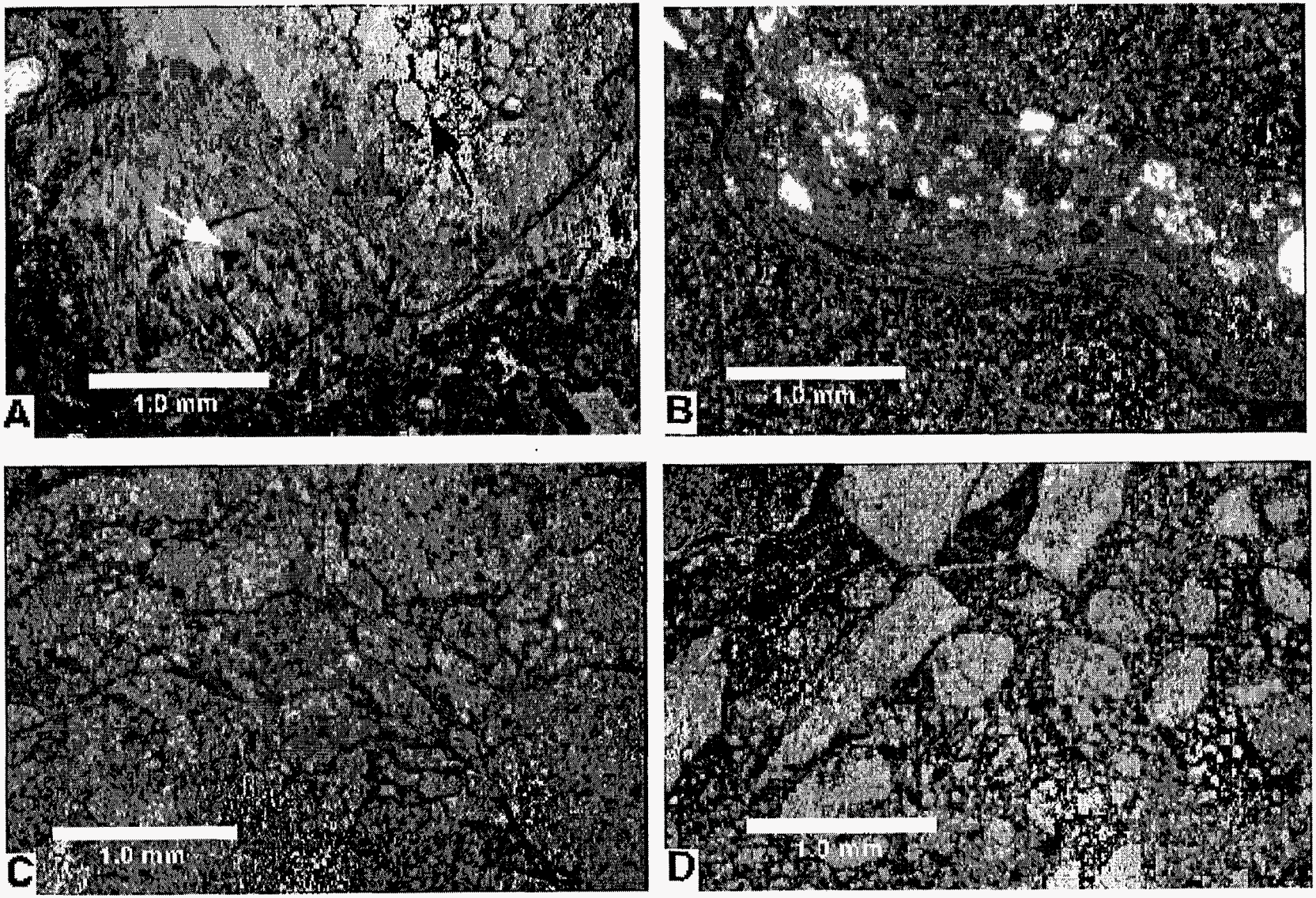

Plate 4

PLATE 5:

A) Echinoderm-rich Dolomitic Wackestone-Packstone-Grainstone facies. Note that grain molds and intercrystalline porosity (blue areas) are lined with oil and connected by fractures (white arrows). Plane polarized light.

B) Coarse calcite cement and poikilotopic calcite (red-stained areas) that is common below the MO. White arrow points to a dolomite rhomb "floating" in calcite. Plane polarized light.

C) Poikilotopic replacive calcite just below post-Mississippian unconformity. Here the calcite replaces sponge spicule-rich facies. The dark areas (white arrow) are extinction patterns of poikilotopic calcite. Crossed nicols.

D) Dolomitic matrix below the MO surface with abundant fenestral pores (white areas). Note one pore filled with coarse calcite cement (red-stained area). Plane polarized light.

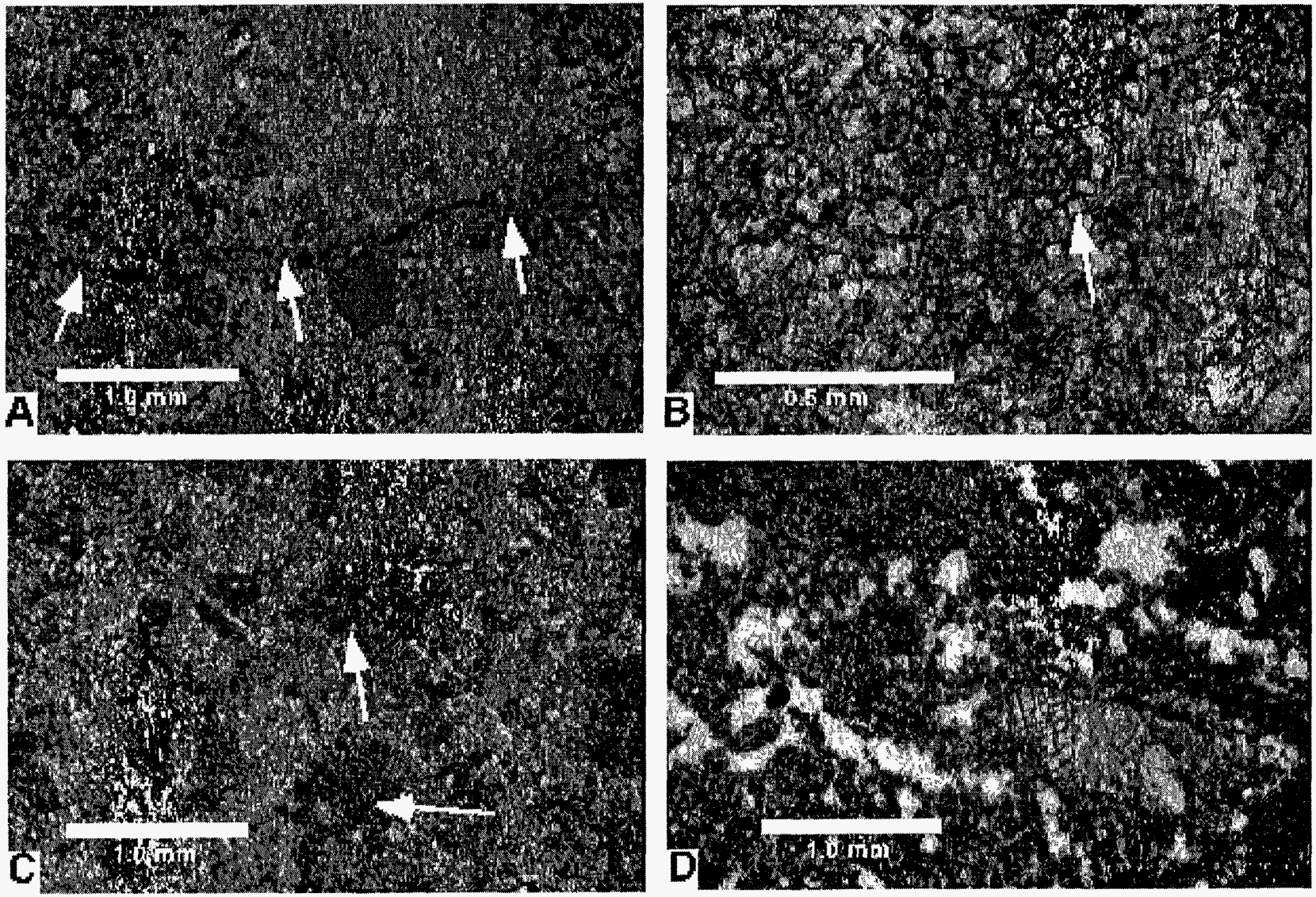

Plate 5

PLATE 6:

A) Fracture below the MO surface filled with dolomite, clay, detrital quartz (white arrow) clasts and matrix that is cemented by coarse calcite cement (blue arrow). Plane polarized light.

B) Fracture below the MO surface that contains angular poikilotopic calcite clasts (red-stained) and detrital quartz in very finely crystalline dolomitic matrix. Plane polarized light.

C) Altered facies below the MO surface. Some altered areas are characterized by a central area filled with coarse calcite cement (white arrow) surrounded by a halo rich in iron and fenestral pores (white areas) in dolomitic and replacive poikilotopic calcite matrix. Plane polarized light.

D) Poikilotopic calcite replaced facies (red-stained areas) below the MO surface that were subsequently fractured. The fracture is filled with very finely crystalline dolomite from above the MO surface and locally contains clasts of poikilotopic calcite (white arrow). Note the truncated coarse calcite cement filled fracture in the poikilotopic calcite area in the bottom right portion of the photomicrograph. Plane polarized light.

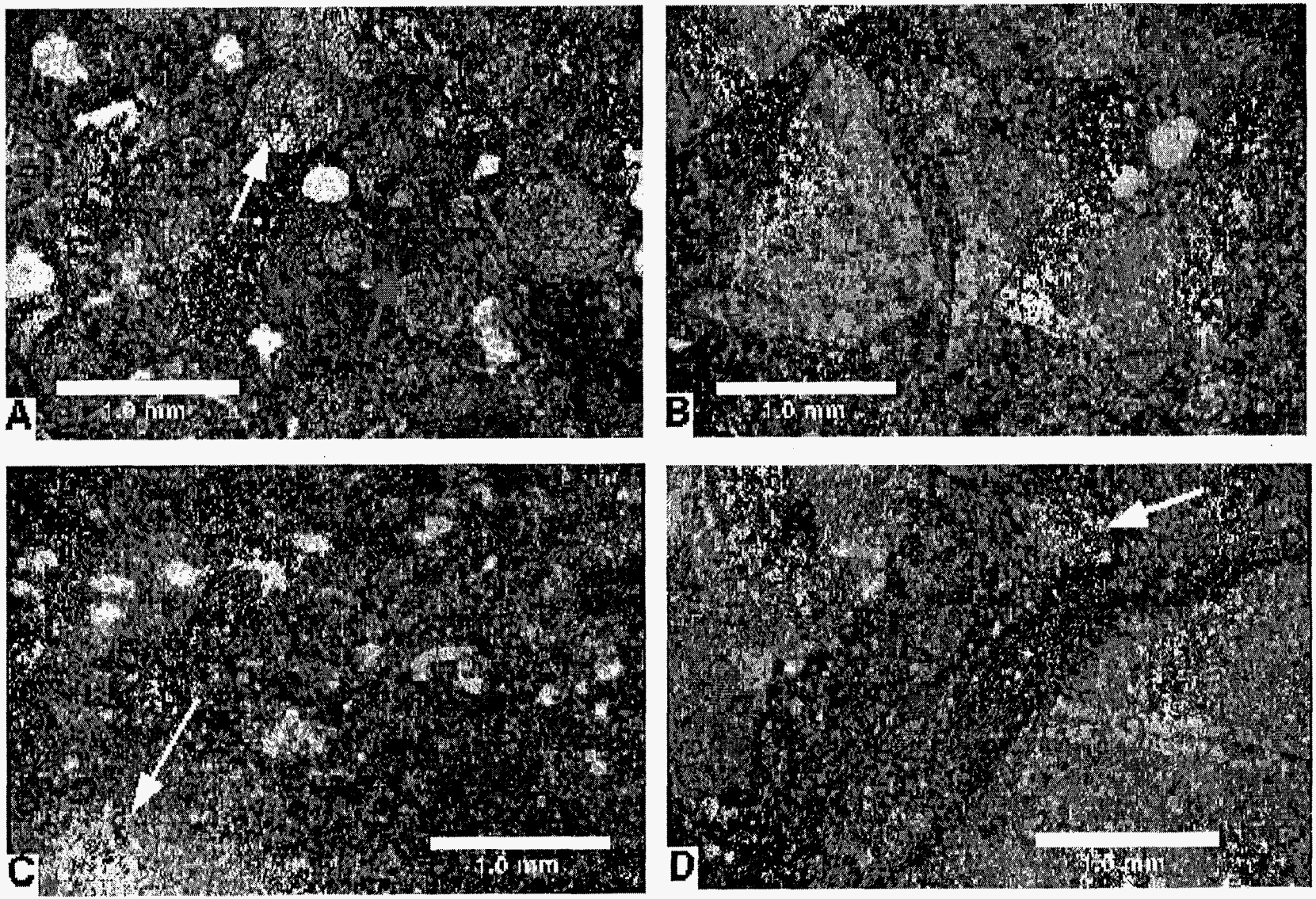

Plate 6

PLATE 7:

A) Silica replaced evaporite mineral blades and nodule cut by later fracture partially filled with very finely crystalline dolomite and evaporite matrix containing evaporite nodule clasts. Plane polarized light.

B) Late stage baroque dolomite (white arrow points to rhomb) and glauconite cement (red arrow). Plane polarized light.

C) Coarse calcite cement and poikilotopic calcite areas (1) cut by fracture filled with Fe-rich dolomite (2). Later open fractures (3) crosscut all previous facies and events. Plane polarized light.

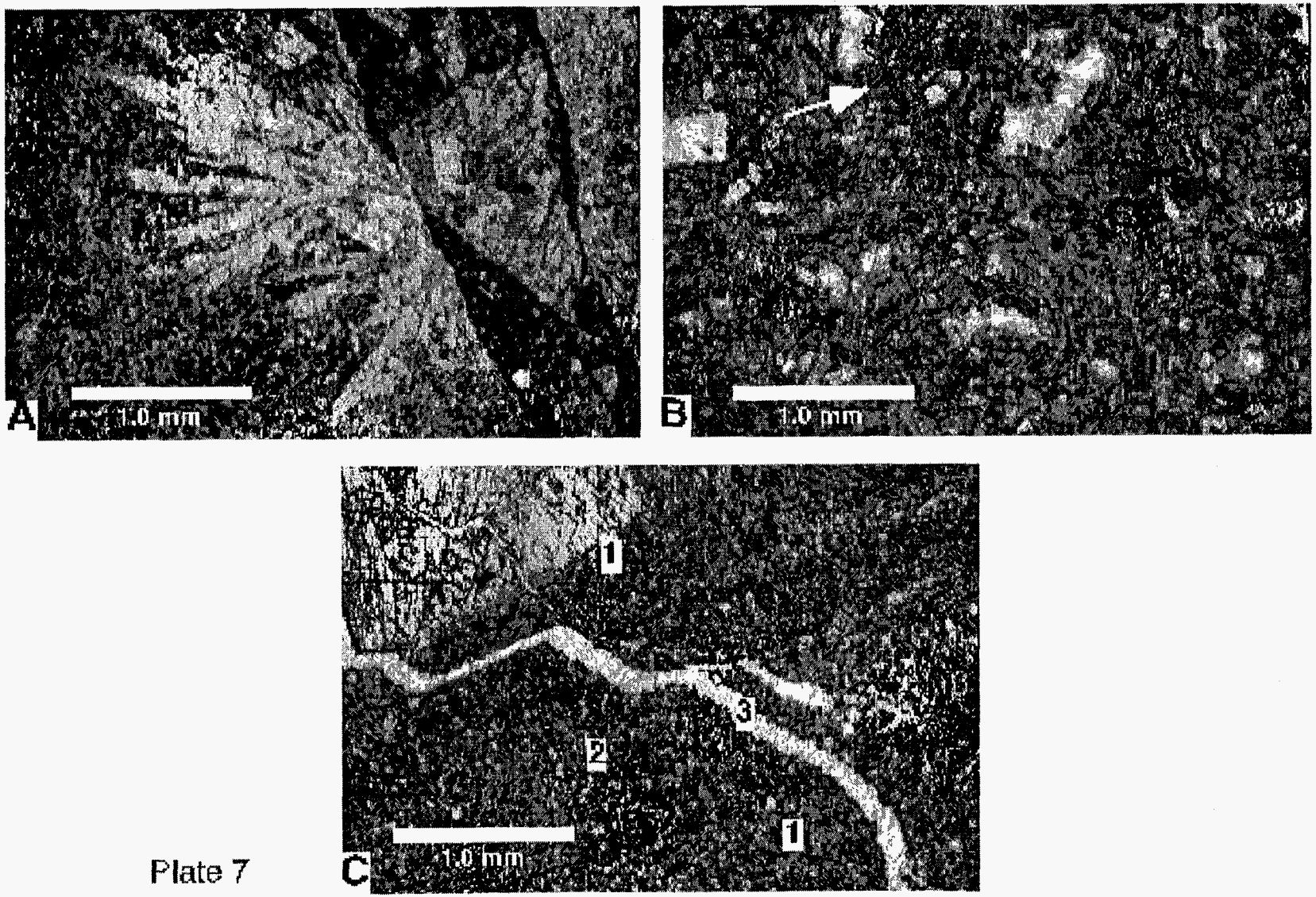

Plate 7

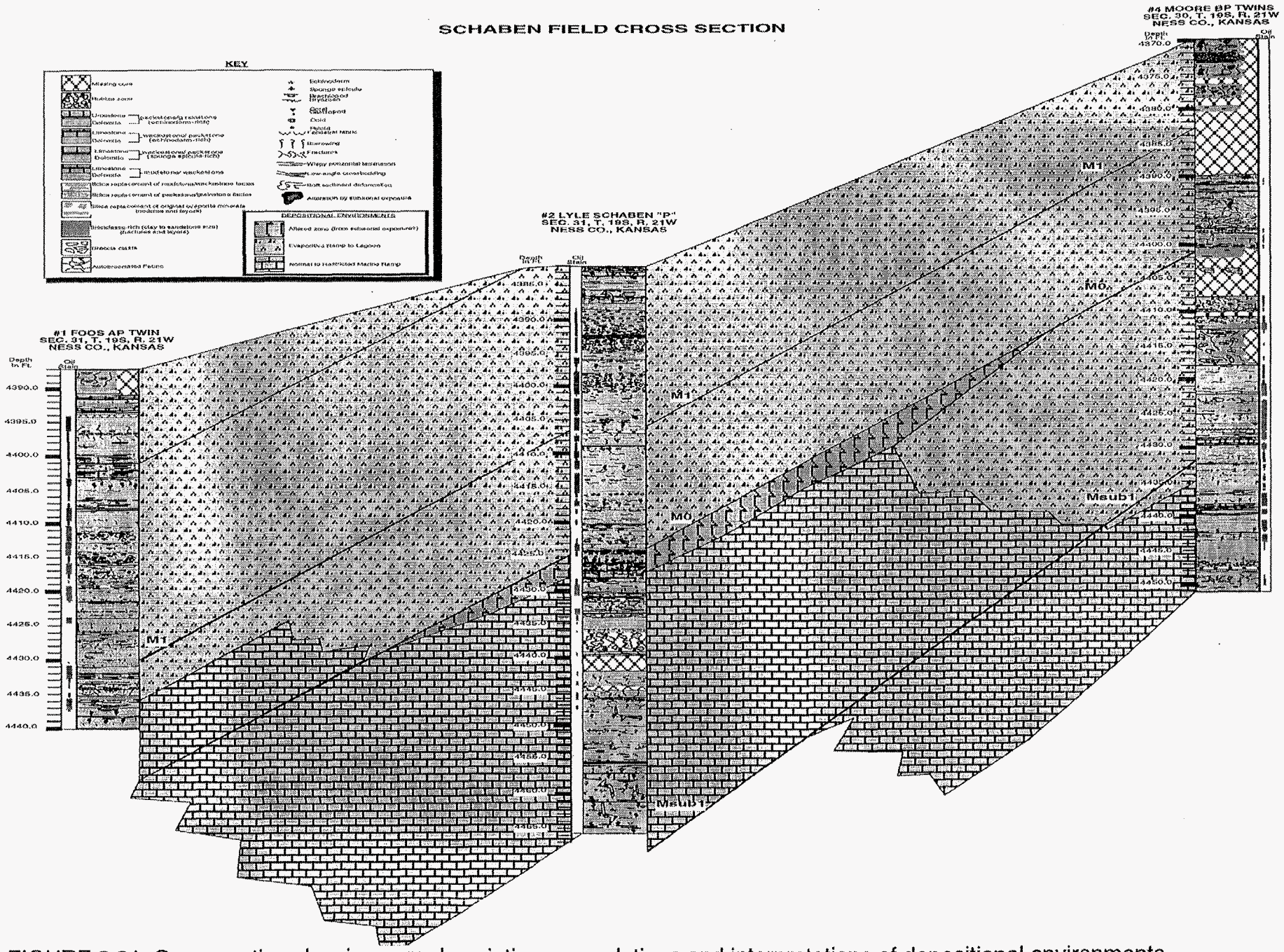

FIGURE 2.21: Cross section showing core descriptions, correlations and interpretations of depositional environments.

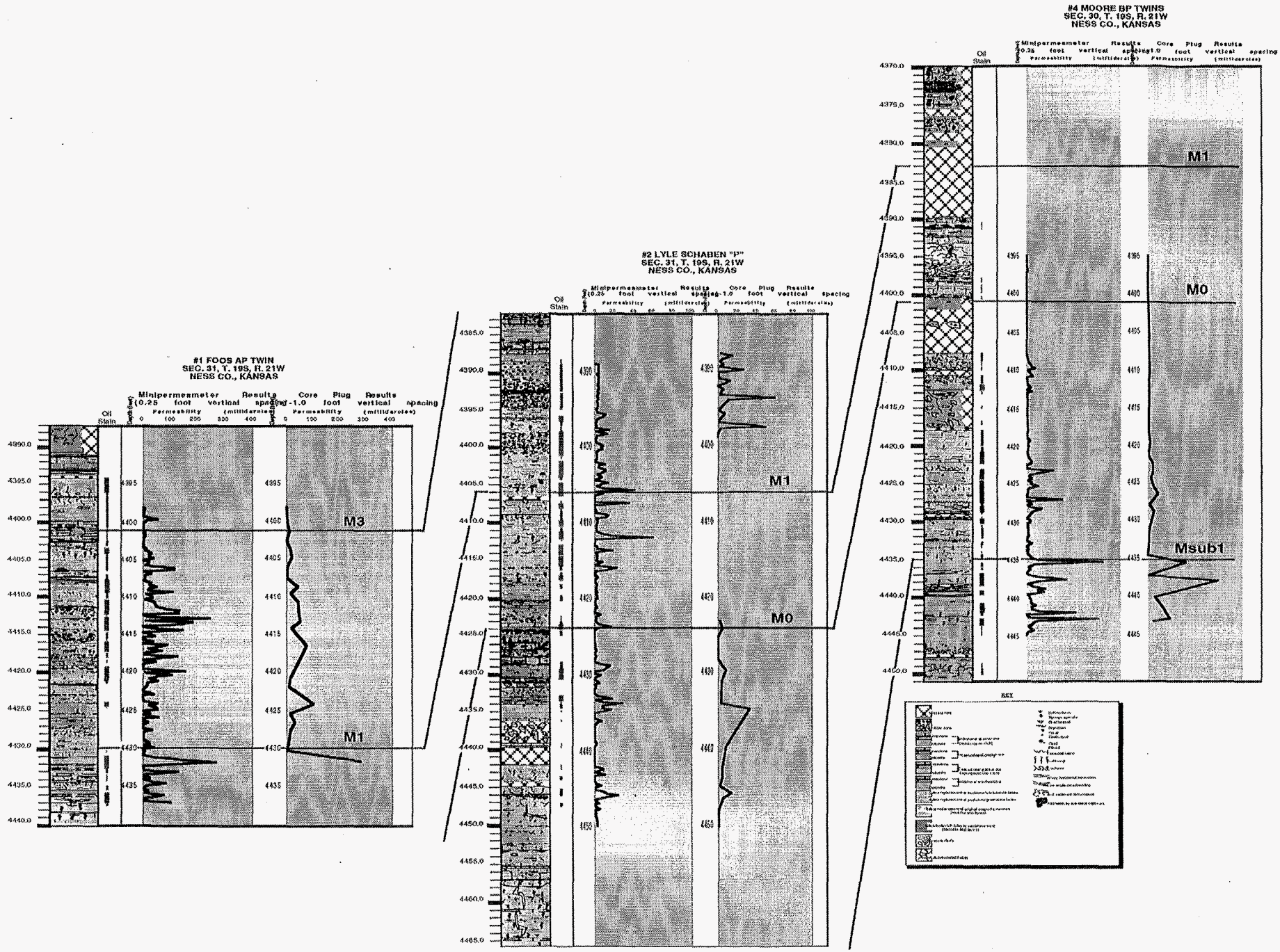

FIGURE 2.22: Cross section showing core features and associated permeability data from minipermeameter measurements and standard core plug measurements.

2.3 RESERVOIR MODEL

2.3.1 Field Data and Full Field Reservoir Parameters

FIELD DATA

GENERAL DATA

State:	Kansas
County:	Ness
Location:	Township 19 South--Range 21 West, Township 20 South--Range 21 West, and Township 19 South--Range 22 West
Discovery Date:	September 4, 1963
Discovery Well(s):	Cities Service Oil Company, #1 Moore 'B' SE SE 30-T19S-R21W Mississippian Oil, 4494' RTD
Field Size:	8,880 acres
Wells	
Total:	90
Operating (1996):	67
Abandoned:	25

RESERVOIR DATA

Producing Formation(s):	Mississippian (Osagian)
Lithology:	Dolomite, Chert, Limestone
Average Depth:	4400' (-2100' subsea)
Original Oil/Water Contact	-2145' subsea
Average Porosity:	17.5 %
Permeability Horizontal (Estimated):	6.5 md to 167.0 md
Permeability Vertical (Estimated):	0.15 times horizontal permeability
Archie Equation Parameters:	a=1, m=2, n=2, Rw =0.13
Temperature:	115 F
Original Field Pressure:	1100 psi
Present Field Pressure:	1100 psi

PRODUCTION DATA

Original Oil In Place (Volumetrics): 40 - 50 MMBO
Cumulative Oil Production (mm/yy): 9.1 MMBO (September 1996)
Estimated Recovery Factor: 17%
Present Oil Production:

Cumulative Produced Water (Estimated):
Present Produced Water (Estimated):

FLUID PROPERTIES:

Crude Oil

API Gravity	40
Viscosity at P_{BP}:	2.5 cp
Initial Solution Gas-Oil Ratio:	50 cu. ft/bbl
Formation Volume Factor at Pi:	1.037 RB/STB
Bubble Point Pressure:	225 psia

Gas

Viscosity at P_{BP}:	0.0108 cp
Formation Volume Factor at P_{BP}:	0.0123 RB/SCF

Produced Water:

Total Dissolved Solids:	30,000 ppm
Viscosity at P_{BP}:	0.65 cp

FULL FIELD SIMULATION PARAMETERS

1. Number of grid blocks:

A first step in a simulation study is establishing a pattern of grids that is able to properly define the reservoir. Any mapping or gridding software can be used for this purpose. In this study, the Geographix mapping and gridding package was used to generate the grid maps of porosity, saturation, permeability, pressure, and pay thickness.

Grid sizes were selected such that there were 5 grid blocks between wells. This spacing was thought to be sufficient to represent the reservoir. Also, the effects of numerical dispersion in BOAST 3 are reduced if there are about 4 to 5 grid cells between the wells. Figure 2.23 shows the location of wells in the grid pattern generated for Schaben field.

Sub-surface petrophysical cross-sections in Schaben field show that the original oil column has migrated across multiple correlated zones within the Mississippian. This suggests that the oil migrated into the anticlinal structure through a fracture system rather than by capillarity. The presence of fractures in the cores, obtained from the 3 recently drilled wells, confirms a fracture system within the reservoir. Also, reservoir heterogeneity is a typical characteristic for most Mississippian carbonate reservoirs. However, limited petrophysical and core data in the Schaben field do not allow a complex description of the reservoir. Fluid production data over the life of the field shows an increasing rate of water production with time. DST results from recently drilled wells indicate that the current reservoir pressure is close to the original reservoir pressure. These observations suggest a strong recharge of the reservoir by an underlying aquifer. Considering these observations, the Schaben field simulation was simplified as a two-layer model in the z direction that included a reservoir layer with an underlying aquifer layer.

2. Grid block dimensions:

The grid block dimensions are 220 feet by 220 feet and are same for both the reservoir layer and the aquifer. From petrophysical logs covering the Mississippian at the Schaben demonstration site, it is difficult to distinguish between productive and non-productive zones, therefore gross and the net pay thickness is assumed to be equal. Gross/net pay was selected from petrophysical logs as the interval from the top of the reservoir to the oil water contact (OWC) at -2145 feet subsea. Figure 2.24 shows the gross/net pay thickness of layer 1. OWC was established from DST data, production test data, and petrophysical analysis. All petrophysical analyzes were generated using PfEFFER (see section 2.2.2.4). A uniform aquifer thickness of 100 feet was assumed in this study. Petrophysical logs from some of the deep wells surrounding the Schaben field show an approximate aquifer thickness of 100 feet.

3. Dip angle:

The regional dip of the Mississippian formation across the demonstration area is a quarter of 1-degree (0.25°). Given the negligible regional dip angle, a zero dip angle was used in this simulation study.

4. Depth to the top of the grid blocks in the top most layer.

The depth to the top of layer 1 (pay-zone) is the distance between the datum of sea level and the top of the reservoir. This interval was obtained from the petrophysical logs. Figure 2.25 is a map showing the depth to the top of the reservoir from a datum of sea level.

5. Reservoir Porosity and Permeability:

The PfEFFER log analysis package (see Section 2.2.2.4) was used to determine the total reservoir porosity at each well. Calculated porosity at each well is the average value obtained over the net pay interval. Porosity values in Schaben field were obtained from a wide suite of logs, both old and new, and run over a period of 35 years. For the simulation, porosity obtained from the log calculations was labeled total porosity and assumed to be made up of both micro- and macro-porosity. Based on core analysis, under reservoir pressures the micro-pores do not appear to contribute to fluid flow within the reservoir, and are saturated with immobile water. Under reservoir pressures, it was assumed that the fluid-flow took place only through macro-pores. Hydrocarbons are assumed to reside only in the macro-pores. Correlation between core porosity and macro-porosity, at reservoir pressure, was obtained from the NMR studies on 18 core plugs selected from wells drilled as part of the project (Figure 2.26). Based on the results of core studies, core porosity was assumed to equal to the log porosity. Since the pore volume making up the macro-pores is believed to contribute solely to the fluid-flow in the reservoir, the macro-porosity was used as the effective porosity in the simulation. Figure 2.27 is the effective porosity map of Schaben field.

A horizontal matrix permeability to effective porosity cross-plot (Figure 2.28) was obtained from laboratory measurements on 104 cores plugs taken from cores of the three most recently drilled wells. The permeability range observed from core plugs is 1.3 to 33.4md.. As mentioned earlier, fluid-flow in Schaben field is influenced by a fracture-matrix system. Examination of the permeability obtained from DST tests in 5 wells indicate average permeability values ranging between 73 to 246md. Matrix permeabilities appear to underestimate the effective permeability in the reservoir. Simulation runs using only the matrix permeability were unable to support the historical production rates of oil and water. Sensitivity analysis and history matching from iterative simulation runs resulted in the use of an effective horizontal permeability that was five times the matrix permeability (Figure 2.29). The permeability values adjusted for the simulation are similar to observed values from Mississippian DST test and ranged from 6.5 to 167.0 md.

Horizontal permeability measurements were obtained from approximately 150 core plugs, taken from cores of seven different wells, was available. A plot of maximum horizontal matrix permeability against the direction 90^{o} to the maximum resulted in a slope near 1 (Figure 2.30). Based on this plot, it was assumed that the horizontal permeability in the X and Y directions is equal.

In fractured reservoirs, an assumption is often made that the vertical permeability is one tenth that of the horizontal permeability. A histogram plot of the ratio of horizontal and vertical permeability from 48 core plugs from the Schaben demonstration site is shown as figure 2.31. The highest frequencies are between the permeability ratios of 0.05 and 0.2 with a mean value of 0.15. Initial simulation runs used a horizontal to vertical matrix permeability ratio of 0.1. Sensitivity analysis and production history matching from iterative simulation runs were used to adjust the vertical permeability to 0.15 times the horizontal permeability (Figure 2.32).

6. Relative Permeability & Capillary Pressure:

Data relating relative permeability ratio (K_{rw}/K_{ro}) at different water saturations were available from standard laboratory core plug measurements from the well #1 Moore D. This relative permeability ratio curve was used to generate relative permeability curves (i.e., K_{ro} vs. S_w and K_{rw} vs. S_w). Initial simulation runs were carried out using these relative permeability curves. However, the end points and the shape of both the curves were modified in order to match the historical production data of the field. The final relative permeability data used in the simulation were obtained from the exercise of history matching over a period of 34 years (Figure 2.33).

Eighteen core plugs from the pay zone were selected from the cores of three different wells, and capillary pressure tests were carried out on them. The irreducible water saturation was obtained from the relative permeability data. From the series of 18 capillary pressure curves, the curve showing an asymptotic rise closest to the irreducible water saturation was selected as the representative capillary pressure curve.

7. PVT data:

Historical production data from Schaben demonstration site indicates that gas production was never significant during the history of the field. Thus, a solution gas-oil-ratio of 50 cu. ft/bbl was assumed in this study. The gas gravity was assumed to be 0.7 (air=1.0). Production records show that the average API tank gravity of the oil is 40 degrees and the average reservoir temperature is 115°F.

A bubble point pressure of 225 psi was calculated from standard correlations. The subsea depth corresponding to this bubble point pressure was -2100 feet. This is the average subsea depth of the reservoir across the field. The oil viscosity above and below the bubble point was calculated with the help of standard correlations. The viscosity of dead oil at reservoir temperature was determined as 2.5 cp, with a slope of oil viscosity above bubble point of 0.000495 cp/psi.

The oil formation volume factor at bubble point and above the bubble point was also calculated using standard correlations. The oil formation volume factor at bubble point was determined as 1.037 RB/STB with a slope of oil formation volume factor above bubble point of -0.000005 RB/(STB.psi).

Water analyzes available from wells in the Schaben demonstration area indicate average total dissolved solids are 30,000 ppm. Correlations were used to calculate the water viscosity corrected to average reservoir temperature and pressure (Water viscosity = 0.65 cp). Standard correlations were also used to calculate the formation volume factor of water at pressures above the bubble point.

The calculated average reservoir porosity for all the grid blocks is 17.5%. This average porosity was used to determine the total rock compressibility of the reservoir from standard correlations (Total rock compressibility = $3.8*10^{-6}$ psi^{-1}).

Gas formation volume factor and gas viscosity was calculated at bubble point pressure, and also at pressures above the bubble point with the help of standard correlations. The gas viscosity at bubble point was determined as 0.0108 cp with a slope above bubble point of 0.0123 RB/scf.

The stock tank properties of oil, gas and water used in the simulation are:

density of oil = 51.46 lb/cu. ft;
density of water = 64.55 lb/cu. ft;
density of gas = 0.0535 lb/cu. ft.

8. Oil saturation:

Since the Schaben field has not produced significant volumes of gas, the sum of water and oil saturation was assumed to be unity. Initial water saturation at individual wells was determined from well log analysis using the PfEFFER log analysis package (see Section 2.2.2.4). Total water saturation as calculated at individual wells and effective porosity as determined from log calculations and NMR analysis (Figure 2.26) were used to create a effective oil saturation (1-water saturation) map for the Schaben demonstration area. Effective oil saturation in each 220' X

220' grid cell was obtained by dividing the total volume of oil present in each grid by the effective pore volume of that grid (Figure 2.27). This effective oil saturation was then normalized so that no grid cell had a value of effective oil saturation more than 75% (Figure 2.34). This normalization was carried out because the relative permeability curves indicate that the water stops moving at saturations below 25%.

9. Water saturation:

The water saturation in the effective porosity of each grid cell was obtained by subtracting the effective oil saturation from 1.

10. Pressure:

The average DST shut-in pressures in the Mississippian reservoir at Schaben Field were used to generate an initial reservoir pressure map (Figure 2.35). The reservoir pressure map showed that most of the reservoir had pressures above 1100 psi. However, two regions at the periphery of the field showed pressures in the region of 400 psi. These anomalous low pressures were removed from the analysis and the final map normalized so that all the grid cells had a minimum pressure of 1100 psi. (Figure 2.35).

11. Aquifer:

Schaben field appears to have an active bottom water drive. Simulation was based on a two-layer model with the bottom layer acting as the aquifer. The aquifer in this simulation was designed solely to supply the necessary water required to recharge the reservoir layer and maintain reservoir pressure over time. An uniform porosity of 25% was used for the aquifer. The aquifer porosity was obtained from the well logs of Humburg #1. This is one of the few deep wells in the field with an adequate electric log suite across the aquifer. Oil flow in the reservoir is restricted to the upper layer, and is unaffected by the aquifer permeability. Vertical permeability in the aquifer plays a critical role in controlling the water production at the wells. A good field match was obtained (within 18% of what is believed to be the water production in the field) when a value of 25md was assumed as the horizontal permeability of the aquifer along with a vertical permeability ranging between 0.1 to 4.5md. As in the reservoir layer, aquifer permeability in the X and Y direction was assumed to be equal. The aquifer pressure was assumed to be higher than the maximum pressure value in the reservoir, and was assigned a constant value of 1400 psi.

12. Limiting factors imposed on the simulation:

Maximum number of time steps allowed in the run = 9999
Limiting maximum water/oil ratio = 100
Limiting maximum gas/oil ratio = 1000
Limiting minimum field average pressure = 100 psi
Limiting maximum field average pressure = 2000 psi
Maximum saturation change permitted over a time step = 0.3
Maximum pressure change permitted over a time step = 200 psi

Boast 3 Simulation
Schaben Field

Well Locations and Grid Cells

Grid Cell Dimensions
220 ft X 220 ft

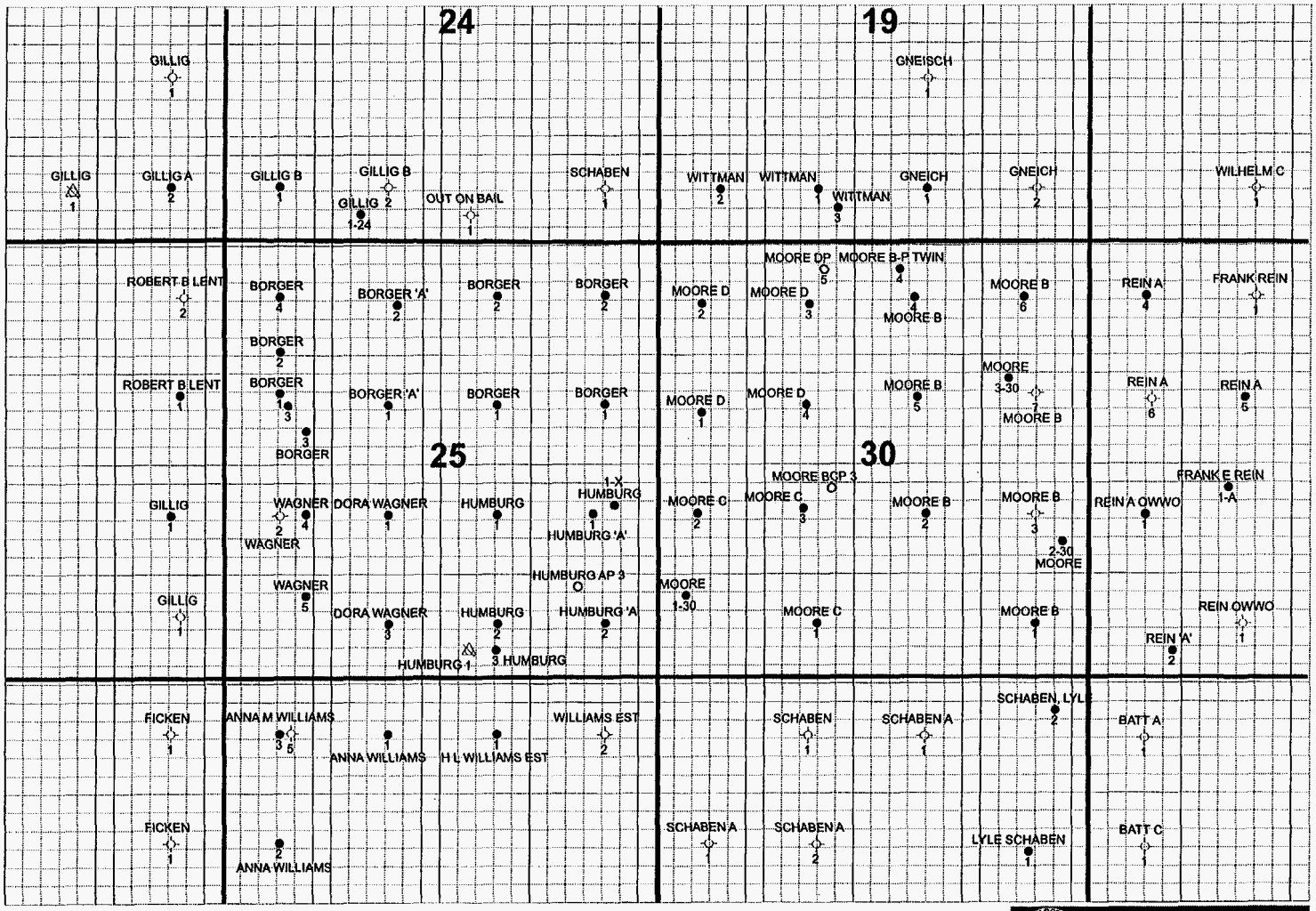

Upper Left Cell is Row 1 / Column 1
Lower Right Cell is Row 49 / Column 72

Kansas Geological Survey

Figure 2.23

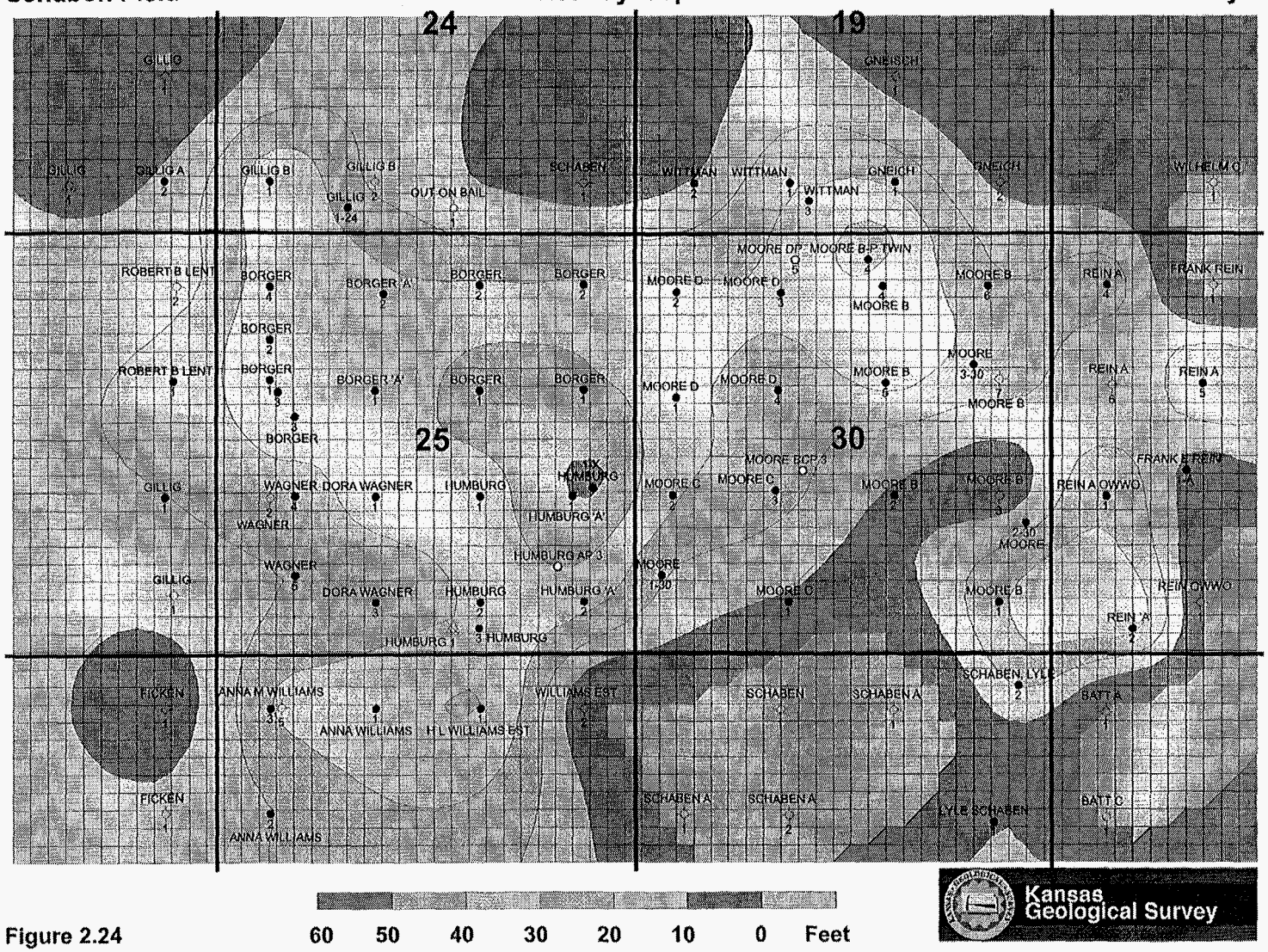
Boast 3 Simulation
Schaben Field
Layer 1
Net Pay Isopach
Date: 1963
Time = 0 Days
24
19
25
30
60 50 40 30 20 10 0 Feet
Kansas Geological Survey

Figure 2.24

Boast 3 Simulation
Schaben Field

Depth to Layer 1
Datum: Sealevel

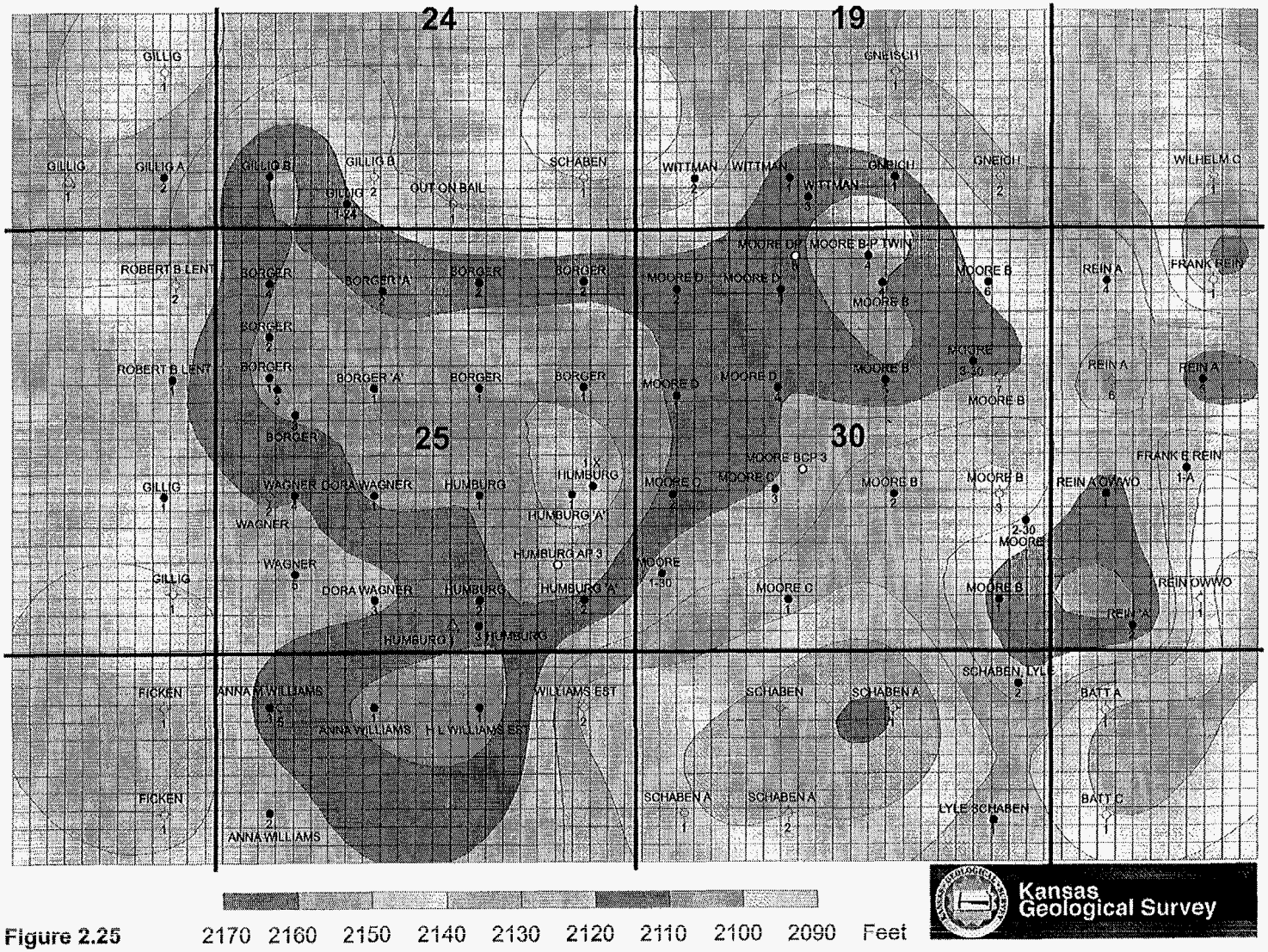

Figure 2.25

Boast 3 Simulation
Schaben Field

NMR Derived Effective Porosity vs. Core Pororsity

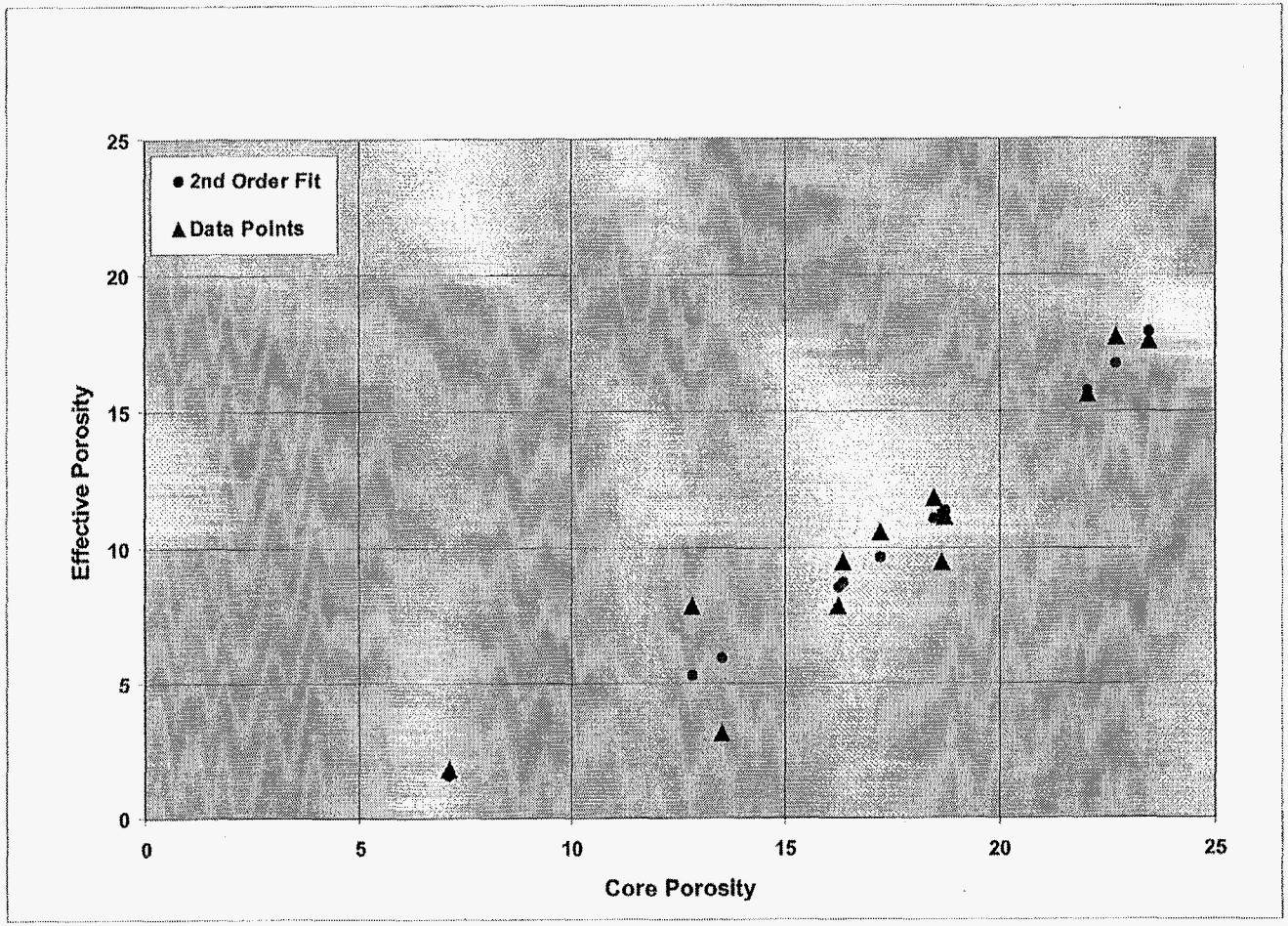

Kansas Geological Survey

Figure 2.26

Boast 3 Simulation
Schaben Field

Effective Porosity
[Total Porosity - Micro Porosity]

Layer 1
Payzone

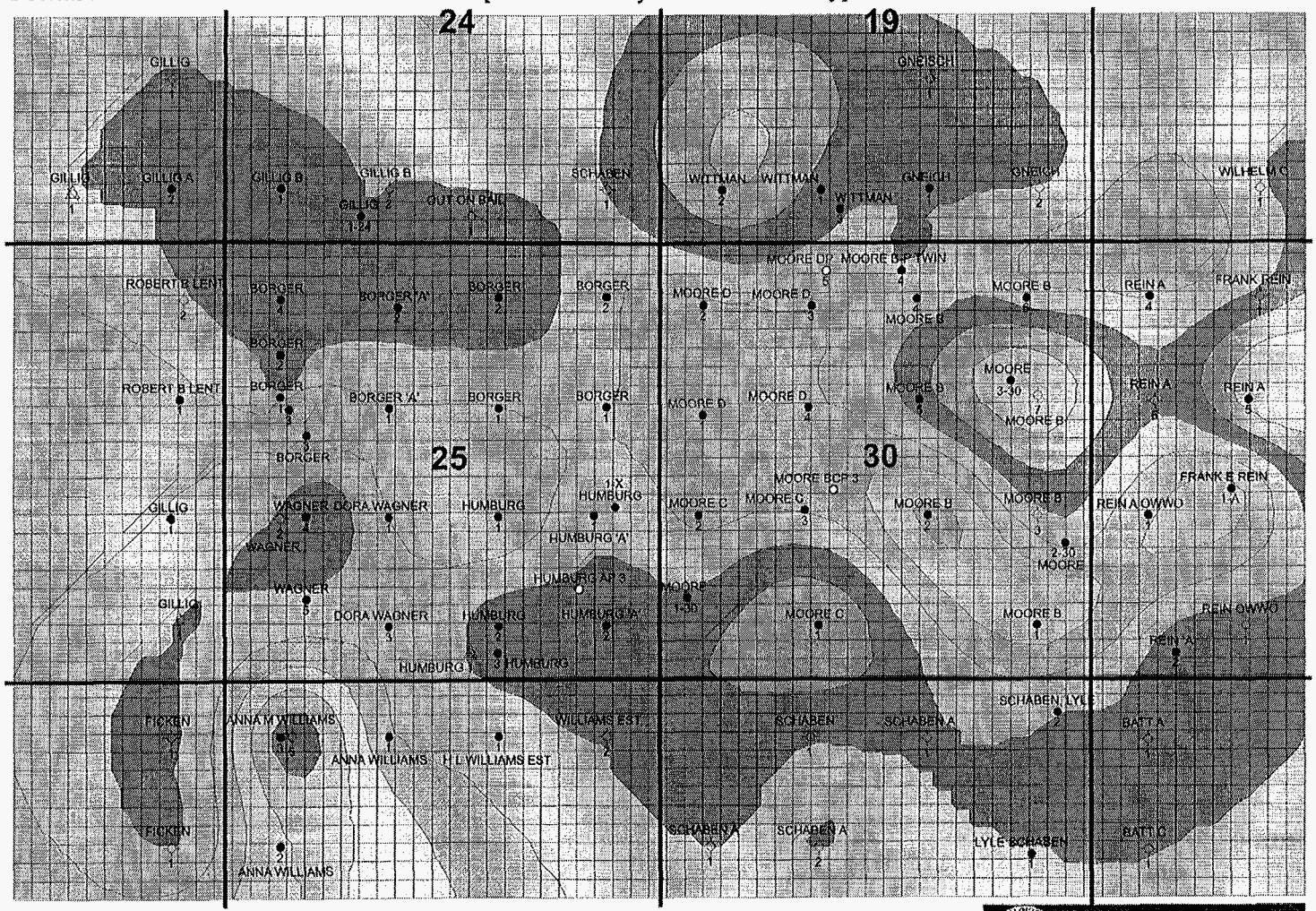

.170 .155 .140 .125 .110 .095 .080 .065 .050 **Porosity**

Kansas Geological Survey

Figure 2.27

Boast 3 Simulation
Schaben Field

Horizontal Matrix Permeability vs. Effective Pororsity

Layer 1
Payzone

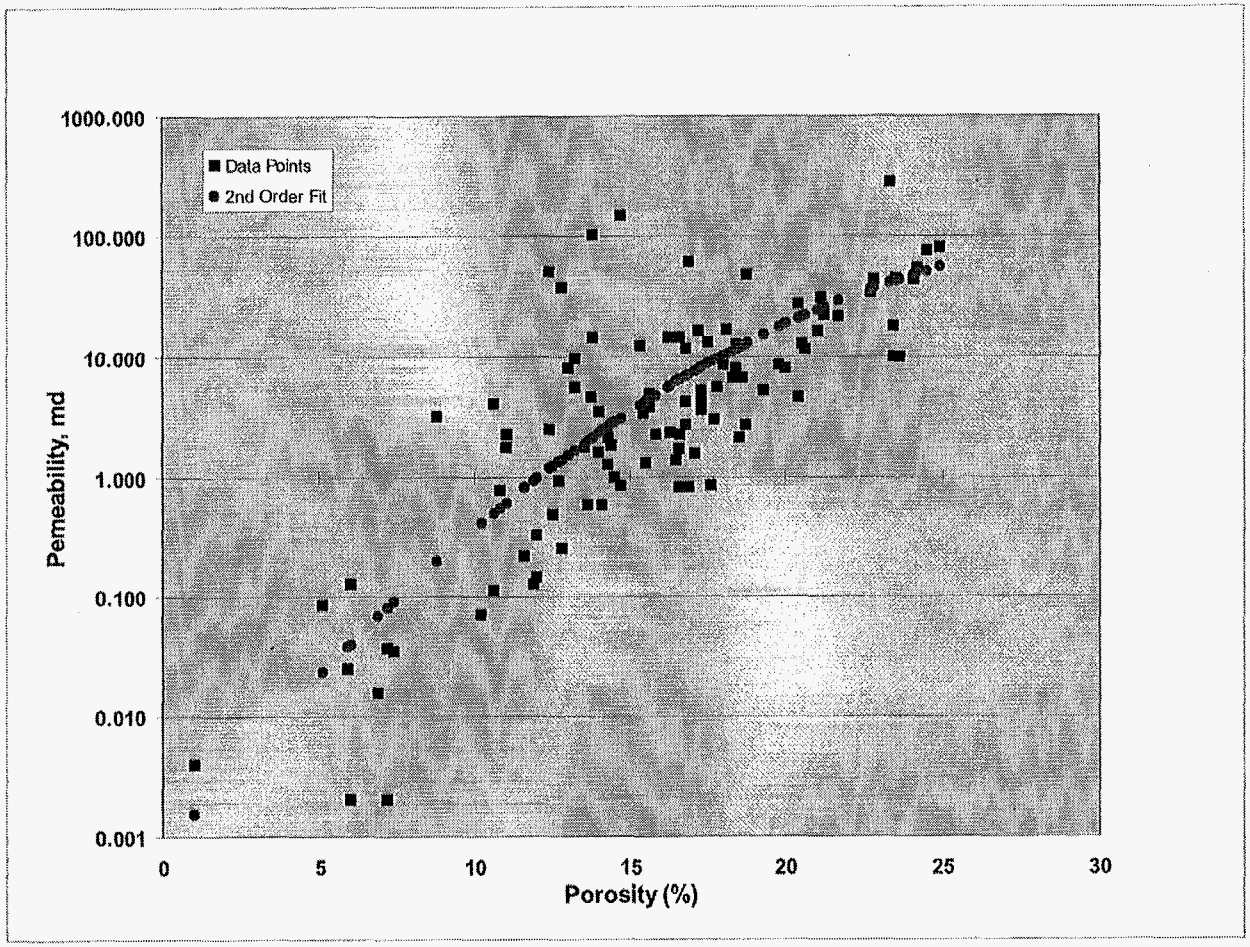

Kansas Geological Survey

Figure 2.28

Boast 3 Simulation
Schaben Field

Horizontal Permeability
(5*Kx Matrix)

Layer 1
Payzone

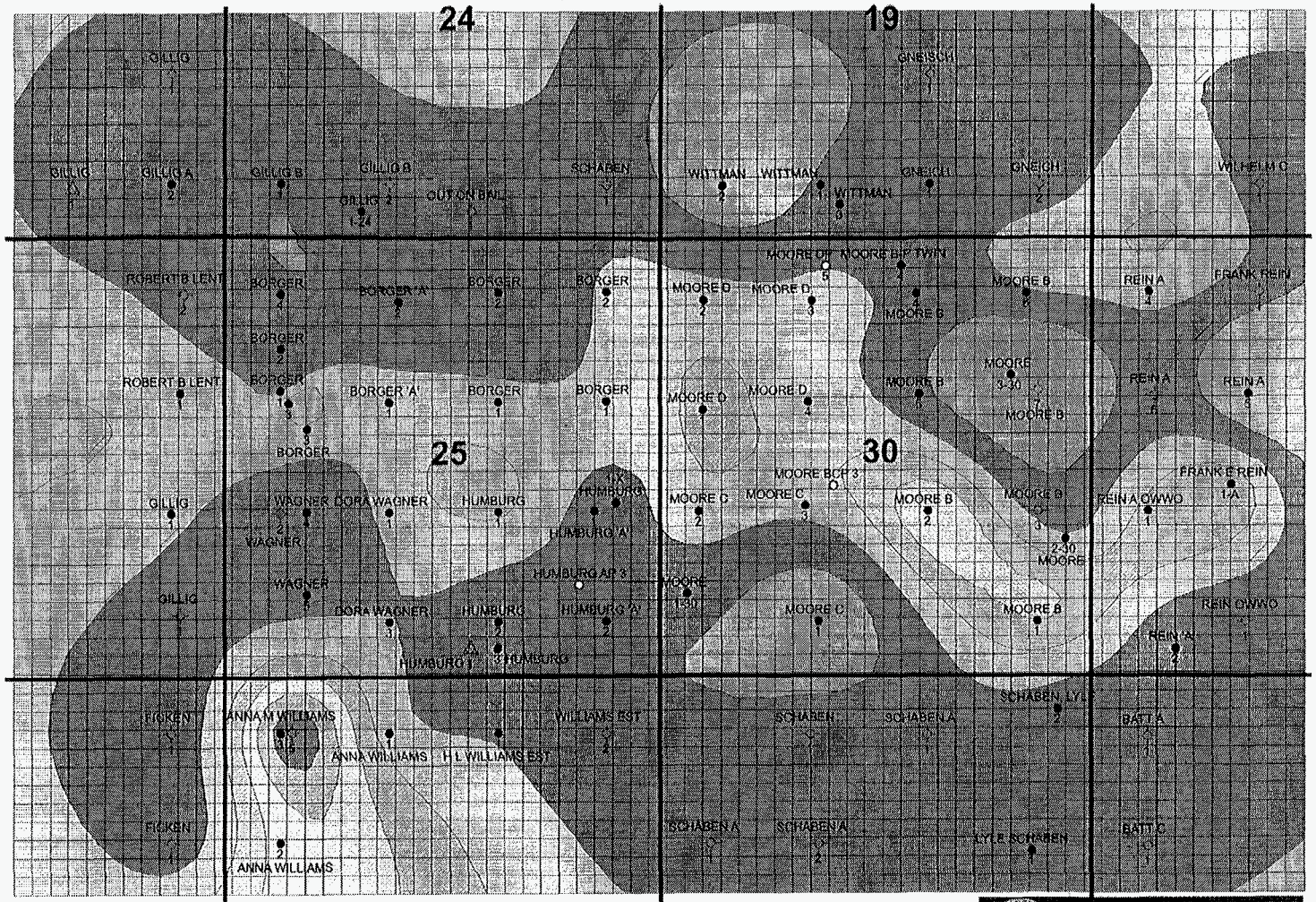

175 150 125 100 75 50 25 0 Permeability (md)

Kansas Geological Survey

Figure 2.29

Boast 3 Simulation
Schaben Field

Horizontal Matrix Permeability
in X and Y Direction

Layer 1
Payzone

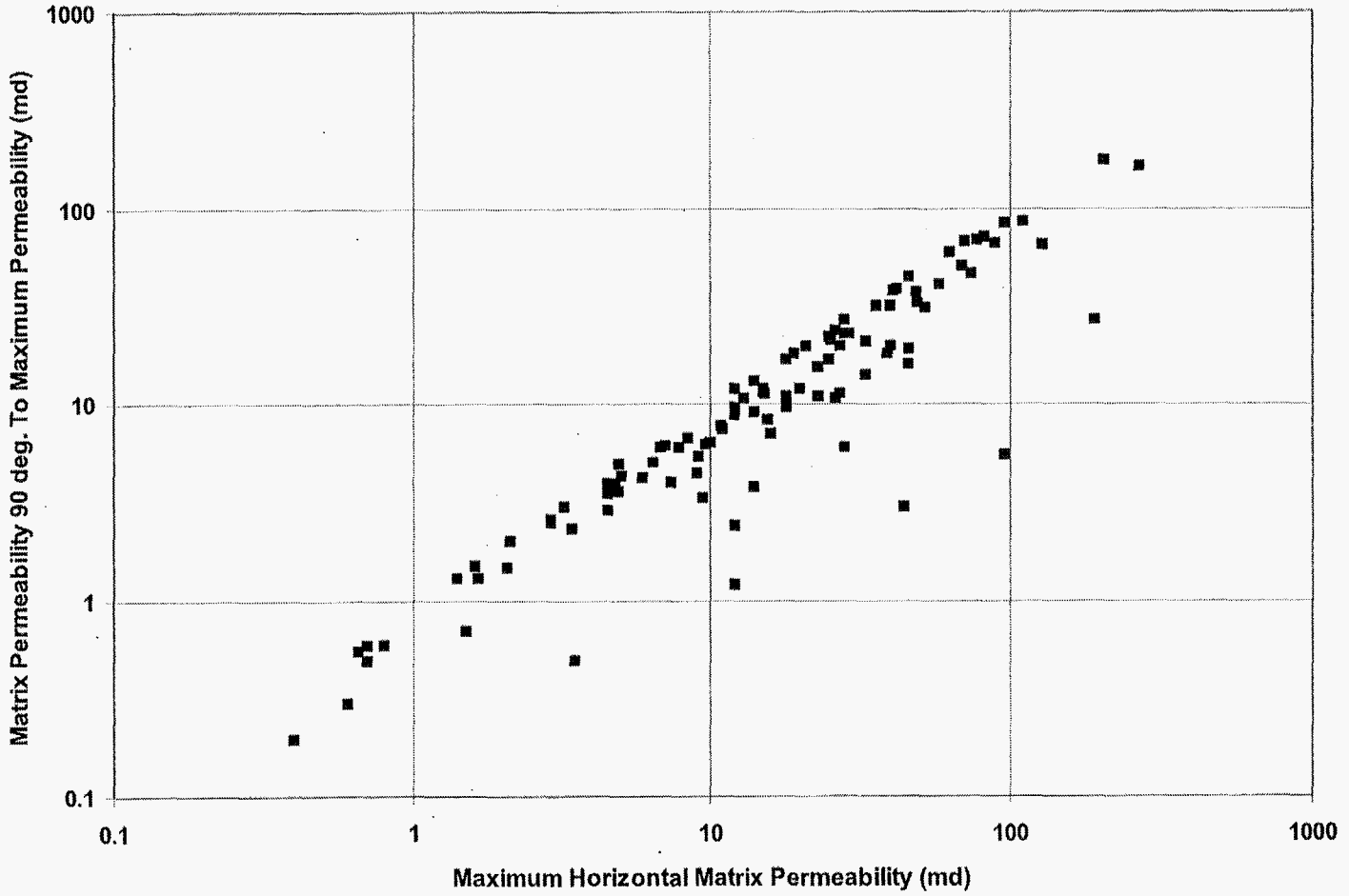

Kansas Geological Survey

Figure 2.30

Boast 3 Simulation
Schaben Field

Histogram of Kh / Kv Ratio

Layer 1
Payzone

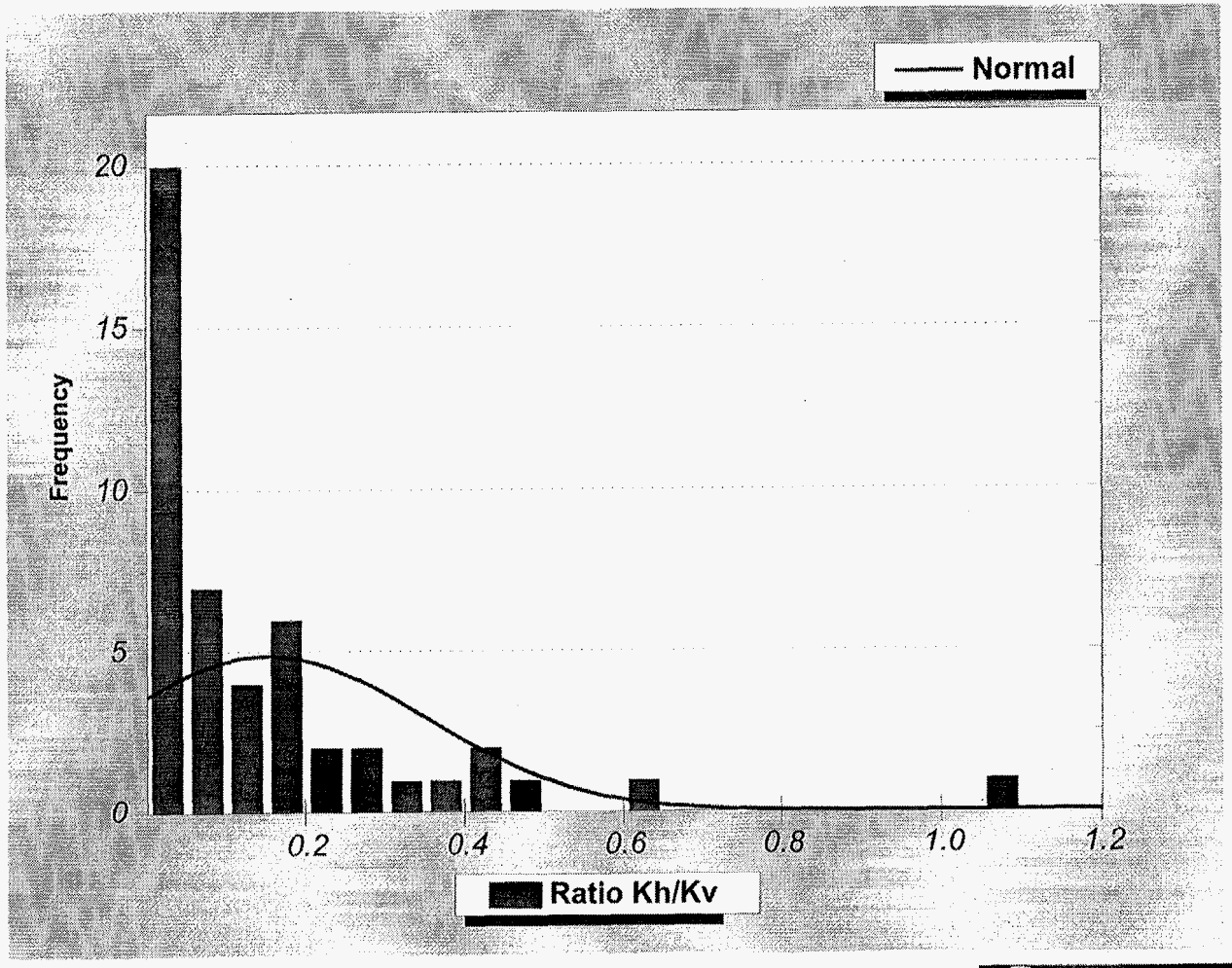

Kansas Geological Survey

Figure 2.31

Boast 3 Simulation
Schaben Field

Vertical Permeability
(.15*Kx)

Layer 1
Payzone

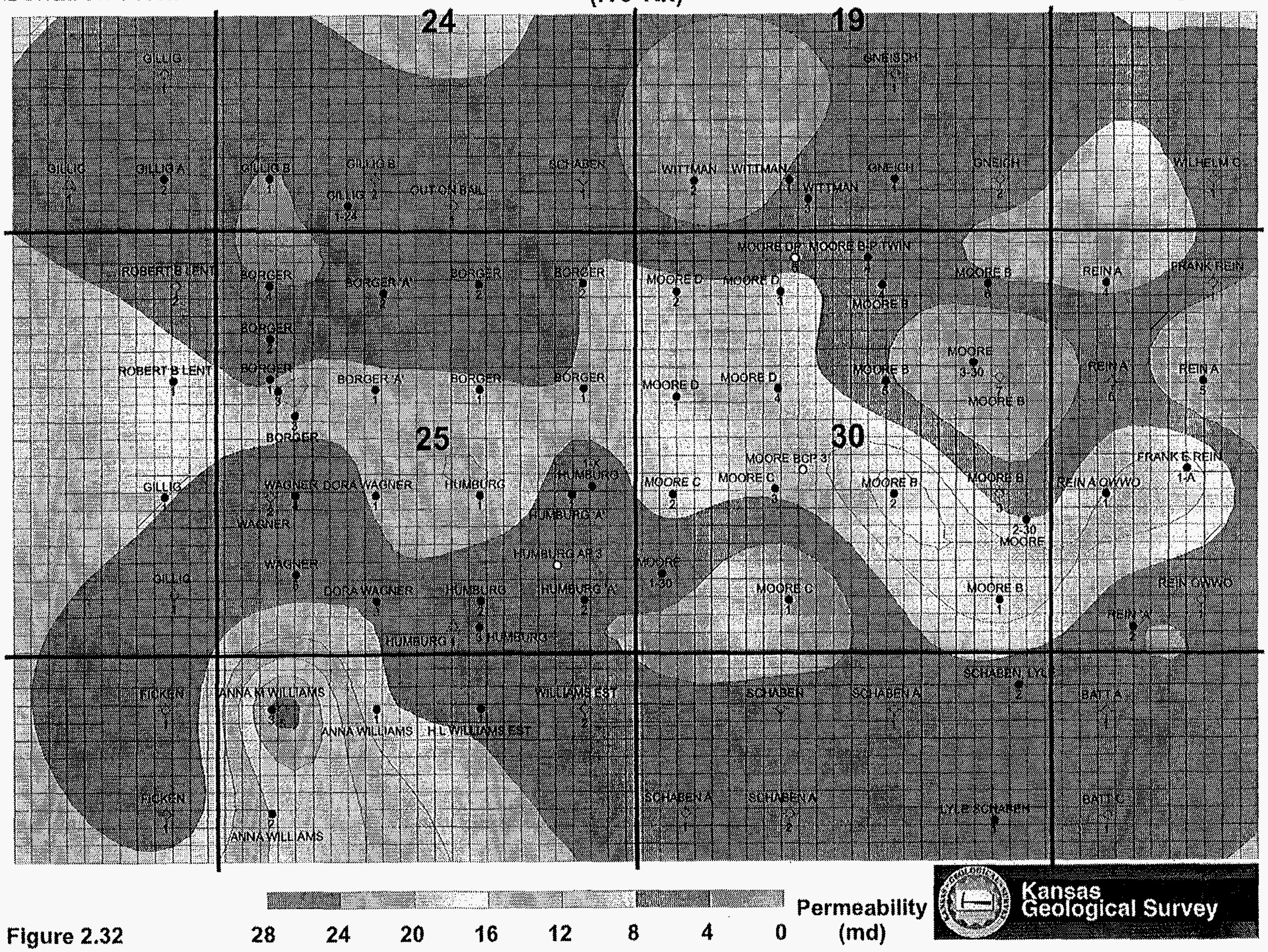

Kansas Geological Survey

Figure 2.32

Boast 3 Simulation
Schaben Field

Relative Permeability Curves

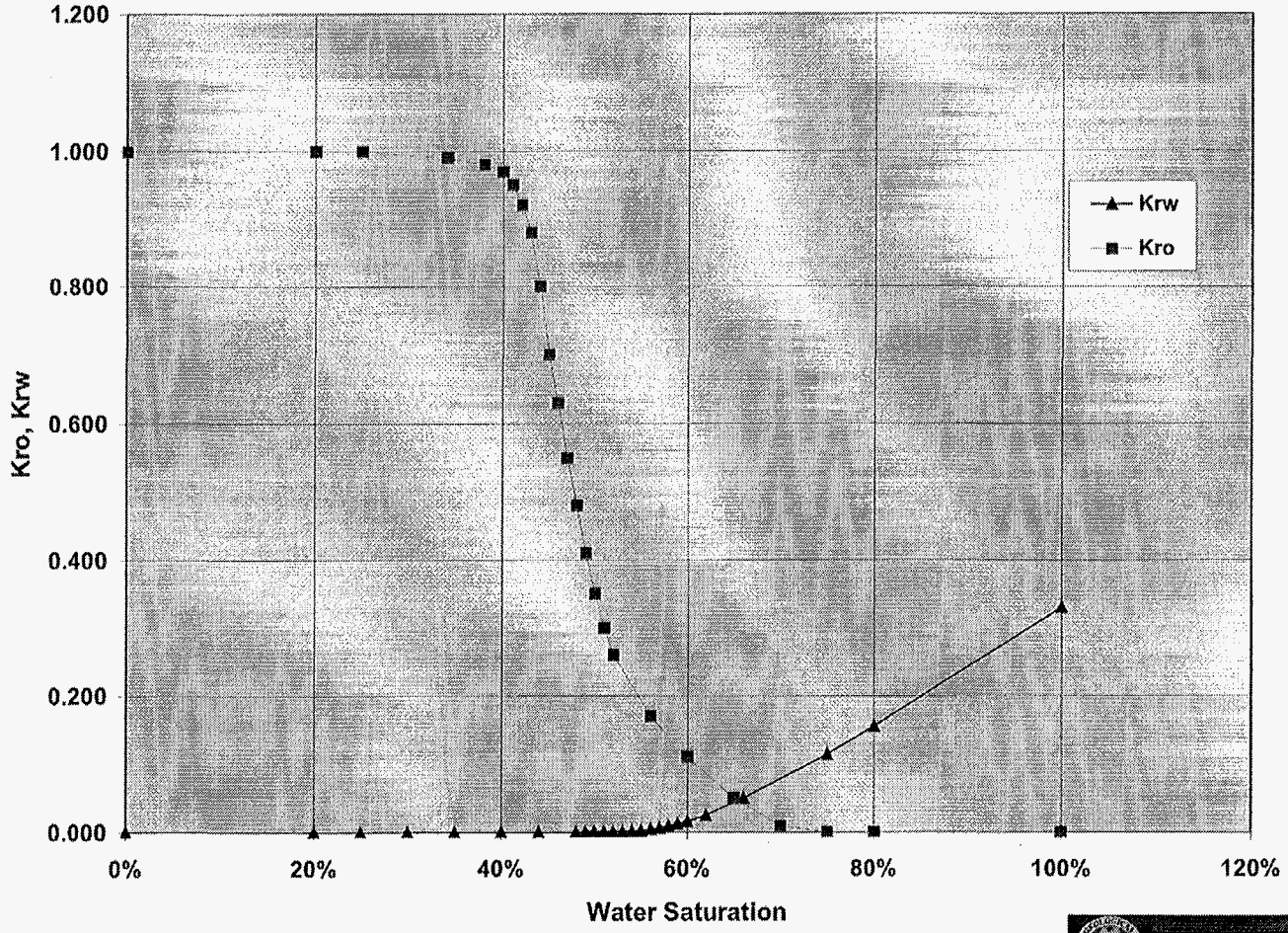

Kansas Geological Survey

Figure 2.33

Boast 3 Simulation
Schaben Field

Layer 1
Oil Saturation

Date: 1963
Time = 0 Days

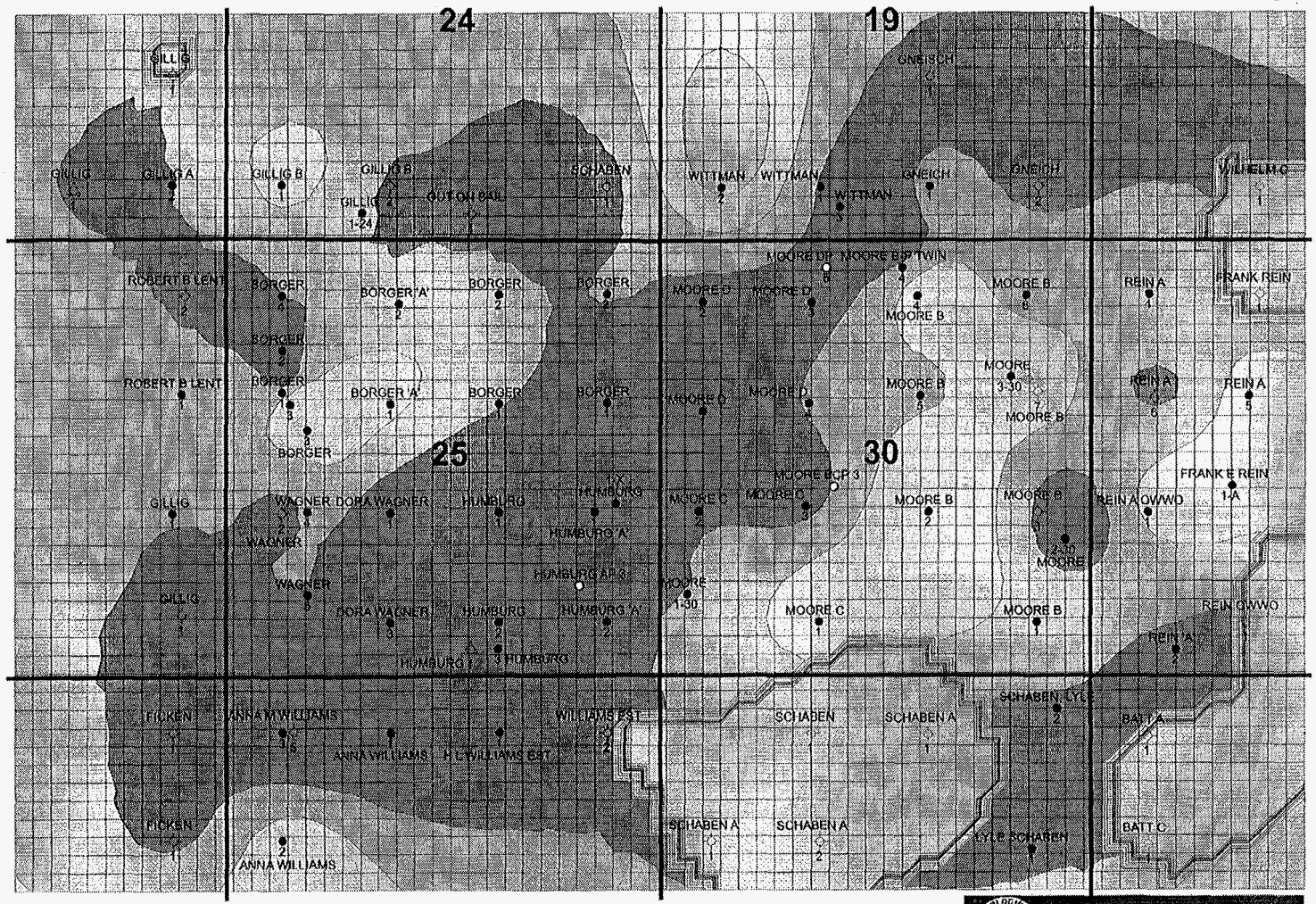

.80 .73 .66 .59 .52 .45 .38 .31 .24 So

Kansas Geological Survey

Figure 2.34

Boast 3 Simulation
Schaben Field

Layer 1
Initial Pressure (normalized FSIP)

Date: 1963
Time = 0 Days

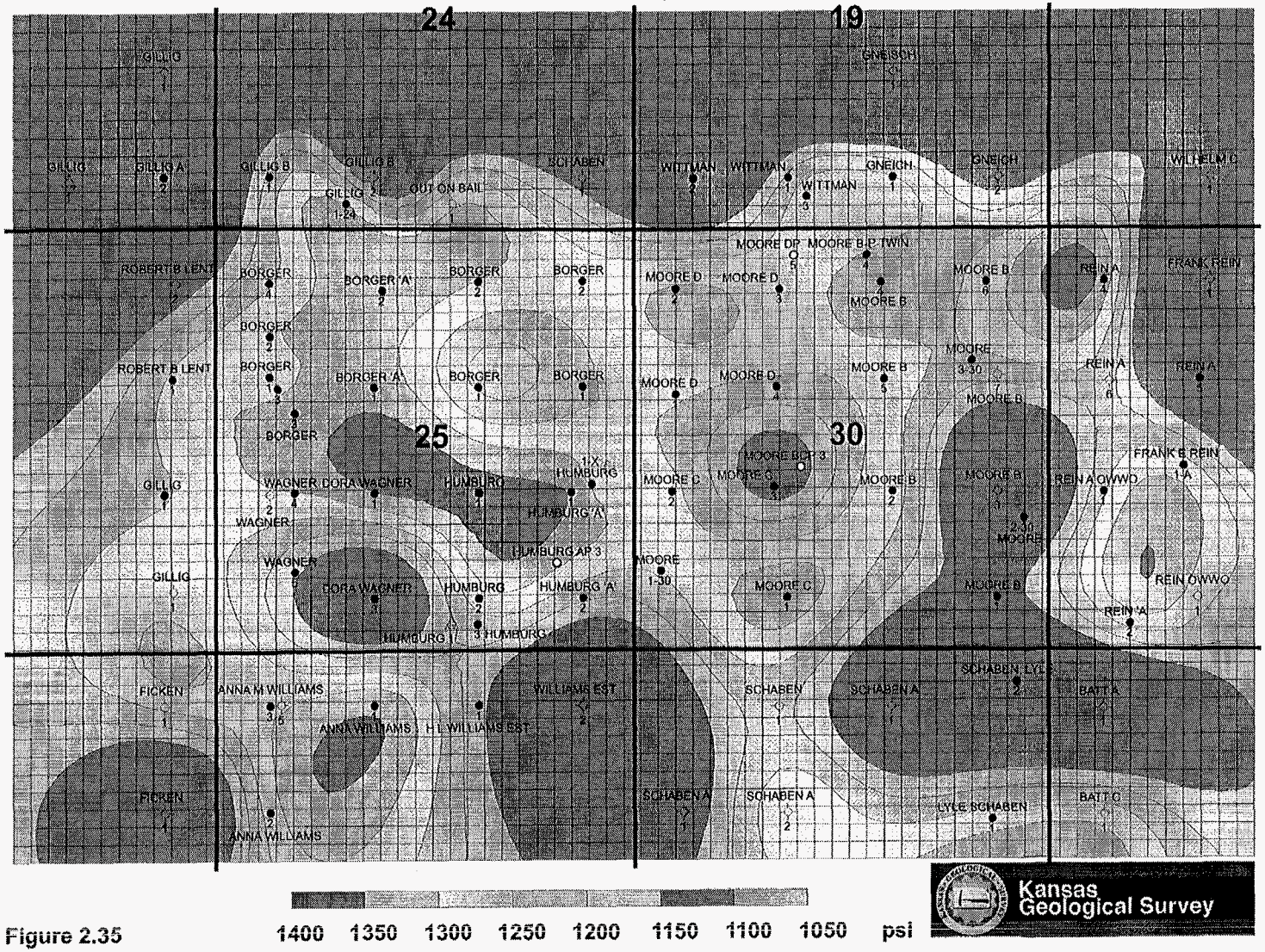

1400 1350 1300 1250 1200 1150 1100 1050 psi

Kansas Geological Survey

Figure 2.35

2.3.2 Full Field Reservoir Volumetrics

A volumetric study for the Schaben Field demonstration area was completed on a grid-by-grid basis prior to the start of simulation. The volumetric calculations were performed to check if the different reservoir parameters such as effective porosity, net pay thickness, and water saturation in the effective porosity were able to support the observed historic production data.

Review of the production data indicates that most of the wells produce less than 15% water for a 1 to 4 year period after initial production. Average water saturation derived from the well logs show values ranging between 65 to 75%. Analysis of the NMR data from core plugs indicates a significant difference between the total porosity (obtained from well logs) and the effective porosity under reservoir pressures. The total water saturations obtained from the logs show high values especially given the fact that most of the wells show a low water cut during the initial production years. Thus, it was inferred that perhaps not all of the total water saturation is mobile. It was assumed that the reservoir was made up of micro- and macro-pores. The micro-pores are believed saturated with water that is immobile under reservoir pressure. In order to determine effective porosity the correlation between the effective porosity and total porosity developed from the NMR data was used to adjust total porosity determined from logs. The adjusted effective porosity for each grid cell is believed to better represent the pore volume where fluid-flow can occur under reservoir conditions.

Effective oil saturation in each grid cell was obtained using total water saturation from 1, calculated total porosity and calculated effective porosity. Total volume of oil present in each grid cell was obtained by multiplying the grid volume with the total porosity and the oil saturation. The macro-pore volume of each grid was obtained by multiplying the grid volume with the effective porosity. Oil saturation located in the effective porosity was obtained by dividing the total volume of oil present in the grid by the macro pore volume of the grid. Oil saturation in the effective porosity was used in the volumetric calculations.

Mobile water saturation was obtained by subtracting the oil saturation in the effective pores from 1. Thus, the water saturation used in the volumetric calculations represents the water saturation in the effective pore volume of the reservoir (i.e., in the macro pores).

A map of the original oil in place (Figure 2.36) was generated by using the effective porosity, effective water saturation and grid volume. Production data available on a lease basis for 33 years includes the total volume of oil produced per lease in a year. In addition to annual production data, results of an annual productivity test for each well during its operational history were available. This data included total barrels of oil and water for the one-day test and the calculated water-oil-ratio (WOR). Productivity test data were used to allocate annual lease oil production among all the wells on the lease. Individual well water production was obtained by dividing total oil production on a per well basis by the corresponding WOR recorded in the annual one day barrel test. Schaben field is spaced on a relatively uniform 40 acre spacing with each well located near the center of the tract. The grid cell dimension used in the volumetric study was 220 feet by 220 feet. The result is that each 40 acre tract has 36 grid cells. Cumulative

oil production at each well was gridded to generate a cumulative production per grid cell map for the whole field. Cumulative production from each grid cell divided by 36 was gridded to generate a map showing the calculated distribution of the cumulative well production among the 36 surrounding grid blocks (Figure 2.37).

Remaining oil in place in each grid cell was generated by subtracting the calculated volume of oil produced in each grid cell from the original oil in place in that grid cell. The remaining oil saturation at each grid cell was multiplied by the pay thickness in the grid cell to obtain a residual oil saturation-thickness map as of 1995 (Figure 2.38). An irreducible oil saturation of 0.25 was assumed to be applicable in Schaben field. Subtracting 0.25 from the remaining oil saturation in each grid cell was used to calculate the residual mobile oil saturation. To highlight the productive potential remaining areas of the Schaben Field, a mobile saturation - thickness map (Figure 2.39) was generated by multiplying the mobile residual oil saturation in each grid cell by the pay thickness at the grid cell.

The residual mobile oil saturation-thickness map identifies areas with significant production potential. Also, absence of negative oil saturation values in any of grid cells in the field indicate that the combination of reservoir parameters such as effective porosity, effective water saturation and pay thickness is consistent with the historical production figures for the Schaben field.

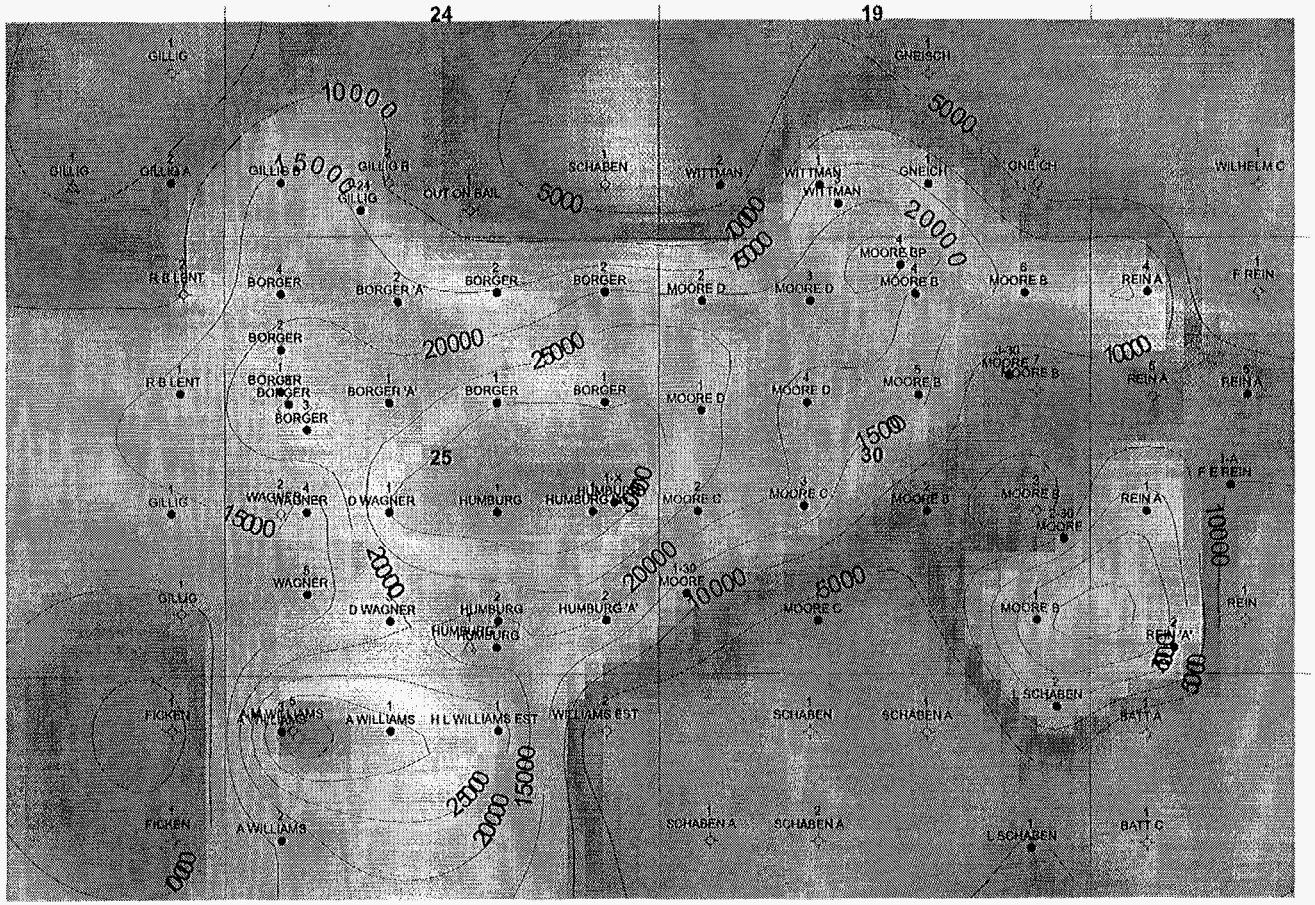

Figure 2.36

Schaben Field - Vol. Calc. Original Oil in Place in Reservoir (reservoir barrels per grid cell)

Saibal Bhattacharya	Engineer	4/16/97
Paul Gerlach	Geologist	

Scale 1:24000.

Kansas Geological Survey

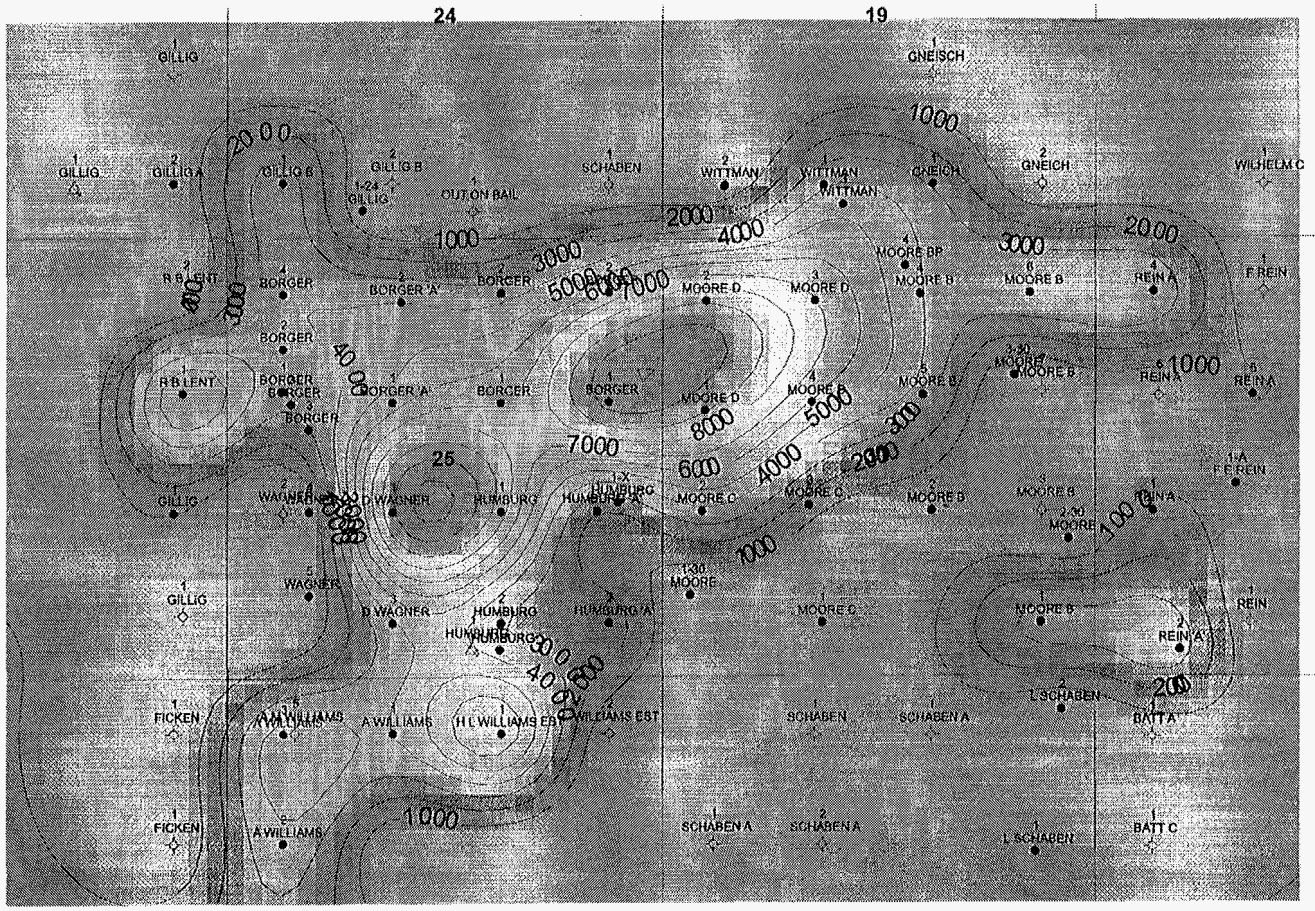

Figure 2.37

Schaben Field - Vol. Calc.
Cumulative Oil Produced
(reservoir barrels per grid cell)

Saibal Bhattacharya	Engineer	4/16/97
Paul Gerlach	Geologist	

Scale 1:24000.

Kansas Geological Survey

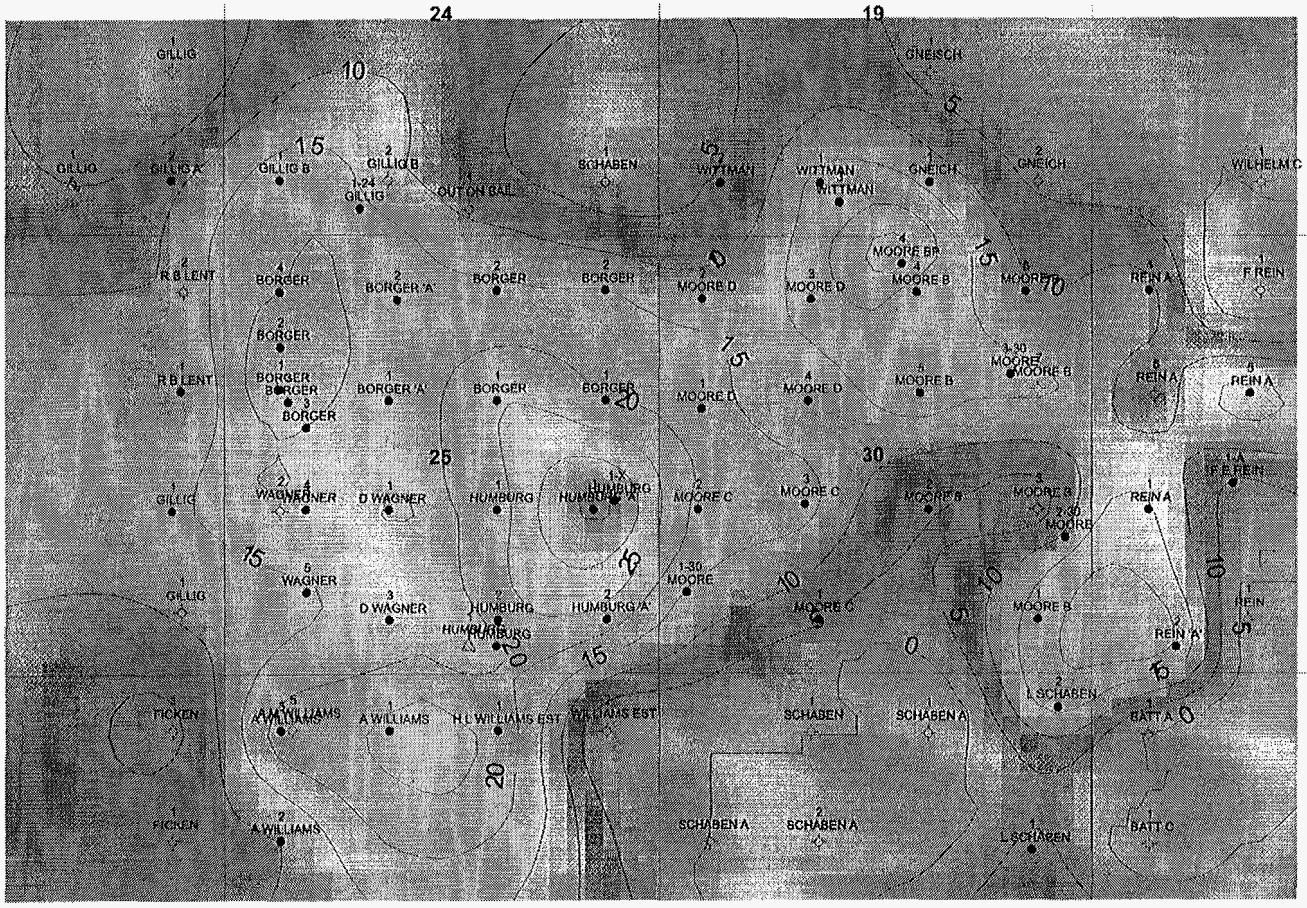

Figure 2.38

Schaben Field - Vol. Calc.
Rem. Oil Saturation Ft. (Date:1996)
(saturation% * payzone isopach ft)

Saibal Bhattacharya	Engineer	4/10/97
Paul Gerlach	Geologist	

Scale 1:24000.

Kansas Geological Survey

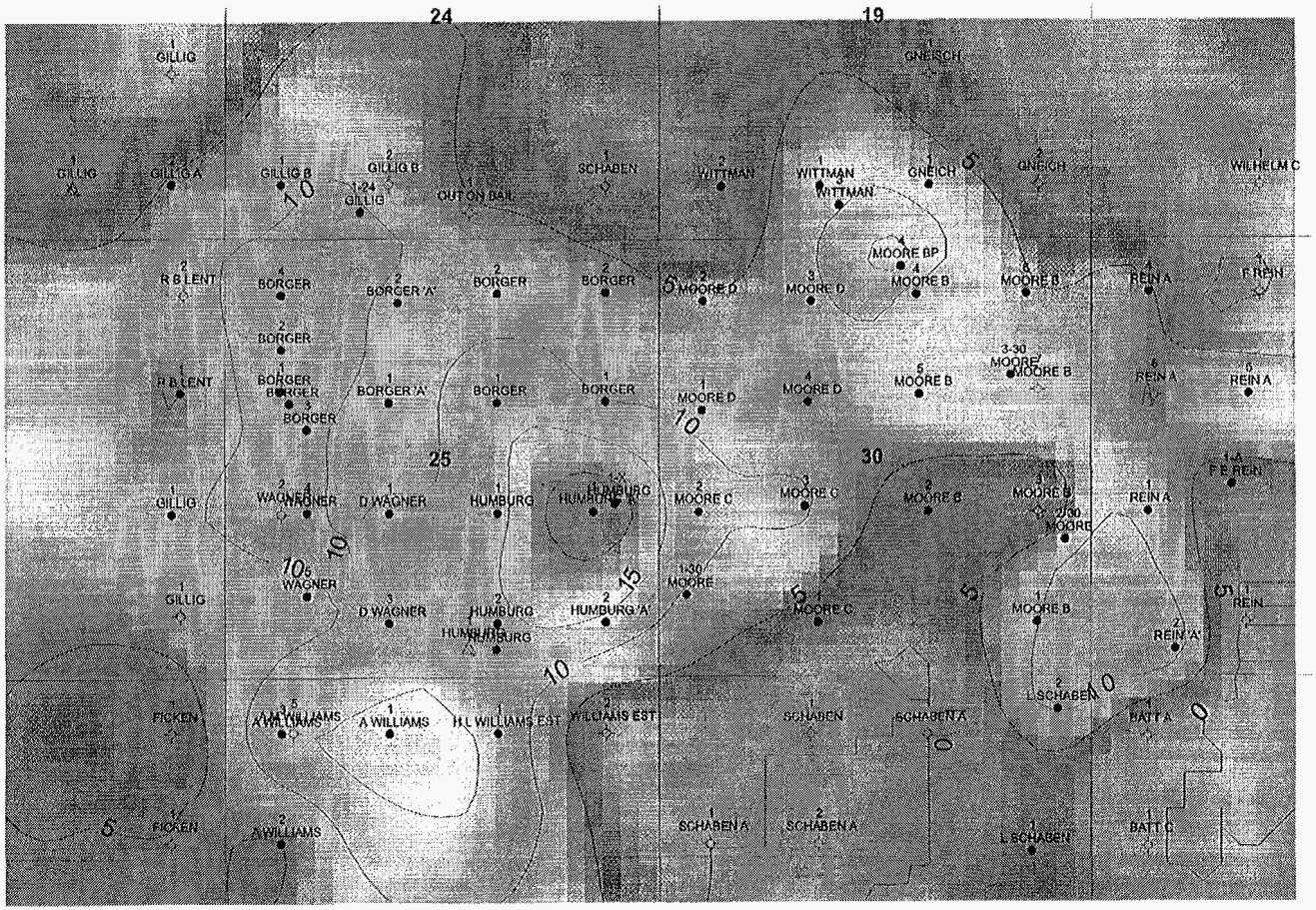

Figure 2.39

Schaben Field - Vol. Calc.
Rem. Mobile Oil Sat. Ft. (Date:1995)
(Mobile sat.% * payzone isopach ft)

Saibal Bhattacharya	Engineer	4/16/97
Paul Gerlach	Geologist	

Scale 1:24000.

Kansas Geological Survey

2.3.3 Full-Field BOAST 3 Simulation

2.3.3.1 BOAST 3 Simulator :

Simulation studies for Schaben Field were carried out with BOAST 3 simulator. BOAST 3 is a public domain PC based reservoir simulation tool from the U.S. Department of Energy. BOAST 3 is black oil applied simulation tool that performs reservoir evaluation and can be used to design solutions to different petroleum engineering problems. BOAST 3 is an isothermal, 3D, three phase simulator that assumes reservoir fluids with constant composition and physical properties dependent solely on reservoir pressure. These reservoir fluid approximations are applicable for a large percentage of the world's oil and gas reservoirs. The BOAST 3 simulator has wide range of applicability and can be used to simulate the oil and gas recovery under different scenarios such as primary depletion, pressure maintenance by gas/water injection, evaluation of secondary operations by waterflooding operations.

BOAST 3 is a finite-difference implicit pressure/explicit saturation (IMPES) numerical simulator. The well model in BOAST 3 allows specification of rate or pressure constraints on well performance, and the user is free to add or recomplete wells during the coarse of the simulation. Multiple rock and PVT regions can be defined, and three aquifer models are available as options.

2.3.3.2 History Match and Prediction

The major premise of this simulation study was to enter eleven years of historical data and have the simulator predict and match the next 23 years of known field production data. The historical data entered into the simulator input file included the daily oil production rate for each well. Daily oil production rate at each well was obtained by dividing the cumulative oil produced by the well in a year by the number of days the well operated in that year. During the first eleven years, the simulator calculated the bottom hole flowing pressure at each well that was necessary to produce the given oil production rate, and then used this bottom hole pressure to calculate the water production at each well. As the simulator was able to predict the water production rates during the first eleven years within a reasonable degree of accuracy, the corresponding flowing bottom hole pressure at the end of eleven years were thought to be acceptable. The calculated bottom hole flowing pressure at each well at the end of the first eleven years was noted. During the prediction phase, only the flowing bottom hole pressure at each well was entered in the input file and the simulator calculated both the oil and water production rates. The flowing bottom hole pressure entered for each well during this prediction phase was based on the corresponding bottom hole flowing pressure calculated by the simulator at the end of the eleventh year. Production profiles show that the water-oil ratio at each well remains almost constant after eleven years. Thus it was assumed that the flowing bottom hole pressure at each well during the prediction phase was close to that calculated by the simulator at the end of the eleventh year. It was also assumed that as the well aged, the flowing bottom hole pressure at each well would decline.

The flowing bottom hole pressure at each well that was entered in the input file during the prediction phase was a percentage of the pressure calculated by the simulator at the end of the eleventh year. This percentage value varied from 100% to 85% (in a descending manner) over the period of prediction (i.e. from the thirteenth to the thirty-fourth year).

2.3.3.3 Simulation Results

At the field level, a good match between simulated and observed was obtained for both oil and water production rates during the 34 years encompassed by the historical and predictive periods (Figure 2.40). The only exceptions are two years (between 7300 to 8030 days). Field production records indicate that a large number of wells were shutin during this period for administrative and economic reasons. Due to certain technical problems faced during the construction of the input file for BOAST 3, individual wells could not be shut off or reactivated after the first eleven years. Thus the simulation is unable to match the daily field production rates during the anomalous period when many of producing wells were idled.

A good match was also obtained for the simulated and observed cumulative oil and water production for the field from 1963 to 1996 (Figure 2.41). After matches were obtained within acceptable tolerances for both oil and water at a field scale, attention was focused on the performance of the individual wells. Figures 2.42 and 2.43 show the match obtained for individual wells between the simulated cumulative oil and water production and the historical cumulative production. The ratio as defined in both plots is the ratio between observed cumulative production and predicted cumulative production for each well generated from the simulation. A ratio of 1 would indicate that simulated cumulative production is equal to the corresponding historical production. Most of the wells have a ratio between 0.9 to 1.1 indicating a good match of the cumulative oil production on a well to well basis (Figure 2.42). In case of water production the majority of the wells have a ratio varying between 0.8 to 1.2 (Figure 2.43). However, a number of wells have a ratio value as high as 10 and some as low as 0.1. The simulator appears to over and under predict the water in some wells.

The mismatch of water production in some of the wells may be due to inaccurate description of the reservoir properties around the concerned wells. Schaben field is a fractured reservoir with an active bottom water drive. The vertical permeability in the reservoir and more especially in the aquifer around the well plays a very important role in controlling the water production at the well. Several reruns were carried out on the simulator with the vertical permeabilities lowered around wells where the simulator over predicted water resulting in drastically reduced water production. Similarly, increasing the vertical permeability around the wells resulted in the increase of the simulated water production at the well. This process of local adjustment of the vertical permeability could be applied on every well to make the simulated results match more closely the historical production. Another important point to note is that the historical water production data may not be very accurate because it was derived from the oil production values and the corresponding water-oil ratios.

Oil saturation maps generated from the simulation output at different time periods of the field history show the oil saturation across the field at the beginning of 1963, the end of 1973 (i.e., at the beginning of the prediction phase), and at the end of 1996 (figures 2.44 and 2.45). The

simulation indicates that by the end of 1973 areas of low oil saturation have started to develop around wells, especially wells with a high production rate (Figure 2.44). At the end of 1996 the simulation shows oil saturation dropping around most wells to just above the irreducible oil saturation (i.e., between 0.31-0.35). However, significant pockets of high oil saturations are left unswept in between the drainage areas of surrounding wells (Figure 2.45).

Using the simulation results a residual oil saturation-thickness map for Schaben field at the end of 1996 was generated (Figure 2.46). The relative permeability curves used in the simulation indicate an irreducible oil saturation of 0.25. If the relative permeability curves are correct, it will be difficult to produce oil from zones having an oil saturation that is approaching 0.30. A conservative oil saturation cut off of 0.40 along with a pay thickness cut off of greater than 20 feet was employed to construct a map showing areas with the highest predicted infill potential (Figure 2.47). All grid cells with a residual oil saturation less than 40% or with a net pay thickness less than 20 feet were zeroed.

Based on the infill potential map and in consultation with one of the operators of Schaben field, three sites were chosen to locate new wells. These sites are marked with a white circle on the map (Figure 2.47). Subsequent simulation runs were carried out with the three new wells coming on production in the simulator during the year 1996. The simulation with the three new wells was run through the year 2006 and an oil saturation map was generated from the simulation output (Figure 2.48). Predicted daily field production rate of oil and water after the three new wells has been put in operation indicates the addition of significant additional oil production (Figure 2.49). The three new wells were simulated to produce under a backpressure (i.e., a flowing bottom hole pressure) equal to that of the nearest well at the end of 1996. The daily production rate simulated for the Moore BCP #3 is calculated to produce a total of 47,200 barrels of oil and 227,600 barrels of water over a period of ten years (Figure 2.50). The simulator also predicts daily oil production above 10 barrels during the first 5 years.

Figure 2.40

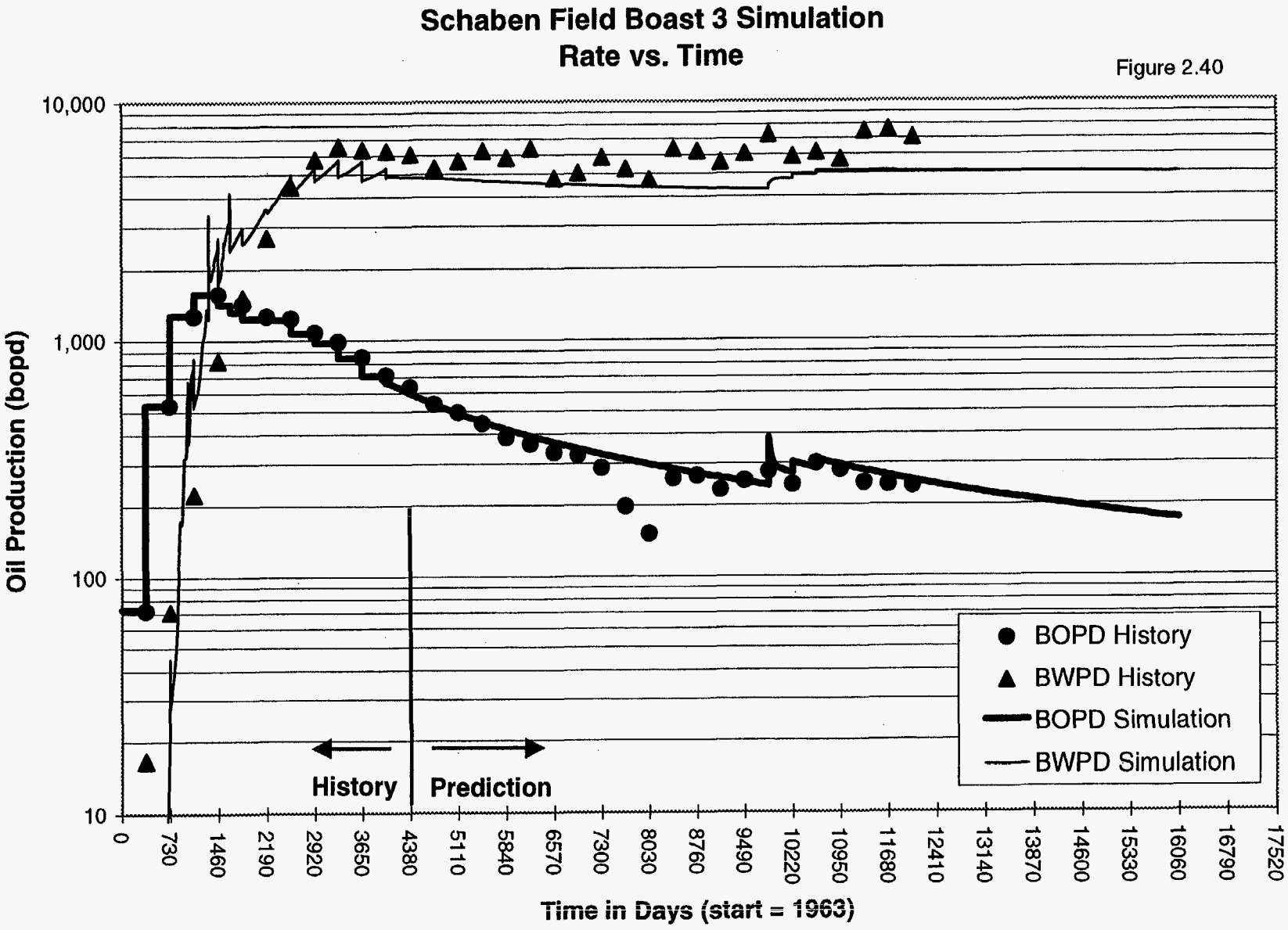
Schaben Field Boast 3 Simulation
Rate vs. Time
Oil Production (bopd)
10,000
1,000
100
10
0
730
1460
2190
2920
3650
4380
5110
5840
6570
7300
8030
8760
9490
10220
10950
11680
12410
13140
13870
14600
15330
16060
16790
17520
Time in Days (start = 1963)
History
Prediction
BOPD History
BWPD History
BOPD Simulation
BWPD Simulation

Schaben Field Boast 3 Simulation
Cumulative vs. Time

Figure 2.41

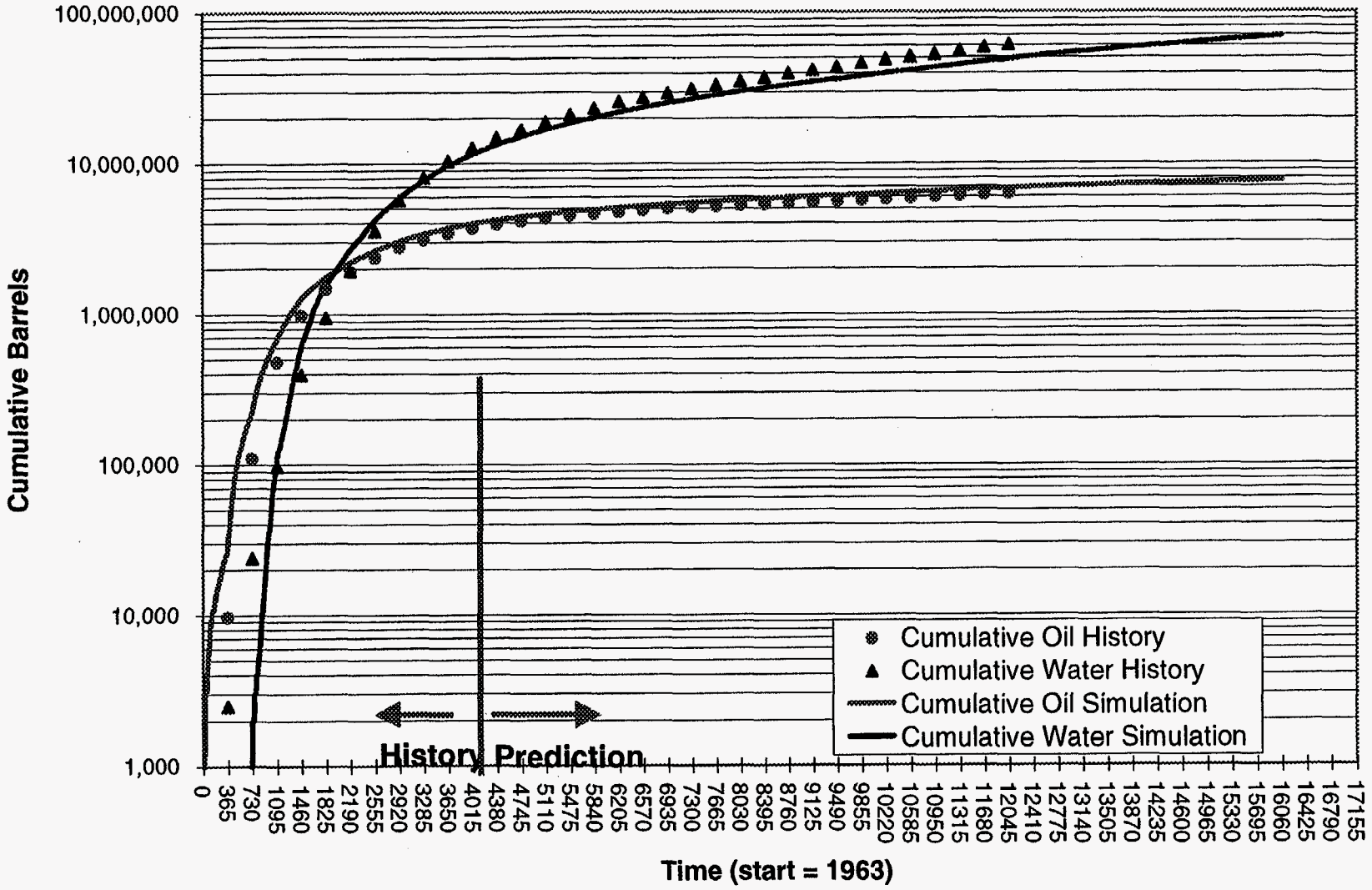

Figure 2.42

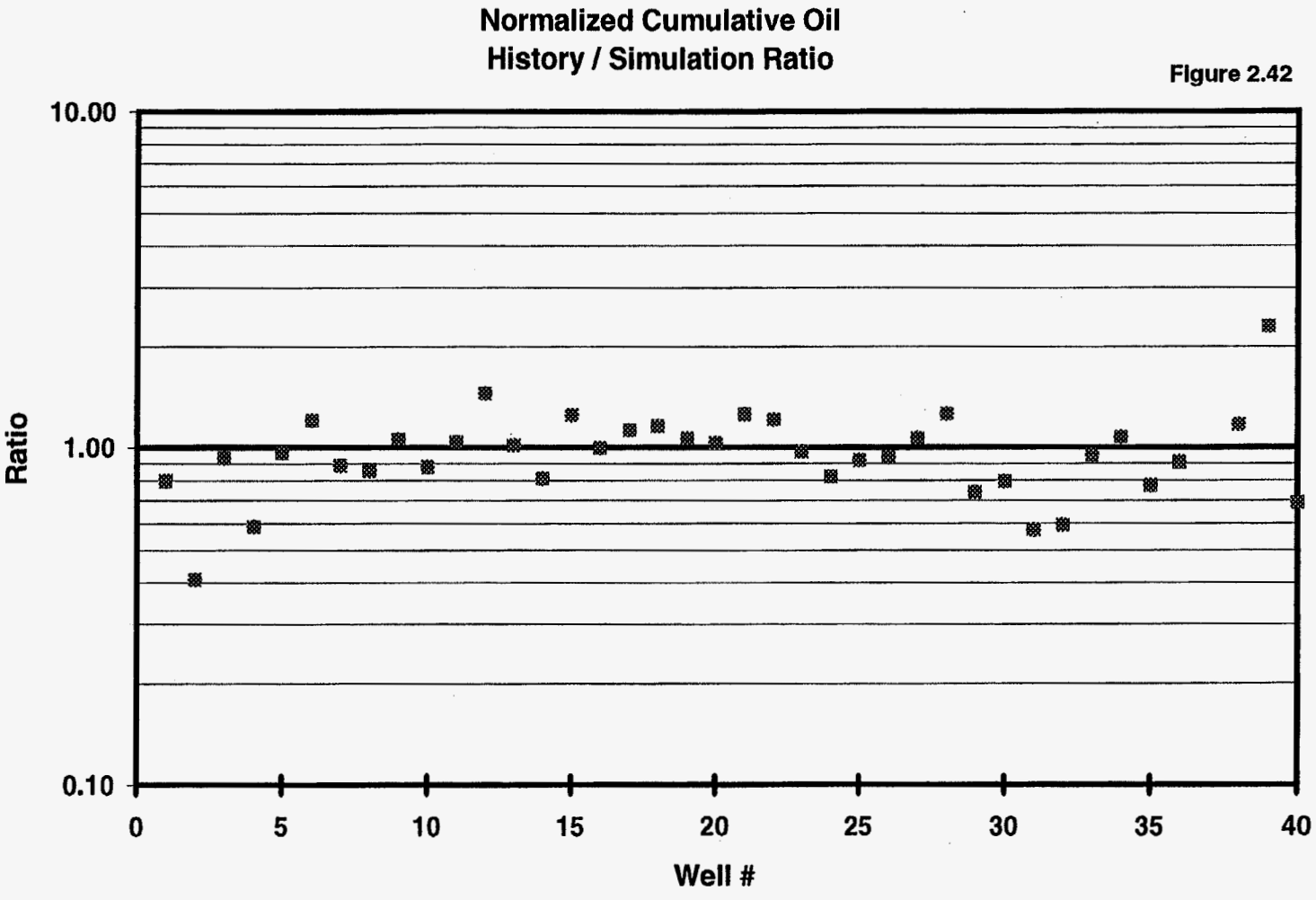
Normalized Cumulative Oil
History / Simulation Ratio
10.00
1.00
0.10
Ratio
0
5
10
15
20
25
30
35
40
Well #

Normalized Cumulative Water History / Simulation Ratio

Figure 2.43

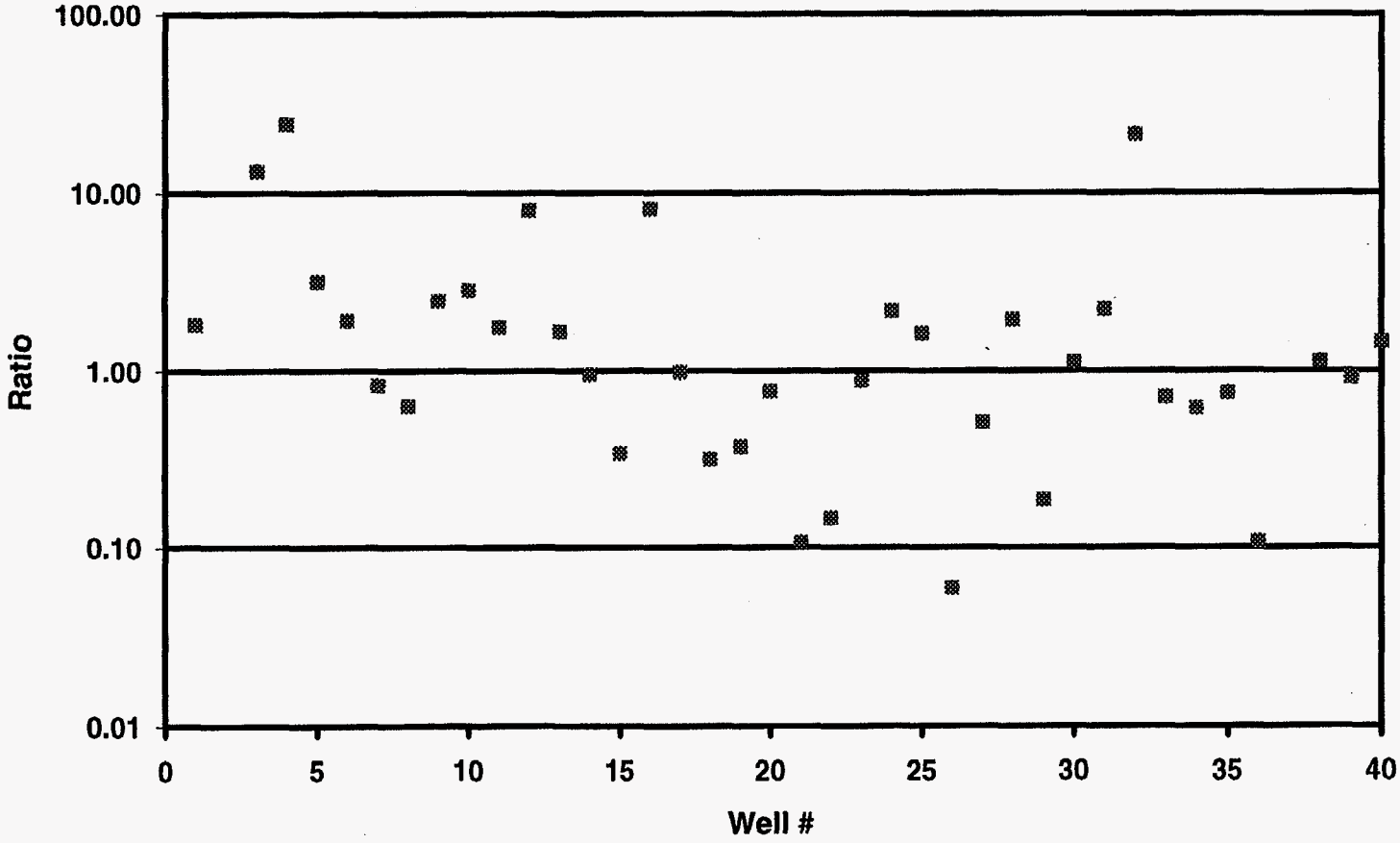

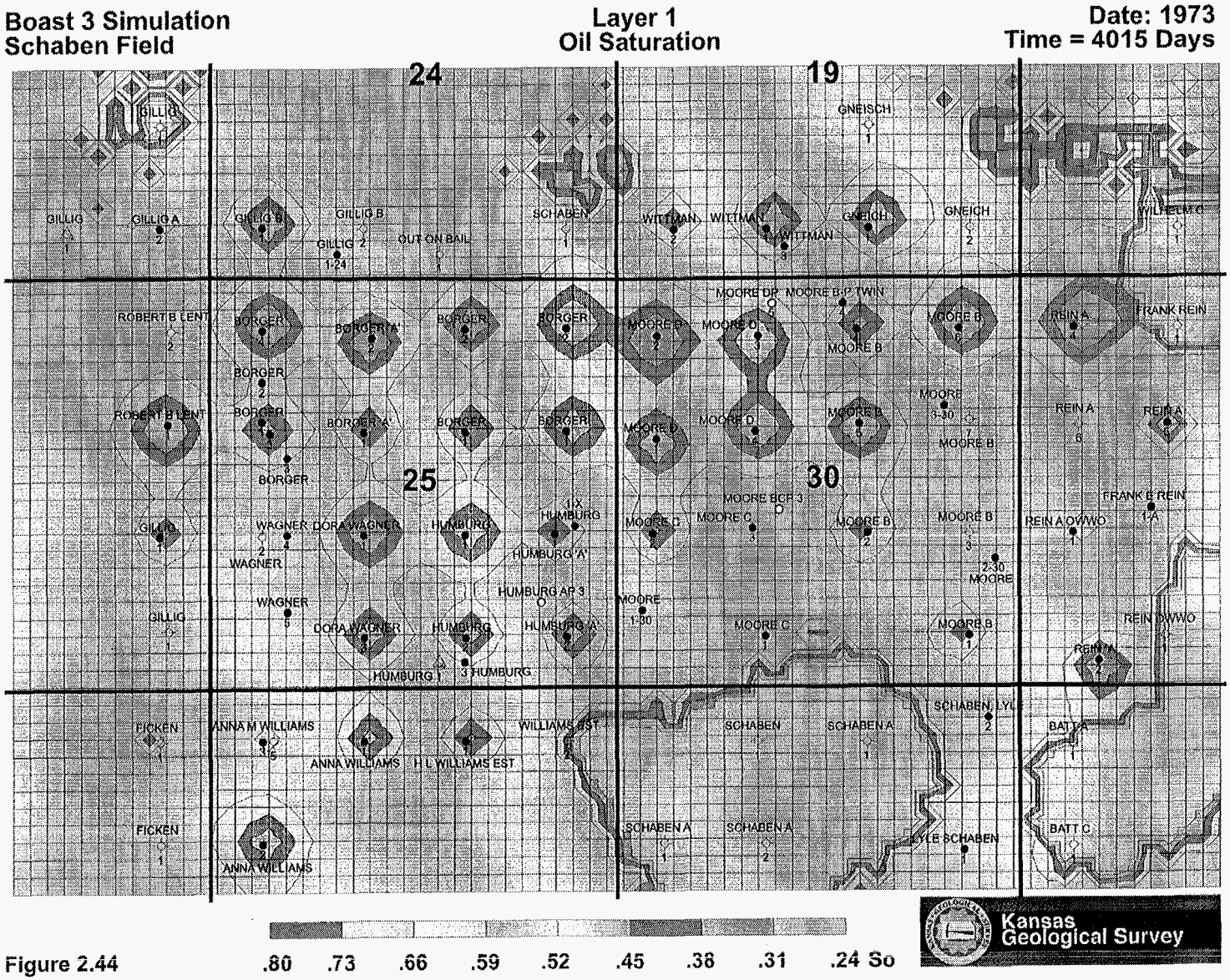
Boast 3 Simulation
Schaben Field
Layer 1
Oil Saturation
Date: 1973
Time = 4015 Days
24
19
25
30
GILLIG
GILLIG A
GILLIG B
GILLIG 2
1-24
OUT ON BAIL
SCHABEN
WITTMAN
GNEISCH
WILHELM C
ROBERT B LENT
BORGER
BORGER A
MOORE D
MOORE B
MOORE B-2 TWIN
MOORE DP
REIN A
FRANK REIN
REIN A OWWO
MOORE
2-30
HUMBURG
HUMBURG A
HUMBURG AP 3
1X
WAGNER
DORA WAGNER
MOORE C
MOORE BCP 3
1-30
2-30
HUMBURG 1
3 HUMBURG
FICKEN
ANNA M WILLIAMS
ANNA WILLIAMS
H L WILLIAMS EST
WILLIAMS EST
SCHABEN A
SCHABEN LYLE
LYLE SCHABEN
BATT A
BATT C
.80
.73
.66
.59
.52
.45
.38
.31
.24 So
Kansas
Geological Survey

Figure 2.44

Boast 3 Simulation
Schaben Field

Layer 1
Oil Saturation

Date: 1996
Time = 12410 Days

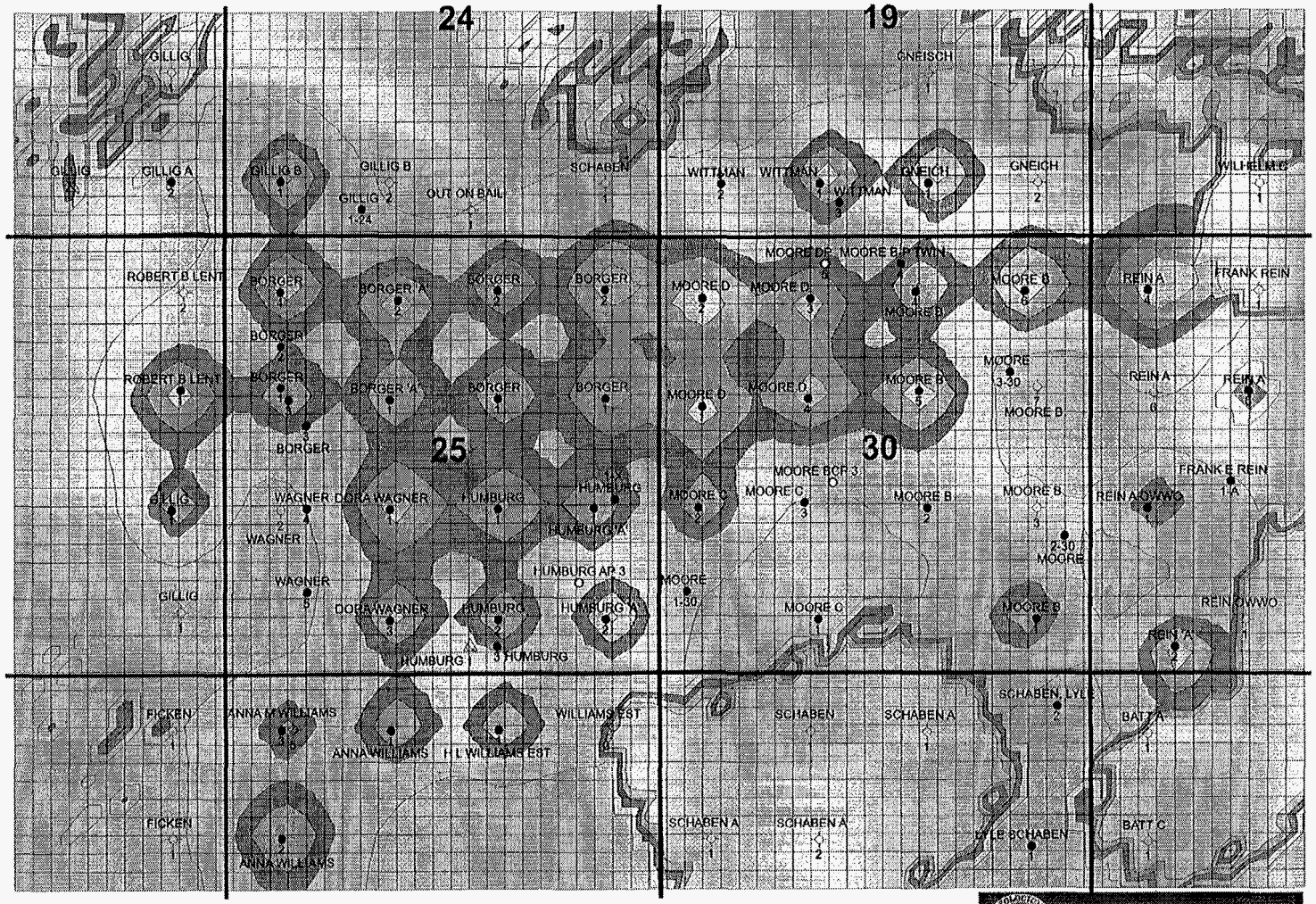

.80 .73 .66 .59 .45 .52 .38 .31 .24 So

Kansas Geological Survey

Figure 2.45

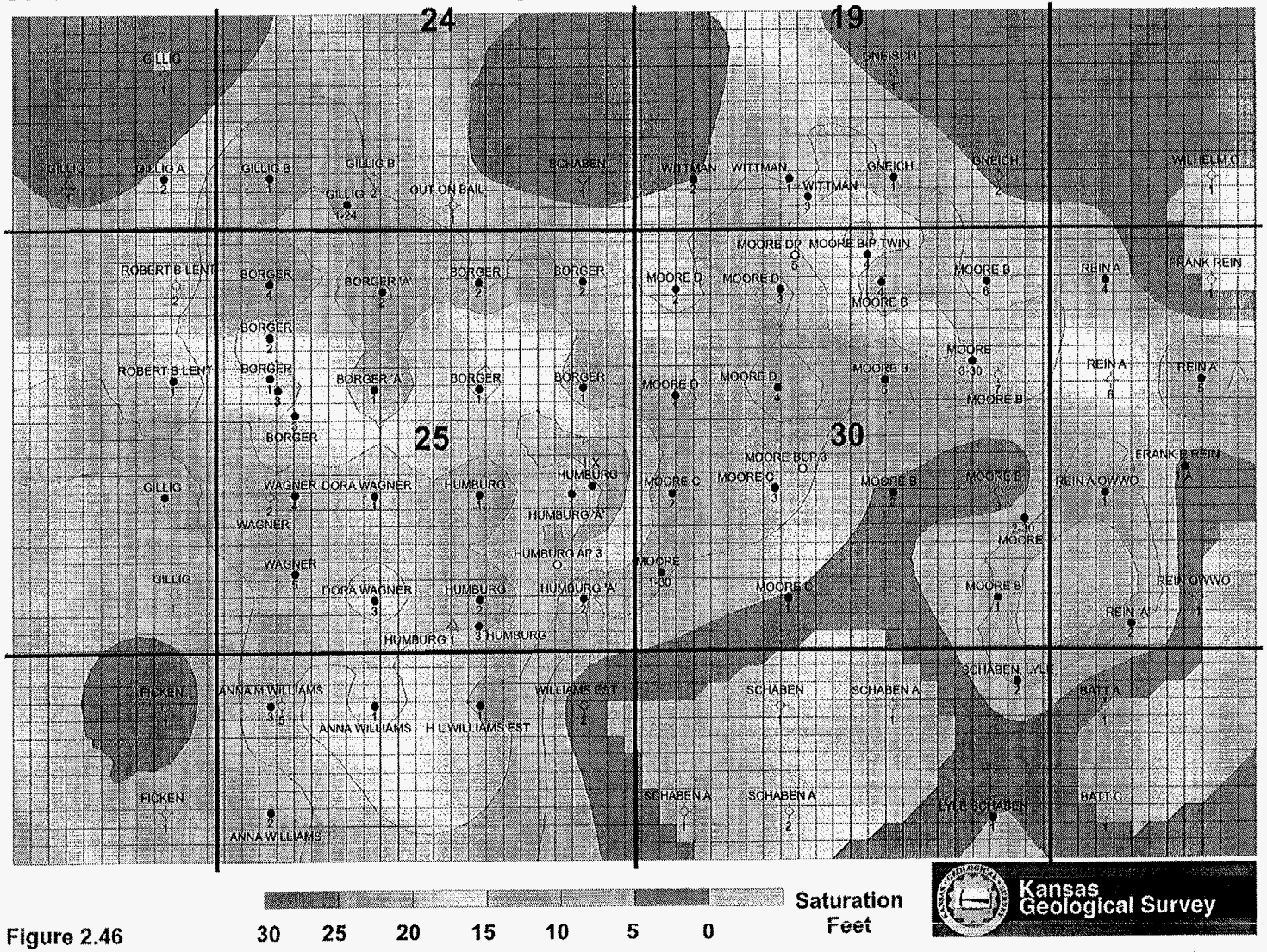
Boast 3 Simulation
Schaben Field
Saturation Feet
[Oil Saturation * Net Pay]
Date: 1996
Time = 12410 Days
24
19
25
30
GILLIG
GILLIG A
GILLIG B
GILLIG 2
OUT ON BAIL
SCHABEN
WITTMAN
WITTMAN
WITTMAN
GNEICH
GNEICH
WILHELM C
ROBERT B LENT
BORGER
BORGER 'A'
BORGER
BORGER
MOORE D
MOORE D
MOORE DP
MOORE BP
TWIN
MOORE B
MOORE B
REIN A
FRANK REIN
MOORE
3-30
REIN A
REIN A
WAGNER
DORA WAGNER
HUMBURG
HUMBURG
HUMBURG 'A'
MOORE C
MOORE C
MOORE BCP 3
MOORE B
MOORE B
REIN A OWWO
FRANK P REIN
2-30
MOORE
1-30
MOORE C
MOORE B
REIN OWWO
REIN 'A'
HUMBURG 1
HUMBURG
HUMBURG AP 3
FICKEN
ANNA M WILLIAMS
ANNA WILLIAMS
H L WILLIAMS EST
WILLIAMS EST
SCHABEN
SCHABEN A
SCHABEN, LYLE
BATT A
SCHABEN A
SCHABEN A
LYLE SCHABEN
BATT C
Saturation Feet
30 25 20 15 10 5 0
Kansas Geological Survey

Figure 2.46

Boast 3 Simulation
Schaben Field

Grid Cells with Best Infill Potential
(So 1995 > 40% * Net Pay >20 ft)

Date: 1996
Time = 12410 Days

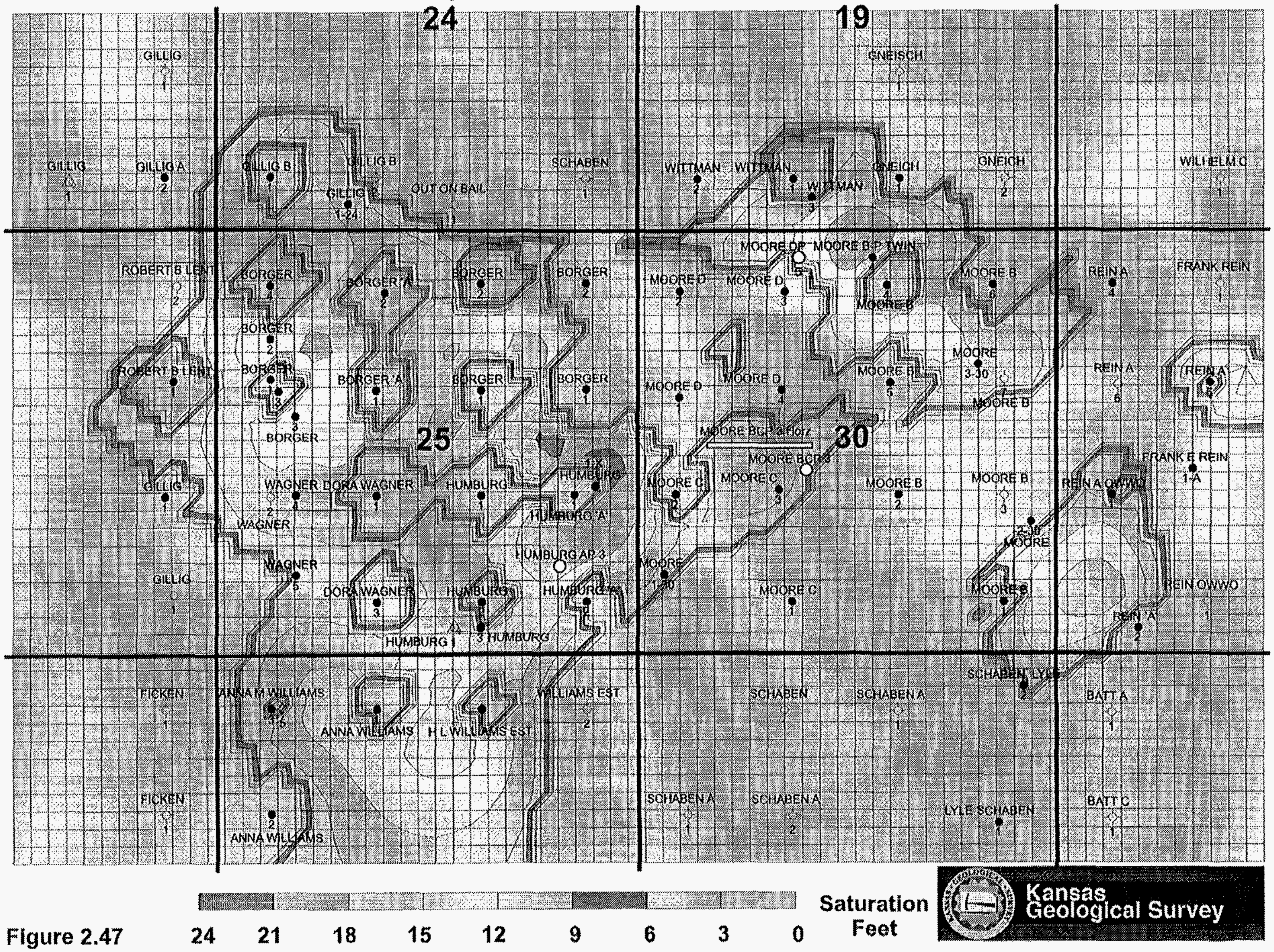

Figure 2.47

Boast 3 Simulation
Schaben Field

Layer 1
Oil Saturation

Date: 2006
Time = 16060 Days

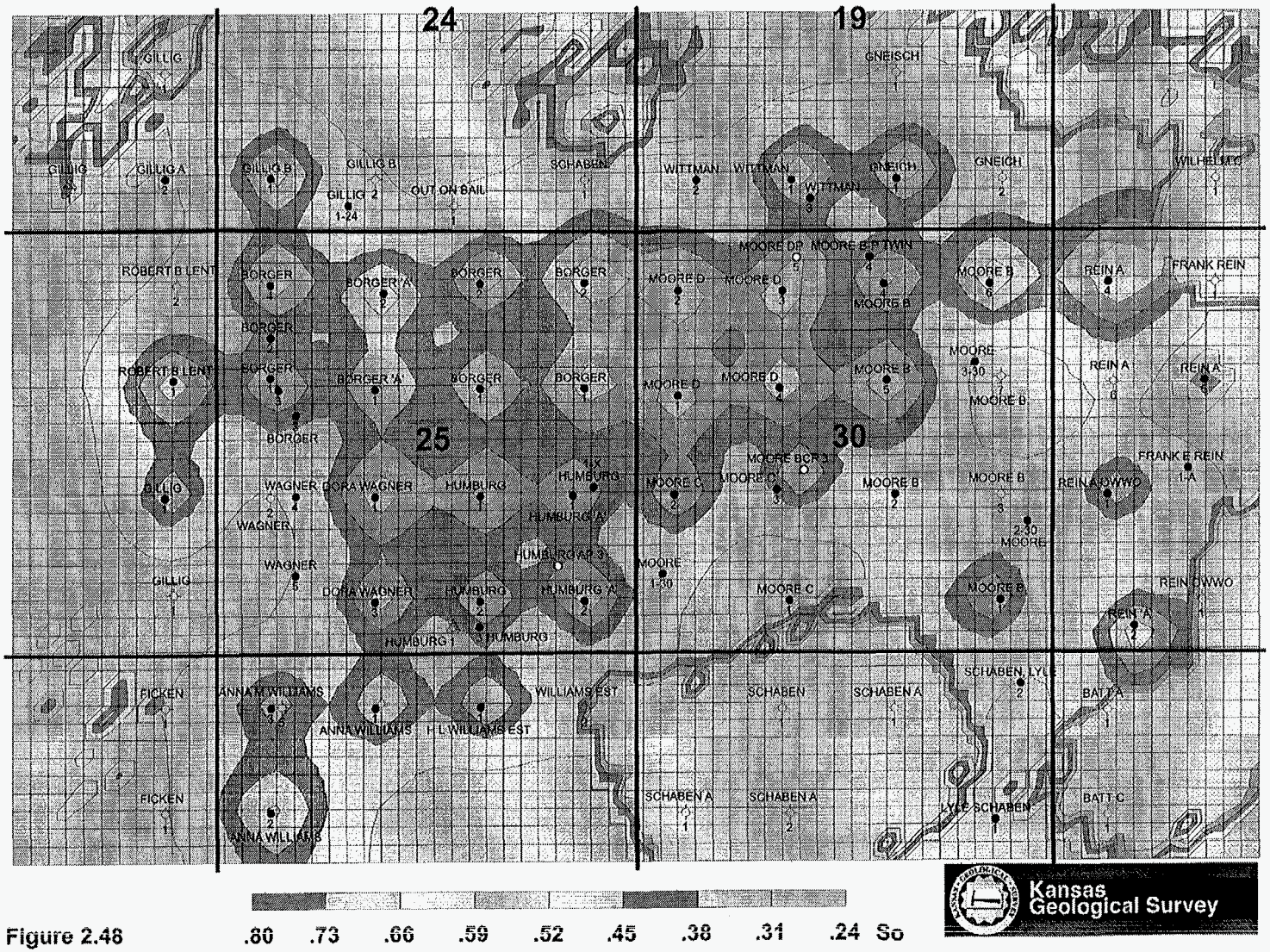

.80 .73 .66 .59 .52 .45 .38 .31 .24 So

Kansas Geological Survey

Figure 2.48

Schaben Field Boast 3 Simulation
Rate vs. Time

Figure 2.49

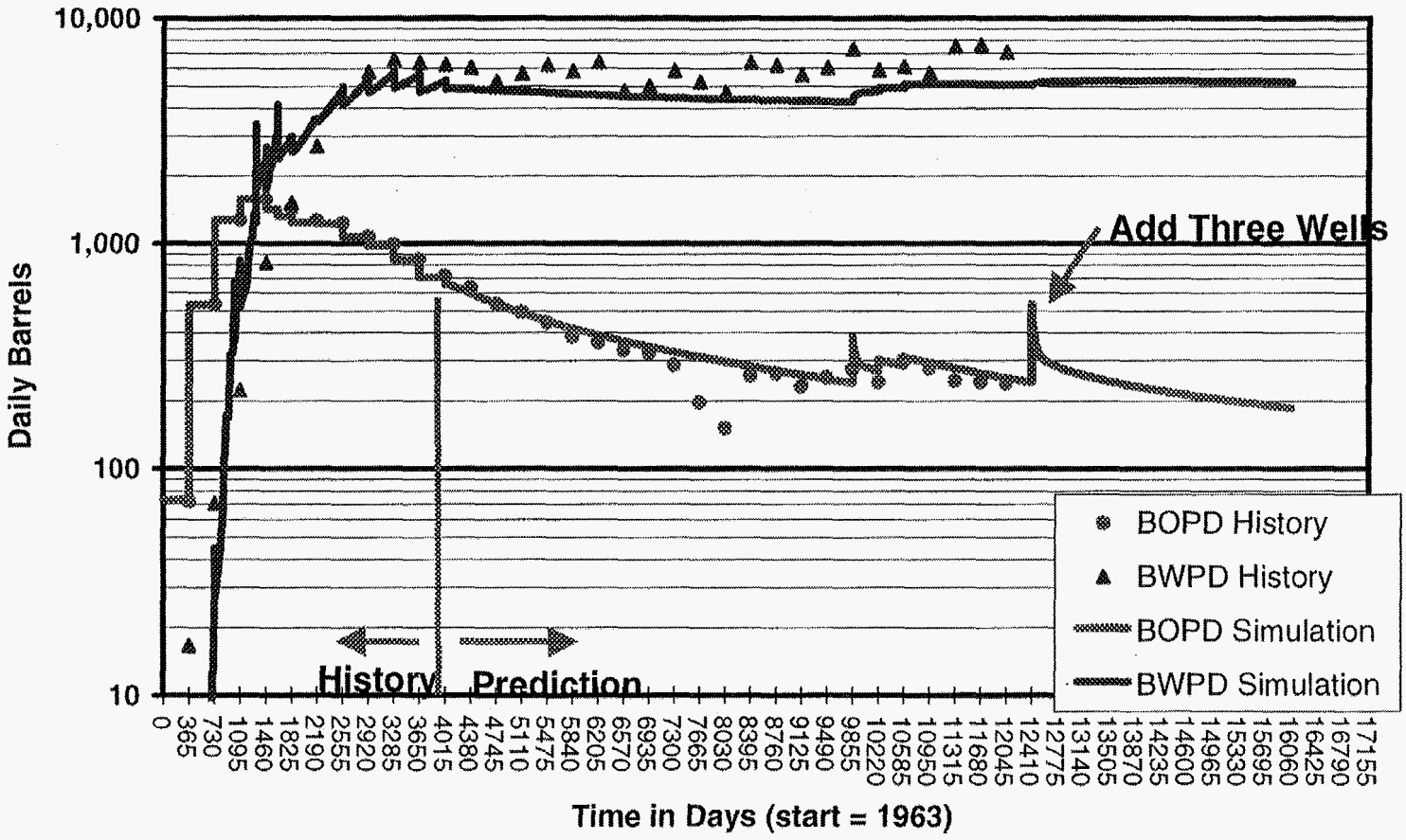

Figure 2.50

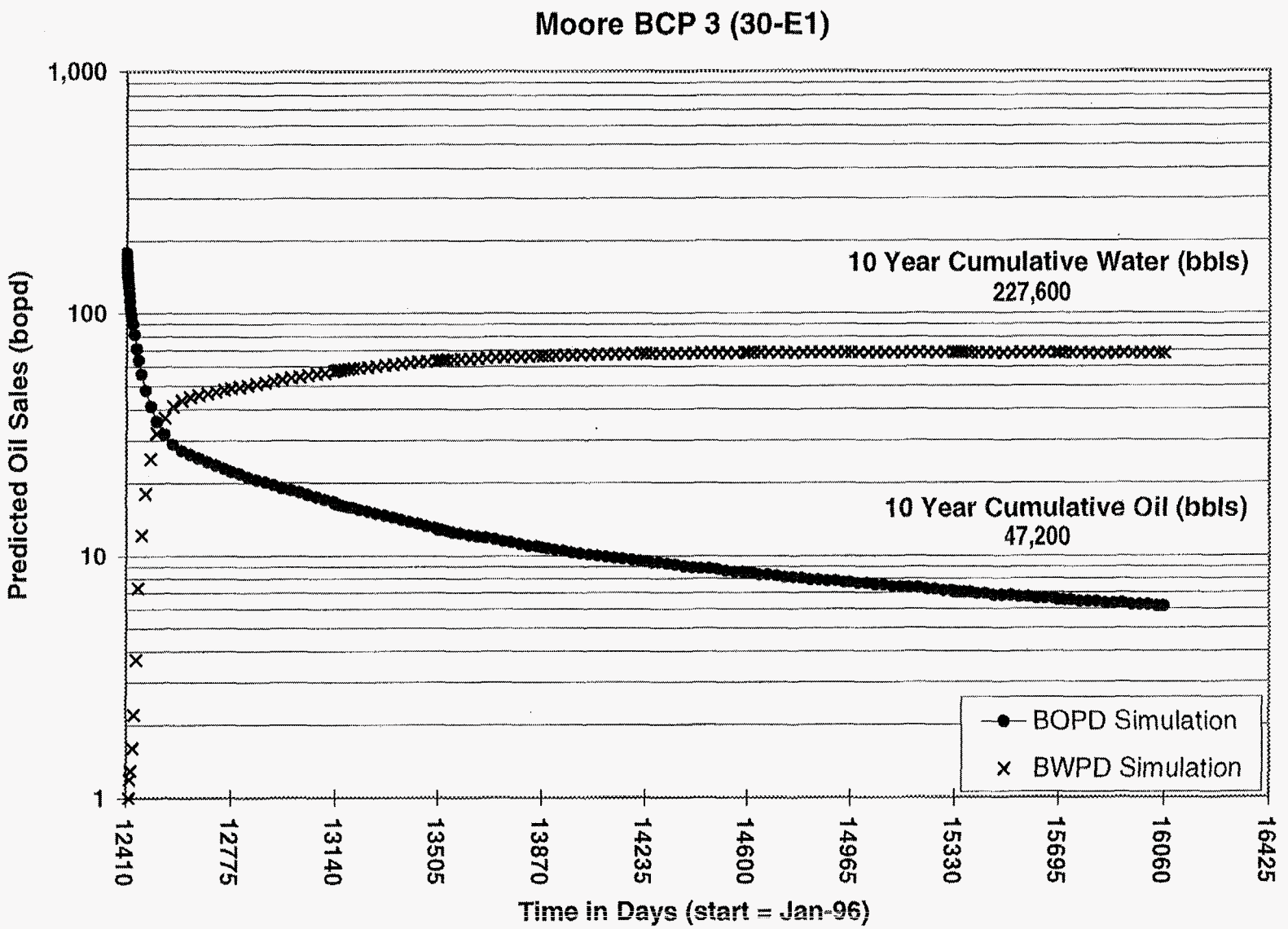
Moore BCP 3 (30-E1)
Predicted Oil Sales (bopd)
1,000
100
10
1
10 Year Cumulative Water (bbls)
227,600
10 Year Cumulative Oil (bbls)
47,200
BOPD Simulation
BWPD Simulation
12410
12775
13140
13505
13870
14235
14600
14965
15330
15695
16060
16425
Time in Days (start = Jan-96)

2.3.4 Section 30 VIP Simulation

The objectives of the reservoir simulation were: (1) evaluate the characterization and distribution of various reservoir parameters, (2) obtain a history match of the past production performance, (3) determine the remaining oil in place, (4) assess the viability of infill drilling, and (5) identify optimal sites for infill wells.

Personnel in the Tertiary Oil Recovery Project did simulation of the Schaben Field performance in Section 30 by matching production history from discovery of the field to 1995. Following development of the history match, production histories for potential locations of infill wells were simulated. Results of these simulations provide the basis for selection of sites for development in Budget Period 2.

In this section, the methodology for developing the reservoir simulation is summarized. A brief overview is presented describing the input data for the simulation. The procedure for obtaining the history match is outlined and results are presented for field and the individual wells. Finally, the rationale for selection of potential infill well sites is presented with results from simulation of thirteen possible infill locations.

Reservoir Simulator

The reservoir simulation was completed using Western Atlas VIP Executive simulation software installed on a Silicon Graphics workstation. The VIP simulator is a conventional black oil simulator, equipped with a graphics interface. VIP consists of a series of software products developed to perform simulation, pre-processing, and post-processing functions. The graphics package allows visualization of the reservoir depletion using three dimensional displays including recording on video tape for subsequent presentations.

The model developed in this study consisted of a two layered reservoir, with both layers having identical properties and an infinite acting water aquifer at the bottom of the reservoir. The area modeled was Sec.30-T19S-R21W. This area was selected based upon: (1) being the most prolific producing area within the field, (2) Ritchie Exploration's interest and ownership rights, and (3) time constraints associated with the development of an accurate geological model which was needed as data input for the simulation model.

Reservoir Description

Most of the data required for simulation was provided based upon the geological model developed at the Kansas Geological Survey. The data received were in the format of contour files, which were transferred electronically from KGS to the Silicon Graphics workstation at TORP. The data files consisted of top and bottom of the reservoir, net pay interval, porosity, horizontal permeability, and water saturation. Additional files necessary for simulation were developed at TORP for directional permeability, oil saturation, well locations, and PVT data. Adjustments were made in the initial data based on simulated production history. These adjustments are described in the section on the history match.

Production Data

The primary source of production data was from commercial oil sales records. This provided information on oil sales by lease, with no water production or individual well production data. A search was conducted to obtain individual well oil and water production from operators in the field. The only operator that supplied individual well oil and water production was Pickrell Drilling Company.

Annual productivity tests for Schaben Field wells were obtained from the file at the Kansas Corporation Commission. These tests were required as the production from the field was prorated by the KCC from 1964 to present. Annual productivity tests were used to allocate annual oil production from sales records to individual wells. Although overall oil production for the field should be accurate, there is uncertainty associated with the water production and individual well production.

An important parameter in the reservoir simulation is the bottom hole pressure in the production wells during production. The bottom hole pressure must be known to accurately match field performance using the reservoir simulator. When the history match is completed properly, the reservoir simulator will match production performance when the bottom hole pressure is specified in each production well.

Fluid levels and operating practices were obtained from individual well files and discussions with Ritchie field production personnel. Table 1 (Appendix J) summarizes initial production data and information on the fluid level in each well. It is difficult to tell whether the wells were pumped off following the initial completion. It appears that most of the wells were initially capable of producing in excess of their daily oil allowable.

Oil production declined fairly rapidly following initial completion and some water production began to appear. Well tests indicated reduced productivity following initial completion of less than 100 bbls of total fluid per day. During this time all the wells were pumped off. Periodic acid jobs provided minor stimulation of production, but the wells remained pumped off. The majority of the water production occurred following recompletion with the perforation of additional Mississippian or Ft. Scott pay. A few wells have consistently high fluid levels.

Rock/Fluid and Fluid Property Data

Limited data were available for reservoir rock and fluids in this field. Oil gravity is 40.2 ° API. Viscosity of dead oil at reservoir temperature (Rein "A" Lease June 24, 1965) was 2.5 cp. There was no evidence of significant solution gas in this field so the bubble point pressure is low. Reservoir temperature is about 125 °F. Viscosity of the reservoir brine at reservoir temperature (0.64 cp) was estimated from the a correlation based on the TDS analysis from a water sample from Rein A-1(26,134 ppm). Residual oil saturation varied from 20-25% from core analysis so a value of 23% was selected for simulation.

Relative permeability data are required for the reservoir simulation. A limited amount of data were available from core samples on Moore "D" No. 1, Moore "B" No. 1, and Humberg "A" No. 1. Data included end point permeabilities, water/oil permeability ratios at several water saturations, initial water saturations and residual oil saturations. Initial water saturations from the core data varied from 31 to 56%. The relative permeability to water at residual oil saturation averages 0.25 which was selected for the simulation. The correlation developed from this data for the Schaben simulation is given below:

Relative Permeability Curves

$$k_{ro} = \__1(1 - S_{wD})^m$$
$$k_{rw} = \__2(S_{wD})^n$$

where,

$$S_{wD} = (S_w - S_{iw})/(1 - S_{iw} - S_{or})$$

In these correlations, S_{iw} = initial water saturation, S_{or} = residual oil saturation, while $\__1$,m,and n are determined by fitting the data. The parameter $\__2$ is the relative permeability to water at residual oil saturation was determine from core data to be 0.25.

History Match

The reservoir was divided by 20 x 20 x 2 grids in x, y, and z direction respectively. The simulator allowed non-uniform gridding with the well forced to be located at the center of the grid block. The grid layout is shown in Figure 2.51 which depicts the pore volume of each grid block. All the wells were perforated in the top layer. An infinite aquifer with strength set to 100 was used to support the field from the bottom. The total pressure drop in the reservoir was less than 100 psi for the entire production period of the field which is consistent with the pressure observation of the field.

The process of matching the history of the reservoir from 1963 to 1995 involved running numerous simulations to determine if the reservoir properties were consistent with the observed production response. It is not unusual to find that the initial reservoir description cannot be used to match oil and water production history. Rock properties such as permeability are often adjusted in an attempt to secure a satisfactory history match.

In simulating the Schaben field, the initial runs indicated that production response could not be matched for any reasonable changes in permeability. Large volumes of water were produced from wells that were known to produce *"water free"* oil in the initial 1-2 years. Initial water saturations provide by KGS ranged from 50 to 80 percent. The average water saturation in Section 30 was 62 percent. It became clear that the initial water saturations provided by KGS were not correct.

A revision in the reservoir description was made by KGS personnel based on the assumption the reservoir has a two phase pore geometry consisting of macro and micro pores. It was further assumed that oil was contained only in macro pores and that micro pores contained 100 percent water, which was assumed to be immobile. The effective porosity was reduced as

well as the water saturation in permeable rock. The revised initial water saturations varied from 19 to 45 percent, with the resulting average water saturation in Section 30 being 30 percent. The oil saturations were changed to correspond with the new water saturation data. Figures 2.52 and 2.53 show the map of the revised initial oil saturation and the porosity distribution in Section 30.

Following adjustment of the porosity and water saturations, a series of simulations were run to determine if a satisfactory history match could be obtained. Criteria for a successful match include matching cumulative oil and water production within 10%. Water production was more difficult to match but was within 10% for most wells. However, the water production data have the highest uncertainty.

Adjustments in permeability modifications were made both laterally and locally to obtain the history match for oil and water production. When it became apparent that a history match could be obtained, bottom hole pressures in production wells were set at values estimated from the data presented in Table 1 and the history match was refined. The changes in the original reservoir description are summarized in Appendix K.

The history match was made in three stages:

Stage 1: Oil production was set to the actual production and water production was matched for each well from 1963 to 1995 by adjusting relative permeability curves. Pressure limitation was set to 15 psi.

Stage 2: Oil and water production was predicted from 1978 to 1995 by adjusting fluid level in each well based on the available data. Local adjustments for each well were made for k_x, k_y, and k_z to get the best match for each well. Figures 2.54-2.56 show the distribution of permeability thickness, X-direction and Z- direction permeability used in the final simulation.

Stage 3: Fluid level in each well was set based on the available data in Table 1. Oil and water production was simulated for each well for the entire period of 1963 to 1995 using the reservoir parameters determined in Stages 1 and 2..

Results from the Stage 3 simulation are summarized in Table 2. Cumulative oil production through 1995 was 1.84 MMSTB and cumulative water production was estimated to be 10.46 MMSTB. Cumulative oil production from the simulation was 1.82 MMSTB and cumulative water production was 11.79 MMSTB. Graphs of the cumulative oil and water production for the field and individual wells are presented in Figures 2.57-2.59. Oil production rate is plotted against time in Figure 2.58. Figure 2.59 shows the water production rate during the same period. Graphs of cumulative oil and water production for individual wells during the life of the project are included in Appendix B. Figures 2.60 and 2.61 show the ratios of actual/simulated oil and water production from each well.

The overall agreement is excellent considering the amount and quality of the data used to develop the reservoir description and history match. The agreement between simulated and actual history could be improved by fine tuning of the reservoir description, particularly

adjustment of initial water saturations in regions where wells produced "clean" oil for 1-3 years after completion.

Potential Infill Locations

Potential locations for infill wells were identified from examination of the oil saturation map at the end of 1997 shown in Figure 2.62. A map of mobile oil was generated from saturation, net thickness and porosity maps. This map is presented in Figure 2.63 in terms of barrels per acre. Figure 2.63 should be used with caution because significant mobile oil is indicated in the region between Wells B-1 and B-6 even though Wells B-3 and B-7 were completed in this region and abandoned.

Figure 2.64 shows the locations of nine potential infill wells selected from Figures 2.60 and 2.61. These are identified as New Wells 5-13 on the map. Wells 6-9 and Well 13 were vertical wells. Wells 10-12 were horizontal wells that were drilled at the same locations as corresponding vertical wells. These wells had horizontal sections 1284 to 1402 ft in length. Grid locations (row and column indices) of these wells are included in Table 3 along with cumulative oil and water production for the period from 1998 to 2005. Simulated production from individual wells is summarized in Tables 4-12. Production from the vertical wells ranged from 32.55 to 116.03 MSTB. Simulated oil production from five of the six wells was in excess of 60 MSTB. Thus, there is potential for significant additional oil production from Section 30 by drilling vertical infill wells and these well would be economic at current oil prices.

Estimated cumulative production from horizontal wells ranged from 133 MSTB to 352 MSTB. Production from these wells (Wells 11-13) is summarized in Tables 10-12. Production is characterized by high initial rates in first year or two followed by a rapid decline. Estimated production rates are on the order of several thousand barrels of fluid per day which will require installation of high volume pumps and will increase operating costs but appear to be economic if high initial oil production rates are found.

Four additional vertical infill wells were simulated at locations identified by Ritchie Exploration Co as potential sites with offsetting lease considerations. These wells are identified as Wells 1-4 and are shown in Figure 2.64. Cumulative oil and water production for the period 1998-2005 is summarized in Table 13. Simulated production from individual wells is presented in Tables 14-17. Cumulative oil production from these wells varies from 21 MSTB to 28 MSTB. These sites are considered marginal and would not be supported as potential sites in Budget Period II.

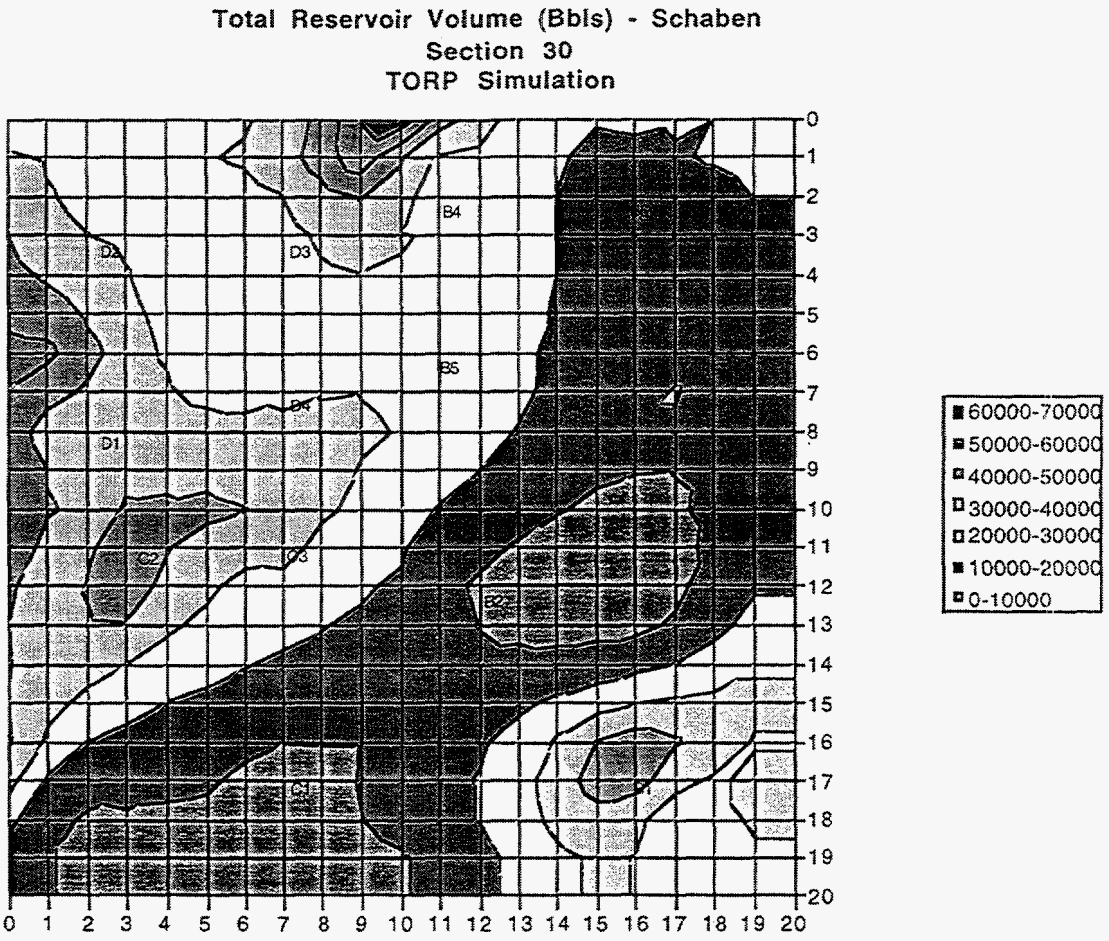

Figure 2.51. Grid layout with reservoir volume for Section 30 simulation.

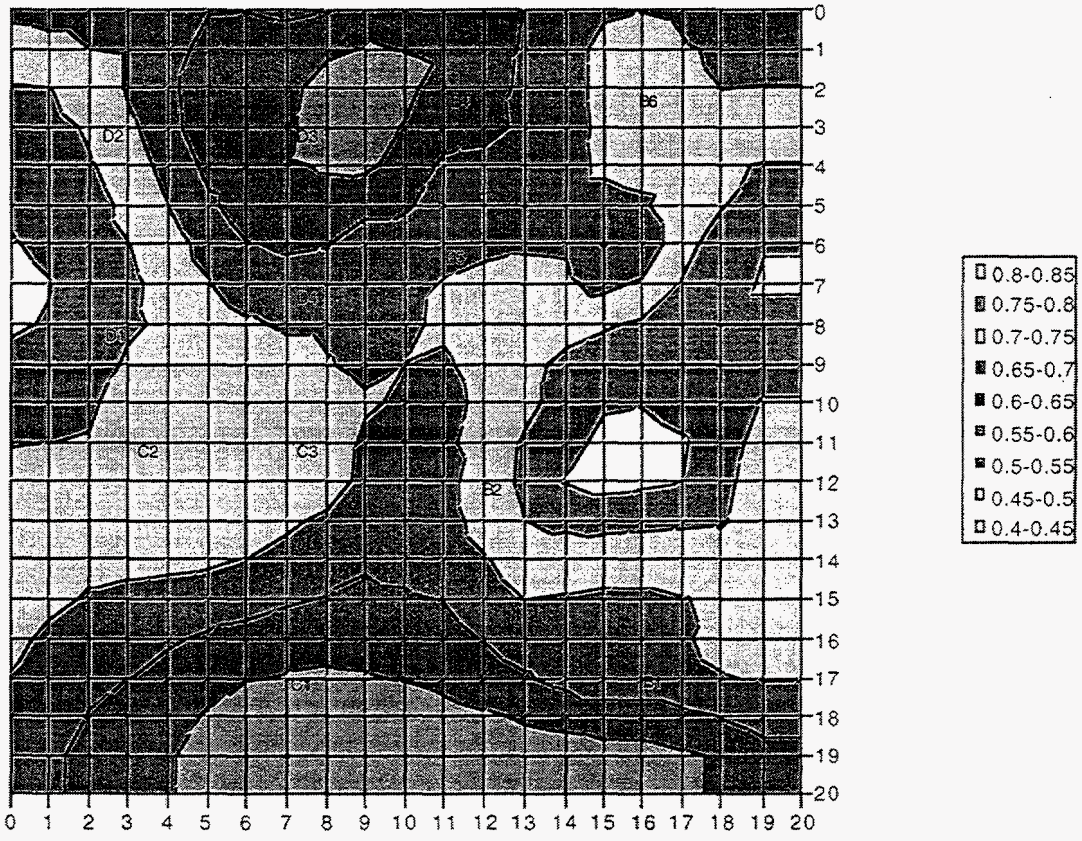

Figure 2.52 Revised initial oil saturation Section 30

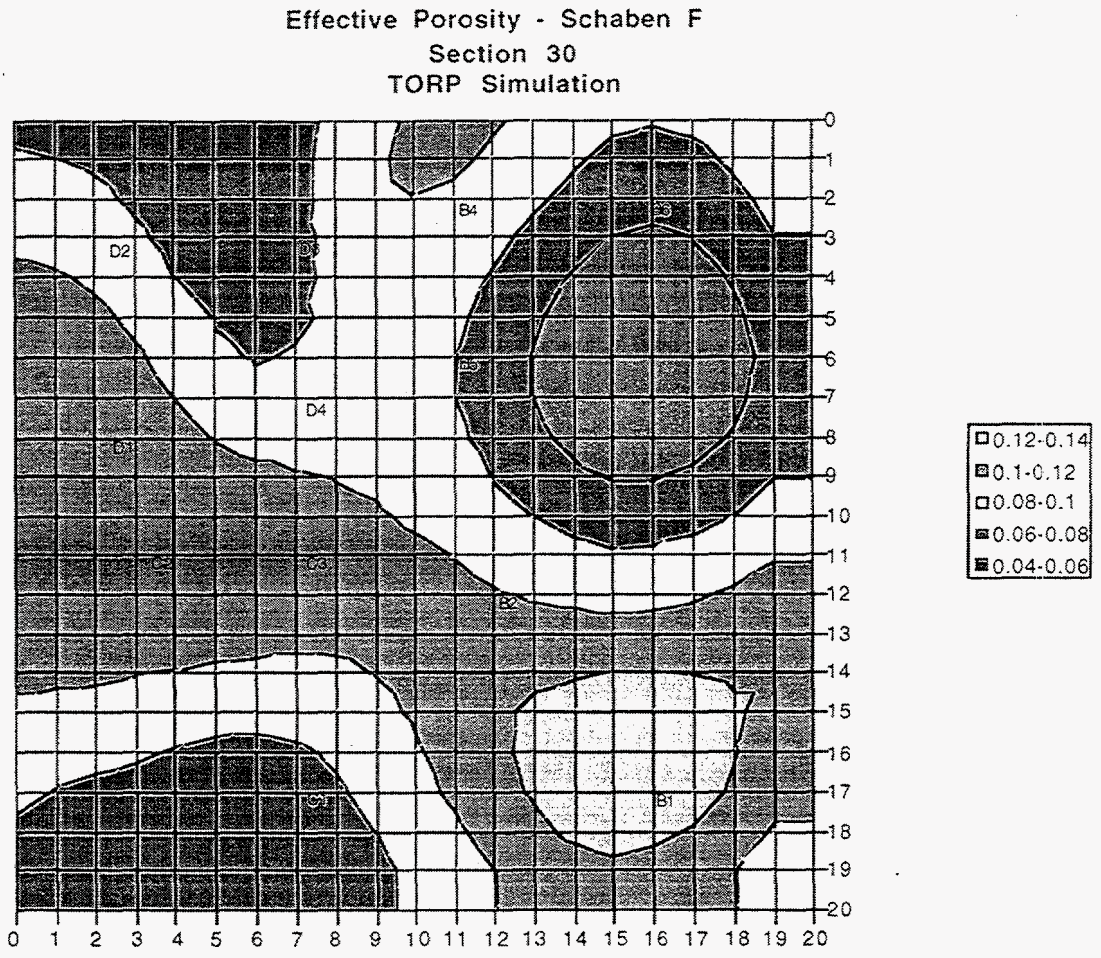

Figure 2.53 Effective porosity Section 30

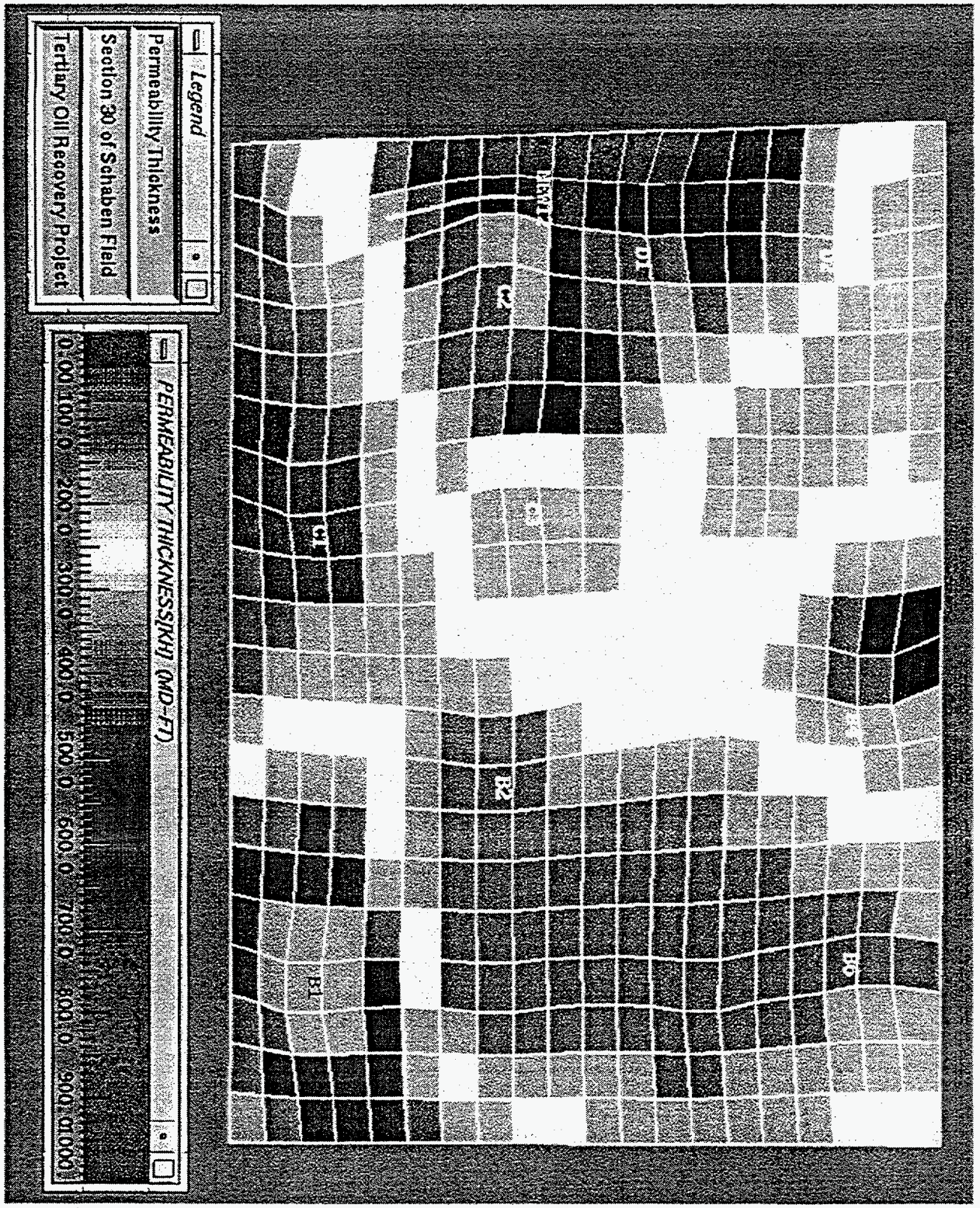

Figure 2.54 Permeability thickness distribution Section 30.

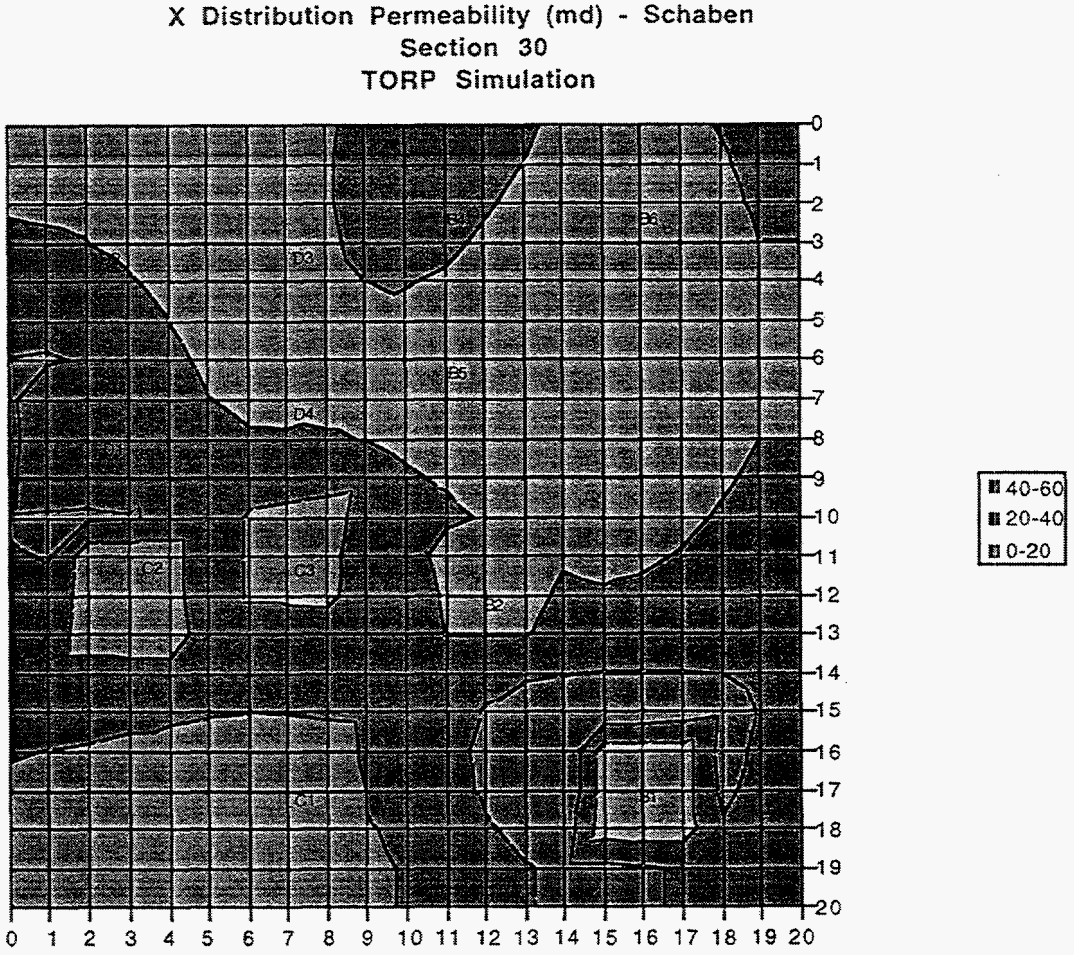

Figure 2.55 X Distribution permeability in Section 30

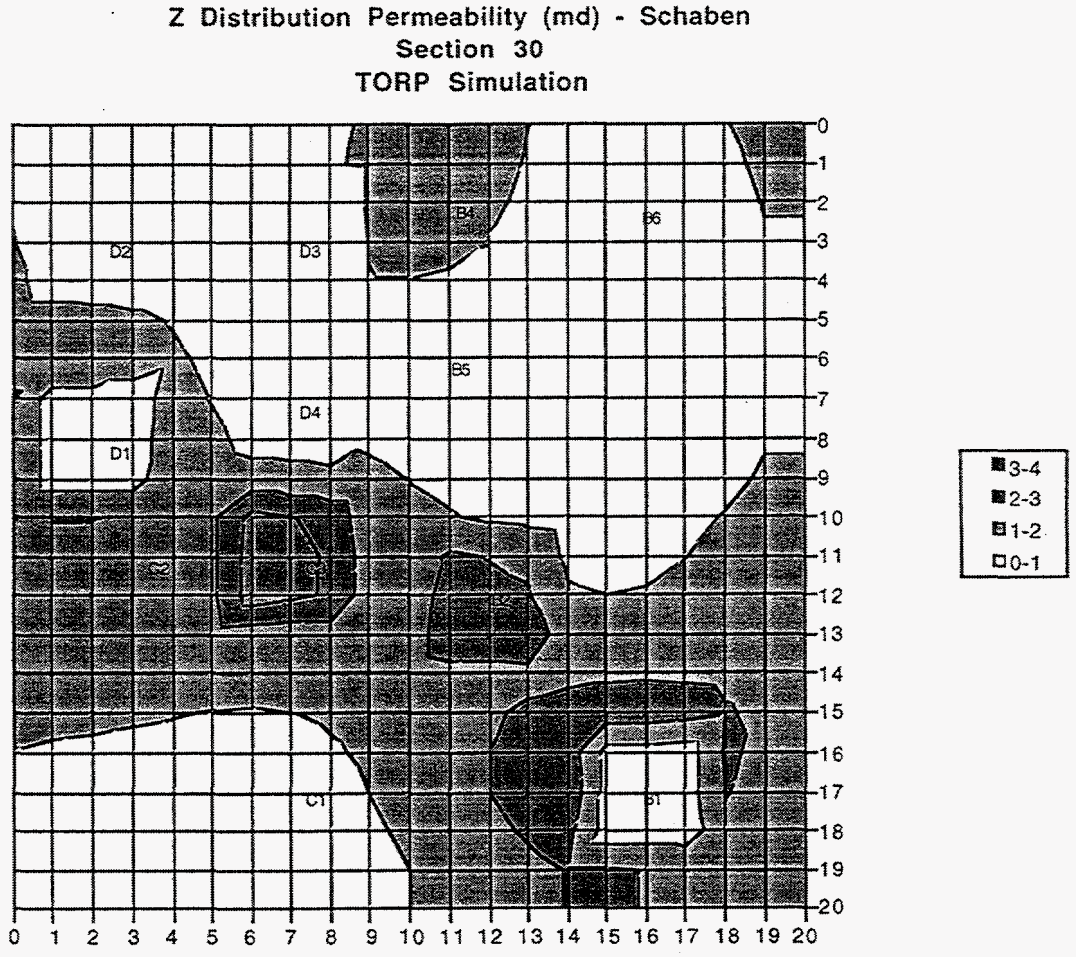

Figure 2.56 Z Distribution permeability in Section 30

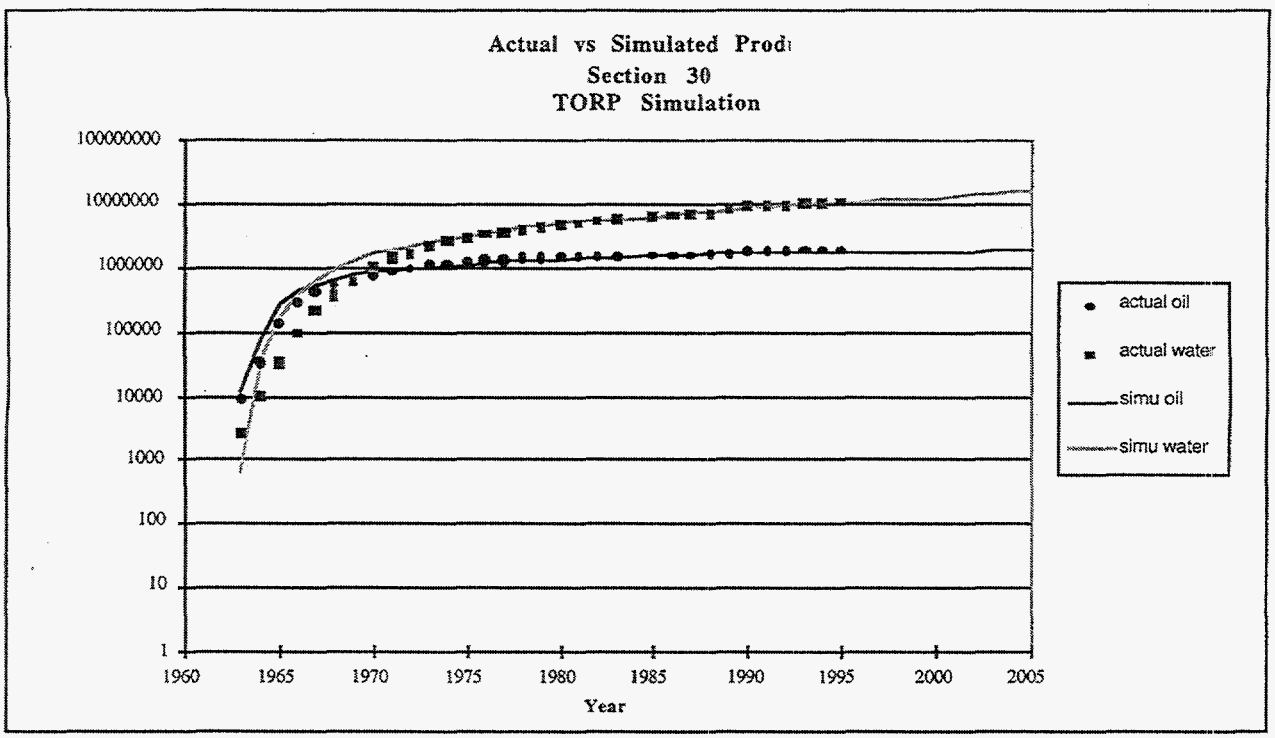

Figure 2.57 Actual vs. Simulated oil production rates in Section 30

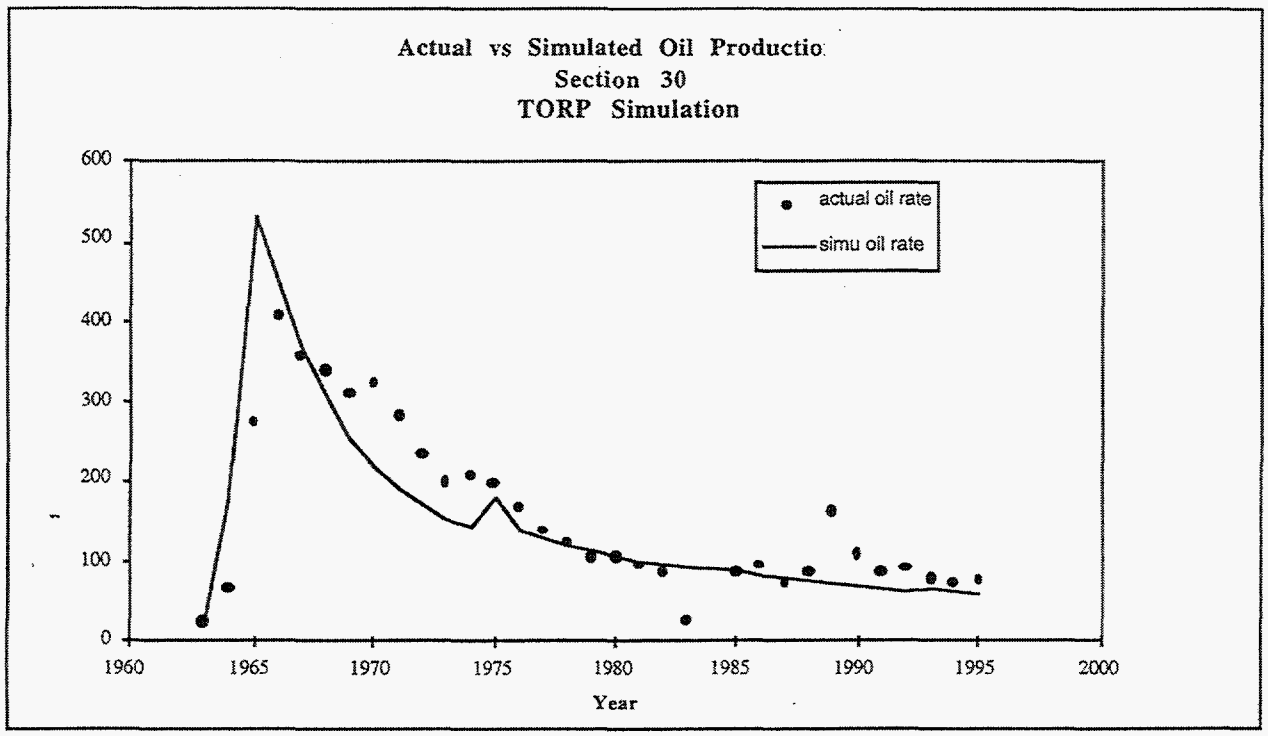

Figure 2.58 Actual vs. Simulated oil production rates in Section 30

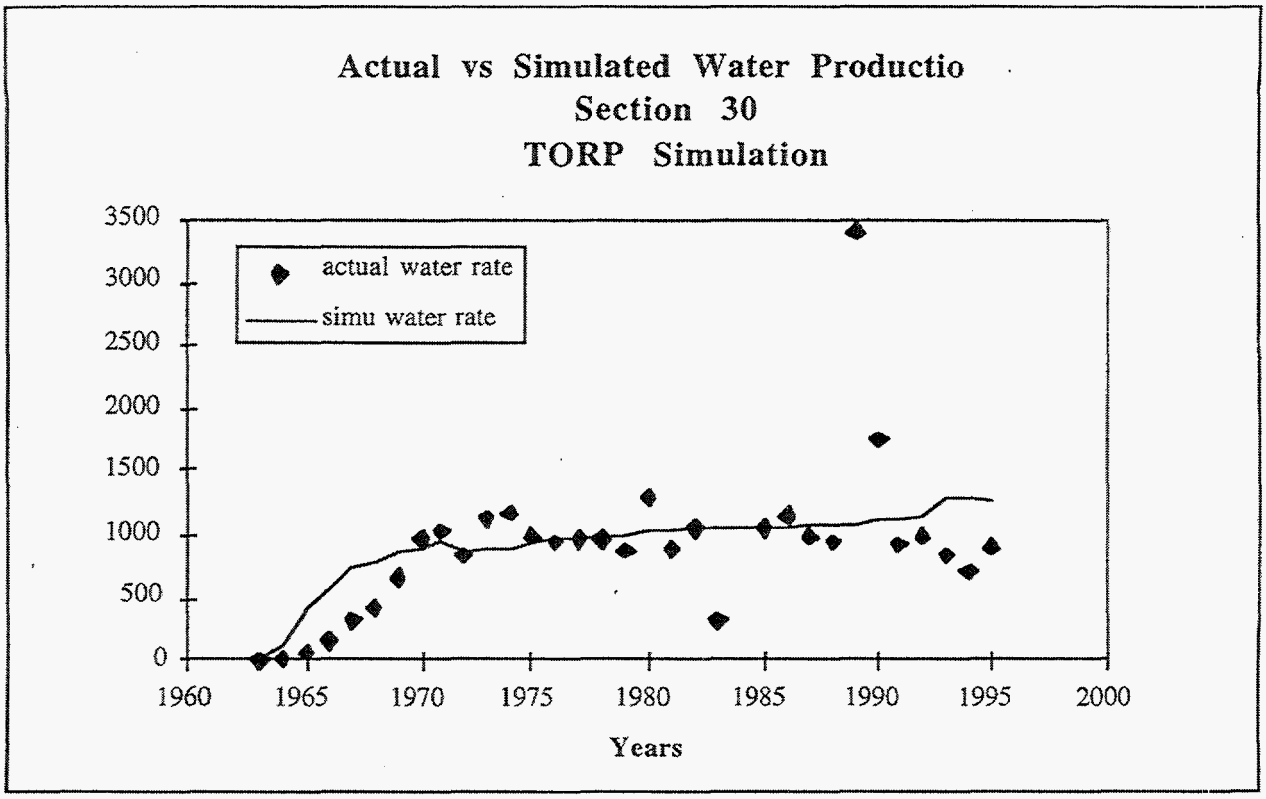

Figure 2.59 Actual vs. Simulated water production rates in Section 30

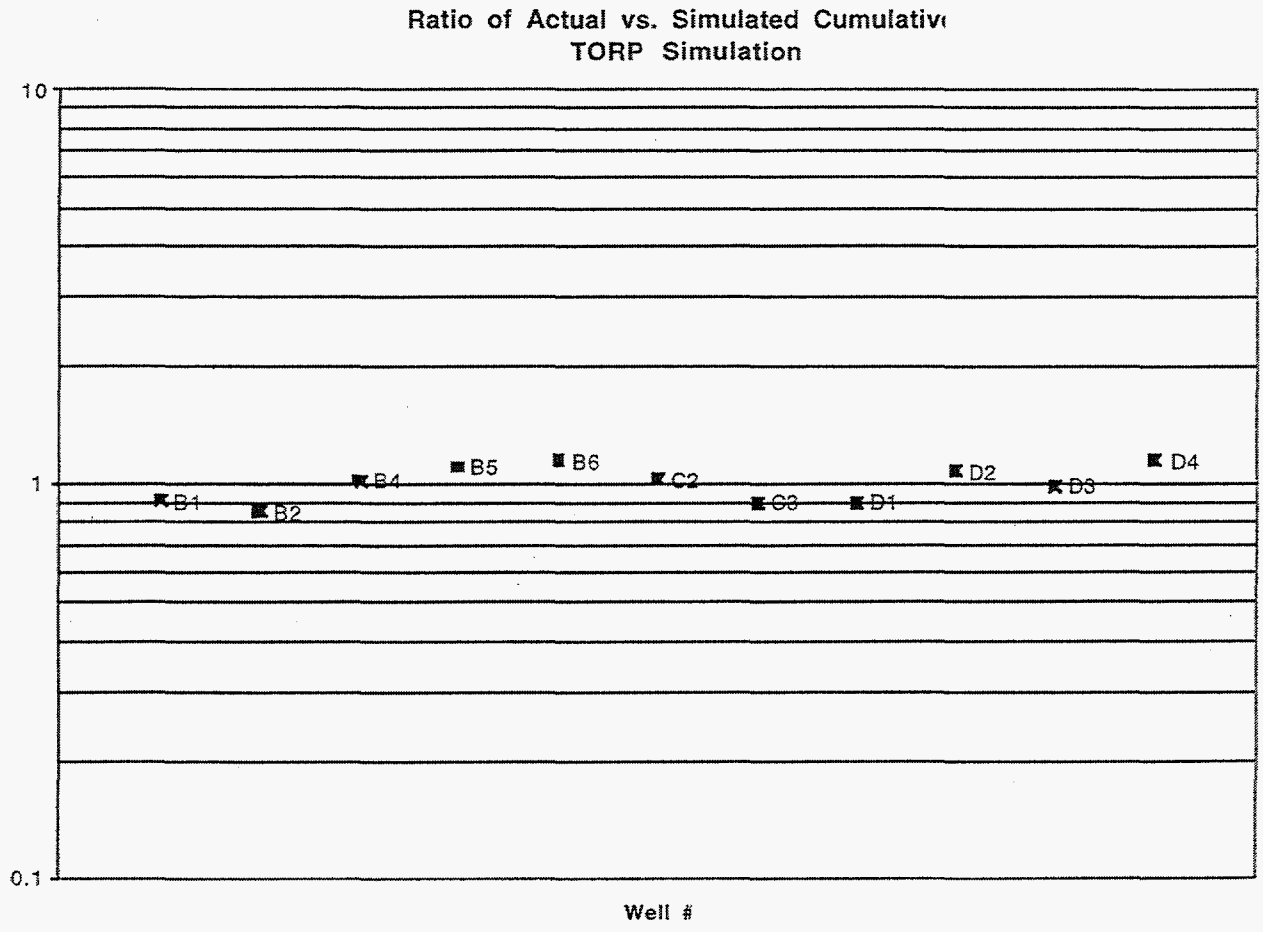

Figure 2.60 Ratio of actual vs. simulated cumulative oil

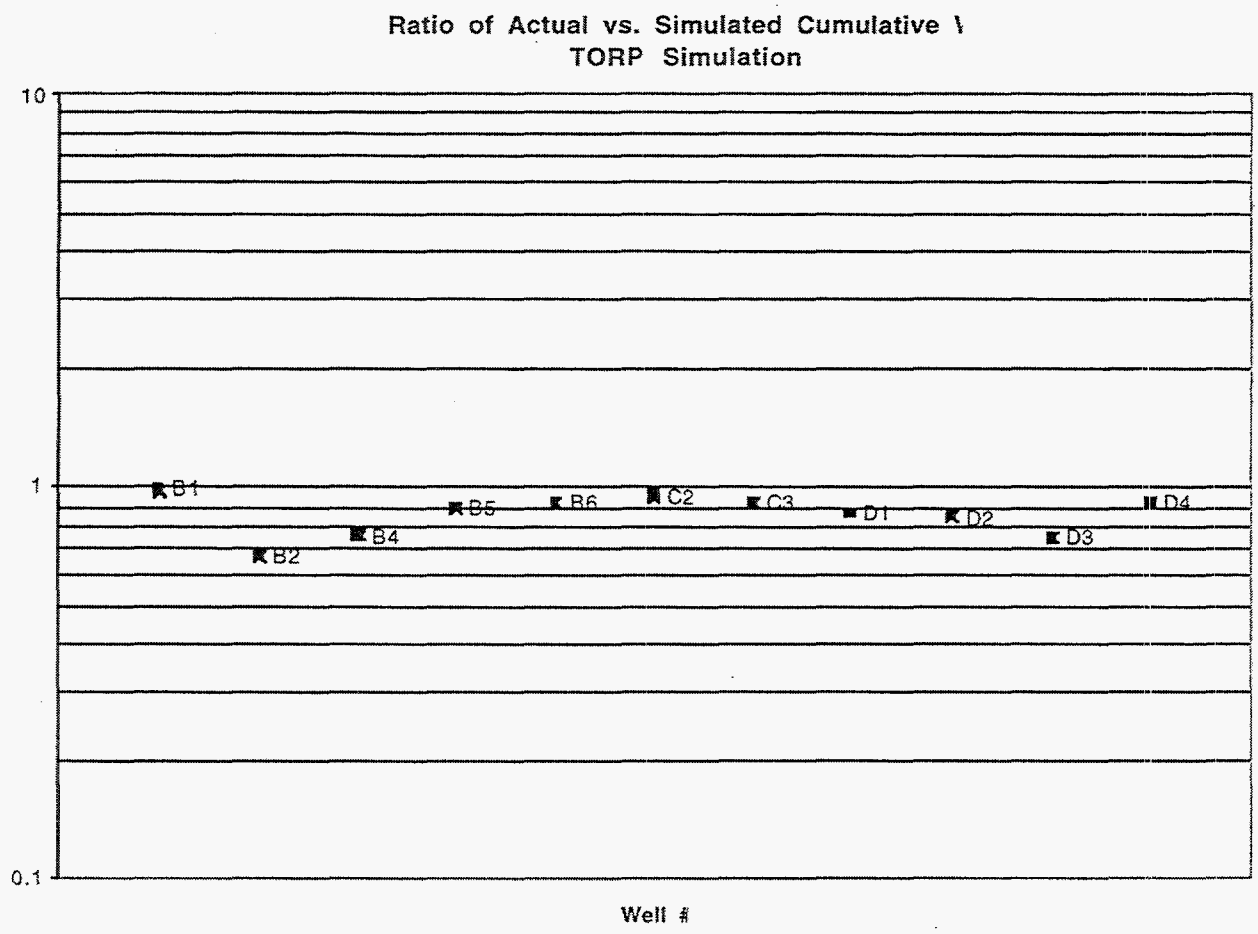

Figure 2.61 Ratio of actual vs. simulated cumulative water

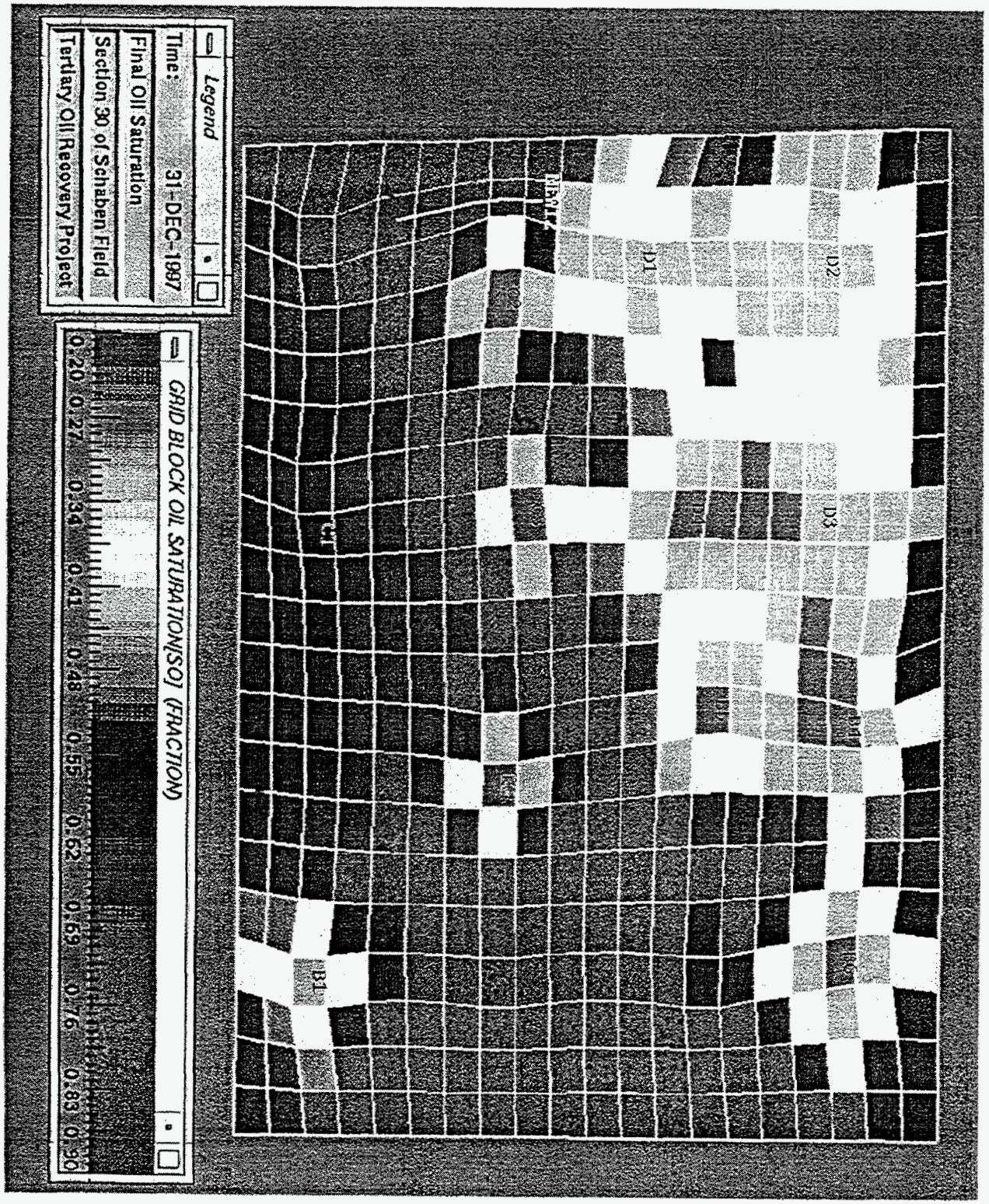

Figure 2.62 Oil saturation in Section 30, end 1997.

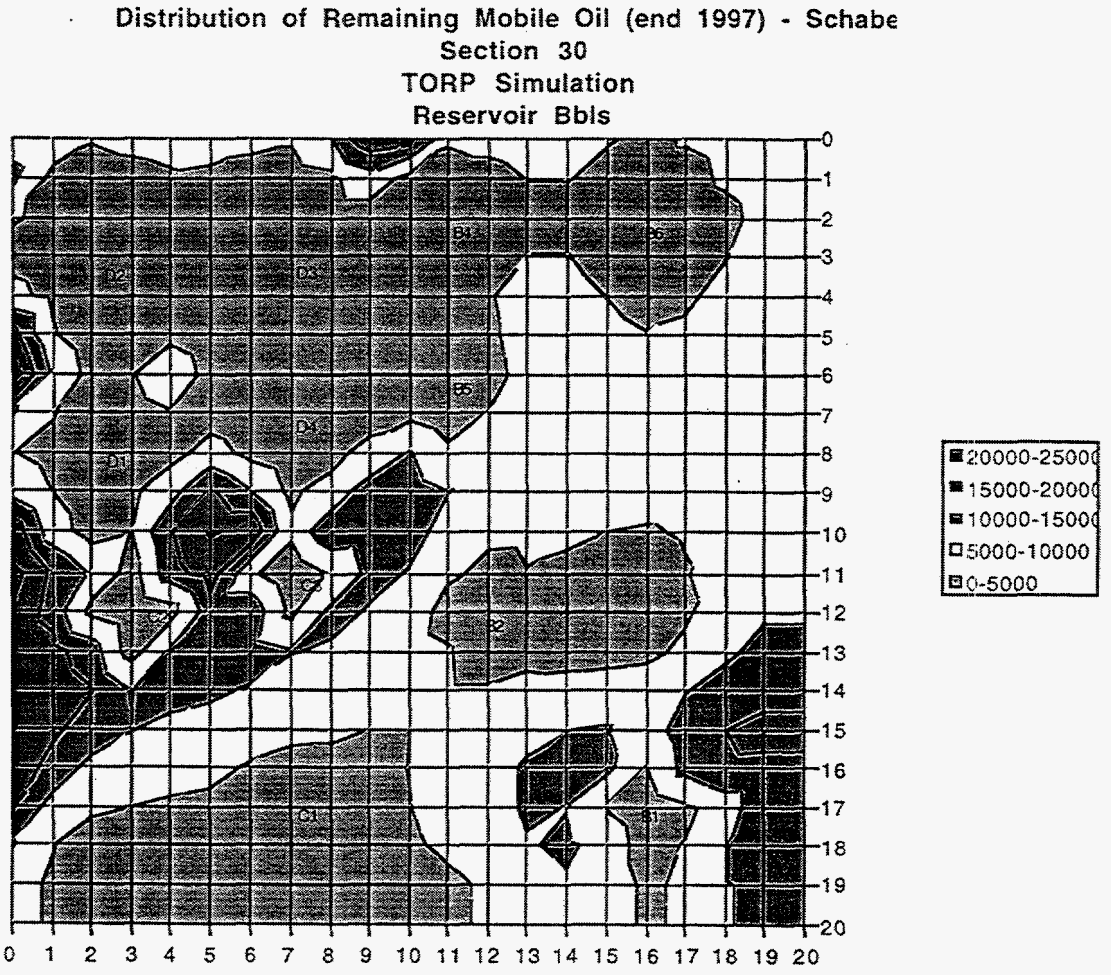

Figure 2.63 Distribution of mobile oil in Section 30, end 1997

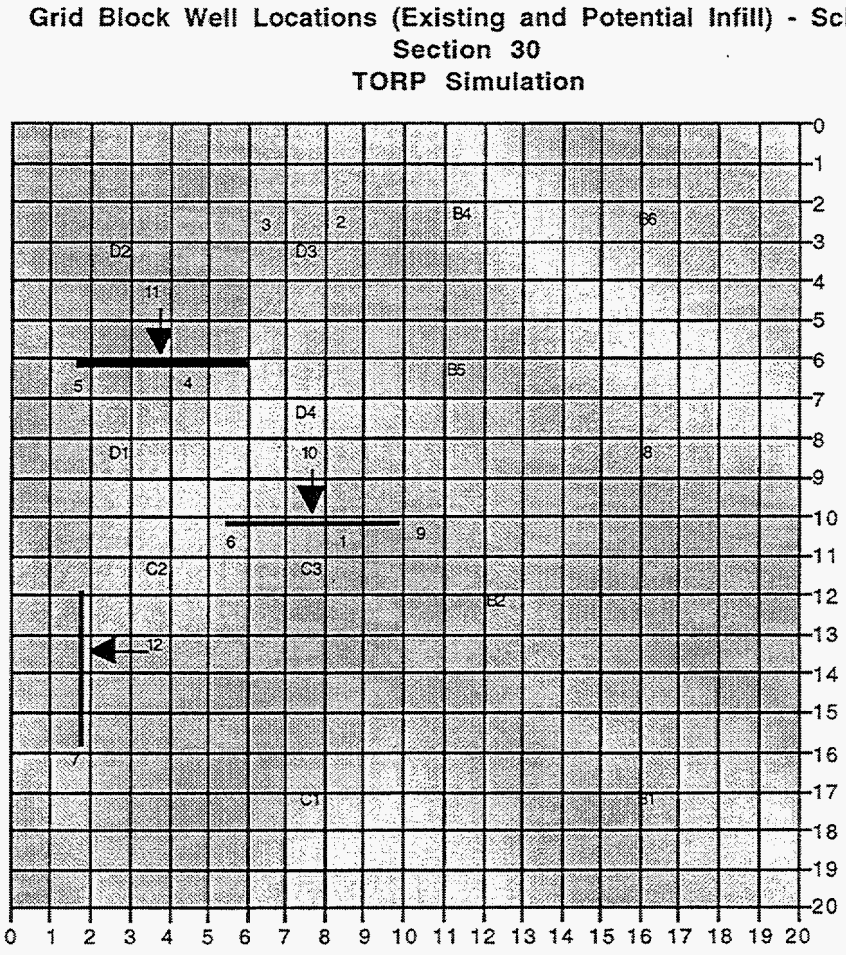

Figure 2.64 Location of existing and potential infill wells.

2.4 TECHNOLOGY TRANSFER ACTIVITIES

2.4.1 Traditional Activities

The data, results and technology have been presented at numerous technical meetings and published in technical papers in local, regional and national publications. PfEFFER a software package using a widely available spreadsheet was developed tested and demonstrated as part of the Class 2 project. In addition, BOAST 3 a public-domain program for reservoir simulation has been modified and demonstrated for full-field simulation. All technologies, developed and demonstrated as part of the Kansas Class 2 project, were tailored specifically to the scale appropriate to the operations of Kansas producers. The majority of Kansas production is operated by small independent producers that do not have resources to develop and test advanced technologies (90% of the 3,000 Kansas producers have less than 20 employees). For Kansas producer's, access to cost-effective new technology is important for sustaining production and increasing viability

2.4.2 Non-Traditional Activities (Internet)

All data and results of the Schaben project are being added to a world-wide-web server. The Internet protocol provides independent operators with on-line access to digital information, digital data bases, results of the field study, related regional geologic and production data, and purposeful transfer of technology. Access is through the Ness County page of the Digital Petroleum Atlas prototype (Figure 1.6; the uniform resource locator [URL] is http://crude2.kgs.ukans.edu:80/DPA/County/ness.html). It should be emphasized that the Schaben Project is an additional play/field to the Digital Petroleum Atlas and is not a substitute. The Internet provides just-in-time accessibility to fundamental well, reservoir, and geographic data (such as e-logs, production volumes, and digital map data), to petroleum related data compilations (such as the Schaben field study, regional maps [see Ness County page] and bibliographies), and to the latest research ideas. The virtual resource center provides a flexible and efficient method to disseminate data and technology to a geographically dispersed high technology industry.

We provide to independent operators, through on-line access, an evaluation of the technologies best suited for additional hydrocarbon recovery at Schaben and other Mississippian sub-unconformity fields. Information is available when and where operators need it (figuratively on the operator's desk). The digital structure permits the operator to access comprehensive reservoir data and customize the interpretative products (for example, maps and cross-sections) to their needs. Schaben Field and regional data sets along with technical studies are free-standing, but linked, entities that will be made available on-line through the Internet to users as they are completed.

Data sets have relational links that provide opportunity for history-matching, feasibility, and risk analysis tests on the Schaben demonstration site. The flexible "web-like" design provides ready access to data, and technology at a variety of scales from regional, to field, to lease, and finally to the individual bore. The digital structure permits the operator to access comprehensive reservoir data and customize the interpretative products (for example, maps and cross-sections) to their

needs. The results of the Schaben study are accessible in digital form on-line using a World-Wide-Web browser as the graphical user interface.

2.5 PROBLEMS ENCOUNTERED

Permitting problems in the Schaben Field demonstration area delayed wells, but has not had a significant impact on project results. A recent ruling by the Kansas Corporation Commission provides some flexibility and should assist continued operations. The project is well within budget and cost sharing is in excess of 50%.

2.6 RECOMMENDATIONS FOR BUDGET PERIOD 2

Tasks for Budget Period 2 as outlined in the original Statement of Work remain as originally proposed. Modifications in subtasks reflect the results and knowledge gained in Budget Period 1. The tasks, subtasks and recommendations for Budget Period 2 are listed below.

Task 2.1 DEMONSTRATION OF RESERVOIR MANAGEMENT STRATEGY

Subtask 2.1.1 Infill Drilling-Schaben Demonstration Site

On the basis of the results of the advanced reservoir characterization and the simulation results for Schaben field, four well locations will be selected for infill drilling and possible horizontal reentry/drilling. An optimal drilling, completion, and production strategy will be demonstrated for each well. It is anticipated that the strategy will include the following components. Each well will be drilled, cored and logged. All cores will be petrophysically analyzed, photographed, slabbed, and boxed. Petrophysical analysis will include porosity, multi-directional permeability, oil and water saturation, capillary pressure and NMR. Cores will also be analyzed to determine fracture density and orientation. Drilling information, drillstem test data, and log evaluation will provide the basis for the casing point decision. If warranted, the wells will be completed and equipped for production. All pertinent well data will be entered into the digital computer database for use in modifying the reservoir simulation and evaluation of additional vertical wells and potential horizontal well.

Subtask 2.1.2 Production Performance Evaluation-Schaben Demonstration Site

Following drilling, deepening, and completion of the demonstration wells, production will be monitored and reservoir performance will be evaluated. The incremental contribution to recoverable reserves of all wells completed or recompleted as producing wells will be evaluated. Wells drilled during Budget Period 1 and completed as producers will continue to be evaluated for their contribution to incremental reserves, and the implications for infill drilling potential. The results of drilling, completion, and production of the demonstration wells will be compared to the predictions of the advanced reservoir characterization and reservoir simulation. The incremental contribution to recoverable reserves and the implications for additional infill and horizontal drilling will be evaluated using commercial and public domain simulators. These simulators will include BOAST 3 and BOAST-VHS.

Subtask 2.1.3 Regional Comparison

The detailed reservoir models developed and demonstrated at the Schaben Field demonstration site will provide the basis for evaluating the critical reservoir parameters characterizing the sub-unconformity Mississippian reservoirs of the central Kansas and the Mid-continent. In conjunction with a regional database consolidated from Kansas Geological Survey, Kansas Corporation Commission and operator data sources, reservoir models from the field site will provide a basis for comparison to other sub-unconformity reservoirs, and will facilitate transfer of technology developed and demonstrated to other nearby reservoirs in the producing trend. All data and interpreted products will be available on-line through the Internet. Regional potential for recovery of additional reserves will be evaluated.

Task 2.2 TECHNOLOGY TRANSFER

Subtask 2.2.1 Preparation of Technology Transfer Materials

Continued development and publication of manuscripts and software.

Develop an improved interface between BOAST 3 and PfEFFER along with improve preprocessing (e.g., spreadsheets), data management and post-processing (graphics) tools.

Develop a teaching manual and improved user's manual for BOAST 3.

Preparation of presentation figures, maps and core displays.

Development of improved on-line access to digital databases, information and technologies developed as part of the project.

Subtask 2.2.2 Technology Transfer Activities.

Continued on-line, open-file publication of technical results.

Presentation of results in at least two seminars/workshops targeted to Kansas and other operators of Class II reservoirs. These will include integrated short courses involving the Schaben Demonstration project and cost-effective technologies developed and demonstrated in Budget Period 1. These technologies include PfEFFER, BOAST 3 and the Internet. A first round of classes has been scheduled for June 23-27 in Lawrence, Kansas.

Continued presentation of results via oral or poster presentations at local, regional, and national meetings. Upcoming scheduled presentation include the National AAPG Meeting (Dallas) and the National SPE Meeting (San Antonio)

Continue publication of technical papers in local, regional, and national professional/technical publications.

Task 2.3 FULFILLMENT OF REPORTING REQUIREMENTS

All reporting requirements of the Department of Energy, other federal agencies and state and local governments will be fulfilled in a timely fashion.

3.0 REFERENCES CITED

Akkurt, R., 1990, Effects of tool motion in pulsed NMR logging: Ph.D. Dissertation, Colorado School of Mines.

Barry, Cavers, and Kneale, 1975, Recommended standards for digital tape formats: Geophysics, v. 40, no. 2, p. 344-352.

Canadian Well Logging Society's LAS Committee, 1993, New features of LAS 2.0 the floppy disk standard for log data: The Log Analyst, March-April 1993, p. 60-68.

Carr, T. R., D. Beene, and D. R. Collins, 1995a, Kansas Oil and Gas Production Trends: Kansas Geological Survey Open File Report 95-42, 8p.

Carr, T. R., Hopkins, J. H., Feldman, H. R., Feltz, A., Doveton J. H., and D. Collins, D. R., 1995b, Color 2-D and 3-D Pseudo-Seismic Transforms of Wireline Logs: A Seismic Approach To Petrophysical Sequence Stratigraphy; Landmark Computer Graphics UserNet, 6p.

Chandler, R.N., Drack, E.O., Miller, M.N., and Prammer, M.G., 1994, Improved log quality with a dual-frequency pulsed NMR tool: Soc. Petroleum Engineers: SPE 28365, p. 23-35.

Collins, D. R., and Doveton, J. H., 1986, Color images of Kansas subsurface geology from well logs; Computers and Geoscience, v. 12, 519-526.

Collins, D. R., and Doveton, J. H., 1989, Applying color information theory to the display of lithologic images from wireline logs, Geobyte, v. 4, p. 16-24.

Doveton, J. H., Guy, W., Watney, W. L., Bohling, G. C., Ullah, S., and Atkins-Heljeson, D., 1995, PfEFFER 1.0 Manual, Kansas Geological Survey Open File Report 95-86.

Doveton, J.H., Guy, W.J., Watney, W. L., Bohling, G.C., Ullah, S., and Adkins-Heljeson, D., 1996, Log analysis of petrofacies and flow-units with microcomputer spreadsheet software: 1995 AAPG Mid-Continent Meeting.Transactions, p.224-233.

Doveton, 1994, Geologic Log Analysis Using Computer Methods, A. A. P. G. Computer Applications in Geology 2, 169p.

Ebanks, W.J., Jr., 1991, Bindley field-U.S.A. Anadarko Basin, Kansas *in* Beaumont, E.A., and N.H. Foster, compilers, Stratigraphic TrapsII: AAPG Treatise of Petroleum Geology Atlas of Oil and Gas Fields, p. 117-136.

Goebel, E. D., and Merriam, D. F., 1957, Trend players look to western Kansas Cherokee; Oil and Gas Journal, v. 55, p. 126-135.

Johnson, R. A., and Budd, D. A., 1994, The utility of continual reservoir description: An example from Bindley Field, Western Kansas: AAPG Bulletin, v. 78, p. 722-743.

Kenyon, W.E., 1992, Nuclear magnetic resonance as a petrophysical measurement: Nuclear Geophysics, v. 6, no. 2, p. 153-177.

Keller, P.J., 1990, Basic principles of magnetic resonance imaging: General Electric Medical Systems.

Kleinberg, R.L., and Horsfield, M.A., 1990, Transverse relaxation processes in porous sedimentary rocks: J. Magnetic Resonance, v. 88, p. 9-19.

Murphy, D.P., 1995, NMR logging and core analysis--simplified: World Oil, v. 66, p. 65-70.

Rogers, J.P., Spiculitic Chert reservoir in Glick Field, South-Central Kansas: The Mountain Geologist, v. 32, p. 1-22.

SPWLA, 1995, Nuclear Magnetic Resonance Logging, 1995, Soc. Prof. Well Log Analysts, one day short course, Paris, France.

Thomas, M.A., 1982, Petrology and diagenesis of the Lower Mississippian, Osagean Series, Western Sedgwick Basin, Kansas: Kansas Geological Survey Open-file Report 82-24, 87 p.
Warren, J. K. 1989, Evaporite sedimentology: Englewood Cliffs, New Jersey, Prentice Hall, 285 p.

4.0 APPENDICES

4.1 Appendix A

PfEFFER "Super Pickett" PLOTS
from
Ritchie 4 Moore "B-P" Twin
NW NE Sec. 30-T19S-R21W
Ness County, Kansas

Resistivity-porosity plots on depth with an attribute of computed Gamma Ray indicate a reservoir with a high bulk volume water (.08-.11), a relatively constant porosity (20%), and a medium high water saturation (up to 60%). This would agree with Franseen's core description of the reservoir as a very fine-to-fine crystalline dolomite. The reservoir presently open by perforations has a BVW of 0.11 and a SW of 50-60%. The upper section is more heterogeneous. The multi-coarsening upward cycles are indicated by the plots cyclically changing direction.

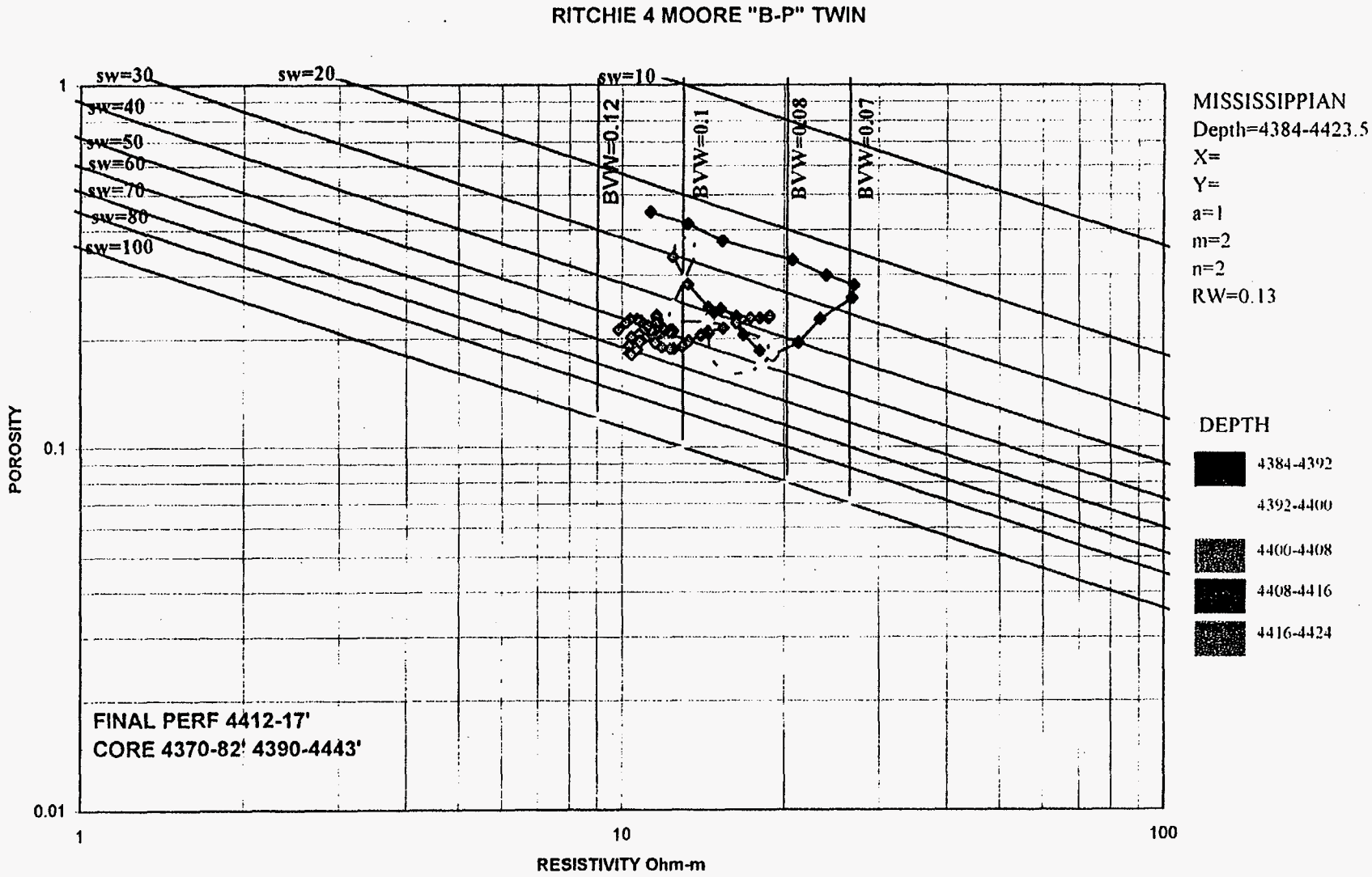
RITCHIE 4 MOORE "B-P" TWIN
sw=30
sw=20
sw=10
sw=40
sw=50
sw=60
sw=70
sw=80
sw=100
BVW=0.12
BVW=0.1
BVW=0.08
BVW=0.07
1
0.1
0.01
POROSITY
1
10
100
RESISTIVITY Ohm-m
FINAL PERF 4412-17'
CORE 4370-82' 4390-4443'
MISSISSIPPIAN
Depth=4384-4423.5
X=
Y=
a=1
m=2
n=2
RW=0.13
DEPTH
4384-4392
4392-4400
4400-4408
4408-4416
4416-4424

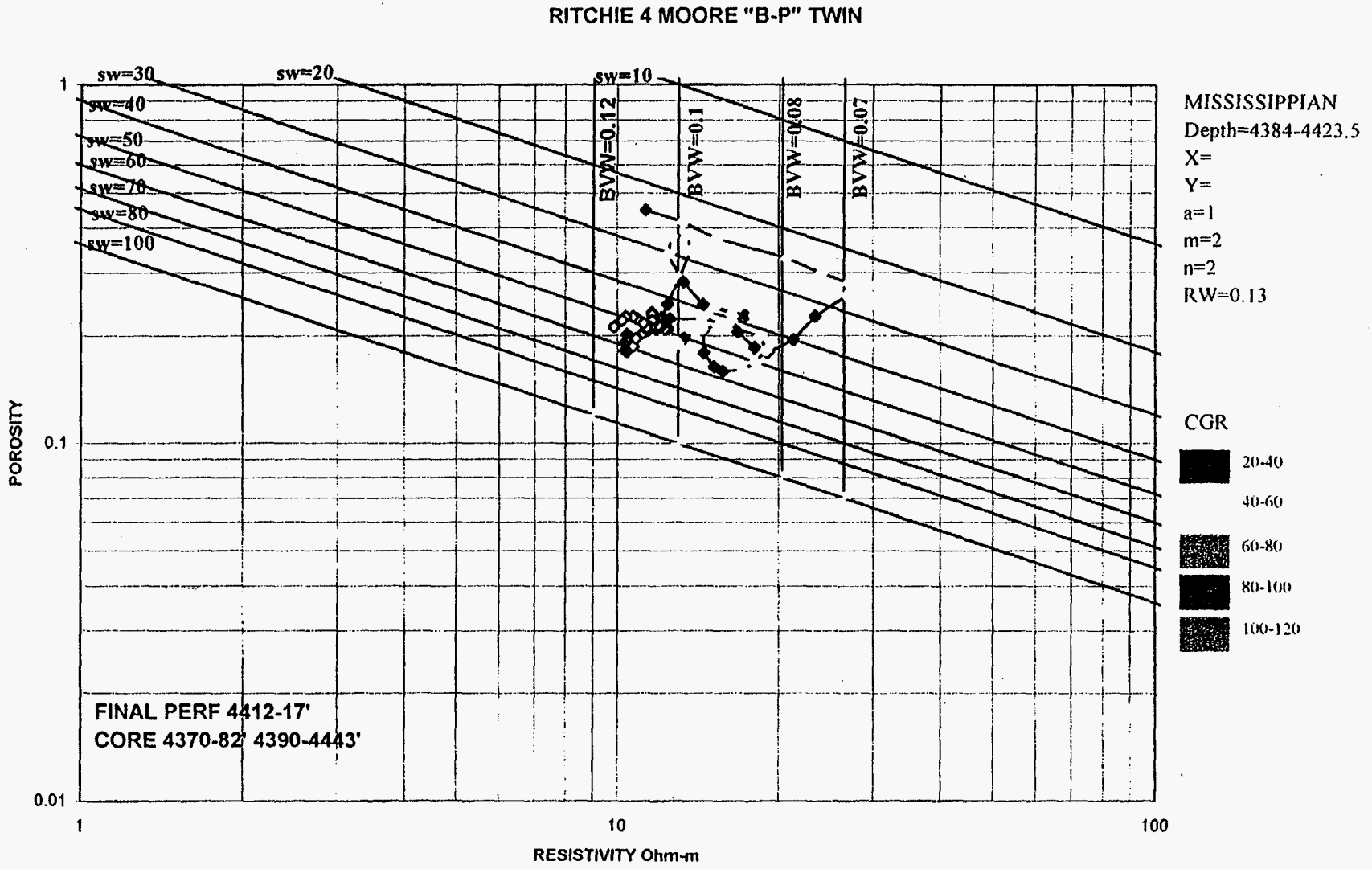
RITCHIE 4 MOORE "B-P" TWIN
sw=30
sw=20
sw=10
sw=40
sw=50
sw=60
sw=70
sw=80
sw=100
BVW=0.12
BVW=0.1
BVW=0.08
BVW=0.07
POROSITY
1
0.1
0.01
1
10
100
RESISTIVITY Ohm-m
FINAL PERF 4412-17'
CORE 4370-82' 4390-4443'
MISSISSIPPIAN
Depth=4384-4423.5
X=
Y=
a=1
m=2
n=2
RW=0.13
CGR
20-40
40-60
60-80
80-100
100-120

MISSISSIPPIAN

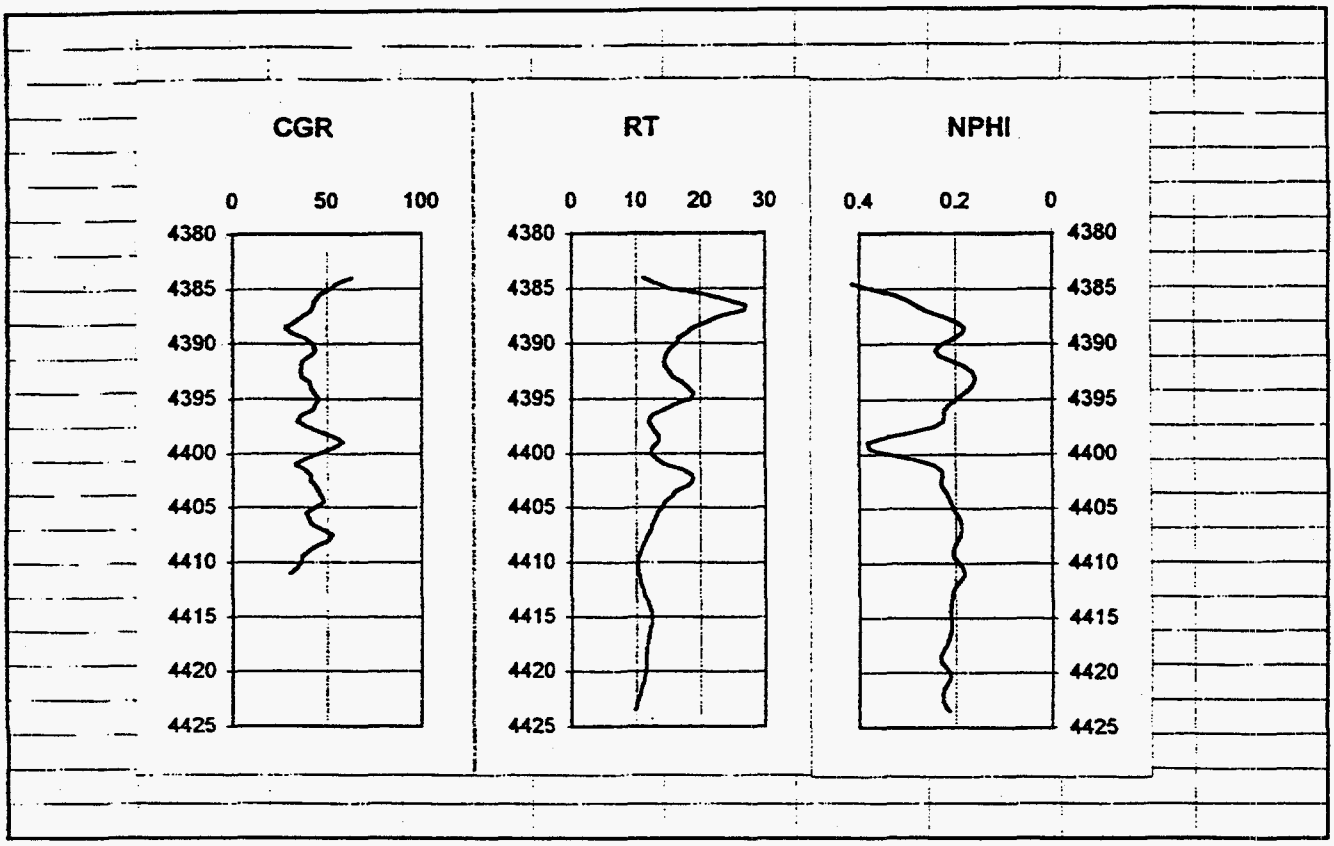

4.2 Appendix B

PfEFFER "Super Pickett" PLOTS

from

Ritchie 1 Foos "A-P" Twin

NE SW SW Sec. 31-T19S-R21W

Ness County, Kansas

Resistivity-porosity cross plots on depth attributes of computed Gamma Ray and Photo-Electric effect indicate a reservoir that is very heterogeneous of the top with a high bulk volume water (.09-.12), varying porosity (10-30%), and a varying water saturation (30-100%). The lower section indicates a more constant porosity (17-20%), an increasingly high BVW with depth (0.1 to 0.17), a increasing water saturation with depth (60%-100%). This indicates that the reservoir is in a long transition zone from oil to water. The Photo-Electric effect readings of 2.5-3 indicates a dolomite and chert reservoir. The Rhomaa-Umaa plot indicates that the reservoir is a mixture of chert and dolomite. The multi-coarsening upward cycles are indicated by the plots cyclically changing direction.

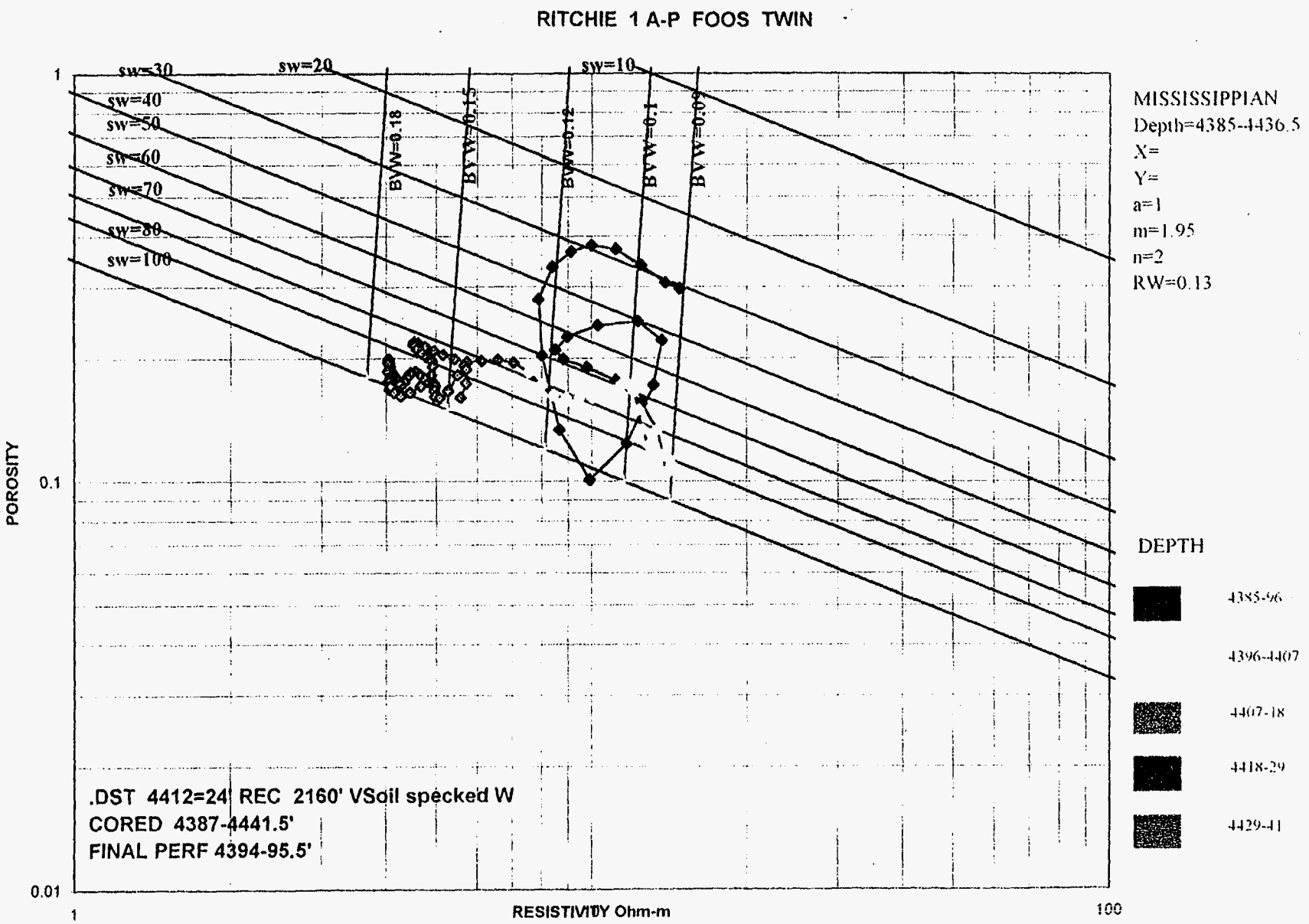
RITCHIE 1 A-P FOOS TWIN
sw=30
sw=20
sw=10
sw=40
sw=50
sw=60
sw=70
sw=80
sw=100
BVW=0.18
BVW=0.15
BVW=0.12
BVW=0.1
BVW=0.09
1
0.1
0.01
POROSITY
1
100
RESISTIVITY Ohm-m
MISSISSIPPIAN
Depth=4385--4436.5
X=
Y=
a=1
m=1.95
n=2
RW=0.13
DEPTH
4385-96
4396-4407
4407-18
4418-29
4429-41
.DST 4412=24' REC 2160' VSoil specked W
CORED 4387-4441.5'
FINAL PERF 4394-95.5'

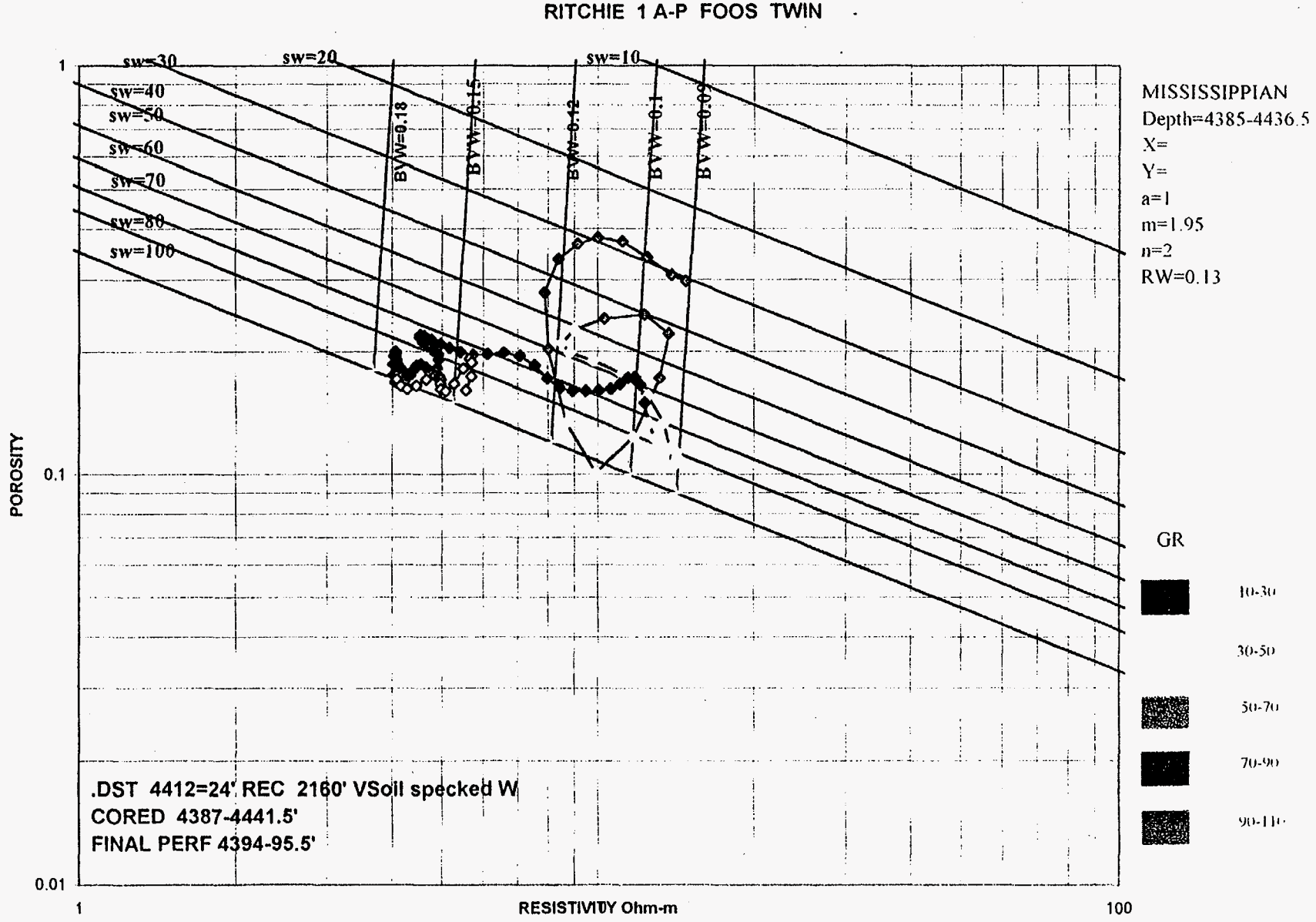
RITCHIE 1 A-P FOOS TWIN
sw=30
sw=20
sw=10
sw=40
sw=50
sw=60
sw=70
sw=80
sw=100
BVW=0.18
BVW=0.15
BVW=0.12
BVW=0.1
BVW=0.08
MISSISSIPPIAN
Depth=4385-4436.5
X=
Y=
a=1
m=1.95
n=2
RW=0.13
GR
10-30
30-50
50-70
70-90
90-110
.DST 4412=24' REC 2160' VSoil specked W
CORED 4387-4441.5'
FINAL PERF 4394-95.5'
POROSITY
1
0.1
0.01
1
100
RESISTIVITY Ohm-m

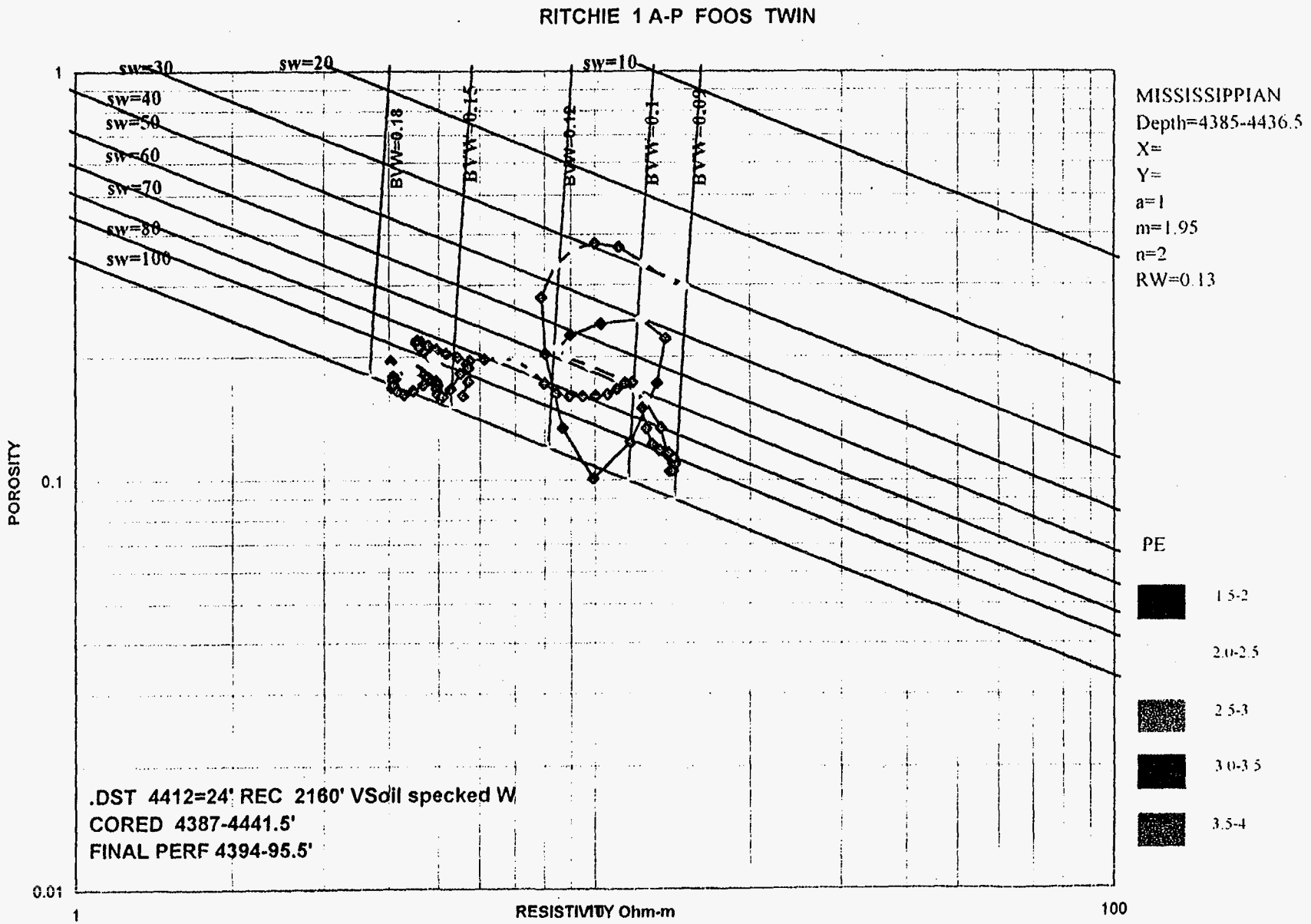
RITCHIE 1 A-P FOOS TWIN
sw=30
sw=20
sw=10
sw=40
sw=50
sw=60
sw=70
sw=80
sw=100
BVW=0.18
BVW=0.15
BVW=0.1
BVW=0.05
1
0.1
0.01
POROSITY
1
100
RESISTIVITY Ohm-m
MISSISSIPPIAN
Depth=4385-4436.5
X=
Y=
a=1
m=1.95
n=2
RW=0.13
PE
1.5-2
2.0-2.5
2.5-3
3.0-3.5
3.5-4
.DST 4412=24' REC 2160' VSoil specked W
CORED 4387-4441.5'
FINAL PERF 4394-95.5'

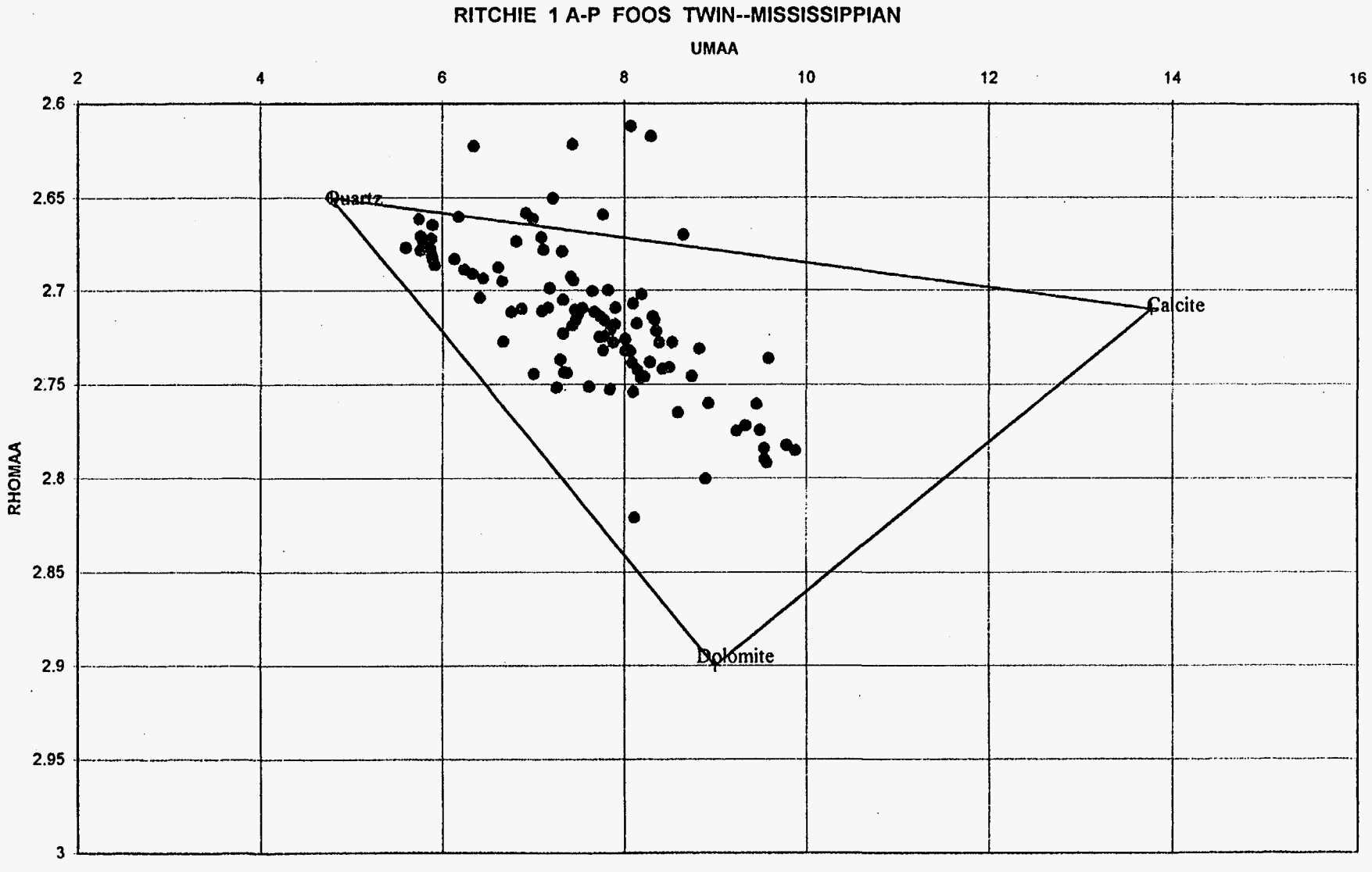
RITCHIE 1 A-P FOOS TWIN--MISSISSIPPIAN
UMAA
2
4
6
8
10
12
14
16
RHOMAA
2.6
2.65
2.7
2.75
2.8
2.85
2.9
2.95
3
Quartz
Calcite
Dolomite

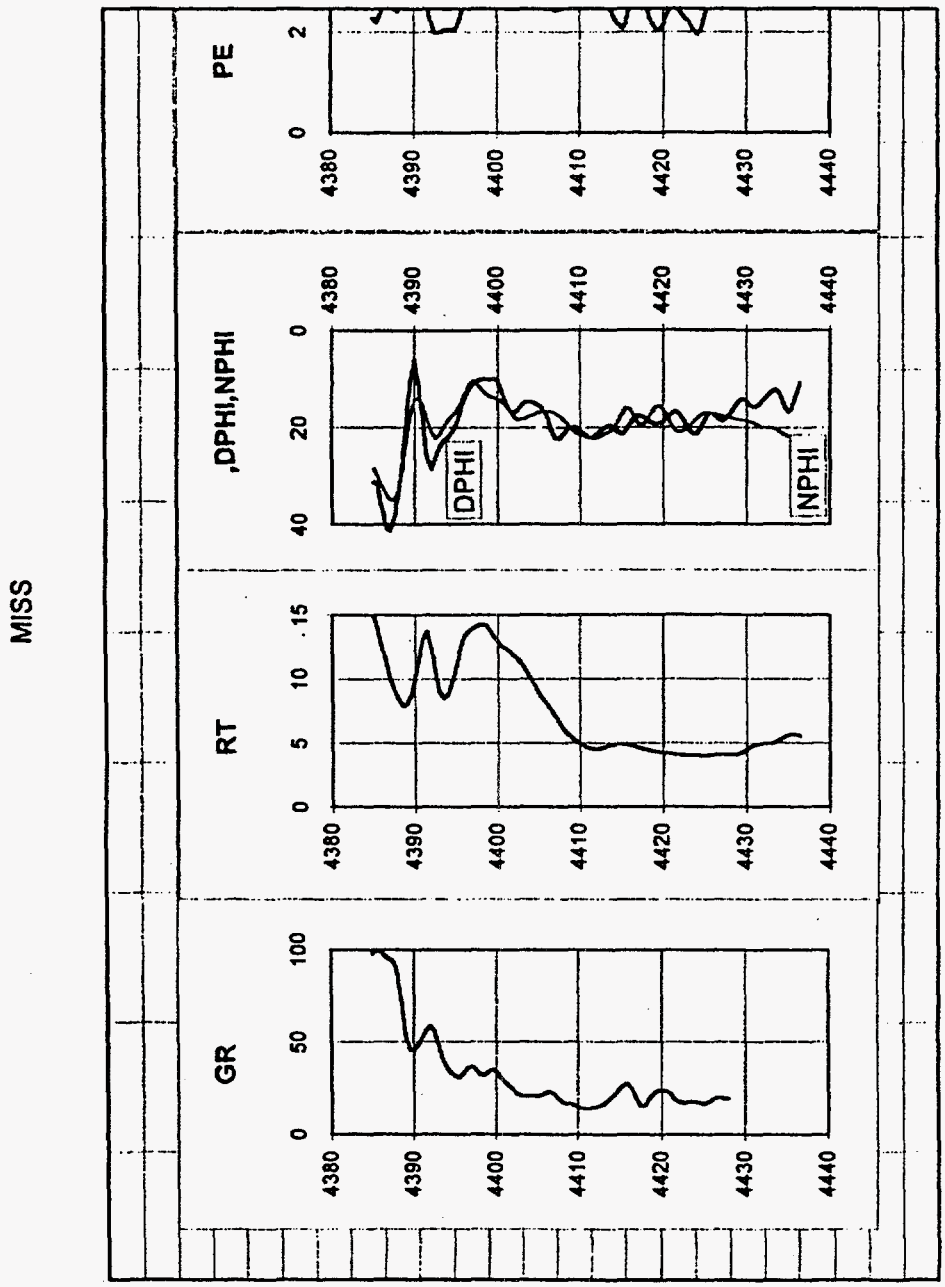
MISS
GR
0
50
100
RT
0
5
10
15
,DPHI,NPHI
0
20
40
DPHI
NPHI
PE
0
2
4380
4390
4400
4410
4420
4430
4440

4.3 Appendix C

PfEFFER "Super Pickett" PLOTS

from

Ritchie 2 Lyle Schaben "P"

400' FNL and 400" FEL, NE/4 Sec. 31-T19S-R21W

Ness County, Kansas

Resistivity-porosity cross plot on depth showing transition zone from oil to water ("irreducible" to aquifer).

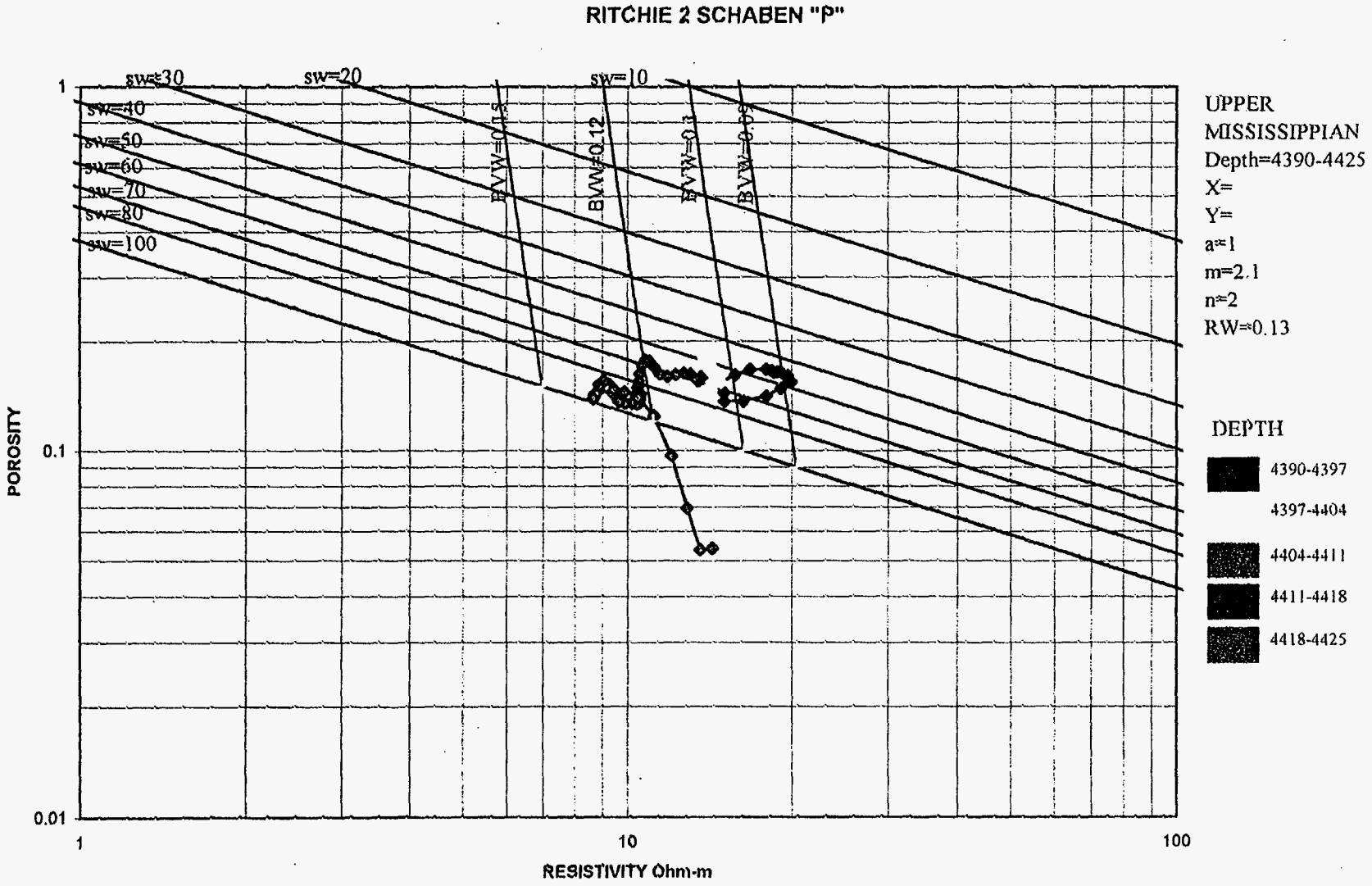
RITCHIE 2 SCHABEN "P"
sw=30
sw=20
sw=10
sw=40
sw=50
sw=60
sw=70
sw=80
sw=100
BVW=0.15
BVW=0.12
BVW=0.1
BVW=0.09
1
0.1
0.01
POROSITY
1
10
100
RESISTIVITY Ohm-m
UPPER
MISSISSIPPIAN
Depth=4390-4425
X=
Y=
a=1
m=2.1
n=2
RW=0.13
DEPTH
4390-4397
4397-4404
4404-4411
4411-4418
4418-4425

4.4 Appendix D
Individual Well Fluid Matches
TORP Simulation for Section 30 of Schaben Field

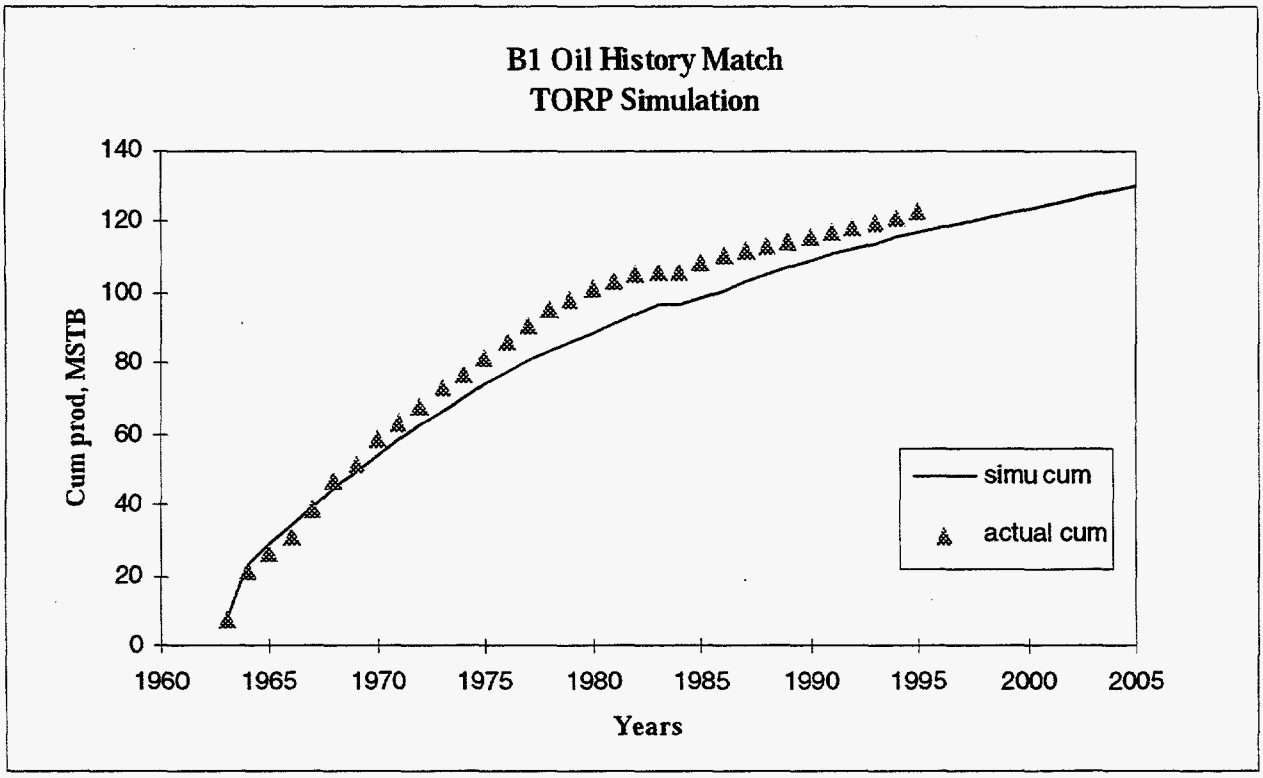

Figure D.1

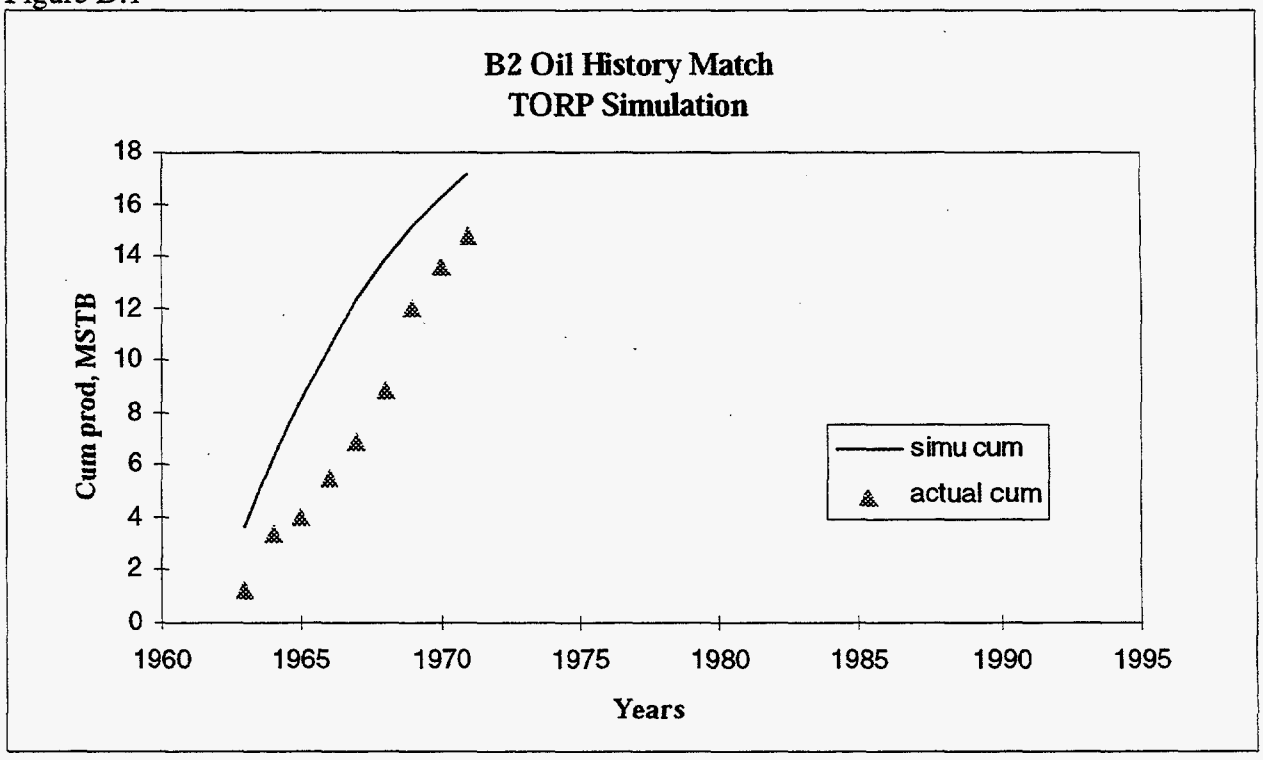

Figure D.2

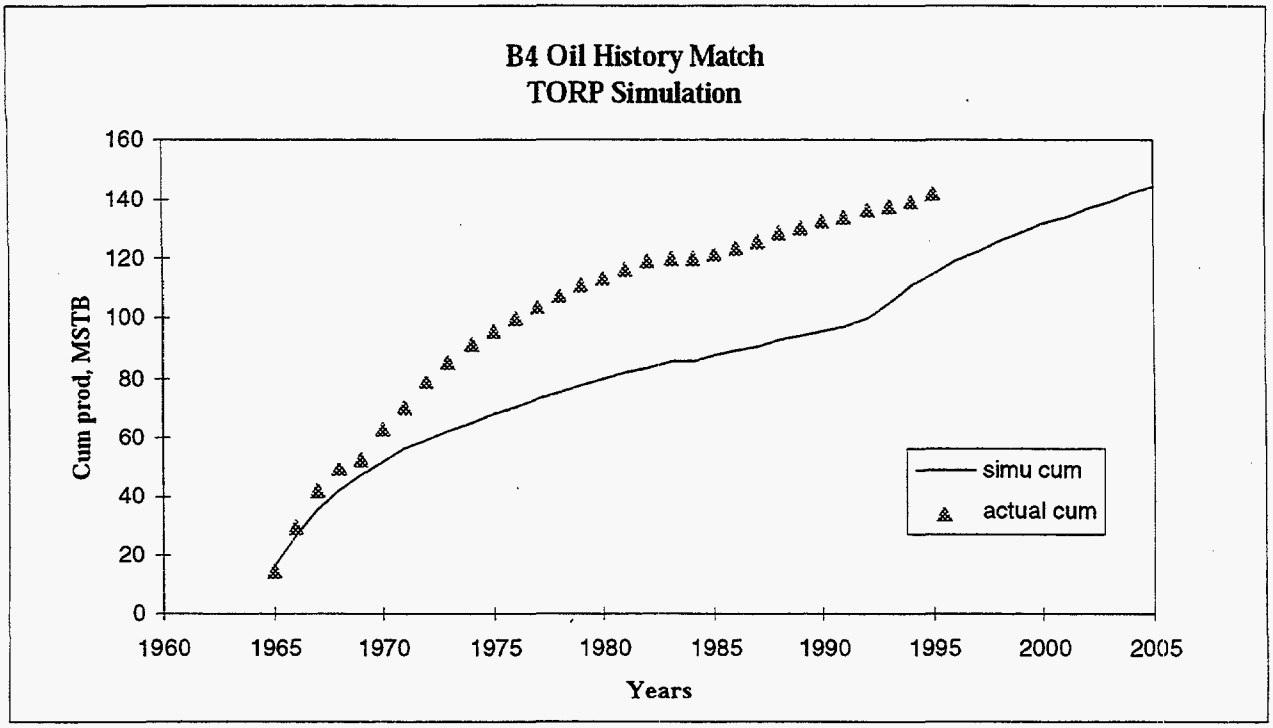

Figure D.3

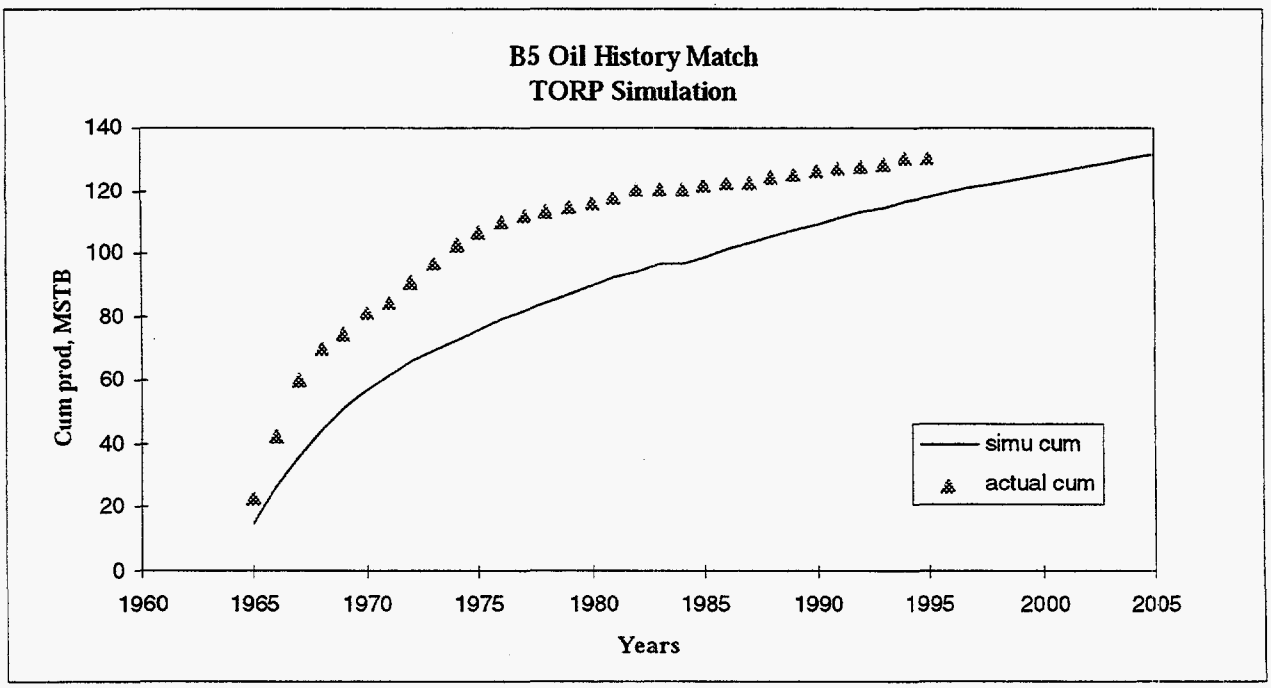

Figure D.4

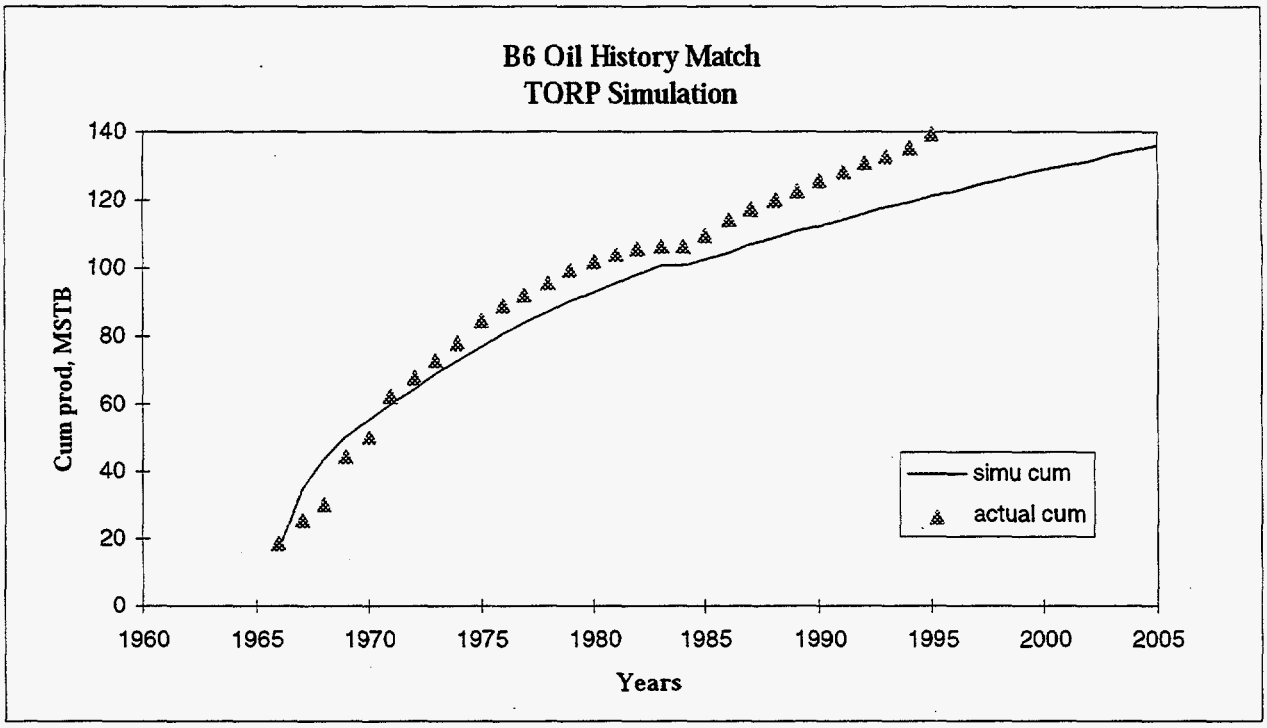

Figure D.5

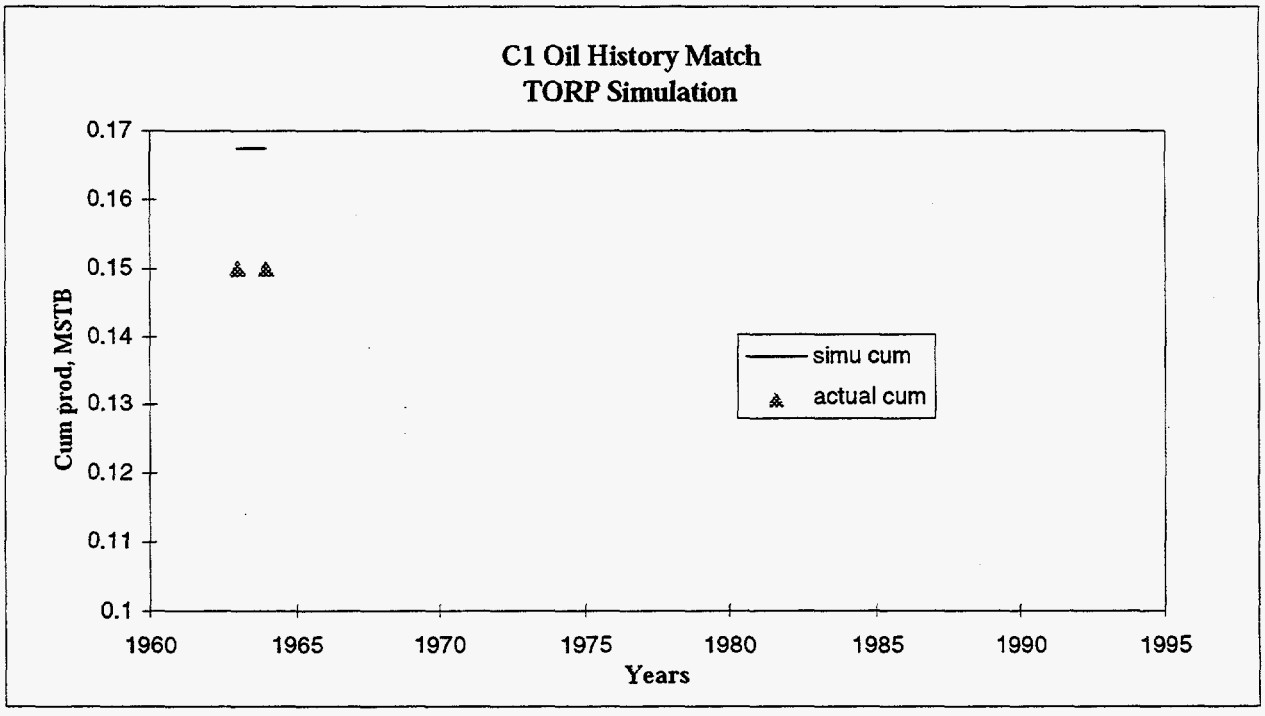

Figure D.6

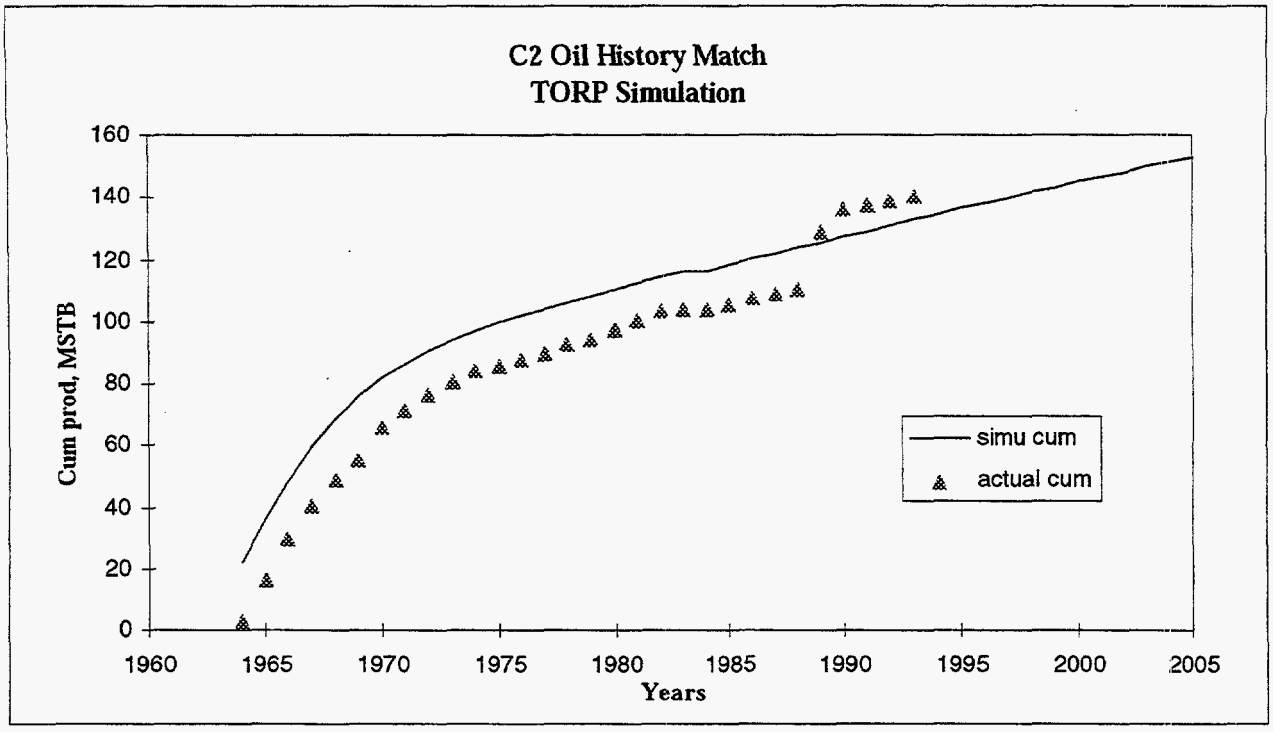

Figure D.7

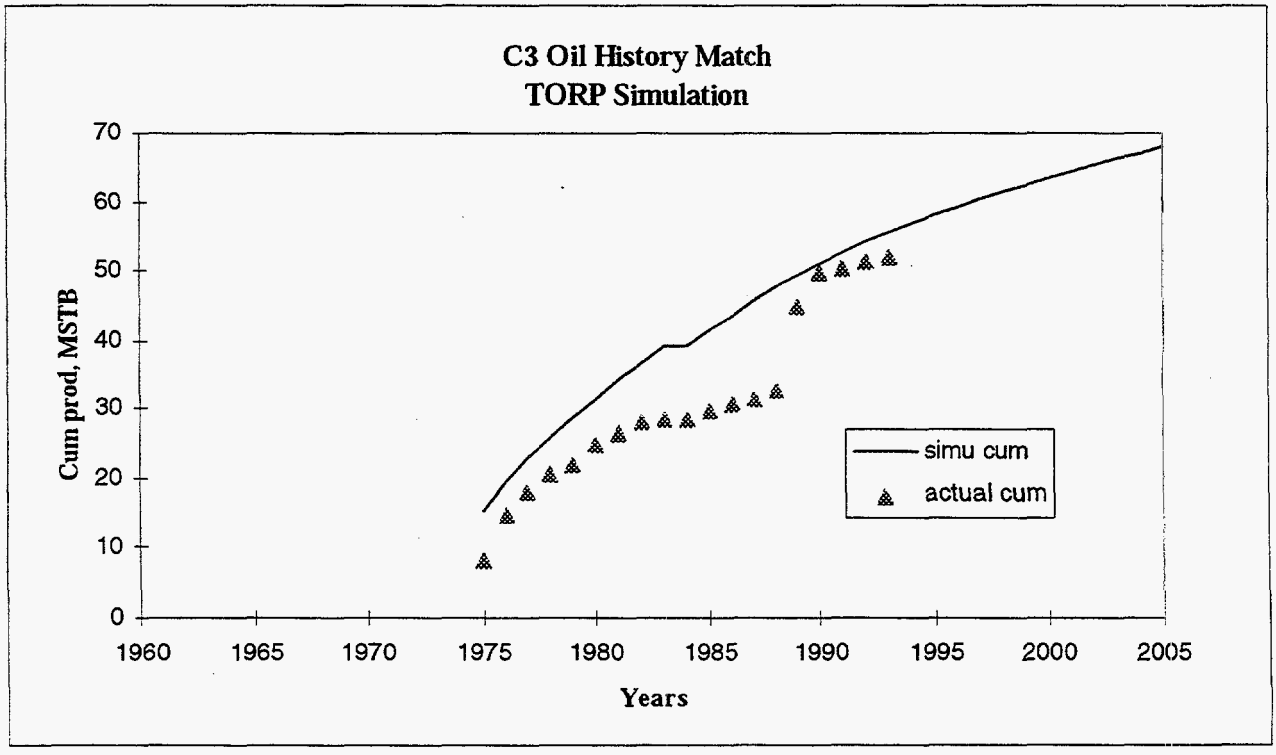

Figure D.8

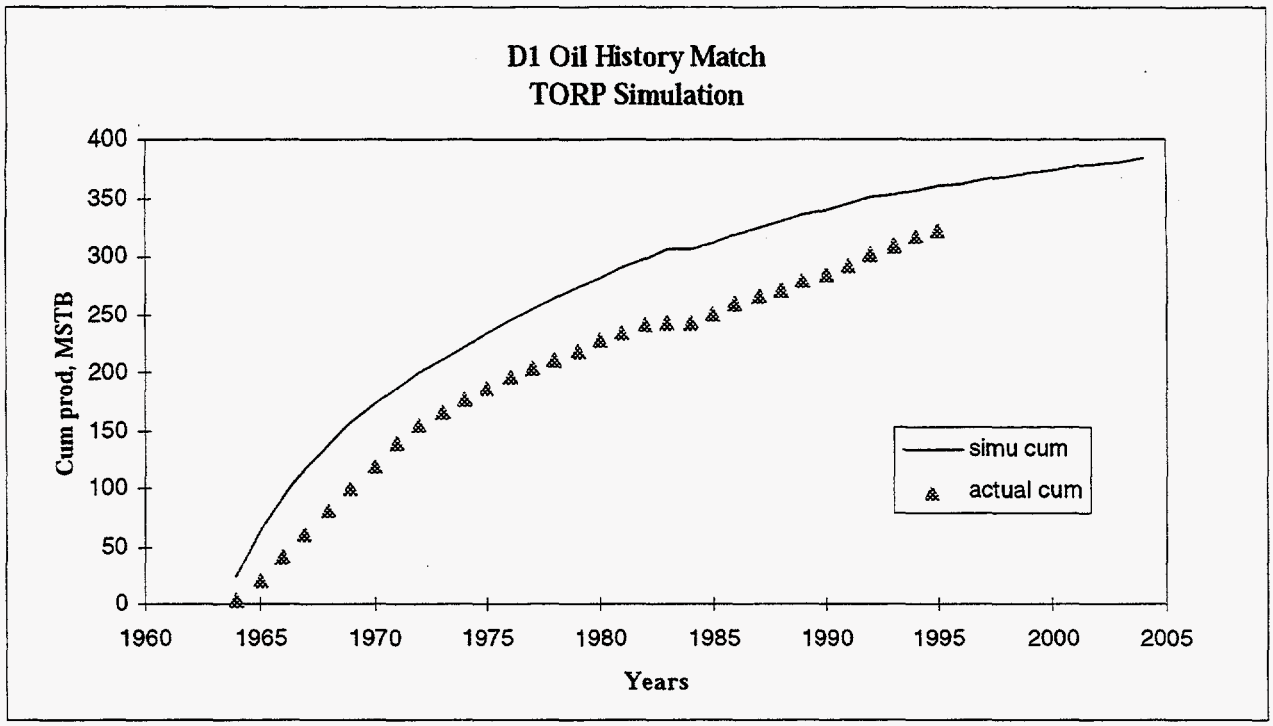

Figure D.9

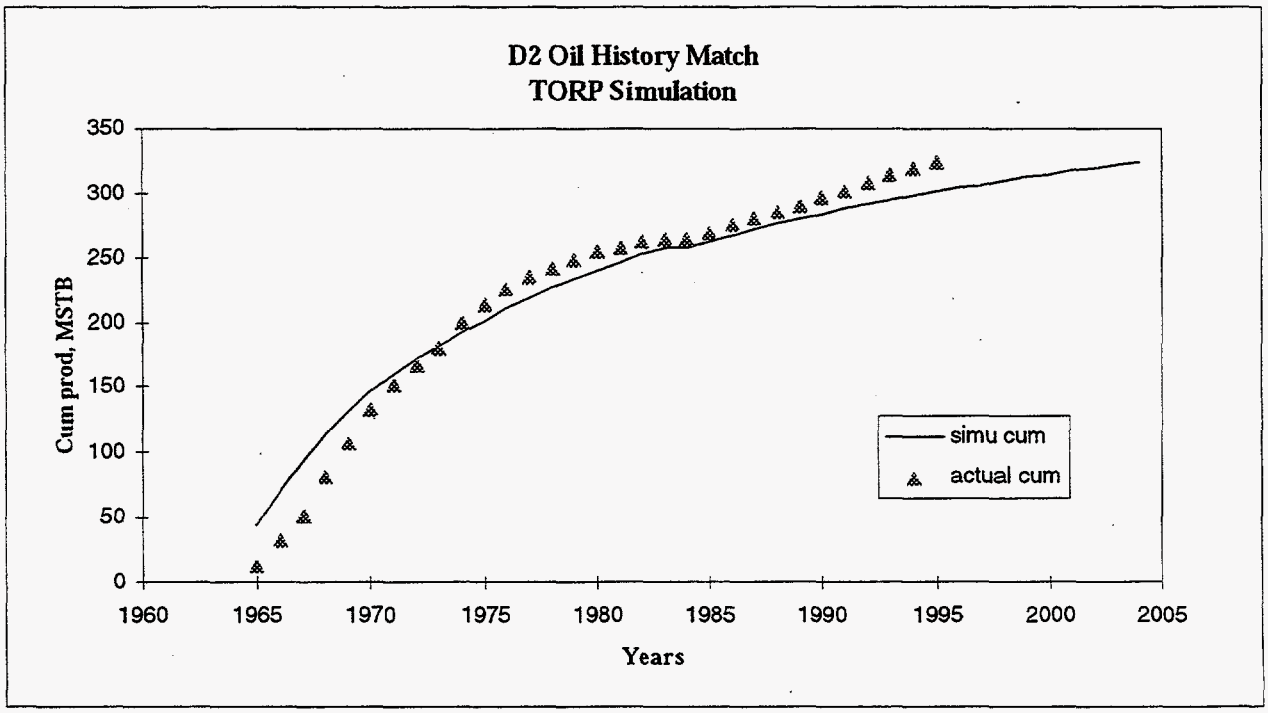

Figure D.10

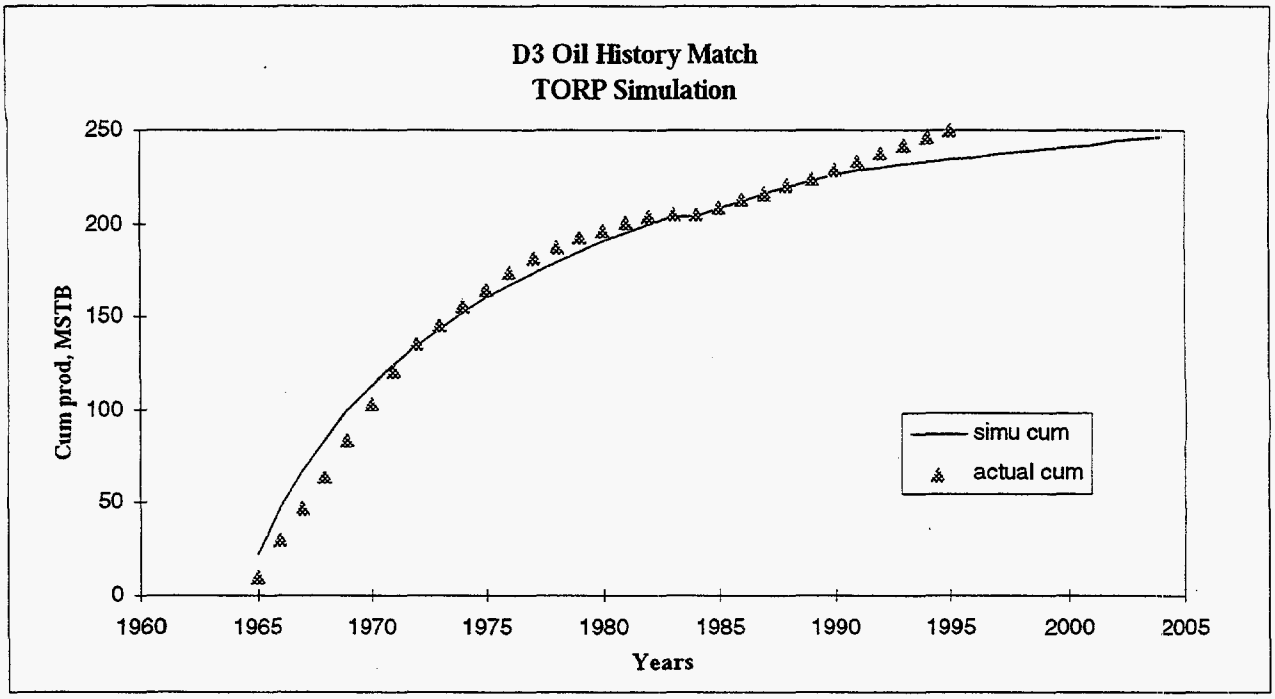

Figure D.11

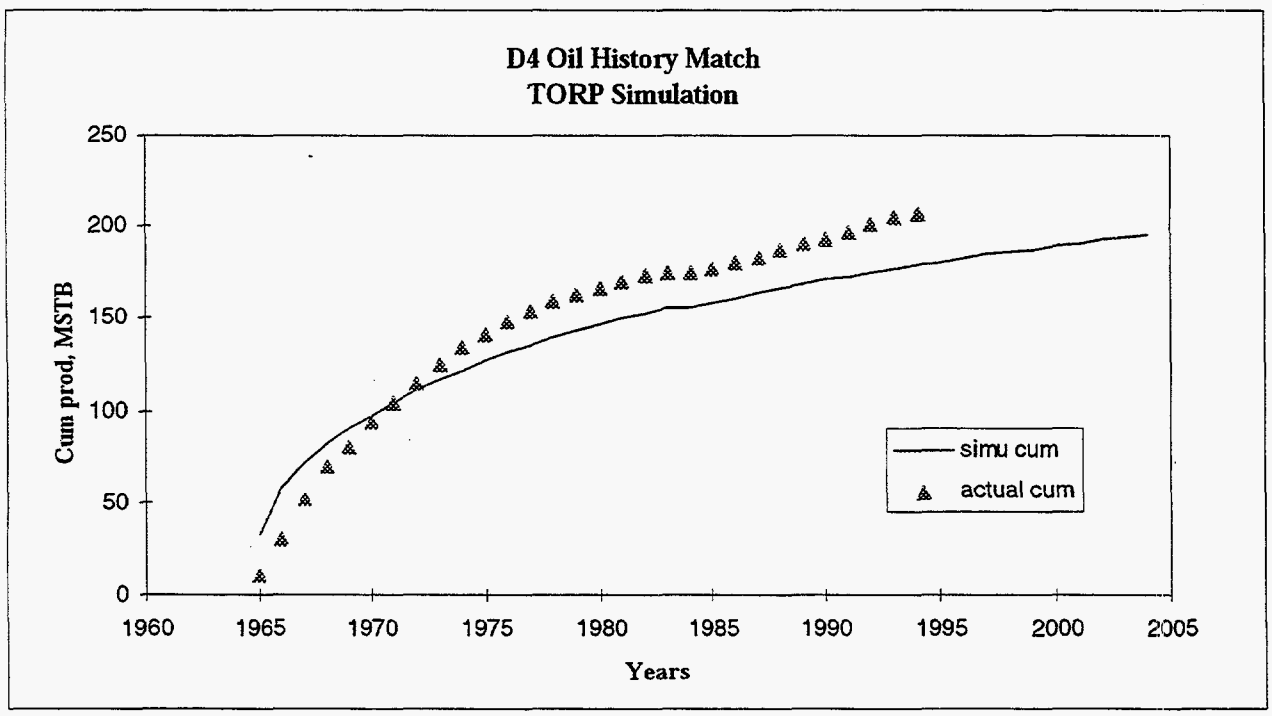

Figure D.12

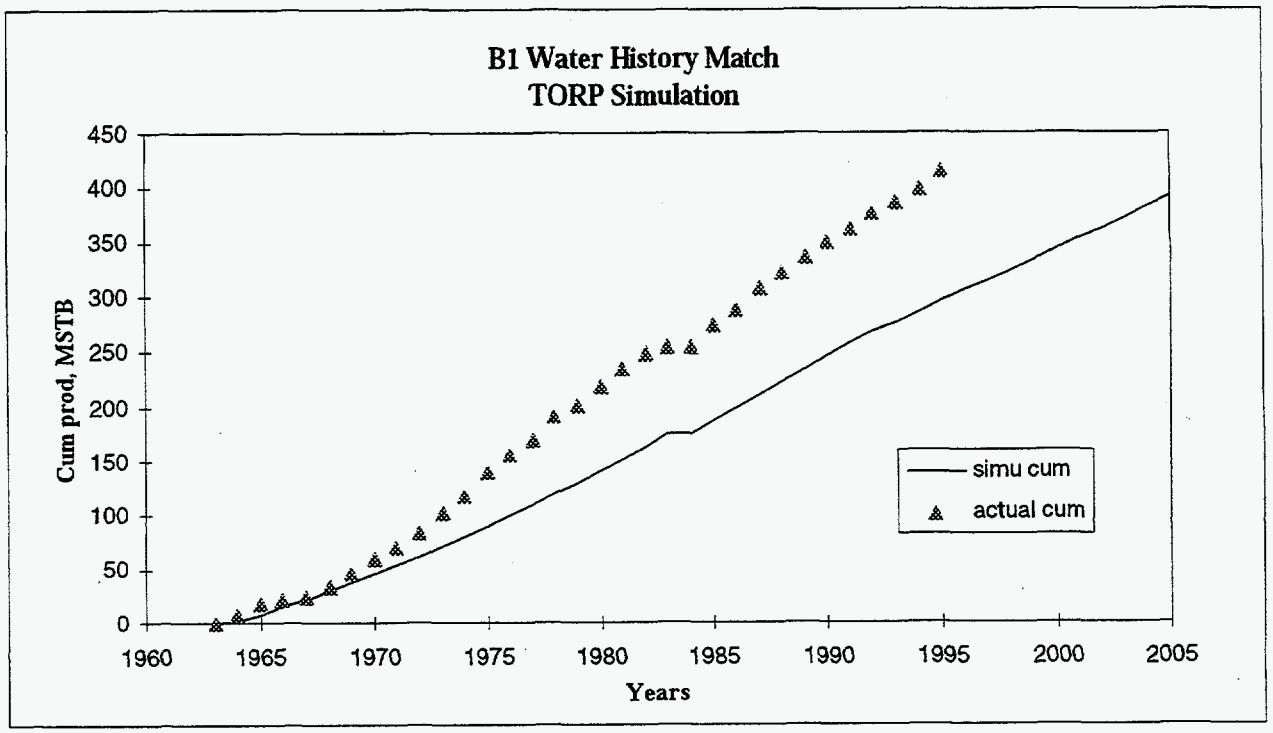

Figure D.13

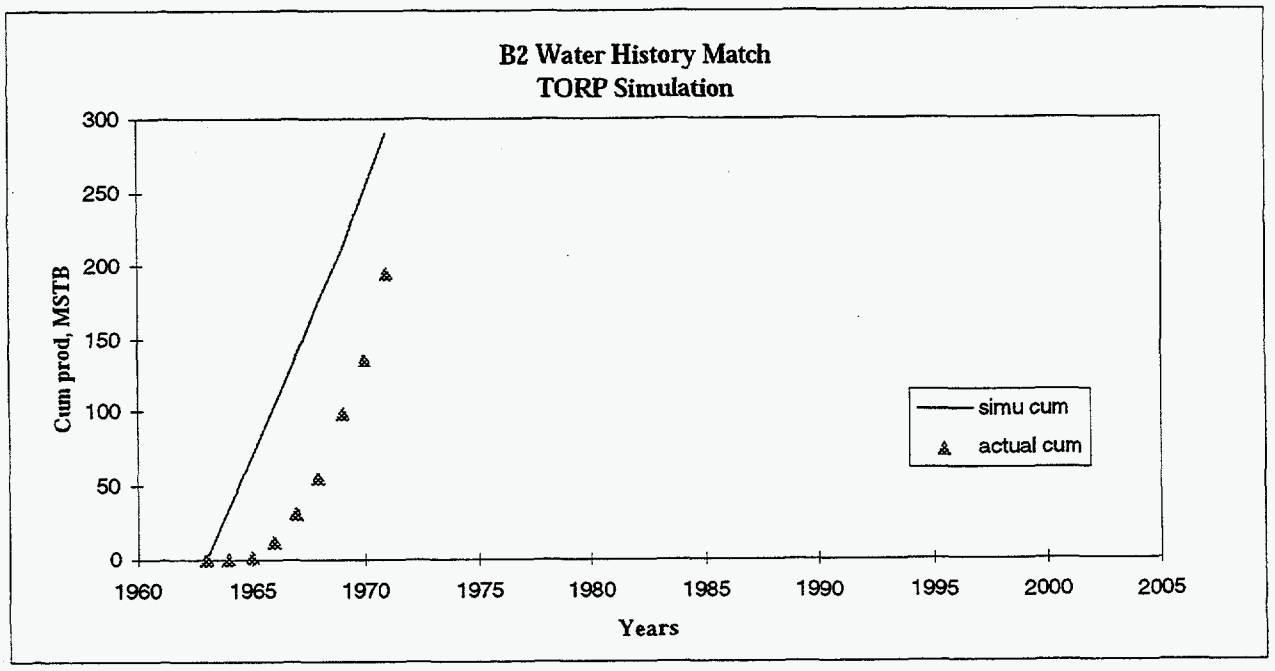

Figure D.14

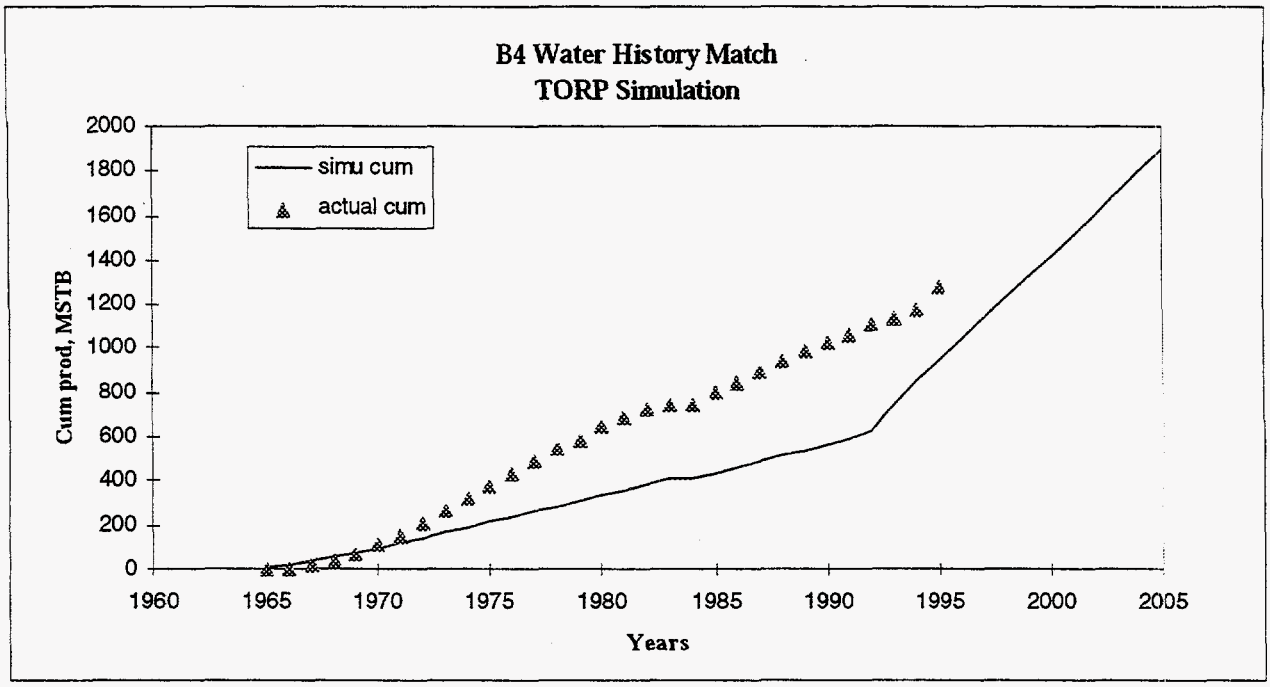

Figure D.15

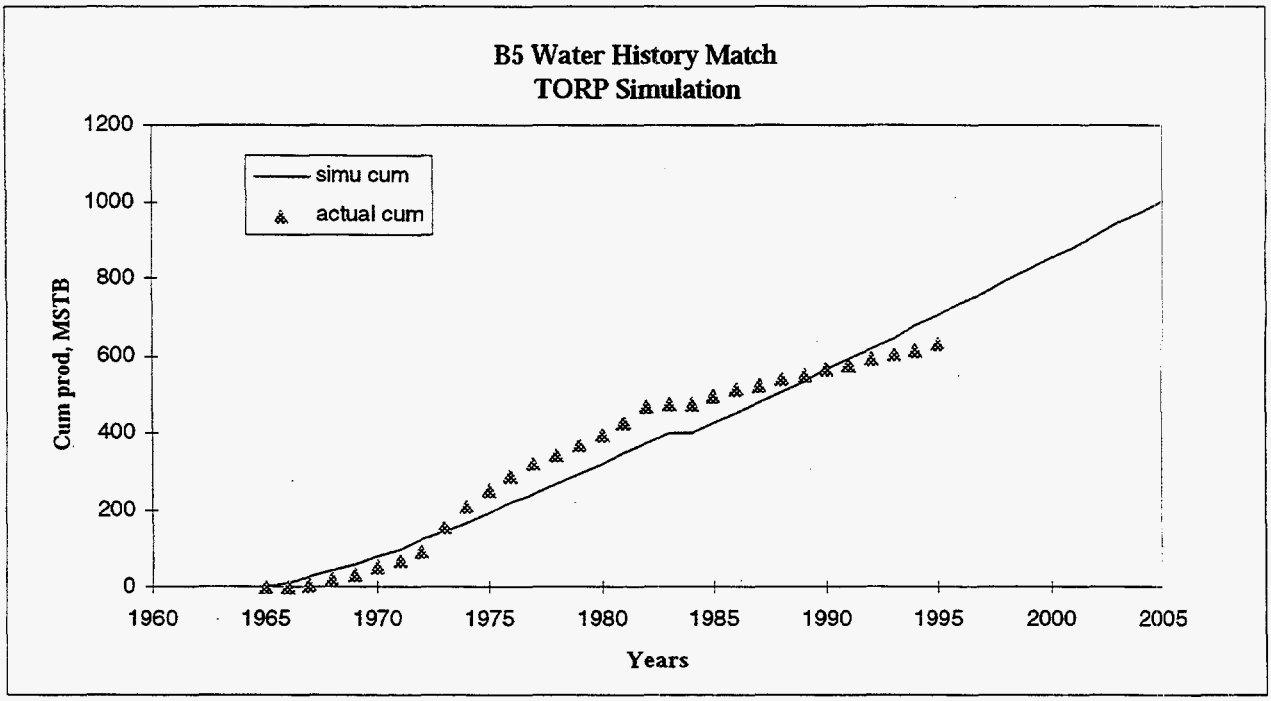

Figure D.16

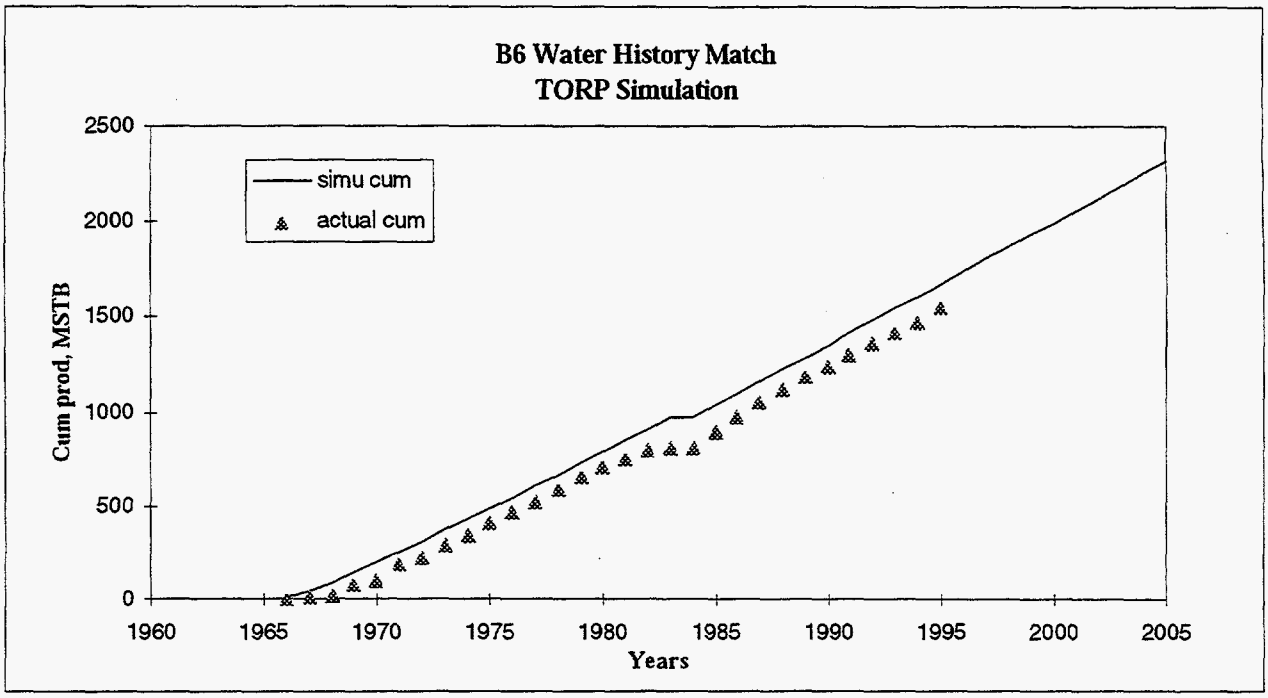

Figure D.17

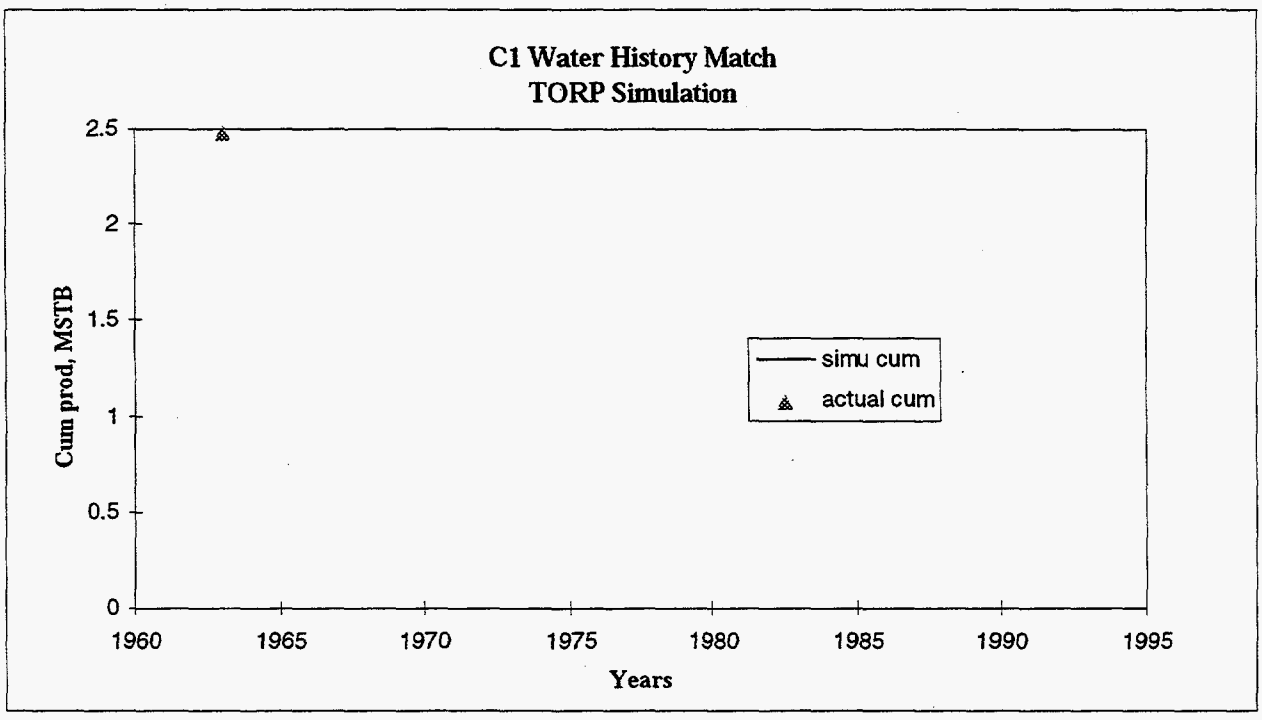

Figure D.18

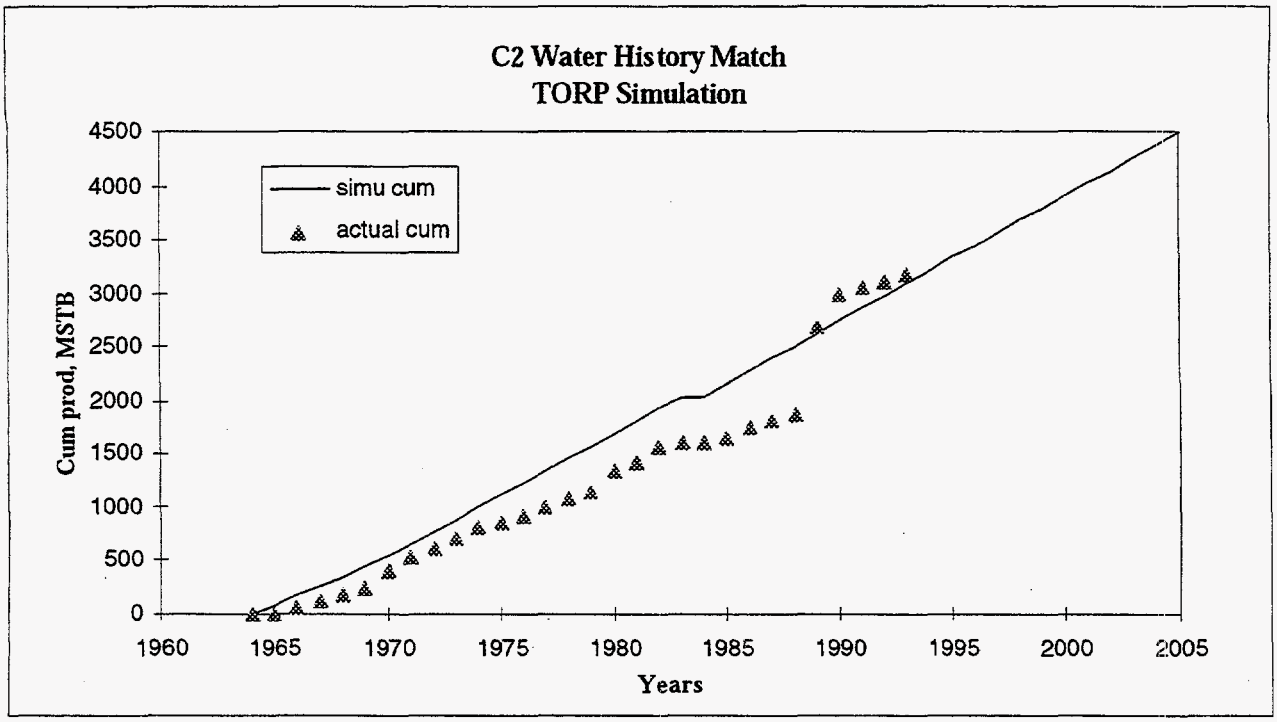

Figure D.19

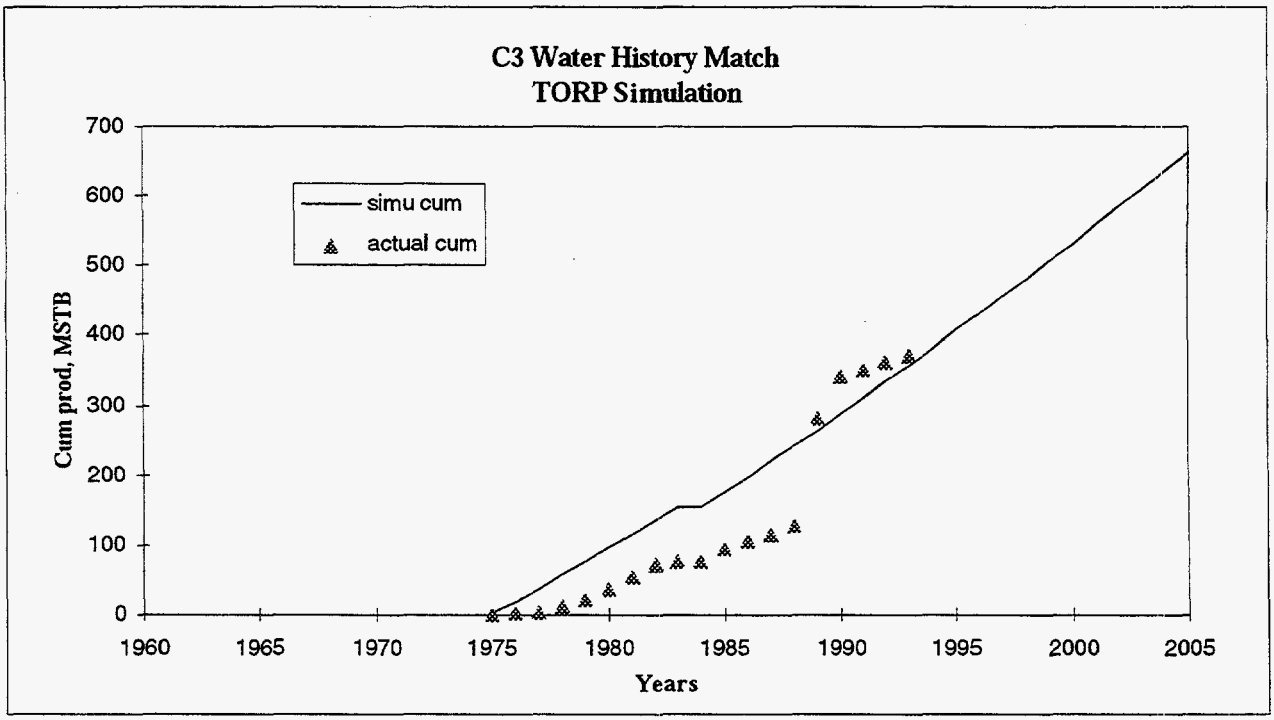

Figure D.20

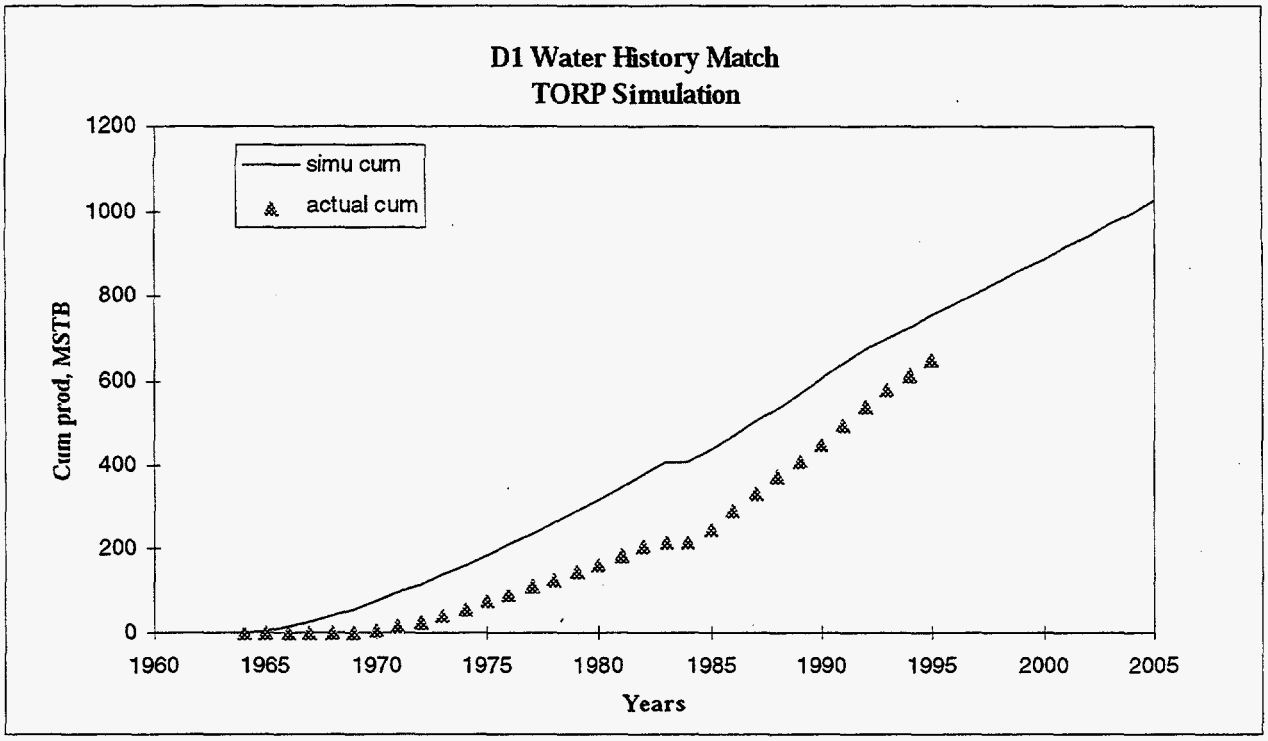

Figure D.21

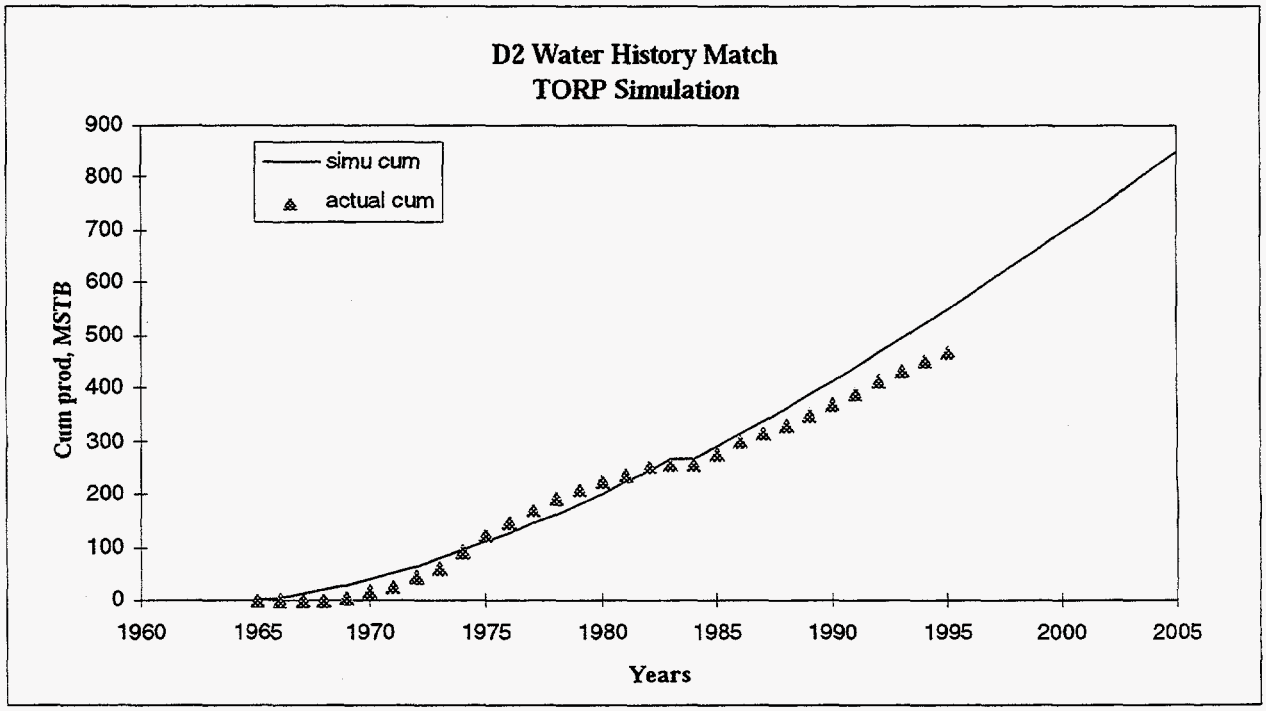

Figure D.22

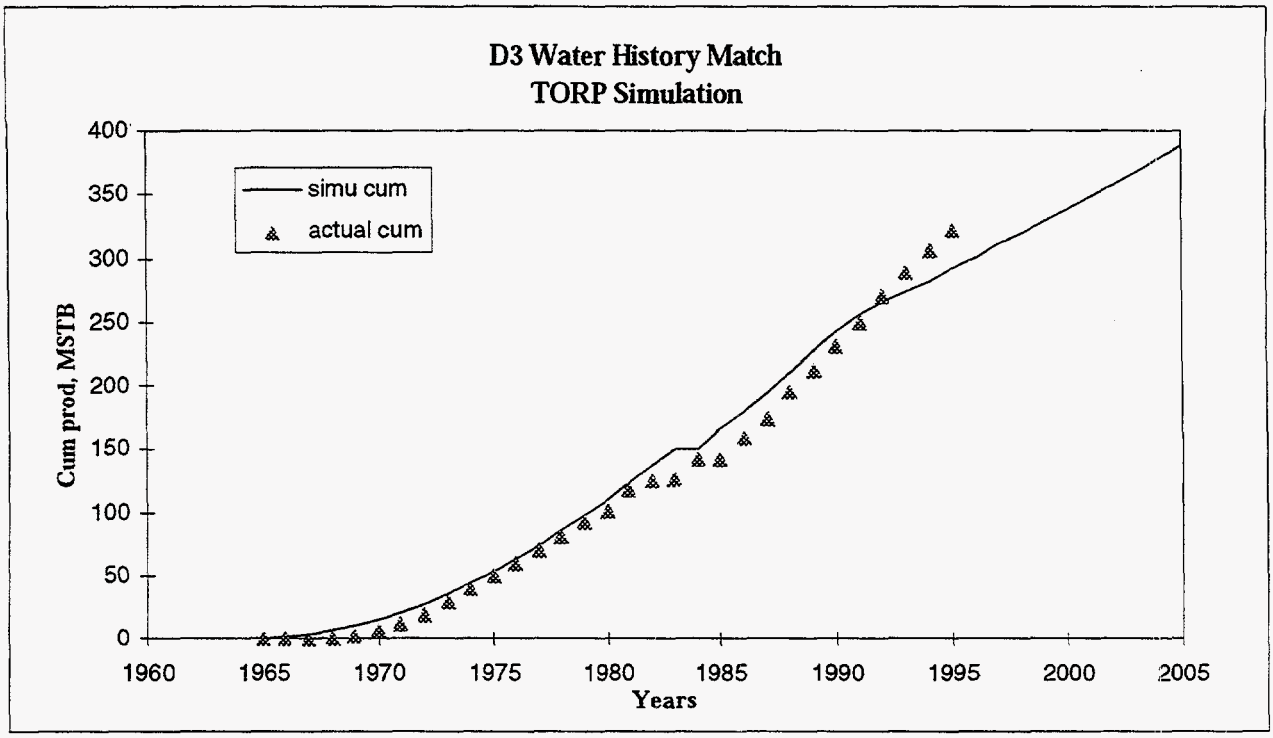

Figure D.23

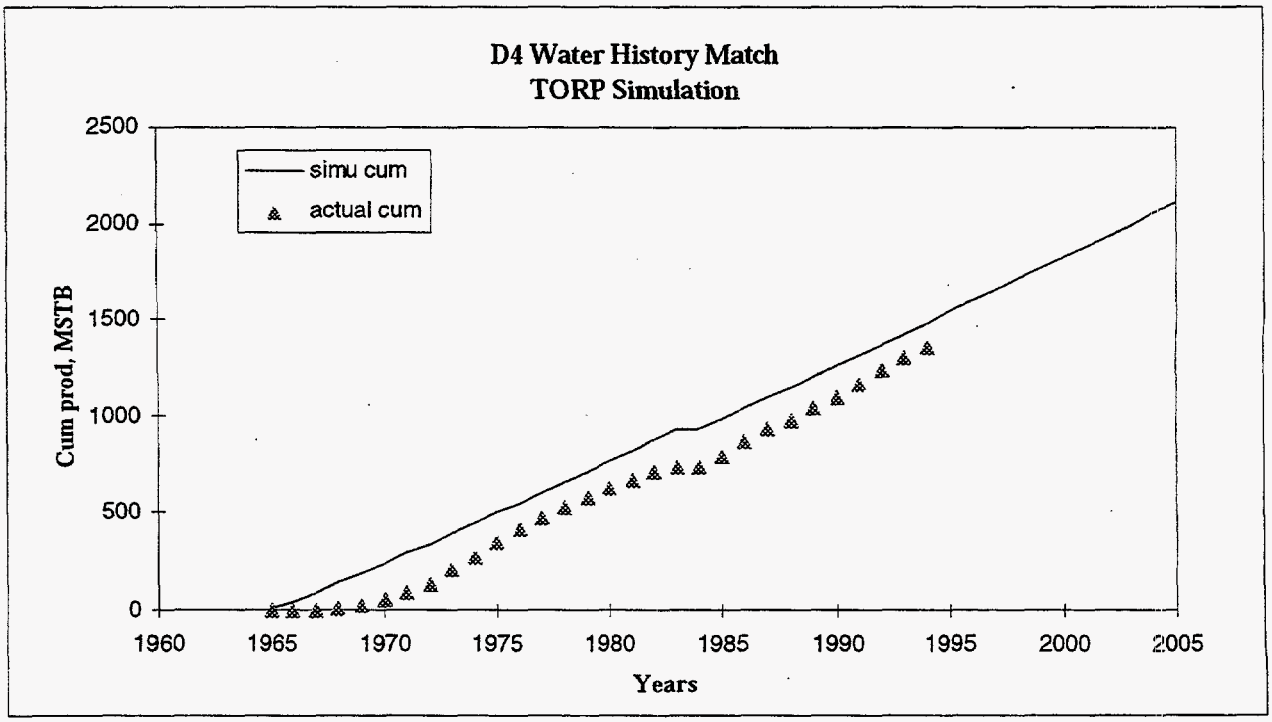

Figure D.24

4.5 Appendix E
Summary of Tables for TORP Simulation of Section 30

Table E.1
Wellbore Flowing Pressures

Well	Date	Perfs/Formation	Test Rate	Status/Fluid Level	BHP (psi)
Moore B-1	8/24/63	4401-16 (Miss)	122 BOPD, 0 BWPD		
	10/1/82	4316-18 (Ft Scott)	10 BOPD, 52 BWPD	Pumped off	15
	12/3/91	4416-32 (Miss)	10 BOPD, 206 BWPD	3682'	323
	Current			Pumped off	
Moore B-2	1963 - 1971	NA (Miss)	NA	Pumped off	15
Moore B-4 &	5/11/65	4408-14 (Miss)	121 BOPD, 0 BWPD		
B-4 Twin	3/13/74	4394-96 (Miss)			
		4398-4400 (Miss)			
		4408-14 (Miss)	27 BOPD, 247 BWPD		
	12/9/91	4394-4408 (Miss)			
		4418-19 (Miss)	4 BOPD, 284 BWPD	2100'	997
	10/7/92		0 BOPD, 184 BWPD	3844'	247
	Current	B-4 Twin	NA	A lot of fluid	
Moore B-5	7/17/65	4388-92 (Miss)	123 BOPD, 0 BWPD	Pumped off	15
	9/20/75	4398-4404 (Miss)	16 BOPD, 175 BWPD		
	10/83		9 BOPD, 196 BWPD		
	12/83		10 BOPD, 187 BWPD		
	Current			Pumped off	15
Moore B-6	7/20/66	4436-45 (Miss)	149 BOPD, 1 BWPD		
	3/20/85	4410-16 (Miss)			
		4420-22 (Miss)			
		4428-32 (Miss)	7 BOPD, 195 BWPD		
	Current			Pumped off	15
Moore C-1	1963	NA	Uneconomical	Pumped off	15
Moore C-2	10/16/64	4402-06 (Miss)	184 BOPD, 8 BWPD		
	4/27/91	4311-20 (Ft Scott)			
		4304-09 (Ft Scott)	7 BOPD, 339 BWPD		
	6/19/91		7 BOPD, 259 BWPD		
	Current			Pumped off	15
Moore C-3	6/10/75	4416-20 (Miss)	60 BOPD, 4 BWPD	Pumped off	15
	10/12/81	4438-42 (Miss)	6 BOPD, 63 BWPD	Pumped off	15
	Current			Pumped off	15
Moore D-1	9/17/64	4388-94 (Miss)	195 BOPD, 0 BWPD		
	10/10/73	4372-78 (Miss)	55 BOPD, 57 BWPD	Pumped off	15
	1991	4365-72 (Miss)			
		4378-88 (Miss)			
		4394-97 (Miss)	10 BOPD, 196 BWPD		
	Current			800-900'	366
Moore D-2	3/18/65	4384-90 (Miss)	153 BOPD, trace wtr		
	5/30/91	4356-96 (Miss)	24 BOPD, 128 BWPD		
	Current			Pumped off	15
Moore D-3	4/5/75	4399-4403 (Miss)	121 BOPD, 0 BWPD		
	1/11/74	4386-90 (Miss)	58 BOPD, 45 BWPD	Pumped off	15
	7/19/91	4378-86 (Miss)			
		4390-99 (Miss)			
		4401-05 (Miss)	12 BOPD, 277 BWPD	3045'	585
	Current			Some fluid ?	
Moore D-4	6/29/65	4421-23 (Miss)	121 BOPD, trace wtr		
	7/17/91	4404-24 (Miss)	18 BOPD, 342 BWPD		
	Current			A lot of fluid	904

Table E.2 Summary of TORP Simulation Results for Section 30

Year of Production	Total Cumulative Oil Production	Total Cumulative Water Production	Simulated Cumulative Oil Production	Simulated Cumulative Water Production
1963	8322	2482	11844.96	656.41
1964	31877	9916	74935.81	41066.47
1965	131275	31147	268774.43	187691.31
1966	279184	91893	430394.14	402963
1967	409449	211536	565798.64	664747.18
1968	533119	362779	675840.44	954734.5
1969	645340	602103	767451.74	1266945.4
1970	763768	956614	846283.74	1595070.8
1971	867194	1329382	915324.54	1936682.9
1972	952000	1636829	976723.34	2249779.7
1973	1024248	2048778	1032956.14	2570433.8
1974	1099302	2476614	1085204.04	2896895.1
1975	1170506	2832896	1149742.24	3232198.5
1976	1230734	3176181	1200672.04	3586307.6
1977	1280718	3527560	1247148.24	3964150.8
1978	1324996	3878557	1290489.34	4310509.7
1979	1363588	4193089	1331768.84	4680869.6
1980	1402226	4662112	1370925.14	5055538.1
1981	1436301	4988763	1407655.64	5432589.6
1982	1467439	5371433	1442257.04	5813236.6
1983	1476659	5487464	1475426.44	6198822.6
1985	1507880	5872734	1506717.84	6587296.6
1986	1541628	6290346	1536450.24	6978586.6
1987	1568437	6649033	1565147.94	7373647.6
1988	1599844	6990680	1592702.94	7771573.6
1989	1658659	8231489	1618988.14	8170403.6
1990	1697855	8870356	1644233.74	8571961.6
1991	1728567	9210034	1668054.04	8972733.6
1992	1761508	9566827	1690968.14	9387527.6
1993	1789601	9871674	1714930.14	9855413.6
1994	1816158	10127983	1737895.34	10327382
1995	1843783	10455807	1759499.14	10788136
1996			1780065.64	11244552
1997			1799820.34	11701391
1998			1818884.94	12159995
1999			1837300.44	12620065
2000			1855143.64	13082555
2001			1872347.64	13544786
2002			1889408.24	14013097
2003			1906227.04	14482482
2004			1922692.94	14953668
2005			1938696.34	15424211

Table E.3 Locations of Potential Infill Wells and Cumulative Production for 1998-2005

Cumulative Production from 1998 to 2005
(MSTB)

Well Name	Orientation	Location i	Location j	Oil Production	Water Production
Well 5	Vertical	2	7	60.56	770.58
Well 6	Vertical	6	11	96.38	528.72
Well 7	Vertical	2	17	72.91	183.15
Well 8	Vertical	17	9	32.55	41.65
Well 9	Vertical	11	11	64.28	215.71
Well 10	Horizontal	6-10	11	266.0	12,222.00
Well 11	Horizontal	2-6	7	132.75	8,650.00
Well 12	Horizontal	2	12-16	352.08	17,073.00
Well 13	Vertical	2	12	116.03	736.40

Table E.4

Well New 5 (Richie5)

(i = 2, j = 7)

Year	Oil Production Rate STB/D	Water Production Rate STB/D
1998	43.81	193.40
1999	25.27	236.77
2000	16.89	263.37
2001	12.80	278.37
2002	10.61	293.90
2003	8.76	302.65
2004	7.30	309.41
2005	6.25	315.07
Cumulative (MSTB)	**60.56**	**770.58**

Table E.5

Well New 6 (Sim6)
(i = 6, j = 11)

Year	Oil Production Rate STB/D	Water Production Rate STB/D
1998	60.71	110.91
1999	37.82	147.03
2000	23.77	178.74
2001	16.59	199.26
2002	13.11	214.45
2003	10.75	223.05
2004	9.19	230.50
2005	8.03	235.87
Cumulative (MSTB)	**96.38**	**528.72**

Table E.6

Well New 7 (Sim7)
(i = 2, j = 17)

Year	Oil Production Rate STB/D	Water Production Rate STB/D
1998	33.70	44.8
1999	28.23	51.76
2000	23.58	58.23
2001	19.10	65.40
2002	16.26	72.50
2003	13.56	78.05
2004	11.70	82.70
2005	10.38	85.90
Cumulative (MSTB)	**73.00**	**184.00**

Table E.7

Well New 8 (Sim 8)
(i = 17, j = 9)

Year	Oil Production Rate STB/D	Water Production Rate STB/D
1998	13.35	10.19
1999	11.46	12.01
2000	10.53	13.06
2001	9.18	14.58
2002	8.07	16.39
2003	6.81	18.23
2004	5.80	19.84
2005	5.07	21.24
Cumulative (MSTB)	**32.64**	**42.04**

Table E.8

Well New 9 (Sim9)
(i = 11, j = 11)

Year	Oil Production Rate STB/D	Water Production Rate STB/D
1998	33.34	49.51
1999	26.59	58.55
2000	20.05	68.97
2001	15.17	78.82
2002	12.49	86.88
2003	10.42	92.15
2004	9.12	95.70
2005	8.25	98.43
Cummulative (MSTB)	**64.28**	**215.71**

Table E.9

Well New 10 (Sim10)

(Horizontal Well: i = 6,7,8,9,10, j = 11)

Year	Oil Production Rate STB/D	Water Production Rate STB/D
1998	195.59	3945
1999	76.31	4355
2000	51.36	4448
2001	38.52	4491
2002	31.99	4544
2003	26.02	4553
2004	21.58	4551
2005	18.37	4540
Cumulative (MSTB)	**266.0**	**12,222.**

Table E.10

Well New 11 (Sim11)

(Horizontal Well: i = 2,3,4,5,6, j = 7)

Year	Oil Production Rate STB/D	Water Production Rate STB/D
1998	80.77	2777
1999	40.68	2953
2000	26.35	3021
2001	19.10	3052
2002	15.37	3096
2003	12.82	3100
2004	11.02	3097
2005	9.64	3091
Cummulative (MSTB)	**132.75**	**8650**

Table E.11

Well New 12 (Sim12)

(Horizontal Well: i = 2, j = 12,13,14,15,16)

Year	Oil Production Rate STB/D	Water Production Rate STB/D
1998	550.00	4144.
1999	106.19	6554.
2000	51.42	6788.
2001	32.44	6840.
2002	25.07	6815.
2003	20.54	6801.
2004	17.44	6776.
2005	15.16	6744.
Cumulative (MSTB)	**353.**	**17491.**

Table E.12

Well New 13 (Sim13)

(i = 2, j = 12)

Year	Oil Production Rate STB/D	Water Production Rate STB/D
1998	78.06	162.11
1999	42.23	223.36
2000	30.19	252.78
2001	23.62	271.35
2002	19.55	289.23
2003	15.96	300.64
2004	13.41	311.79
2005	11.54	320.26
Cumulative (MSTB)	**116.03**	**736.40**

Table E.13

Location of Potential Infill Wells and Cumulative Production for 1998-2005

Cumulative Production from 1998 to 2005 (MSTB)					
Well Name	Orientation	Location i	Location j	Oil Production	Water Production
Well 1	Vertical	9	11	27.93	195.80
Well 2	Vertical	9	3	24.66	310.71
Well 3	Vertical	7	3	20.67	164.88
Well 4	Vertical	5	7	25.18	429.49

Table E.14

Well New 1 (Ritchie 1)

(i = 9, j = 11)

Year	Oil Production Rate STB/D	Water Production Rate STB/D
1998	10.07	58.29
1999	6.77	67.22
2000	6.00	69.71
2001	5.50	71.21
2002	5.29	73.20
2003	4.82	74.68
2004	4.33	76.19
2005	3.91	77.50
Cumulative (MSTB)	**27.93**	**195.80**

Table E.15

Well New 2 (Ritchie 2)
(i = 9, j = 3)

Year	Oil Production Rate STB/D	Water Production Rate STB/D
1998	12.40	93.83
1999	10.31	99.07
2000	8.83	103.62
2001	7.63	107.29
2002	6.79	111.82
2003	6.03	114.22
2004	5.45	116.79
2005	4.92	119.14
Cumulative (MSTB)	**24.66**	**310.71**

Table E.16

Well New 3 (Ritchie 3)
(i = 7, j = 3)

Year	Oil Production Rate STB/D	Water Production Rate STB/D
1998	9.71	49.56
1999	8.36	52.56
2000	7.37	54.91
2001	6.57	56.82
2002	6.02	59.26
2003	5.50	60.84
2004	5.03	62.25
2005	4.62	63.49
Cumulative (MSTB)	**20.67**	**164.88**

Table E.17

Well New 4 (Ritchie 4)
(i = 5, j = 7)

Year	Oil Production Rate STB/D	Water Production Rate STB/D
1998	14.59	118.86
1999	8.82	137.01
2000	6.17	147.74
2001	4.61	155.30
2002	3.72	162.26
2003	3.12	165.97
2004	2.68	169.08
2005	2.34	171.40
Cumulative (MSTB)	**25.18**	**429.49**

4.6 Appendix F

TORP Simulation Summary for Section 30 of Schaben Field

Final Simulation Input Data

Fluid Properties:

Oil Gravity: 40°API
Reservoir Temperature: 125°F
Water Viscosity at Reservoir Temperature: 0.647 cp

PVT data:

PSAT	R_s	B_o	Z_g	GR	μ_o	μ_g
194.7	50	1.038	0.9054	0.123	1.9	0.01
15	0.0	1.0	0.993	0.123	2.5	0.00972

Reservoir Properties:

Two layers of identical properties with top layer perforated

Permeability:

K_x and K_y set equal and both multiplied by 3.1 for all grids

Local modification of K_x and K_y:

i = 16-18, j = 17-19, k = 1-2	K_x and K_y multiplied by 0.2
i = 3-5, j = 12-14, k = 1-2	K_x and K_y multiplied by 0.21
i = 7-9, j = 11-13, k = 1-2	K_x and K_y multiplied by 0.5
i = 7-9, j = 17-19, k = 1-2	K_x and K_y multiplied by 0.1
i = 12-14, j = 12-14, k = 1-2	K_x and K_y multiplied by 0.6
i = 2-4, j = 8-10, k = 1-2	K_x and K_y multiplied by 0.7

Local modification of K_z:

i = 16-18, j = 17-19, k = 1-2	K_z multiplied by 0.21
i = 3-5, j = 12-14, k = 1-2	K_z multiplied by 0.8
i = 2-5, j = 3-5, k = 1-2	K_z multiplied by 0.27
i = 6-9, j = 3-5, k = 1-2	K_z multiplied by 0.11
i = 12-14, j = 12-14, k = 1-2	K_z multiplied by 1.8
i = 7-9, j = 11-13, k = 1-2	K_z multiplied by 0.2
i = 7-9, j = 7-9, k = 1-2	K_z multiplied by 0.65
i = 2-4, j = 8-10, k = 1-2	K_z multiplied by 0.3
i = 11-13, j = 2-4, k = 1-2	K_z multiplied by 1.2
i = 16-18, j = 2-4, k = 1-2	K_z multiplied by 1.1
i = 11-13, j = 6-8, k = 1-2	K_z multiplied by 1.1

Relative Permeability Curves:

$$k_{ro} = \alpha_1(1 - S_{wD})^m$$
$$k_{rw} = \alpha_2(S_{wD})^n$$

where,

$$S_{wD} = (S_w - S_{iw})/(1 - S_{iw} - S_{or})$$
$$S_{iw} = 0.305139$$
$$S_{or} = 0.23$$
$$\alpha_1 = 1.0922$$

$m = 1.6$
$\alpha_2 = 0.25$
$n = 2.9$

k_{ro} at S_{iw} was set at 1.0

Capillary Pressure Data:

$$P_{cow} = a + b \exp(-S_{wD}/c)$$

where,

$a = -7.4799213$
$b = 12.751247$
$c = 1.896574$

Well Data:

Well No.	Skin	BHP, psi
D2	+2	15
D3	-4.5, +1.5	15 (up to 1991), 584.8 (in 1991 and after)
B4	-4.5, -3.0	997.2 (up to 1992), 247.25 (in 1992), 438 (in 1995 and after)
B6	-3.7	15
C2	-4	15
D1	+3	15 (up to 1992), 366 (in 1992 and after)
B2	0.0	15
C3	+2	15
B5	+1	15
B1	-3, +4	15(up to 1991), 322.5 (in 1991 and after)
C1	-1	15
D4	-4.5	904

4.7 Appendix G
List of Publications and Presentations
Resulting from Class 2 Project

Bhattachatya, S, and P. M. Gerlach, 1997, Carbonate Reservoir characterization and field simulation using boast 3: The Schaben Field (Mississippian), Ness County , Kansas; Presentation at University of Kansas / TORP Conference, March 19-20, 1997

Carr, T. R., 1996, Technology transfer for the independent; Society of Independent Professional Earth Scientists National Convention Abstracts, p. 10. Invited Talk/Panel Discussion at Society of Independent Petroleum Earth Scientists (SIPES) National Convention, March 20 - - 23, Dallas, TX.

Carr, T. R., J. Hopkins, H. Feldman, A. Feltz, J. Doveton, and D. Collins, 1994, Color Image Transforms of Wireline Logs: A Seismic Approach to Petrophysical Sequence Stratigraphy, Landmark Worldwide Technology Symposium, p. 36. Invited Talk at Landmark Worldwide Technology Forum, November, 29 - December 1, 1994, Houston, Texas.

Carr, T. R., Hopkins, J. H., Feldman, H. R., Feltz, A., Doveton J. H., and D. Collins, D. R., 1995, Color 2-D and 3-D Pseudo-Seismic Transforms of Wireline Logs: A Seismic Approach To Petrophysical Sequence Stratigraphy; Landmark Computer Graphics UserNet, 6p.

Carr, T. R., W. R. Guy, E. K. Franseen, and S. Bhattacharya, 1996, Enhanced Carbonate reservoir model for an old reservoir utilizing new techniques: The Schaben Field (Mississippian), Ness County, Kansas; American Association of Petroleum Geologists, Annual Meeting Abstracts, p. A23-A24.

Carr, T. R., H. R. Feldman, W. J. Guy, 1996, A new look at the reservoir geology of the Mississippian Schaben Field, Ness County, Kansas; Oklahoma Geological Survey Workshop on "Platform Carbonates in the Southern Midcontinent" Abstracts, p. 8.

Carr, T. R. , 1996, New Techniques for Sequence Stratigraphic Analysis Using Wireline Logs. Invited Talk, at San Joaquin Geological Society, December 3, 1996.

Doveton, J. H., Guy, W., Watney, W. L., Bohling, G. C., Ullah, S., and Atkins-Heljeson, D., 1995, PfEFFER 1.0 Manual, Kansas Geological Survey Open File Report 95-86.

Doveton, J.H., Guy, W.J., Watney, W. L., Bohling, G.C., Ullah, S., and Adkins-Heljeson, D., 1996, Log analysis of petrofacies and flow-units with microcomputer spreadsheet software: 1995 AAPG Mid-Continent Meeting.Transactions, p.224-233.

Guy, W. J., T. R. Carr, E. K. Franseen, S. Bhattacharya, and S. Beaty, 1997, Combination of magnetic resonance and classic petrophysical techniques to determine pore geometry and characterization of a complex heterogeneous carbonate reservoir: American Association of Petroleum Geologists Annual Meeting Abstracts, Dallas.

Hopkins, J. F., T. R. Carr, H. R. Feldman, 1996, Pseudoseismic Transforms of Wireline Logs: A Seismic Approach to Petrophysical Sequence Stratigraphy, in J. A. Pacht, R. E. Sheriff and B. F. Perkins, eds., Stratigraphic Analysis Utilizing Advanced Geophysical, Wireline and Borehole Technology for Petroleum Exploration and Production: Gulf Coast SEPM Seventeenth Annual Research Conference, p. 133-144.

Watney, W.L., W.J. Guy, J.H. Doveton, S. Bhattacharya, P. M. Gerlach, G. C. Bohling, T. R. Carr, 1997, Petrofacies Analysis - A petrophysical tool for geologic/engineering reservoir characterization, Manuscript for USDOE Reservoir Characterization Workshop, Houston, Texas, March 3- 5.